

Doctorate Program in Molecular
Oncology and Endocrinology
Doctorate School in Molecular
Medicine

XXIV cycle - 2008–2011
Coordinator: Prof. Massimo Santoro

**“Oncolytic adenovirus *dl922-947*
targets the DNA damage signaling
pathway and enhances the effects
of radiation therapy”**

Antonella Abagnale

University of Naples Federico II
Dipartimento di Biologia e Patologia Cellulare e
Molecolare
“L. Califano”

Administrative Location

Dipartimento di Biologia e Patologia Cellulare e Molecolare “L. Califano”
Università degli Studi di Napoli Federico II

Partner Institutions

Italian Institutions

Università degli Studi di Napoli “Federico II”, Naples, Italy
Istituto di Endocrinologia ed Oncologia Sperimentale “G. Salvatore”, CNR,
Naples, Italy
Seconda Università di Napoli, Naples, Italy
Università degli Studi di Napoli “Parthenope”, Naples, Italy
Università degli Studi del Sannio, Benevento, Italy
Università degli Studi di Genova, Genova, Italy
Università degli Studi di Padova, Padova, Italy
Università degli Studi “Magna Graecia”, Catanzaro, Italy
Università degli Studi di Udine, Udine, Italy

Foreign Institutions

Université Libre de Bruxelles, Bruxelles, Belgium
Universidade Federal de Sao Paulo, Brazil
University of Turku, Turku, Finland
Université Paris Sud XI, Paris, France
University of Madras, Chennai, India
University Pavol Jozef Šafàrik, Kosice, Slovakia
Universidad Autonoma de Madrid, Centro de Investigaciones Oncologicas
(CNIO), Spain
Johns Hopkins School of Medicine, Baltimore, MD, USA
Johns Hopkins Krieger School of Arts and Sciences, Baltimore, MD, USA
National Institutes of Health, Bethesda, MD, USA
Ohio State University, Columbus, OH, USA
Albert Einstein College of Medicine of Yeshiwa University, N.Y., USA

Supporting Institutions

Dipartimento di Biologia e Patologia Cellulare e Molecolare “L. Califano”,
Università degli Studi di Napoli “Federico II”, Naples, Italy
Istituto di Endocrinologia ed Oncologia Sperimentale “G. Salvatore”, CNR,
Naples, Italy
Istituto Superiore di Oncologia, Italy.

Italian Faculty

| | |
|-------------------------------------|---------------------------|
| Salvatore Maria Aloj | Paolo Emidio Macchia |
| Francesco Saverio Ambesi Impiombato | Barbara Majello |
| Francesco Beguinot | Rosa Marina Melillo |
| Maria Teresa Berlingieri | Claudia Miele |
| Bernadette Biondi | Nunzia Montuori |
| Francesca Carlomagno | Roberto Pacelli |
| Gabriella Castoria | Giuseppe Palumbo |
| Maria Domenica Castellone | Silvio Parodi |
| Angela Celetti | Nicola Perrotti |
| Lorenzo Chiariotti | Maria Giovanna Pierantoni |
| Vincenzo Ciminale | Rosario Pivonello |
| Annamaria Cirafici | Giuseppe Portella |
| Annamaria Colao | Giorgio Punzo |
| Sabino De Placido | Maria Fiammetta Romano |
| Gabriella De Vita | Antonio Rosato |
| Monica Fedele | Giuliana Salvatore |
| Pietro Formisano | Massimo Santoro |
| Alfredo Fusco | Giampaolo Tortora |
| Domenico Grieco | Donatella Tramontano |
| Michele Grieco | Giancarlo Troncone |
| Maddalena Illario | Giancarlo Vecchio |
| Massimo Imbriaco | Giuseppe Viglietto |
| Paolo Laccetti | Mario Vitale |
| Antonio Leonardi | |

*Ai due
grandi amori
della mia vita*

**“Oncolytic adenovirus
dl922-947 targets the
DNA damage signaling
pathway and enhances
the effects of radiation
therapy”**

TABLE OF CONTENTS

| | |
|---|-----------|
| LIST OF PUBLICATIONS | 5 |
| LIST OF ABBREVIATIONS..... | 6 |
| ABSTRACT..... | 7 |
| 1. BACKGROUND..... | 8 |
| 1.1 Oncolytic viruses as anticancer drugs..... | 8 |
| 1.2 Herpes simplex virus | 9 |
| 1.3 Polyomavirus..... | 10 |
| 1.4 Poxvirus..... | 11 |
| 1.5 Parvovirus | 11 |
| 1.6 Reovirus..... | 12 |
| 1.7 Paramyxovirus | 12 |
| 1.8 Picornavirus | 13 |
| 1.9 Adenovirus | 13 |
| 1.10 Oncolytic adenovirus and cell death | 17 |
| 1.11 Oncolytic viruses in cancer therapies..... | 19 |
| 1.12 Oncolytic adenoviruses in combination cancer therapies..... | 20 |
| 1.13 OVs and IR: understanding the molecular mechanism. Role of the DNA damage pathway..... | 22 |
| 2. AIM OF THE STUDY | 30 |
| 3. MATERIALS AND METHODS | 31 |

| | | |
|-----------|--|-----------|
| 3.1 | Cell lines and drug | 31 |
| 3.2 | Preparation of adenoviruses | 31 |
| 3.3 | Viability assay | 31 |
| 3.4 | Quantitative PCR of adenovirus | 32 |
| 3.5 | AdGFP infection..... | 32 |
| 3.6 | Cell cycle analysis..... | 33 |
| 3.7 | FACS analysis: P-H2AX and cell cycle..... | 33 |
| 3.8 | Western blot | 33 |
| 3.9 | Antibodies for western blot | 34 |
| 3.10 | Tumorigenicity assays | 34 |
| 3.11 | Statistical analysis | 35 |
| 3.12 | Micronuclei counting | 36 |
| 4. | RESULTS..... | 37 |
| 4.1 | Ionising radiation enhances the effects of the oncolytic adenovirus <i>dl922-947</i> | 37 |
| 4.2 | Ionising radiation does not increase viral entry upon infection | 40 |
| 4.3 | IR induces G2 accumulation and caspase-3 activation: effects of the combined treatment on ATC cell cycle and cell death..... | 42 |
| 4.4 | Ionising radiation in combination with <i>dl922-947</i> reduced the growth of ATC tumor xenografts | 47 |
| 4.5 | <i>dl922-947</i> modulates the DNA damage signaling pathway to enhance ionising radiation effects | 50 |
| 5. | DISCUSSION..... | 60 |
| 6. | CONCLUSION..... | 65 |
| 7. | ACKNOWLEDGEMENTS | 66 |

8. REFERENCES 68

LIST OF PUBLICATIONS

This dissertation is based upon the following publications:

- Esposito F, Libertini S, Franco R, **Abagnale A**, Marra L, Portella G, Chieffi P.
Aurora B expression in post-puberal testicular germ cell tumours. *J Cell Physiol.* 2009;221(2):435-9.
- Libertini S, **Abagnale A**, Passaro C, Botta G, Portella G.
Aurora A and B kinases--targets of novel anticancer drugs. *Recent Pat Anticancer Drug Discov.* 2010;5(3):219-41. Review.
- Botta G, Perruolo G, Libertini S, Cassese A, **Abagnale A**, Beguinot F, Formisano P, Portella G.
PED/PEA-15 modulates coxsackievirus-adenovirus receptor expression and adenoviral infectivity via ERK-mediated signals in glioma cells. *Hum Gene Ther.* 2010;21(9):1067-76.
- Libertini S, **Abagnale A**, Passaro C, Botta G, Barbato S, Chieffi P, Portella G.
AZD1152 negatively affects the growth of anaplastic thyroid carcinoma cells and enhances the effects of oncolytic virus dl922-947. *Endocr Relat Cancer.* 2011;18(1):129-41.
- Botta G, Libertini S, Passaro C, **Abagnale A**, Barbato S, Hallden G, Beguinot F, Formisano P and Portella G.
Inhibition of autophagy enhances the effects of E1A defective oncolytic adenovirus dl922-947 against glioma cells in vitro and in vivo. *Hum Gene Ther.* Under Review.

LIST OF ABBREVIATIONS

| | |
|--|--|
| ATC: Anaplastic Thyroid Carcinoma | EBRT: external beam radiation therapy |
| OVs: Oncolytic viruses | DSB: double strand break |
| IR: ionising radiation | NHEJ: non homologous end-joining |
| NDV: Newcastle disease virus | HR: homologous recombination |
| HSV: herpes simplex virus | ATM: ataxia-telangiectasia mutated |
| CNS: central nervous system | ATR: ATM-Rad3 related protein |
| VV: vaccinia virus | SMC-1: structural maintenance of chromosomes 1 |
| AAV: adeno-associated virus | Chk1/2: checkpoint kinase 1/2 |
| IRES: internal ribosome entry site | BRCA1: breast cancer susceptibility gene 1 |
| CAR: coxsackie and adenovirus receptor | DNA-PK: DNA-dependent protein kinase |
| CR1/2: conserved region 1/2 | Mdc1: mediator of DNA damage checkpoint |
| HAT: histone acetyltransferase | MOIs: multiplicity of infection |
| 5-FU: 5-fluorouracil | HPI: hours post infection |
| LV: leucovorin | |
| DSBR: double strand break response | |
| PFU: plaque forming unit | |
| CSC: cancer stem cell | |
| EMT: epithelial-mesenchymal transition | |

ABSTRACT

Replication selective oncolytic viruses (OVs) are a rapidly expanding therapeutic platform for cancer treatment. OVs are characterized by genetic alterations that ablate critical viral protein functions essential for viral replication in normal cells, but non-essential in tumor cells, thus targeting viral replication to tumor cells.

dl1520 was the first oncolytic virus described, and we have demonstrated that *dl1520* is effective against anaplastic thyroid carcinoma (ATC) cells and tumor xenografts; its antineoplastic effects are enhanced by paclitaxel, doxorubicin, lovastatin and ionising radiation. We have also shown that the second generation oncolytic adenovirus *dl922-947* possesses a greater antitumor effect than *dl1520* against ATC cells, and that the anti-VEGF monoclonal antibody, Bevacizumab, increased the effects of *dl922-947* by improving viral distribution within the tumor mass. Furthermore, we have also shown that AZD1152, a selective Aurora B kinase inhibitor, negatively affects the growth of anaplastic thyroid carcinoma cells and enhances the effects of oncolytic virus *dl922-947*.

So far, preclinical and clinical studies have clearly shown the antineoplastic potential of oncolytic viruses, at least for local treatment, but have also highlighted the need to find associations that could improve their activity. Association of viruses with specific combinations, not only able to directly kill tumor cells but also to increase viral oncolytic activity, would represent a powerful therapeutic tool for the treatment of human neoplasia, in particular for diseases lacking of effective treatment.

The main treatment of ATC consists of irradiation plus chemotherapeutic drugs. In order to identify novel treatment able to enhance the effects of OVs, I have evaluated the effects of ionising radiation in combination with *dl922-947*, focusing my attention on which type of cell death was activated in the combined treatment. Moreover, I have studied the effects of *dl922-947* on the DNA damage response pathway and I have also evaluated the effects of an ATM inhibitor on *dl922-947*'s activity.

1. BACKGROUND

1.1 Oncolytic viruses as anticancer drugs

The notion that viruses may be able to eradicate cancer has existed since the early 20th century (Sinkovics and Horvath 1993; Sinkovics and Horvath 2000; Southam and Moore 1952). Several viruses were tested both in experimental settings and in humans during the 1950s and 1960s. Among the first viruses to be used in a controlled fashion in clinical studies was a vaccine strain of rabies virus to treat 30 patients with melanomatosis, eight of whom showed tumor regression (Pack 1950). A few years later the oncolytic efficacy of adenovirus serotype type 4, (which at that time was referred to as RI (respiratory infectious) virus), was tested in humans (Southman et al. 1956), as well as the flavivirus West Nile virus (Southam and Moore 1952) and the paramyxoviruses mumps and Newcastle disease virus (NDV) (Asada 1974; Okuno et al. 1978). Many viruses were tested in animal models. For instance, bovine enterovirus showed efficient lysis of syngeneic tumors in immunocompetent mice (Taylor et al. 1971). These studies provided the first evidence of therapeutic potential in humans. However clinical studies were unimpressive and many viruses elicited side-effects which ultimately ended the trials. As a result, the initial interest in viruses as anti-cancer agents declined during the following decades, as deduced from the number of publications from that time, and studies were mainly conducted using experimental models. Later in the 1990s interest in viruses as a treatment for cancer was rekindled, and today virotherapy is asserting itself as a novel treatment option alongside surgery, chemo- and radio-therapy. Many genetic and physiological features specific for malignant cells relating to particular gain-of-function or loss-of-function mutations explain why cancer cells are so generous hosts for viruses. Cancer cells have undergone a mini-evolution (point-mutations, larger chromosomal shifts and alterations), providing them with selective growth advantages over normal cells (Cahill et al. 1999). While cancer cells gain growth-enhancing attributes, they may simultaneously lose critical components of the intracellular defense mechanisms and thus become fertile ground for the replication of many viruses. Moreover, malignant cells may express higher levels of virus receptors compared to normal cells, which makes them more susceptible to infection (Vaha-Koskela et al. 2006). Cancer-selective oncolytic viruses replicate preferentially in cancer cells, thereby amplifying the initial input dose, and as a result destroy those cells at the end of replication cycles by lysis. The viral progeny are then released, enabling them to infect neighboring cells, which results in multiple self-perpetuating rounds of infection, replication, lysis and spread throughout the tumor, all while sparing normal cells, hence toxicity is limited. Of note, oncolytic viruses can kill apoptosis-resistant tumor cells, and hence do not have cross-resistance with existing therapies. Despite the advances made in oncolytic viral therapies, the field

awaits a true revolutionary breakthrough success, as was initially envisioned with the development of the field. The limitations in success may be due to the intrinsic biological properties of the tumor targets. Notably, a subpopulation of cancer cells that are often resistant to conventional treatment regimens and are responsible for the initiation of tumors in xenograft models have recently been discovered and characterized. This treatment resistant subpopulation still lacks full definition but has been characterized as cancer-initiating cells or cancer stem (or stem-like) cells (CSC). As with other treatment modalities, previous oncolytic virus agents have targeted the general tumor cell population and have not specifically targeted the CSC subpopulation. From the viewpoint of disease phenotype, CSCs embody the refractory nature observed among many cancers; very competent initial tumor establishment (Li et al. 2007) and extremely aggressive metastatic nature (Hermann et al. 2007). Furthermore, recent discoveries indicate that CSCs embody chemo- and radioresistance (Shah et al. 2007; Ishii et al. 2008), and have been correlated with advanced disease and resistance to current therapies (Hermann et al. 2007), and thus help explain the clinical treatment resistance of these cancers. As CSCs are critical for tumor initiation, progression, persistence, and the development of metastasis, the success or failure of cancer treatment approaches may be influenced greatly by the presence and treatment sensitivity of these cells. Oncolytic vectors conceptually provide the means to effectively target and eradicate CSCs, kill the general tumor cell population, and carry therapeutic transgenes to alter the tissue microenvironment to make it unfavorable for the EMT (epithelial-mesenchymal transition) phenomena as well as tumor propagation. Specifically, Ad-based oncolytic vectors, or CRAds, have shown the ability to accomplish all of these goals and have provided favourable patient safety profiles in early clinical trials. CRAds offer a targeted therapy directed toward CSCs and can affect the general tumor cell population directly through shared targets or indirectly via synergistic effects with chemotherapy and radiation therapy, favoring a multiple modality approach to CSC targeting and eradication with overall cancer cure. Additionally, viral replication within a tumor may help mobilize the immune system by inducing the release of cytokines and by liberating tumor antigens (Ries et al. 2000; Cody and Douglas 2009), contributing to a more efficient anti-tumor immune response. Members from an increasing number of virus families are being considered for cancer gene therapy. In the following some further details will be given about some of these viruses.

1.2 Herpes simplex virus

Vectors based on herpes simplex virus (HSV)-1 are, together with the adenoviruses, further along in their development and testing for virotherapy. HSV-1 is an enveloped, double-stranded linear DNA virus whose genome spans 152 Kb encoding over 80 genes. Approximately half of the genes are

necessary for virus replication. The HSV-1 genome is composed of unique long (U_L) and unique short (U_S) segments, which are both flanked by inverted repeats. Infection can be either lytic or latent. During lytic infection, HSV-1 genes are expressed in a temporally regulated cascade consisting of three phases, designed α , β , and γ . HSV-1 offers a number of advantages over other viral vectors system. These advantages include: the potential for incorporating a large foreign DNA; neurotropism, rendering gene delivery to the CNS more effective; the sensitivity to antiherpetic agents like ganciclovir provides a safety mechanism by which viral replication could be abrogated; moreover, HSV-1 never integrates and persists as an episome even during latency so the risk of insertional mutagenesis is not an issue. There are two general strategies that are employed to target HSV-1 replication to cancer cells. The first involves deletion or inactivation of viral genes that are essential for viral replication in normal cells but dispensable in tumor cells, such as HSV-tk, ribonucleotide reductase, and $\gamma 134.5$. The initial HSV-1 mutant studied for tumor-selective replication, *dlsptk*, contains a 360-bp deletion within HSV-tk, and it was used to treat malignant gliomas in rodents (Martuza 1992). Accordingly, *dlsptk* replicates well in cultured tumor cells and induces significant growth inhibition of human U87 gliomas growing in the brains of nude mice. However, this HSV-1 mutant has not been tested in clinical trials because it produces neurotoxicity at higher titers, and it is resistant to the antiviral agents acyclovir and ganciclovir by virtue of its disrupted HSV-tk gene. Investigators looked instead at developing HSV-1 mutants that maintain sensitivity to acyclovir and ganciclovir and that exhibit less neurovirulence by deletion of the $\gamma 134.5$ gene. One such $\gamma 134.5$ -null mutant is G207 (MediGene, Inc.; San Diego, CA) which exhibits tumor-cell-specific replication and antitumor efficacy in both *in vitro* and *in vivo* models of malignant glioma (Mineta 1995) and a study of a phase I was conducted in patients with glioma (Shah 2003). However, there are challenges that arise when working with HSV-1 vectors. First, genetic manipulation of HSV-1 is difficult due to the large size of the viral DNA. A second potential obstacle when using HSV-1 recombinant vectors is the fact that most humans have pre-existing herpes immunity, which could potentially impair gene delivery. Potential neurotoxicity is a third problem inherent to HSV-1 vectors when delivered into the central nervous system.

1.3 Polyomavirus

Polyomaviruses are double-stranded DNA viruses with a relatively small circular genome (5.3 Kb). Recombinant polyomavirus vectors based on the SV40 virus have been around since the turn of the millennium, and although inherently non-lytic, Cordelier et al. (2007) recently demonstrated significant tumor-specificity *in vitro* and growth inhibition in a mouse model of pancreatic cancer using tumor-specific promoters to drive the expression of an inhibitory protein from such a vector. The main advantages of polyomavirus

vectors is their remarkable ability to escape immune recognition, they do not evoke a neutralizing antibody response, and durable transgene expression (Strayer et al. 2005).

1.4 Poxvirus

Poxviruses are large, enveloped, dsDNA viruses with a complex genome harboring multiple immune-modulating genes. The most commonly used poxvirus in cancer targeting is vaccinia virus (VV). As the wildtype strain WR causes local tissue destruction (necrosom), the derived vectors have been attenuated by removal of thymidine kinase or other genes (Guo et al. 2005; McCart et al. 2001). Many VV vectors efficiently kill tumors in preclinical settings. However, although replication-competent vectors have been able to enhance the survival of both immunodeficient and immunocompetent mice carrying different types of tumors, significant infection of other organs has also been observed, indicating that VV vectors still need to be optimized (Guo et al. 2005). As an example, the novel replication-competent vector JX-594 based on strain Wyeth showed impressive oncolysis of tumors and metastases in syngeneic models in both rats and rabbits upon i.v. administration (Kim et al. 2006). JX-594 is an oncolytic poxvirus engineered for replication, transgene expression and amplification in cancer cells harbouring activation of the epidermal growth factor receptor (EGFR)/Ras pathway, followed by cell lysis and anticancer immunity. In a recent clinical trial it has been demonstrated that JX-594 selectively infects, replicates and expresses transgene products in cancer tissue after intravenous infusion, in a dose-related fashion. Normal tissue were not affected clinically. This platform technology opened the possibility of multifunctional products that selectively express high concentration of several complementary therapeutic and imaging molecules in metastatic solid tumors in humans (Breitbach et al. 2011).

1.5 Parvovirus

Parvoviruses are non-enveloped single-stranded DNA viruses (5Kb genome). The family includes the helper-dependent viruses, including the adeno-associated viruses (AAV), which require molecular functions supplied in trans via co-infection with herpes- or adenoviruses, whereas the autonomous parvoviruses can replicate with the help of cellular factors. Of these, only the autonomous parvoviruses are oncolytic, although both display oncosuppressive effects. Parvoviruses can inhibit the transforming capacity of other oncogenic viruses (Mousset and Rommelaere 1982), and have been shown to suppress the proliferation of some cancer cell lines by inducing cell cycle arrest and terminal differentiation (Bantel-Schaal 1995). Anti-tumor efficacy by these

viruses may involve both oncolysis and tumor suppression/reversion (Cornelis et al. 2004).

1.6 Reovirus

Reoviruses are very common in the human respiratory and gastrointestinal tract. While attenuated in healthy tissue, reoviruses are inherently oncolytic and show high tumor-specificity upon remote administration. Marked inhibition of tumor growth and prolonged survival of immunocompetent mice was observed upon multiple i.v. injections in a model of lung-metastasizing mammary cancer (Hirasawa et al. 2003). In this study, the oncolytic efficacy was reduced in pre-immunized animals, indicating that pre-existing immunity poses an obstacle with this virus. The first indications that reovirus could be used to treat established or inhibit metastases came from xenografts models of human cancer in immunocompromised animals (Norman et al. 2002; Yang et al. 2003; Alain et al. 2002; Yang et al. 2004). Xenografts of a human breast cancer cell line were inoculated over both the left and right hind flanks and reovirus was injected into only one flank tumor (Norman et al. 2002). Reovirus replication and regression was observed at both injected and non-injected contralateral sites. In another study, reovirus administered intracranially was able to eradicate breast cancer metastases in the CNS of nude mice and to prolong survival of immunocompetent rats with leptomeningeal breast cancer metastases when administered intrathecally (Yang et al. 2004).

1.7 Paramyxovirus

This vast group of viruses includes prototypic members such as measles virus, mumps virus and the Newcastle disease virus (NDV), all of which have been used in cancer targeting. The history of NDV as an anti-tumor agent in humans began in 1965 with a clinical trial led by Dr's Cassel and Garrett who used the live attenuated 73-T strain to treat a patient with cervical carcinoma (Cassel and Garrett 1965). Subsequently, NDV has been used both as oncolysate and live virus in several clinical trials. As an example of the latter, in one study a purified poultry vaccine dubbed MTH-68/H based on live attenuated NDV was administered i.v. to a total of 14 patients with grade IV glioblastoma multiforme since 1996 (Csatary et al. 2004). Of these patients, five died of the cancer, two died of other causes and the remaining seven were alive at the time of the publishing of the paper in 2004. Four of these patients who had been alive for 5-9 years had received i.v. virus as their sole form of treatment. A phase I/II clinical trial using i.v. administration of another live attenuated neurotropic NDV strain, NDV-HUJ, to treat glioblastoma and three phase I trials using the live NDV vector PV701 to treat patients with multiple

types of cancers were recently completed (Freeman et al. 2006; Lorence et al. 2003).

1.8 Picornavirus

Several members of these positive strand RNA viruses are being developed into tools for virotherapy. Poliovirus infects a wide variety of human cancer cell lines and primary explants (Ansardi et al. 2001). By attenuation of a neurovirulent poliovirus strain by replacement of the viral internal ribosome entry site (IRES) with the corresponding sequence from the closely related human rhinovirus type 2, Gromeier et al. (2000) were able to obtain a highly efficacious recombinant virus, PV1(PVS)-RIPO, which displayed significant tumor tropism and oncolytic potential in subcutaneous and i.c. human astrocytoma xenografts in nude mice. Whereas the subcutaneous tumors were efficiently eradicated upon a single i.v. administration, the brain tumor xenografts responded only to i.t. injection despite that the vector was neurotropic and replication-competent. In another study, this virus was able to cause complete tumor regression in a small number of athymic rats harbouring i.c. human glioma xenografts upon intrathecal administration. In addition to the recombinant vectors, a live attenuated strain of poliovirus 1 has shown promise as an oncolytic agent (Toyoda et al. 2004).

1.9 Adenovirus

Adenoviruses were isolated in 1953 from human adenoid tissue samples in culture undergoing “spontaneous” regression, and were dubbed adenoidal—pharyngeal—conjunctival viruses based on their capacity to induce disease symptoms in experimentally infected humans (Rowe et al. 1953). The 51 distinct serotypes of human adenovirus have been classified into six groups (A–F) based on sequence homology and their ability to agglutinate red blood cells (Shenk 1996). Most studies have been carried out on adenovirus serotype 2 (Ad2) and 5 (Ad5). Human adenoviruses contain a linear, double stranded DNA genome of 30-36 Kb, and present an icosahedral symmetry. The hexon, penton base, and knobbed fiber, are the most important capsid proteins for gene delivery. Adenovirus infection occurs through binding of the adenoviral fiber to cellular receptors such as the coxsackie-adenovirus receptor (CAR) or integrins.

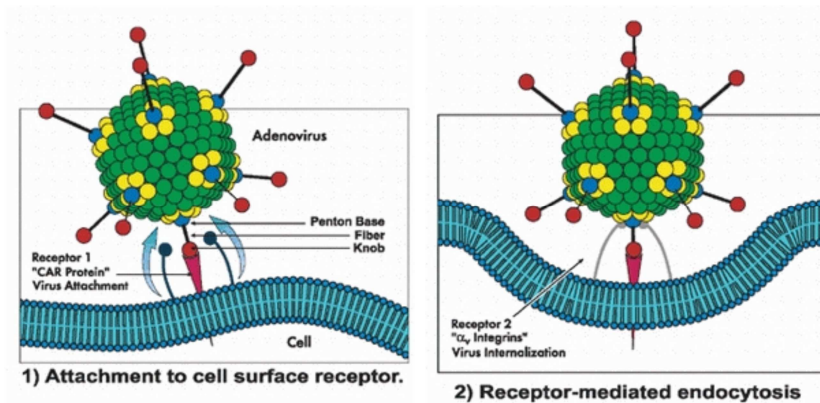


Figure 1. Adsorption and entry of adenovirus into the cell

Attachment of adenovirus to cell surface receptor (on the left) and receptor-mediated endocytosis (on the right).

After the virus internalization through endocytosis the virus escapes the endosome and translocates to the nuclear pore complex, where the viral DNA is released into the nucleus and transcription begins. Transcription, replication and viral packaging take place in the nucleus of the infected cell. A complex series of splicing accompanies transcription, and genes are transcribed from both strands. Adenoviral transcription occurs in two phases: early and late (Fields et al. 1996).

During the early phase, the host cell is transformed into an efficient producer of the viral genome. The first gene that is transcribed in the viral genome is E1A. The adenovirus E1A protein is encoded by several alternatively spliced mRNAs, with the predominant forms being the 12S and 13S mRNAs (Heise et al. 2000). Two regions of conserved sequence among E1A proteins of different adenovirus types are conserved regions 1 and 2 (CR1 and CR2). CR1 and CR2 contribute to E1A-induced cell cycle progression and transformation (Fueyo et al. 2000, Rodriguez et al. 1997). During infection, the primary mechanism by which E1A forces quiescent cells to actively cycle is by interfering with proteins of the retinoblastoma (Rb) pathway (Harlow et al. 1986; Moran 1993) and this interaction is mediated primarily by CR2. Rb acts as a tumor suppressor via binding to E2F, a transcriptional activator that promotes expression of genes necessary for driving the cell into S phase (Nevins 1995). The E1A product is able to sequester Rb and release repression of E2F, allowing it to activate its target genes. E1A proteins have also been shown to modulate the activity of p107 and p130, two members of the Rb family that are also involved in regulating cell cycle progression (Parreno et al. 2001). In addition to binding to Rb, E1A also binds to p300, an important nuclear integrator of diverse signalling pathways that possesses intrinsic histone acetyltransferase (HAT) activity and is implicated in the activation of genes that maintain cell differentiation and inhibit the cell cycle. p300 regulates and activates transcription by acetylating multiple other transcription factors, E2F and p53 being two important examples. E1A has been shown to repress directly the HAT activity of p300 and to inhibit p300-dependent transcription

(Hamamori et al. 1999; Chakravarti et al. 1999). All these actions of E1A result in the accumulation of p53. p53 is a cellular growth suppressor that acts as a G1 checkpoint control and in response to viral challenge, p53 may induce a G1 growth arrest by inducing genes such as the cyclin-dependent kinase inhibitor p21/WAF1/Cip1 gene (El-Deiry et al. 1993, Xiong et al. 1993) or apoptosis by inducing genes such as Bax1 (Miyashita and Reed 1995). The induction of apoptosis is inhibited by the products of the E1B gene. The E1B transcription unit encodes two proteins, E1B-55kDa and E1B-19kDa. The E1B-19kDa protein is a functional homologue of the proto-oncogene-encoded Bcl-2 and prevents apoptosis by similar mechanisms (Debbas et al. 1993; Rao et al. 1992). The E1B-55kDa protein complexes with the amino-terminal end of p53 and inhibits its activity as a transcription factor (Kao et al. 1990; Yew and Berk 1992; Yew et al. 1994). It is thought that these mechanisms for inhibiting apoptosis keep the cell alive as long as possible in order to maximize viral yields (Rao et al. 1992). In addition to its antiapoptotic functions, the E1B-55kDa protein facilitates the transport of nuclear viral mRNAs to the cytoplasm during the late stages of infection (Pilder et al. 1986). The E2 region encodes proteins necessary for replication of the viral genome: DNA polymerase, preterminal protein, and the 72-kDa single-stranded DNA-binding protein (De Jong et al. 2003). Products of the viral E3 region function to subvert the host immune response and allow persistence of infected cells. The immune system has evolved a number of mechanisms for destroying virus-infected cells, including cell lysis by cytotoxic T lymphocytes and activation of receptor-mediated apoptotic pathways by chemokines. The E4 transcription unit encodes a number of proteins that have been known to play a role in cell cycle control and regulation of DNA replication. The viral structural proteins and the proteins necessary for assembly of the virion are encoded by genes expressed during the late phase of viral replication. Once viral progeny assembly is complete, new viral particles are released by cytolysis (figure 2).

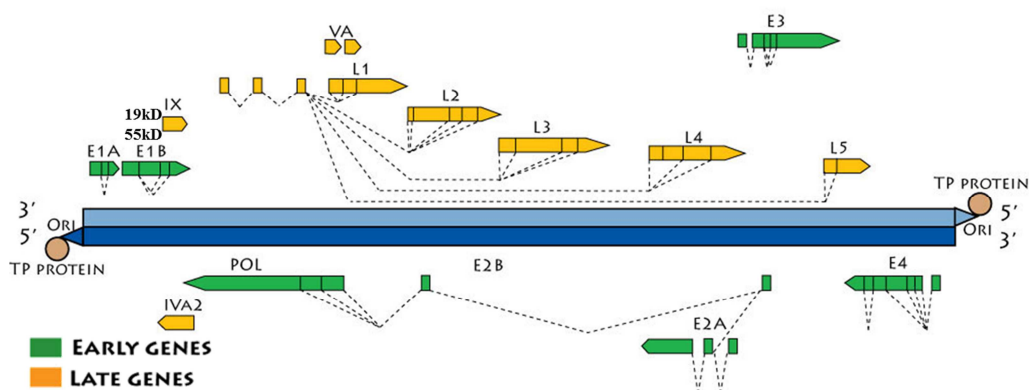


Figure 2. Adenoviral genome.

Adenoviruses have become the most widely used and most extensively studied viruses for gene delivery/therapy purposes, being easy to manipulate and very safe *in vitro* and *in vivo*. Numerous pre-clinical studies were conducted using adenoviral vectors to transfer tumor suppressor genes or as oncolytic viruses (Alemany et al. 2000). In China, oncolytic adenovirus mutants in combination with chemotherapy have been accepted as a standard treatment form for refractory nasopharyngeal cancer.

Oncolytic adenoviruses are genetically manipulated human adenoviruses that acquired a replication phenotype in tumor cells, but show a more restricted phenotype in normal cells. Several features of wild type adenoviruses can be modified to acquire tumor replication properties (Chiocca 2002).

There are different ways in order to developing tumor specificity in oncolytic adenoviruses:

- by altering viral genes that attenuate replication in normal tissue but not in tumor cells;
- by placing viral genes that initiate viral replication under the control of promoter sequences that are active only in tumor cells;
- by the modification of viral coat proteins that function in host cell infection.

The most widely-used strategy consists in the creation of replication-conditional adenoviruses genetically modified such as *dl1520* and *dl922-947*.

Mutant adenovirus *dl1520* (also known as ONYX-015) contains a deletion in the E1B gene, preventing the formation of a functional E1B-55kDa protein. With this mutation, *dl1520* was expected to replicate only in p53-deficient cells (Bischoff et al. 1996). For example, by altering a region of the E1B gene, the adenovirus can selectively replicate in p53-deficient (i.e. tumour) cells and leave p53-competent cells intact. In addition to its role in the degradation of p53, the E1B-55kDa protein has several other important late-phase functions. E1B-55KDa mediates late-viral RNA transport and the loss of E1B-55KDa restricts the viral replication to tumor cells capable of taking over the RNA export function of the viral gene product (O'Shea et al. 2005).

The second strategy concerns the regulation of viral replication via cellular promoters that are overactive in certain tumor cells, sometimes referred to as "tumor-specific" promoters. Certain tumor types, such as germ cell tumors, prostate cancer, and hepatocellular carcinoma, express proteins that are not normally present in the human body after fetal development. Oncolytic adenoviruses have been created to take advantage of the expression of these tumor markers or dependence on normally secreted hormones by placing the E1A gene under the control of the promoters derived from the genes of interest (Hallenbeck et al. 1999; Rodriguez et al. 1997; Matsubara et al. 2001; Hsieh et al. 2002). The last strategy used to create oncolytic adenovirus is to alter the structural viral envelope proteins to retarget the virus to tumor cell surfaces and direct the virus away from its normal receptor (Dmitriev et al. 2000).

The safety and antitumor efficacy of *dl2520* have been tested in numerous phase I and II clinical trials (Kim 2001). In all this trials adenovirus was

administered alone and this monotherapy has demonstrated limitations in efficacy. Its limited efficacy has highlighted the need for oncolytic adenoviruses with higher replication efficiency and killing activity.

A second generation adenoviral mutant has been generated. *dl922-947* is an E1A mutant oncolytic adenovirus, which bears a 24-bp deletion in E1A Conserved Region 2 (CR2) therefore, is unable to induce progression from G₁ into S-phase of quiescent cells. The G₁-S checkpoint is critical for cell growth progression and is lost in almost all cancer cells as a result of mutations or deletions of the RB or CDKN2A genes, amplification and overexpression of Cyclin D, and amplification, overexpression or mutation of the CDK4 gene (Sherr 2000, Roussel 1999). The *in vitro* efficacy of *dl922-947* was demonstrated in a range of a cancer cell lines and this efficacy exceeded that of adenovirus 5 wild-type (Ad5wt) and *dl1520* (Heise et al. 2000). A similar adenovirus, $\Delta 24$, with the same deletion in E1A-CR2, has shown activity in preclinical models of glioma (Fueyo et al. 2000). *dl922-947* has also an impressive *in vitro* activity in ovarian carcinoma and was able to produce some long-term survivors in an aggressive xenograft model (Lockley et al. 2006).

1.10 Oncolytic adenovirus and cell death

Although oncolytic viruses have been tested in clinical trials, so far oncolytic virus-induced cell death mechanisms remain to be elucidated. In order to find drugs that could be used for the development of novel therapeutic strategies based on the use of oncolytic viruses, elucidations of the molecular mechanisms of virus-induced cell death are necessary.

The cell death pathways activated by the infection with OVs are only partially understood, however several evidences indicate that they are cell type depending. We have obtained data confirming this hypothesis. The infection with *dl922-947* activates in glioma cells a survival pathway, autophagy and the block of autophagy with pharmacological inhibitors induces a switch toward apoptosis (Botta et al. under review). Conversely, in ATC cells, *dl922-947* infection leads to a programmed cell death lacking the features of classical apoptosis, but showing some apoptotic markers, such as subG₁ accumulation and caspase-3 activation. We did not observe upon *dl922-947* infection autophagy or mitotic catastrophe in ATC cells (Libertini et al. 2011) and we have also obtained data indicating that *dl922-947* in ATC cells induces G₂/M accumulation and block of cell division, as suggested by the observed poliploidy.

Adenovirus-induced cell death was long presumed to be classically apoptotic (Hall et al. 1998). E1A induces potent apoptosis in many cell systems (Rao et al. 1992), while E4-ORF4 can induce caspase-dependent cell death (Robert et al. 2002). Adenoviruses also express several proteins that inhibit cell death early after infection; for example, E1B-19KDa is the viral homologue of Bcl2

(Chiou et al. 1994) and E1B-55KDa, in concert with E4-ORF6, targets p53 for proteasomal destruction (Steegenga et al. 1998) (figure 3).

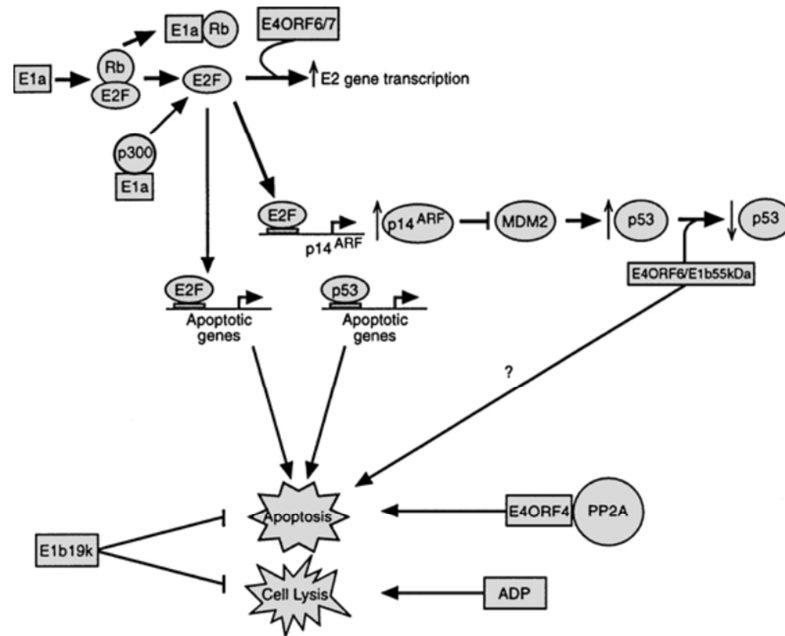


Figure 3. Adenovirus induced cell death pathway.

E1A proteins bind to the cell cycle checkpoint protein pRb105 (pRb)—the retinoblastoma susceptibility gene product—releasing bound transcription factors, such as E2F1 and other E2F family members. E2F1 transactivates p14ARF, the alternative splice product encoded by the p16INK4A locus. P14ARF then binds MDM2 thereby neutralizing its activity. MDM2 normally binds p53 and targets it for proteolysis via the ubiquitin pathway. Disruption of MDM2 function by p14ARF allows p53 levels to rise, which is a prerequisite for induction of cell death by p53, but, although necessary, it is not always sufficient. The increase in p53 level is usually accompanied by posttranslational modification, most often phosphorylation, in order to ‘activate p53’ to become functional (Braithwaite and Russell 2001).

Two groups have made more systematic attempts to monitor the cell death mechanism induced by selectively replicating viral mutants in human cancer cells. One used $\Delta 24$ and $\Delta 24\text{RGD}$ in H460 non-small cell lung carcinoma cells (Abou El Hassan et al. 2004). Both these vectors contain the same 24-bp E1A CR2 deletion as *dl922-947*, but $\Delta 24$ is entirely E3 deleted (Fueyo et al. 2000), whereas $\Delta 24\text{RGD}$ has an intact E3 region and an RGD motif in the fibre knob to redirect binding to α_v integrins (Fueyo et al. 2003). The second group used a mutant with a wild-type E1A region under the control of the human telomerase reverse transcriptase (hTERT) promoter in telomerase-positive cancer cells (Ito et al. 2006). Their conclusions were dramatically different; Abou El Hassan used the term ‘necrosis-like programmed cell death’ to describe the actions of $\Delta 24$ viruses, whereas Ito concluded that autophagy contributed significantly to the death of glioma cells. Baird et al. (2008) clearly shown that classical

apoptosis is not the mechanism by which replicating adenoviruses cause cell death. Some apoptotic morphological features are found, but there are dramatically fewer than with cisplatin treatment.

Replicating adenovirus-induced cell death may therefore be described as a strongly virus-controlled version of non-classical cell death, one that has not been fully characterized before.

1.11 Oncolytic viruses in cancer therapies

Oncolytic viruses are currently under investigation in phase I-III clinical trials (Table 1).

| VIRUS | MECHANISM OF TUMOR TARGETING | PHASE OF DEVELOPMENT | RESULTS |
|------------------------|--|--|--|
| Adenovirus | Targets to tumor antigens; conditionally replicating | Phase III conducted | Greater response in patients who received a combination of virus therapy and chemotherapy than in patients who received chemotherapy alone |
| Reovirus | Selectively infects RAS-transformed cells | Phase I conducted | Currently in trials to compare intratumoral administration with cutaneous administration in patients with melanoma; also in trials for patients with malignant glioma and intravenous administration |
| Herpes simplex virus 1 | Only replicates in tumor cells | Phase I conducted, additional trials planned | G207 and HSV1716 vectors were found to be well-tolerated when given by intratumoral injection in patients with glioma |
| NDV | Selectively replicates in interferon defective cells | Phase I conducted | PV701 vector was found to be well tolerated when given intravenously; some patients had anti-tumor response |
| Vaccinia virus | Gains access to tumor by vascular leakiness | Phase I conducted, Phase II planned | JX-594 vector was found to be well tolerated in phase I clinical trial when given by intratumoral injection into melanomas; trials are being planned to test intravenous delivery |

Table 1. Clinical development of oncolytic viral vectors

The table summarized the different oncolytic viruses that have been tested in preclinical and clinical trials, and their developmental status (Parato et al. 2005).

Most studies have focused on the direct antitumor properties of these viruses, although there is now an increasing body of evidence that the host immune response may be critical to the efficacy of oncolytic virotherapy. Oncolytic viruses represent prime candidate to enhance the immunogenicity of the tumor microenvironment. However, the role of the immune system is controversial. Oncolytic viruses can be administered locally, by direct intratumoral inoculation, or systemically, by intravascular administration. The immune system could antagonize the effectiveness of oncolytic viruses administered

intravascularly by limiting viral delivery to the tumor while, on the other hand, once the virus has reached its target and begins replicating within and destroying tumor cells, the immune response can theoretically augment tumor reduction by redirecting the cytotoxic T lymphocytes response from viral antigens to tumor antigens, also against distal metastasis. In fact, viruses administered by direct intratumoral inoculation elicit a systemic immune response that prevents tumor formation and causes regression of existing tumors at distant sites (Todo et al. 1999).

A number of clinical trials have already been conducted that are based on oncolytic viruses, including those that are naturally selective for tumor cells, such as reovirus and Newcastle disease virus, and those that have been made selective by genetic manipulation, such as adenovirus and herpes simplex virus (Parato et al. 2005).

Although the number of different types of oncolytic viruses that have been tested in preclinical trials is increasing, only a few have made the transition into the clinic. Only 8 years ago, the first patients were treated in the first bona fide clinical trials of oncolytic virus therapy with *dl1520*. When *dl1520* was given to patients intravenously or intra-arterially, it was well tolerated and was associated with tumor shrinkage and/or disease stabilization in some patients (Reid et al. 2002; Reid et al. 2001). So, oncolytic viruses seem to have limited side effects that are less debilitating than those that are associated with many standard cancer therapies, and are beginning to show some signs of efficacy.

A modification of *dl1520*, H101, is the only oncolytic virus to be tested in a phase III study to date (Xia et al. 2004), and is now the only approved world's first oncolytic virus therapy for cancer treatment. In this trial H101 was given by intratumoral injection to patients who received cisplatin-based chemotherapy. The response rate was significantly higher (78%) in patients who received the combination of viral therapy and chemotherapy than in patients who were treated with chemotherapy alone (39%) (Xia et al. 2004; Wakimoto et al. 2004).

1.12 Oncolytic adenoviruses in combination cancer therapies

Preclinical and clinical studies have clearly shown the antineoplastic potential of oncolytic viruses, at least for local treatment. In all cases safety was demonstrated, with the most common associated toxicity being flulike symptoms. Some of the most encouraging data were obtained from a phase II study using intratumoral administration of *dl1520* in patients with advanced head and neck squamous cell carcinoma (Nemunaitis et al. 2000). In this trials adenovirus administered alone as a mono-therapy has demonstrated limitations in efficacy. The best chance for complete tumor eradication lies in a multimodal cancer therapy approach utilizing oncolytic virus in combination with chemotherapy, radiotherapy, or drugs that could improve oncolytic viruses' activity. The rationale for combination therapy was that a greater

antitumor effect was expected with combination treatment compared with single therapies. The therapies have different toxicity profiles and may result in enhanced efficacy without increased adverse events; moreover, no overlapping resistance between oncolytic viruses and chemotherapy and/or radiotherapy was anticipated; and it may be possible to lower treatment doses.

dl1520 has been used in conjunction with chemotherapeutic agents in clinical trials with evidence for potential synergistic antitumor activity. The use of *dl1520* in conjunction with cisplatin (causes intrastrand DNA cross-links that block DNA replication), and 5-fluorouracil (pyrimidine antagonist that inhibits DNA synthesis) has been examined in a phase II clinical trial involving head and neck carcinoma patients. *dl1520* has been used in combination with leucovorin and 5-fluorouracil in a phase II trial in patients with gastrointestinal carcinoma metastatic to the liver and with gemcitabine in a phase I/II trial in patients with unresectable pancreatic carcinoma (Kruyt and Curiel 2002; Post et al. 2003). All these studies have shown that combined treatments increase the therapeutic effects of the virus.

The lack of knowledge about the mechanisms relevant for the oncolytic activity impedes the choice for the best drug to use in the combined treatment. The association of viruses with specific drugs, not only able to directly kill tumor cells but also to increase viral oncolytic activity, would increase the efficacy of the treatment of human neoplasia. It is well known that one of the major obstacle to the successful application of therapeutic strategies based on replicating oncolytic viruses is represented by the poor distribution of viral particles throughout the tumor mass, probably due to physical barriers or to tumor vessels, which are structurally and functionally abnormal and highly disorganized. We have demonstrated that the pre-treatment with Bevacizumab, a recombinant humanized monoclonal antibody to the VEGF, probably decreasing the interstitial pressure or normalizing tumor vessels, improves the delivery and the distribution of the virus into tumor mass and enhances the effects on the inhibition of tumor growth (Libertini et al. 2008).

It has been also hypothesized that the cell cycle may influence the outcome of Ad infection, and it has also been reported that the block in G₂/M phase improves viral entry and replication (Seidman et al. 2001). So interfering with the G₂/M phase, with drugs that block cells in this phase of the cell cycle, could be a potential therapeutic tool to potentiate the effects of oncolytic virus. We have demonstrated that AZD1152, a specific Aurora B kinase inhibitor, is active against ATC cells, inducing G₂/M accumulation, polyploidy and subsequent cell death by mitotic catastrophe. We have also demonstrated that the drug is able to enhance the anti-neoplastic effects of *dl922-947* oncolytic virus in both *in vitro* and *in vivo* models of ATC (Libertini et al. 2011).

The appeal of combining OV's with radiation therapy continues to grow as the relationship between these two therapies is better understood. Through either radiation-mediated enhancement of viral oncolysis or virus-mediated sensitization of cells to radiation therapy, combination of these two treatments has resulted in synergistic antitumor effects in numerous preclinical models.

Combined oncolytic adenovirus therapy and external beam radiotherapy (XRT) has shown significantly improved results over individual therapies in preclinical models (Nandi et al. 2008; Idema et al. 2007; Lamfers et al. 2002; Georger et al. 2003; Bieler et al. 2008; Chen et al. 2001; Dilley et al. 2005). Treatment with Onyx-015, Ad Δ 24, Ad Δ 24-p53 (Idema et al. 2007) or Ad Δ 24RGD (Lamfers et al. 2002) in combination with radiation in a subcutaneous glioma model resulted in 50-100% long-term survival (Ottolino-Perry et al. 2010). Many studies looking at combination of adenovirus and XRT therapy have hypothesized that the radiation-mediated increase in oncolysis is due in part to an increase in viral replication rates. Unfortunately, little information about the underlying molecular mechanism has been uncovered. Increased viral titers correlated with a synergistic cytotoxic effect *in vitro*. *In vivo* combination therapy significantly inhibited tumor growth relative to individual therapies (Chen et al. 2001; Dilley et al. 2005).

1.13 OVs and IR: understanding the molecular mechanism. Role of the DNA damage pathway

Ionising radiation is used as a primary treatment for many types of cancer. Consequently, there is an emphasis in preclinical and clinical studies toward using adenoviruses as part of a combination treatment strategy with radiotherapy (Hingorani et al. 2007). It has been hypothesized that the block in G₂/M phase could enhance viral replication and subsequently the oncolytic effects of the virus.

It is well known that after exposure to ionising radiations, two distinct G₂/M checkpoints are activated:

- the early G₂ checkpoint that prevents the progression of cells irradiated in G₂ into mitosis;
- the G₂/M accumulation that blocks in G₂ cells in earlier phases of the cell cycle at the time of irradiation (Metting and Little 1995)

The combination of viruses and external beam radiation therapy (EBRT) has shown additive or synergistic therapeutic effects in preclinical studies *in vitro* and in subcutaneous prostate, head and neck, lung, colon, thyroid and cholangio-carcinomas, as well as melanoma and malignant glioma (Freytag et al. 2008; Swisher et al. 2003; Immonen et al. 2004; Mundt et al. 2004; Teh et al. 2004; Freytag et al 2007; Harrington et al 2010; Portella et al. 2003). Phase I and II clinical trials investigating the combination of EBRT and viruses have been completed and published. These studies have demonstrated excellent safety and some preliminary evidence of efficacy for adenovirus, HSV and reovirus.

The main results from these studies are summarized in Table 2.

| Author/clinical phase | Patients | Treatment | Comments |
|--------------------------------------|--|--|--|
| Freytag et al. 2003 Phase I | 15 patients with newly diagnosed non metastatic prostate adenocarcinoma | Intraprostatic injection of an oncolytic adenovirus encoding the cytosine deaminase/HSV-TK gene Combination with prodrugs 5-fluorocytosine and valganciclovir, and 70-74 Gy conformal radiation therapy | No dose limiting toxicity Intratumoral transgene expression demonstrated up to 3 weeks after viral injection Mean PSA half-life in patients having received more than 1 week of prodrug therapy shorter than patients having received only 1 week of prodrug therapy (0.6 vs 2 months) |
| Swisher et al. 2003 Phase II | 19 patients with non metastatic non-small cell lung cancer who were not eligible for surgery or chemoradiation | 3 intratumoral injections of a replication defective adenovirus encoding wild type p53 gene Combination with 60 Gy radiation therapy | Antitumoral efficacy after 3 months assessed with clinical findings, CT scan (16 patients) and biopsies (15 patients) |
| Immonem et al. 2004 Phase II/III | 36 patients with operable malignant glioma | Patients were randomized to receive standard treatment alone (surgical excision followed by radiation therapy) (19 patients) or in combination with local injection of adenovirus encoding the HSV-Tk gene in the tumor cavity after resection, followed by intravenous ganciclovir injections for 14 days (17 patients) | Well tolerated treatment Significantly increased mean survival time in experimental arm (39.0 ± 19.7 vs 70.6 ± 52.9 weeks), median survival (62.4 vs 37.7 weeks) |
| Mundt et al. 2004 Phase I | 14 patients with soft tissue sarcoma | 3 escalating doses of TNF-erade, an adenovirus encoding the TNF- α gene under the control of a radio-inducible promoter Combination with 36-50.4 Gy radiation | No dose limiting toxicity Response assessment in 13 patients Of the 11 patients subsequently treated by surgery, 10 patients had a pathological response |
| Senzer et al. 2004 Phase I | 36 patients with solid tumors | Intratumoral injection of TNF-erade Combination with 30-70 Gy radiation | No dose limiting toxicity five patients had synchronous lesions, allowing the comparison between irradiated only lesion and lesions treated by radiation and virus. Four patients had a greater response in the injected lesion |
| Teh et al. 2004 Phase I/II | 59 patients with low to high risk prostate cancer | Intratumoral injection of adenovirus encoding HSV-TK, followed by valacyclovir injections Combination with 76 Gy radiation therapy Combination with hormonal therapy for high risk patients | All patients without pelvic nodes disease had negative biopsy results after 2 years and biochemical control (PSA) at last follow-up. Three out of 4 patients with lymph node disease relapsed |
| Freytag et al. 2007 Phase I | 9 patients with non metastatic prostate adenocarcinoma | Intraprostatic injection of an oncolytic adenovirus encoding the cytosine deaminase/HSV-TK gene combination with prodrugs 5-fluorocytosine and valganciclovir, and 74 Gy intensity-modulated radiotherapy | No dose limiting toxicity 8 patients had post treatment prostate biopsies; 7 were negative at last follow-up (6 or 12 months after treatment) |
| Harrington et al. 2010 Phase I/II | 17 patients with stage III, IVa or IVb squamous cell cancers of the head and neck | Intratumoral injections of herpes simplex virus encoding the GMCSF gene Combination with 70 Gy radiation and cisplatin | No dose limiting toxicity Specific disease survival 82.4% at a median follow-up of 29 months (range, 19-40 months) |
| Harrington et al. 2010 Phase I | 23 patients with advanced solid tumors | Intratumoral injection of reoviru Combination with 20 Gy or 36 Gy radiation | No dose limiting toxicity 14 patients evaluable for response |

Table 2. Main results from phase I and II clinical trials investigating the combination of EBRT and viruses

Although there is a clear evidence that combinations of oncolytic viruses and radiation can enhance viral replication and possibly anti-tumor efficacy when compared with single modality therapy, relatively little is known about the mechanisms involved in enhancing tumor cell death.

Ionising radiation produces a wide variety of lesions in DNA, including base damage, single- and double-strand breaks (DSB) and DNA-DNA or DNA-protein crosslinks (Prise et al. 2005). These lesions can be topographically grouped and clustered within the same region of DNA to comprise so-called “complex damage” (Goodhead 1994).

The DNA damage checkpoint can be defined as a network of interacting pathways operating in concert to recognize damage in the DNA and elicit the response (Elledge 1996; Zhou and Elledge 2000; Nyberg et al. 2002). It shares characteristic of a signal transduction pathway, and the participating proteins can be formally divided into sensors, transducers and effectors. Sensor proteins

recognize DNA damages, directly or indirectly, and function to signal the presence of these abnormalities and initiate the biochemical cascade. Transducers are typically protein kinases that relay and amplify the damage signal from sensors by phosphorylating other kinases or downstream target proteins. Effector proteins include the ultimate downstream targets of the transducer protein kinases. Modification of effector proteins by upstream kinases, directly or indirectly, mediates the inhibition in cell cycle progression. The effector stage is where the DNA damage checkpoint interphases with the cell cycle machinery (Iliakis et al. 2003).

DNA damage detection occurs as an early event after the DNA lesion has occurred. The Mre11-Rad50-Nbs1 (MRN) heterotrimeric protein complex acts as a DSB sensor and localizes to DNA breaks very rapidly, binding DNA free ends (de Jager et al. 2001; Lisby et al. 2004). Relaxation of the chromatin, increasing the accessibility of the DSB to the repair machinery, is also an early event (Downs et al. 2007; Halicka et al. 2009; Kim et al. 2009). Mre11 has both single-stranded endonuclease and 3'-5' exonuclease activity and can process the ends of the DNA lesion to yield regions of microhomology that are between 1 and 5 nucleotides (nt) in length (Paull and Gellert 2000). Rad50 is proposed to be involved in holding the two ends of DNA together by dimerization through the coiled-coil domains (Moreno-Herrero et al. 2005). Rad50 has ATPase activity that is important for regulating DNA binding and Mre11 nuclease activity (Bhaskara et al. 2007; de Jager et al. 2002; Hopfner et al. 2000). Nbs1 is important in directing the localization of the MRN complex. In cells that lack Nbs1, which contains a nuclear localization signal, Mre11 and Rad50 remain cytoplasmic (Desai-Mehta et al. 2001). Also, the forkhead-associated and BRCA1 C-terminal domains of Nbs1 are involved in binding to γ H2AX and retaining the MRN complex at the site of the lesion (Kobayashi et al. 2004). DNA-PK and DNA ligase IV/XRCC4 are involved in ligating the DNA ends together to repair the DSB (Baker et al. 2007). When a DSB occurs in the cellular genome due to a multitude of causes, ranging from ionising radiation (Maser et al. 1997) to viral infection, the MRN complex recognizes the lesion and recruits the protein kinases ataxia-telangiectasia mutated (ATM) and ATM-Rad3 related (ATR) to the site of the break to initiate the process of non-homologous end joining (NHEJ) (Uziel et al. 2003). ATM and ATR are central players in activation of the cellular DNA damage response. Through intermolecular auto-phosphorylation, ATM is phosphorylated on S1981, resulting in the dissociation of dimers into monomers and enzymatic activation (Bakkenist and Kastan 2003). ATM activation leads to the direct or indirect phosphorylation of more than 30 substrates including p53, NBS-1, Structural Maintenance of Chromosomes 1 (SMC-1), E2F1, Checkpoint kinase 1 (Chk1), Chk2, Breast Cancer Susceptibility Gene 1 (BRCA1), DNA-dependent protein kinase (DNA-PK) and H2AX (Darzynkiewicz et al. 2009; Lavin et al. 2006). Large foci form at the site of the DNA break due to the accumulation of γ H2AX, the phosphorylated form of the histone variant H2AX. γ H2AX recruits, among other proteins, Mdc1 (mediator of DNA damage checkpoint 1),

which serves as a bridge to sustain protein-protein interactions at the DNA lesion (Stucki and Jackson 2006). SMC-1 is a member of the cohesion complex that holds sister chromatids together during the homologous recombination process (Watrin and Peters 2006). SMC-1 is recruited to the site of DSB and promotes DNA repair in G₂ phase (Bauerschmidt et al. 2010). E2F1 induces ATM- and NBS-1 dependent Chk2 phosphorylation and promotes apoptosis by cooperating with p53 (Powers et al. 2004; Zhang et al. 2010). Following DNA damage, Chk1 is mainly responsible for the G₂/M cell cycle checkpoint but also mediates cell cycle arrest in S phase. Active Chk1 phosphorylates Cdc25C, inhibiting Cdc25C-mediated activation of cyclin-dependent kinase 2 (Cdk2), a mitosis promoter (Xiao et al. 2003). Activation of Chk2 leads to phosphorylation and degradation of Cdc25A which, in turn, leads to silencing of Cdk2 activity (Falck et al. 2001). Chk2 also phosphorylates and inhibits Cdc25C, providing a further brake on cell cycle progression (Matsuoka et al. 1998). In response to DNA damage, Chk2 phosphorylates many other substrates including p53 and BRCA1 (Darzynkiewicz et al. 2009). Phosphorylated BRCA1 plays a role in promoting both HR and in restricting error-prone NHEJ repair (Zhang and Pwell 2005). DNA-dependent protein kinase plays a major role in NHEJ repair (Lieber 2008). This MRN-ATM pathway is illustrated in figure 4.

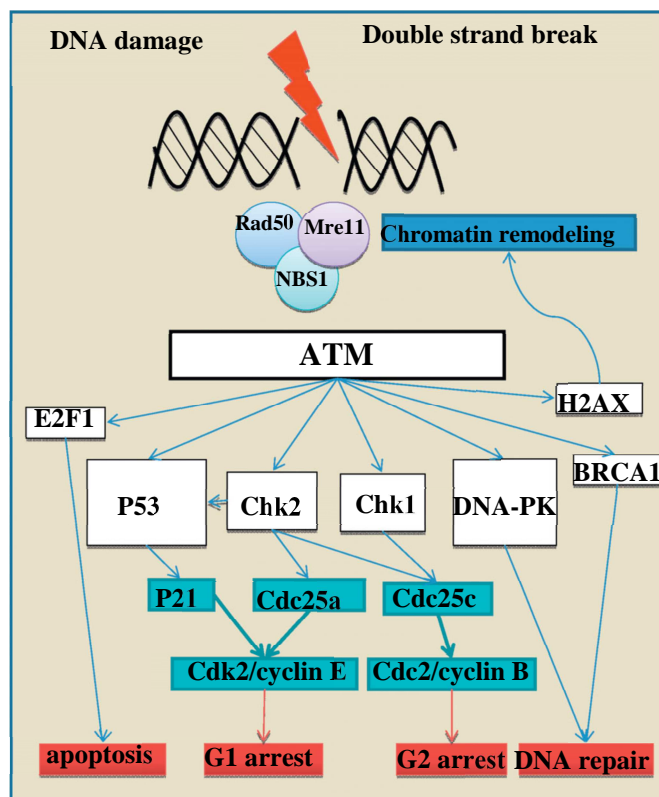


Figure 4. Mre11-Rad50-NBS1 and ATM pathway, in response to a DNA double strand break. The Mre11-Rad50-NBS1 complex localizes to DNA breaks and recruits ataxia telangiectasia mutated (ATM) protein kinase. The relaxation of the chromatin is an early event, initially independently of H2AX and ATM. ATM activation leads to the direct or indirect phosphorylation of more than 30 substrates including p53, E2F1, Checkpoint kinase 1 (Chk1), Chk2, BRCA1, DNA-dependent protein kinase (DNA-PK) and H2AX, controlling apoptotic pathways, cell cycle arrest, and DNA repair pathways.

DSBs play an important role in cell death induced by radiation. Two major mechanisms of repair of DSBs have been described: the non homologous end-joining (NHEJ) mechanisms and homologous recombination (HR) (Jackson 2002). After detection of DNA damage, repair pathways are activated which arrest cell cycle progression at an appropriate cell cycle checkpoint. In normal cells, with an intact p53 signaling, this will occur at the G₁/S checkpoint for cells in G₀ or G₁ of the cell cycle or at the G₂/M checkpoint for cells already in S or G₂ phase at the time of DNA damage. The cell cycle arrest allow cells to assess the extent of DNA damage and to attempt its repair. In case the DNA damage is irreparable, the cell triggers its own death through apoptosis. In cancer cells, a number of the cell cycle checkpoints are deranged and these mechanisms may not operate effectively, allowing neoplastic cells survival.

A number of viral proteins, such as E4-ORF3 and E4-ORF6 products, interact with cellular proteins involved in the DNA damage response (Chaurushiya and Weitzman 2009; Zhou et al. 2009).

Moreover, these viral proteins have found to be key components also in supporting viral DNA replication. In mutant viruses lacking E4-ORF3 and E4-ORF6, early viral transcription and gene expression are normal; however, a significant delay and reduction in viral DNA replication (Halbert et al. 1985; Weinberg and Retner 1986) has been observed. An important function of these Ad E4 proteins is the inhibition of the Mre11-Rad50-Nbs1 (MRN) complex (Lilley et al. 2007; Weitzman and Ornelles 2005).

The role of the MRN complex in NHEJ is relevant to an Ad infection due to the fact that MRN could perceive the linear, double-stranded Ad DNA genomes as DSBs. Following infection with a mutant virus that lacks both E4-ORF3 and E4-ORF6, the cell senses the DNA damage through the sensor complex, ATM is phosphorylated, checkpoint signaling occurs, and the genomes are eventually ligated together to form large concatemers (Lilley et al. 2007; Weitzman and Ornelles 2005). These concatemers are too large to be packaged into virus particles. The origins of replication are located at the termini of the viral genome, therefore mutant viruses would be inefficiently replicated due to the lack of a free terminus in internal genomes. Moreover the junctions of the concatemers also have deletions (Weiden and Ginsberg 1994), suggesting that the ends of the Ad genome are degraded.

Adenoviruses have evolved several mechanisms to counteract the detrimental effects of NHEJ, two of which specifically target the MRN complex. The E4-ORF3 protein can redistribute Mre11, Rad50, and Nbs1 from their normal

diffuse nuclear localization into large nuclear and cytoplasmic accumulations during infections or E4-ORF3 transfection (Evans and Hearing 2005; Stracker et al. 2002; Stracker et al. 2005). This effectively sequesters the MRN complex away from the viral genomes, which are located at the replication centers and do not colocalize with redistributed MRN proteins (Evans and Hearing 2005; Stracker et al. 2005) (figure 5).

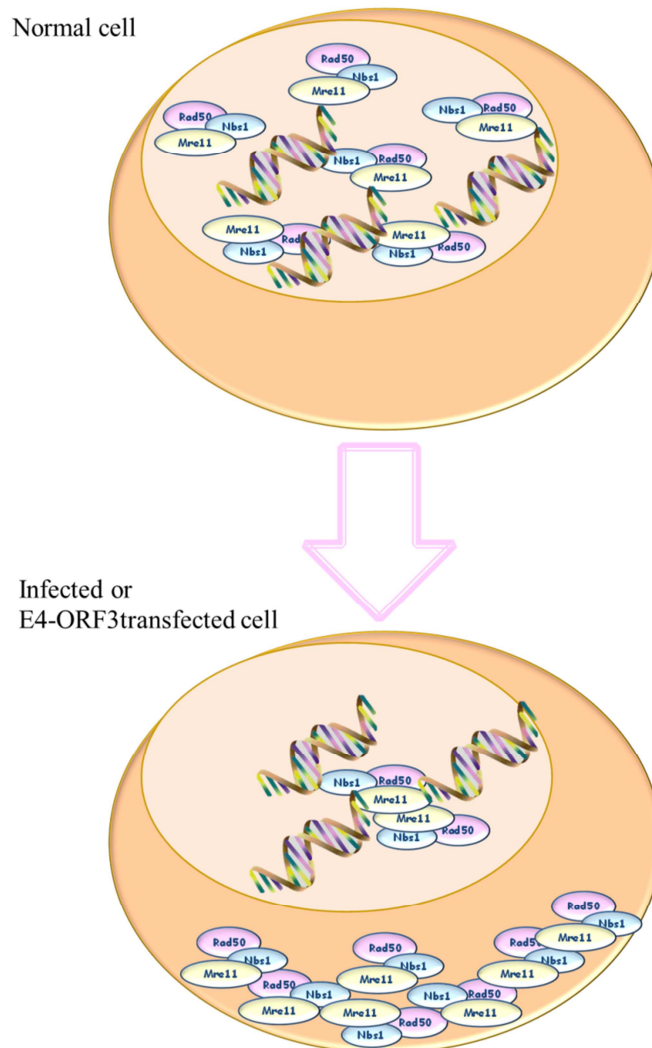


Figure 5. Role of viral E4-ORF3 protein

The E4orf3 protein can redistribute Mre11, Rad50, and Nbs1 from their normal diffuse nuclear localization into large nuclear and cytoplasmic accumulations during infections and transfection.

The E4-ORF6 protein interacts with another viral protein, E1B-55KDa, to form an E3 ubiquitin ligase complex with the cellular proteins Rbx1, Cullin 5 (CUL5), and elongins B and C (Harada et al. 2002; Querido et al. 2001). This complex targets specific proteins, such as p53, Mre11, and DNA ligase IV, for proteasome-dependent degradation (figure 6) (Baker et al. 2007; Harada et al. 2002; Querido et al. 2001). E1B-55KDa and E4-ORF3 also are involved in relocating Mre11 to cytoplasmic aggresomes (Araujo et al. 2005; Liu et al. 2005).

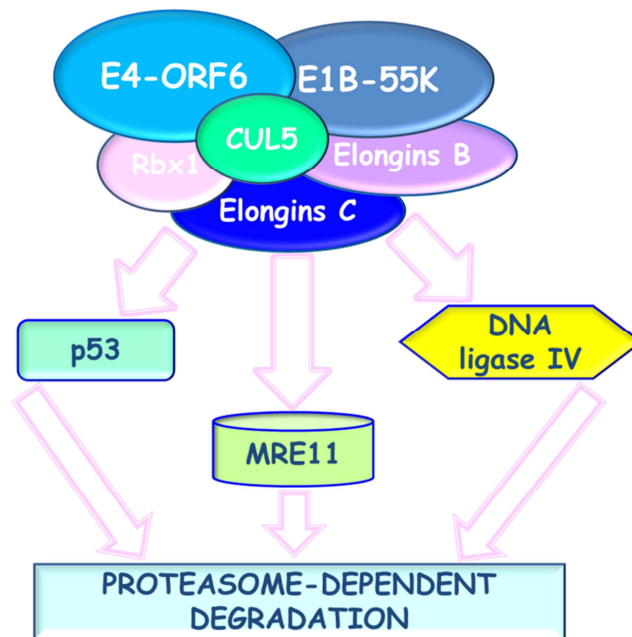


Figure 6. Role of viral E4-ORF6 protein

E4-ORF6 protein interacts with another viral protein, E1B-55K, to form an E3 ubiquitin ligase complex with the cellular proteins Rbx1, Cullin 5 (CUL5), and elongins B and C. This complex targets specific proteins, such as p53, Mre11, and DNA ligase IV, for proteasome-dependent degradation

With either a virus that lacks E4-ORF6 or E4-ORF3 alone, checkpoint signaling and concatemer formation are inhibited, but the deletion of both of these Ad gene products results in checkpoint signaling induction, concatemer formation, and a significant decrease of viral DNA replication (Lilley et al. 2007; Weitzman and Ornelles 2005).

It is not clear if the infection with adenoviruses is sufficient to trigger the DSB response or if viral DNA replication is required. This second hypothesis is more likely to occur since it has been observed that E4-ORF3 protein causes the redistribution of the MRN complex by 6h postinfection (hpi), before viral DNA replication begins (Evans and Hearing 2005). In the absence of the E4-ORF3 protein, when MRN activity is solely inhibited by E4-ORF6/E1B-

55KDa-induced degradation, MRN protein levels are not reduced until later after infection (Liu et al. 2005; Stracker et al. 2002).

2. AIM OF THE STUDY

Replication selective oncolytic viruses (OVs) are a rapidly expanding therapeutic platform for the treatment of aggressive human malignancies, such as anaplastic thyroid carcinoma (ATC). OVs are characterized by genetic alterations that ablate critical viral protein functions essential for viral replication in normal cells, but non essential in tumor cells, thus targeting viral replication to tumor cells. OVs show several advantages for the therapy of cancer: viral replication leads to host cell destruction, and to an amplification of the viral load in a single replicative cycle (Chiocca 2002). Furthermore, OVs lack cross-resistance with current clinical therapies and represent a promising anti-cancer approach (Kumar et al. 2008).

Preclinical and clinical studies have clearly shown the antineoplastic potential of oncolytic viruses, at least for local treatment, but have also highlighted the need to find associations that could improve their activity. The association of viruses with specific drugs, not only able to directly kill tumor cells but also to increase viral oncolytic activity, would represent a powerful therapeutic tool for the treatment of human neoplasia.

ATC is one of the most aggressive human malignancies, responsible for up to 40% of mortality from thyroid cancer. Although multimodality treatments are successfully applied for well-differentiated thyroid carcinomas, ATC survival rates have not been improved for decades: after diagnosis, patients have a median survival time of 4-6 months (Smallridge et al. 2009). Development and evaluation of novel therapeutic strategies are, therefore, desperately required.

In fact, the actual palliative treatment of ATC consists of irradiation plus chemotherapeutic drugs, known DNA damaging agents. In order to identify novel therapeutic approach for the treatment of ATC, during my PhD project I have studied the effects of ionising radiations in combination with *dl922-947* *in vitro* and *in vivo*, in particular focusing my attention on which type of cell death is activated by the combined treatment. Therefore, to identify novel drugs able to enhance the effects of OVs, I have also studied the effects of *dl922-947* on the DNA damage pathway and the effects of the combination between *dl922-947* plus ATM inhibitor on cytotoxic activity of the virus on ATC models.

3. MATERIALS AND METHODS

3.1 Cell lines and drug

Human ATC cell lines, FRO and BHT101-5 have been authenticated as shown previously (Schweppe et al. 2008). These two ATC cell lines have a non-functional p53 gene: in BHT101-5 cells, a 251 Ile/Thr substitution has been reported, while FRO cells are p53 null (Schweppe et al. 2008). FRO cells were obtained by Dr. Juillard (University of California LA), while BHT101-5 cells were established by Dr. Palyi (National Institute of Oncology, Hungary). Both cell lines were grown in DMEM medium supplemented with 10% FBS, 100 IU of penicillin/ml and 100 IU of streptomycin/ml in humidified CO₂ incubator. ATM kinase inhibitor KU55933 (sc-202963, Santa Cruz) was dissolved in DMSO to a final concentration of 10 mM and stored at -20°C.

3.2 Preparation of adenoviruses

dl1520 (ONYX-015), a gift from Dr. A. Balmain and Dr. I. Ganly, is a chimaeric human group C adenovirus (Ad2 and Ad5) that has a deletion between nucleotides 2496 and 3323 in the E1B region that encodes the 55-KDa protein. In addition, there is a C to T transition at position 2022 in region E1B that generates a stop codon at the third codon of the protein.

dl922-947 is a second generation adenoviral mutant that has a 24-bp deletion in E1A Conserved Region 2 (CR2) therefore, is unable to induce progression from G1 into S-phase of quiescent cells.

Ad5wt is a non-mutant adenovirus used as control adenovirus.

AdGFP is a non-replicating E1-deleted adenovirus encoding green fluorescent protein.

Viral stocks were expanded and titered in human embryonic kidney cell line HEK-293, which expresses the E1 region. Stocks were stored at -80°C after the addition of glycerol to a concentration of 50% vol/vol. Virus titer was determined by plaque-forming units (pfu) on the HEK-293 cells.

3.3 Viability assay

For the evaluation of the cytotoxic effects of *dl922-947* in combination with ionising radiation, FRO and BHT101-5 cells were seeded in 96-well plates, 24h later increasing concentration of *dl922-947* were added to the incubation medium, and after additional 24h cells were irradiated with increasing doses of ionising radiation, or *viceversa*. For the evaluation of the cytotoxic effects of *dl922-947* in combination with ATM kinase inhibitor, cells were seeded in 96-well plates, and 24h later were treated with increasing concentration of viruses

in combination or not with the drug. Six days later, cells were fixed with 50% TCA and stained with 0.4% sulforhodamine B in 1% acetic acid. The bound dye was solubilized in 100 μ l of 10 mM unbuffered Tris HCl solution and the optical density was determined at 495 nm in a microplate reader (Biorad). The percent of survival rates of cells exposed to adenovirus vectors were calculated by assuming the survival rate of untreated cells to be 100%.

3.4 Quantitative PCR of adenovirus

To quantify the amount of viral genomes, cells were infected with *dl922-947* (0-0.5-1-2.5-5-7.5-10 pfu/cell) and 24h later were irradiated, or *viceversa*. After 48h of treatment, cell media was collected and viral DNA extracted using a High Pure Viral Nucleic Acid Kit (Roche) and then quantified by Real-Time PCR using assay-specific primer and probe. Real time-based assay was developed using the following primers: 5'-GCC ACC GAG ACG TAC TTC AGC CTG -3' (Upstream primer) and 5'- TTG TAC GAG TAC GCG GTA TCC T -3' (Downstream primer) for the amplification of 143 bp sequence of the viral hexon gene (from bp 99 to 242 bp). For quantification, a standard curve was constructed by assaying serial dilutions of *dl922-947* ranging from 0.1 pfu to 100 pfu. To quantify the amount of viral genomes in cells undergoing the combined treatment (virus plus ATM inhibitor), FRO and BHT101-5 cells were infected with increasing concentration of the virus (0-1-5-10 pfu/cell) in combination with increasing concentration of the drug (0-600-800-1000 nM), or were pre-treated for 24h with the drug and then infected with the virus. After 48h of treatment, cell media was collected and viral DNA extracted using a High Pure Viral Nucleic Acid Kit (Roche) and then quantified by Real-Time PCR using assay-specific primer and probe. To quantify the amount of *dl922-947* virus genome in tumor xenografts, viral DNA was extracted from 50 mg of each sample using a High Pure Viral Nucleic Acid Kit. DNA was resuspended in 200 μ L of elution buffer and 2 μ L used for the Real Time PCR-based assay. For each experiment the DNA was extracted from three different samples of each treatment group.

3.5 AdGFP infection

For the evaluation of adenoviral infectivity in human thyroid carcinoma cell lines after the combined treatment (virus plus IR), cells were detached, counted, and plated in 6 well plate at 70% cell density. After 24h, cells were infected with a green fluorescent protein (GFP)-transducing adenovirus (AdGFP), a non replicating E1-deleted adenovirus encoding GFP, diluted in

growth medium at different multiplicity of infection (MOIs) (0-25-50 pfu/cell). After additional 24h cells were irradiated with increasing doses of IR (0-2-4-8 Gy). Cells were trypsinized 48h after the combined treatment and then washed and resuspended in 300 μ L PBS and analysed for GFP emission in FITC channel. Samples were acquired with a CYAN flow cytometer (DAKO corporation, San Jose, CA, USA) and analysed using SUMMIT software.

3.6 Cell cycle analysis

Adherent FRO and BHT101-5 cells detached with trypsin-EDTA were collected, fixed with 70% ethanol, and stained with a 10% propidium iodide solution (cellular DNA flow cytometric analysis reagent set; Roche) according to the manufacturer's instructions. DNA content was analyzed with a FACScan flow cytometer.

3.7 FACS analysis: P-H2AX and cell cycle

Cells treated with IR, virus or both were harvested by trypsinization, fixed in 70% cold-ethanol over night. The fixed cells were washed with PBS and permeabilized 15 min in 10% FBS/TBS tween 0.1%. TBS tween 0.1% washed pellet was incubated 2h in 50 μ L of anti-phospho-histone H2AX antibody diluted 1:50 in 4% FBS/TBS tween 0.1%. After washing with TBS tween 0.1%, cells were incubated 1h in anti-rabbit IgG FITC conjugated antibody diluted 1:100 in 4% FBS/TBS tween 0.1%. The immunostained cells were then washed with TBS tween 0.1% and stained 20 min with 1 mg/ml propidium iodide plus 500 μ g/ml RNase A in 400 ml PBS. All incubations were performed at room temperature, the last two ones were also performed in the dark. Incubation with H2AX and without primary antibody was performed to assess the specificity of the observed signal. Samples were acquired with a CYAN flow cytometer (DAKO Corporation, San Jose, CA) and analyzed using SUMMIT software.

3.8 Western blot

Cells were homogenized directly into lysis buffer (150 mM NaCl, 1% NP-40, 0,5% sodium deoxycholate, 50 mM Tris pH 8). The lysates were clarified by centrifugation at 14,000 rpm for 20 min. Protein concentrations were estimated by an assay (Bio-Rad) and boiled in Laemmli buffer [60 mM Tris-HCl (pH

6.8), 9,2% SDS, 40% glycerol, 20% 2-mercaptoethanol, and 0.00125% bromophenol blue] for 5 min before electrophoresis. Proteins were subjected to SDS-PAGE (7,5-10-15% polyacrylamide) under reducing conditions. After electrophoresis, proteins were transferred to nitrocellulose membranes (Immobilon, Millipore Corp., Bedford, MA); complete transfer was assessed using trans-blot SD semi-dry transfer cell (BioRad). After blocking with 5% milk solution, the membranes were incubated with the primary antibodies overnight at 4°C. Membranes were then incubated with the horseradish peroxidase-conjugated secondary antibody (1:2000) for 45 min (at room temperature), and the reaction was detected with an enhanced chemiluminescence system (PIERCE, Thermo scientific) with Chemidoc XRS (BioRad).

3.9 Antibodies for western blot

Mouse monoclonal [31A1067] to active + procaspase 3 (ab13585; 1:1000, abcam), anti-actin H-300 (sc-10731; 1:500, Santa Cruz, CA, USA), anti-tubulin (650951; 1:1000, ICN Biomedicals), anti-ATR (09-070; 1:1000, Millipore), anti-NBS1 clone Y112 (04-236; 1:1000, Millipore), anti-phospho-ATM (Ser1981) (10H11.E12) (4526S; 1:1000, Cell signaling technology), anti-phospho-Chk1 (Ser345) (133D3) (2348; 1:1000, Cell signaling technology), anti-adenovirus-2/5 E1A (13 S-5) (sc-430; 1:1000, Santa Cruz, CA, USA), anti-MRE11 (49959; 1:1000, Millipore), anti-phospho-Chk2 (Thr68) (2661; 1:1000, Cell signaling technology), anti-phospho-histone H2A.X (Ser139) (20E3) (9718; 1:2000, Cell signaling technology), anti-RAD50 (07-1781; 1:1000, Millipore), anti-ATM (07-1286; 1:1000, Millipore), anti-integrin β 3 (sc:20058; 1:1000, Santa Cruz, CA, USA), anti-CAR (H-300) (sc-15405; 1:1000, Santa Cruz, CA, USA) are the antibodies used for western blot.

3.10 Tumorigenicity assays

Experiments were performed in six-week-old female athymic mice (Charles-River, Italy). All mice were maintained at the Dipartimento di Biologia e Patologia Animal Facility, in accordance with accepted standards of animal care and with the Italian regulations for the welfare of animals used in studies of experimental neoplasia. The studies were approved by Ethic Committee on animal care of the University Federico II Napoli. FRO cells (8×10^6) were injected into the right flank of 60 athymic mice. The animals were monitored for the appearance of tumors and tumor latency evaluated. After 20 days, when tumors were clearly detectable, tumors volumes were evaluated and the animals were randomised into four groups (15 animals/group) (T=0) with

similar average tumour size: untreated, treated with IR, *dl922-947*, or both. Two groups were irradiated with a single radiation dose (10Gy), on the tumor volume at a distance of 80 cm with a bolus interposition to avoid lower doses at the tumor external edge. Virus was administered three times per week by intratumoral injection to avoid first pass effect. A low viral dose (1×10^6 pfu) was used to better evaluate the effects of the combined treatment. The control group was injected with saline solution. Tumors diameters were measured with calipers and tumors volumes (V) were calculated by the formula of rotational ellipsoid: $V = A \times B^2 / 2$ (A=axial diameter, B=rotational diameter). Experiment was stopped when tumors reached 1 cm^3 in volume and/or symptomatic tumor ulceration occurred. To evaluate the genome equivalent copies of *dl922-947* in tumor xenografts, 10 mice were irradiated with a single radiation dose and 24h after the virus was inoculated intratumorally. After additional 48h animals were sacrificed, the tumor mass excised, DNA extracted and viral replication evaluated by Real Time PCR. To evaluate viral distribution in tumor mass after the combined treatment, FRO cells (8×10^6) were injected into the right flank of 10 athymic mice, and after 20 days, when tumors were clearly detectable, animals were randomized into two groups (5 animals/group). Only one group was irradiated with a single radiation dose (10 Gy). AdGFP (1×10^7 pfu) was injected intratumorally in both groups 24h after. After additional 48h, animals were sacrificed, and tumors were excised, snap frozen in liquid nitrogen, and cut with a cryostat in thick sections for microscopic investigation. Sections were mounted onto untreated slides and coverslipped in slow-fade antifade (Molecular Probes) for microscopic investigation. Ten sections were sampled across the entire tumor mass to ensure they were representative of the distribution of GFP-positive signal into the tumor mass. For each slice, 10 images at high resolution were sampled from the periphery to the core of the section. Images were acquired using a ZeissLSM510 Meta argon-krypton laser scanning confocal microscope, with fluorescence excitation lines at 488 nm and emission filter BP505-550, 20x (Plan Apochromat; numerical aperture, 1.4; Zeiss), pixel depth of 12 bit, fixed box sizes of 512x512 pixels, and pinhole below 1 Airy unit. Four images from each optical section were averaged to improve the signal-to-noise ratio. The color scheme used was green for GFP-labeled structures.

3.11 Statistical analysis

Comparisons among different treatment groups in the *in vivo* experiment were made by the ANOVA method and the Bonferroni *post hoc* test using a commercial software (GraphPad Prism 4). Assessment of differences among rate of tumor growth in mice was made for each time point of the observation period. The analysis of the cell killing effect *in vitro* was also made by ANOVA method and the Bonferroni *post hoc* test. For all the other

experiments comparisons among groups were made by ANOVA method and *t test*.

3.12 Micronuclei counting

FRO and BHT101-5 cells were grown on cover slips and treated with increasing doses of IR (0-4-8-16 Gy). After 24-48h cells were fixed 15' in 3% paraformaldehyde, permeabilized with 0.2% Triton X-100 10' and then stained 5' with Hoechst 33258 (1 µg/ml, Sigma-Aldrich). The washes were followed by mounting the cover slips onto glass slides with glycerol:PBS 1:1.

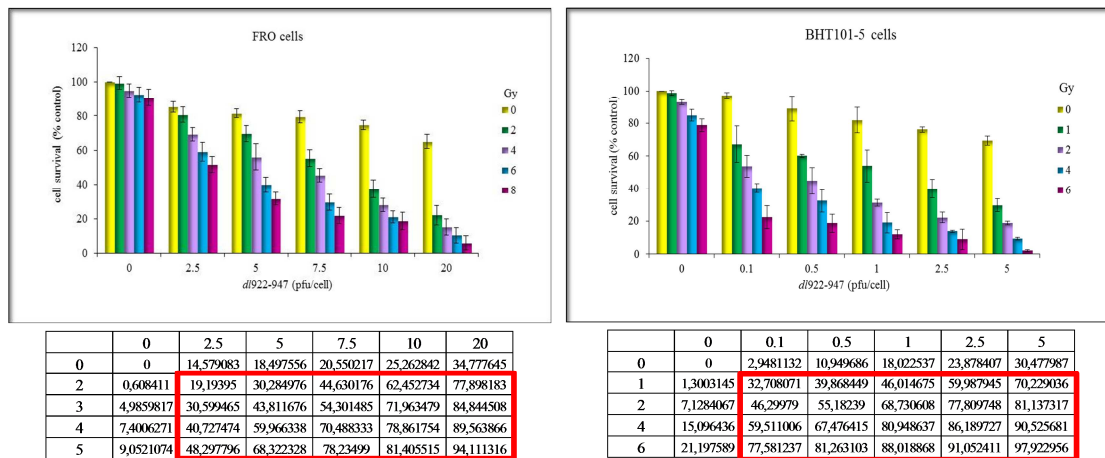
4. RESULTS

4.1 Ionising radiation enhances the effects of the oncolytic adenovirus *dl922-947*

It has been demonstrated in preclinical studies that ionising radiation enhances the efficacy of first generation oncolytic viruses (Portella et al. 2003; Stanziale et al. 2002; Rajecki et al. 2009). To evaluate whether ionising radiation (IR) could enhance oncolytic activity of a second generation oncolytic virus, *dl922-947*, FRO and BHT101-5 cells, were seeded in 96-well plates and infected with different multiplicity of infection (MOIs) of *dl922-947* (0-0.1-0.5-1-2.5-5 pfu/cell), expressed as plaque forming unit (pfu/cell) and irradiated with increasing doses of IR (0-2-3-4-5 Gy), and cell survival was evaluated after seven days. In previous studies it has not been clearly evaluated the best timing for this combined treatment. In order to identify the most appropriate timing, ATC cells (FRO and BHT101-5) have been infected with growing concentration of *dl922-947* and after 24h irradiated or *viceversa*. The results are shown in figure 7 (A-B).

Viability assays show that ionising radiation enhances the effects of *dl922-947* against ATC cells. Both combinations lead to an enhanced effect, although our data clearly show that the most effective treatment is infection followed after 24 hours by irradiation. All combination points show a significant difference with respect to the single treatments. On the contrary, in cells irradiated and then infected an effect is evident only at the higher concentration of the virus. In particular, in cells treated with 7.5 pfu/cell of the virus plus 4 Gy, we can observe a 2.6 fold increase in cells mortality with respect to the single treatments, versus the 1.3 fold increase observed in IR pre-treated cells.

A



B

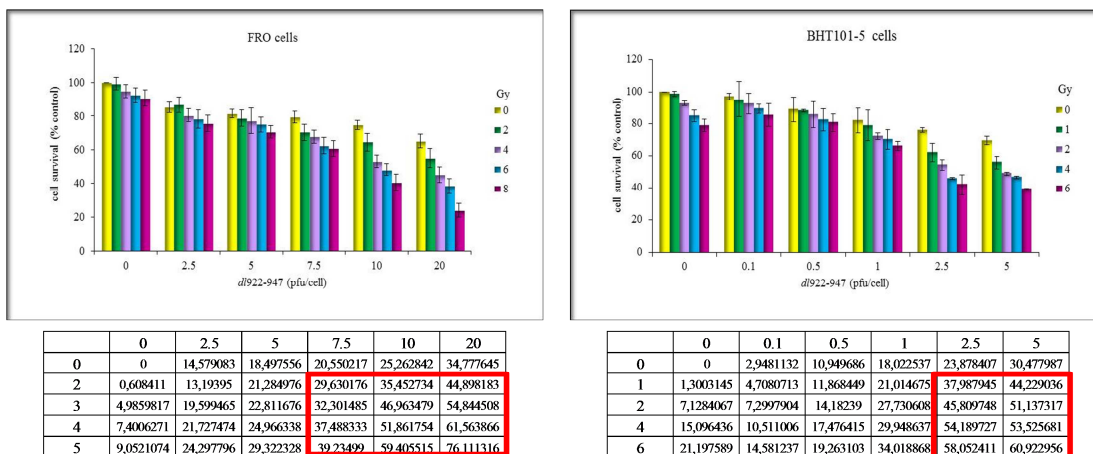


Figure 7. Effects of the combined treatment: *dl922-947/IR* on ATC cell lines.

FRO and BHT101-5 cell lines were infected with increasing concentration of *dl922-947* and 24h after irradiated with different doses of ionising radiation (A) or *viceversa* (B). After seven days cells were analyzed by viability assay. The percentage of survival rates of cells exposed to combined treatment were calculated by assuming the survival rate of untreated cells to be 100%.

To explore the possibility that ionising radiation improves viral replication in ATC cells, I have performed a Real-Time PCR based assay to evaluate the genome equivalent copies of *dl922-947* in ATC cells undergoing the combined treatment.

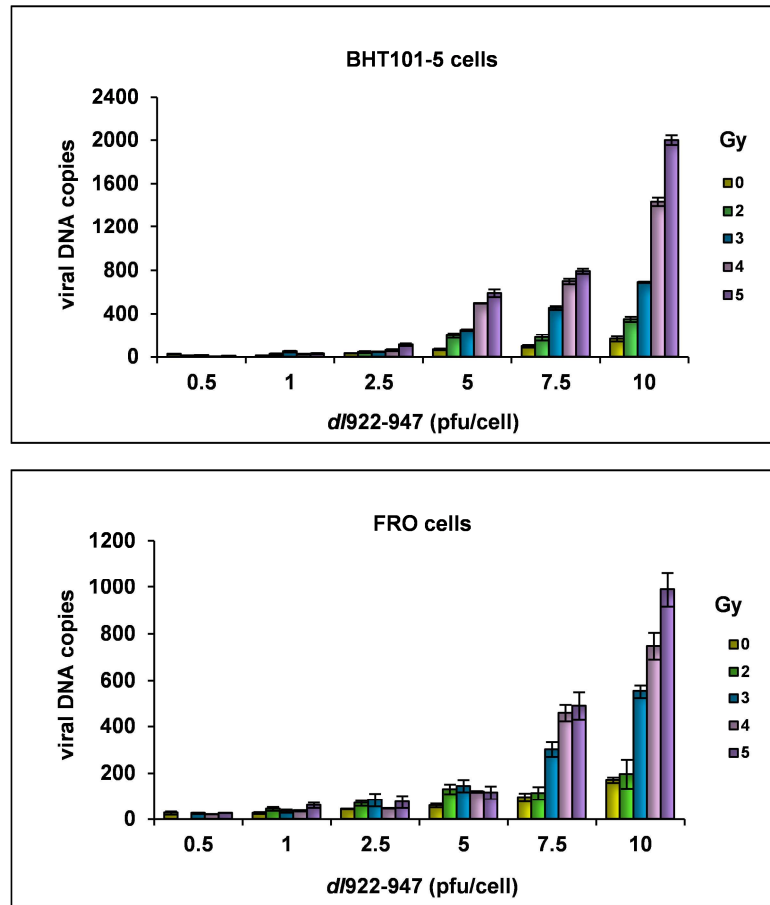
FRO and BHT101-5 cells were irradiated with increasing doses of IR (0-2-3-4-5 Gy) and 24h later infected with different concentration of *dl922-947* (0.5-1-2.5-5-7.5-10 pfu/cell). After additional 48h, viral DNA was extracted and genome equivalent copies analyzed by Real-Time PCR. As shown in figure 8A, a clear increase in viral replication was observed in both cell lines.

Next I have verified whether ionising radiations increase viral genes expression, analyzing expression levels of early E1A viral gene in irradiated or untreated cells.

FRO cells were irradiated (0-2-6 Gy) and then infected with 10 and 25 pfu/cell of *dl922-947*. E1A levels were analyzed by western blot at two different experimental times (16-24h). As shown in figure 8B, E1A levels increase in a dose dependent manner.

This results clearly show that ionising radiation induces an increase of viral replication and enhances the expression of early viral genes in a dose-dependent manner.

A.



B.

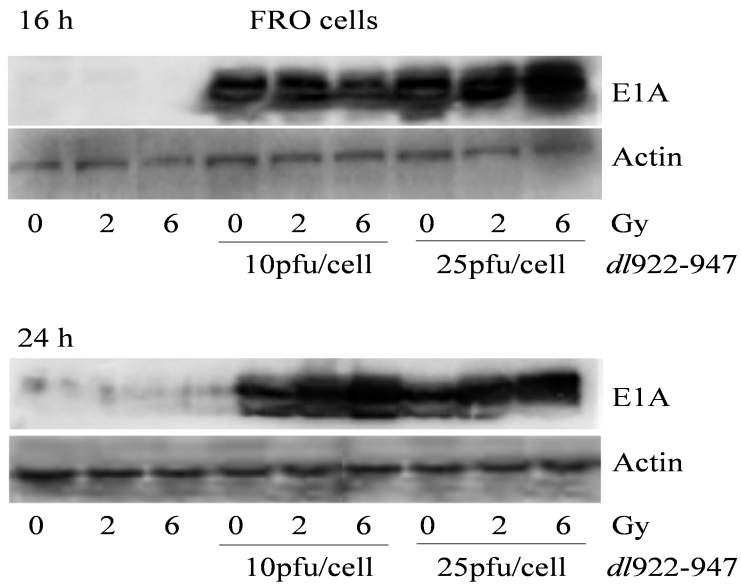


Figure 8. Effects of IR on viral life cycle and gene expression

A. FRO and BHT101-5 cells were irradiated with increasing doses of IR (0-2-3-4-5 Gy) and 24h later infected with different concentration of *dl922-947* (0.5-1-2.5-5-7.5-10

pfu/cell). After additional 48h, viral DNA was extracted and genome equivalent copies analyzed by Real-Time PCR. A clear increase in viral replication was observed in both cell lines.

- B. FRO cells were irradiated (0-2-6 Gy) and then infected with 10 and 25 pfu/cell of *dI922-947*. E1A levels were analyzed by western blot at two different experimental times (16-24h). E1A levels increase in a dose dependent manner.

4.2 Ionising radiation does not increase viral entry upon infection

It has been proposed that radiation can enhance viral oncolytic activity by increasing viral entry in target cells, probably enhancing the expression of the coxsackie and adenovirus receptor (CAR) on the membrane of infected cells or the expression of $\alpha v/\beta 3/5$ integrin subunits, acting as low affinity co-receptors. To monitor this step, FRO cells were irradiated and 24h later infected with a non-replicating reporter adenovirus transducing green fluorescent protein (AdGFP). After additional 48h, GFP emission was evaluated by cytofluorimetric analysis. The percentage of GFP cells was not modified by radiation, although a positive shift in FITC channel was observed. This increase is apparent since IR treatment enlarges the cells enhancing basal fluorescence. Indeed, the analysis of FITC ratio in irradiated and unirradiated cells infected or not with AdGFP showed no significant differences (Fig. 9A). Similar results were obtained with BHT101-5 cells (data not shown).

To confirm that IR do not increase viral entry upon infection, I have also analyzed the expression levels of CAR and $\alpha v/\beta 3$ integrin subunits. FRO cells were irradiated with different doses of IR (0-2-4-6-8 Gy) and 24h later infected with 10 pfu/cell of *dI922-947*. Twenty-four hours after infection CAR and integrin levels were analyzed by western blot. As shown in figure 9B ionising radiation do not increase CAR and integrin levels upon infection. The increase of CAR levels in cells undergoing the combined treatment with respect to the untreated cells, was due to the viral infection, as previously observed by us (unpublished observation).

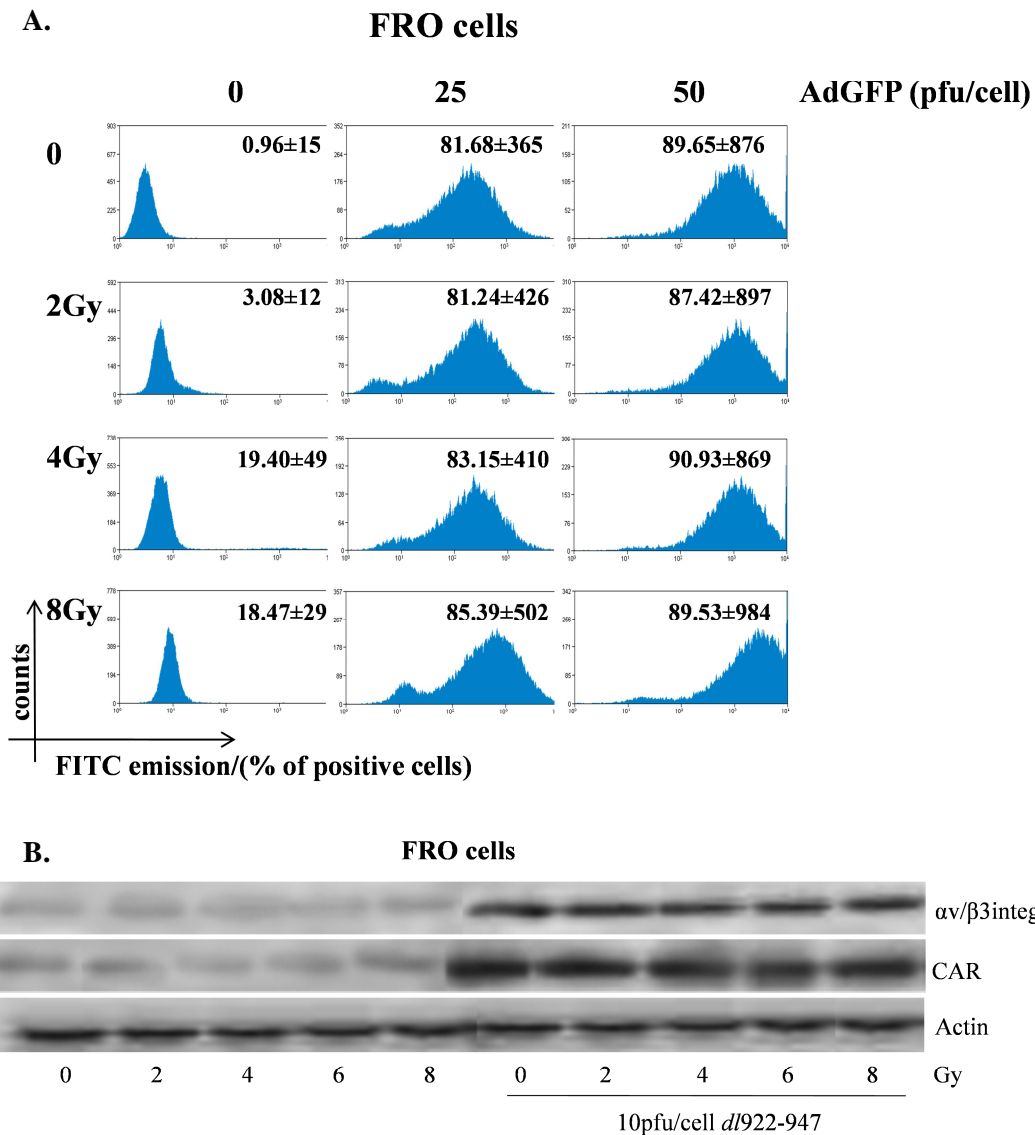


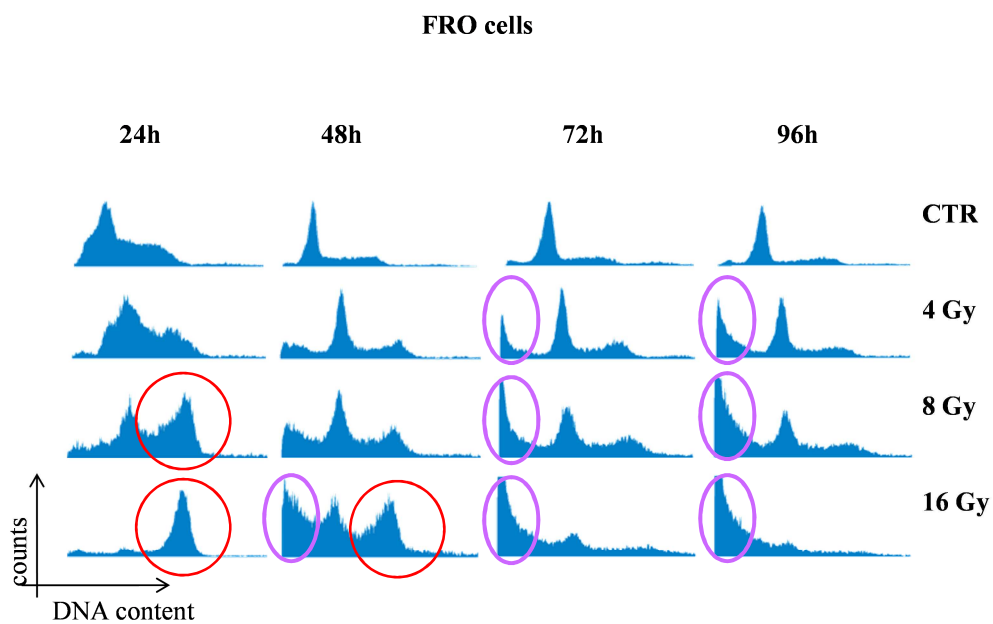
Figure 9. Effects of ionising radiation on viral entry

- A. FRO cells were irradiated and 24h after infected with a non replicating reporter adenovirus transducing green fluorescent protein (AdGFP). After additional 48h, GFP emission was evaluated by cytofluorimetric analysis. The percentage of GFP cells was not modified by radiation.
- B. FRO cells were irradiated with different doses of IR (0-2-4-6-8 Gy) and 24h later infected with 10pfu/cell of *dl922-947*. Twenty-four hours after infection CAR and integrin levels were analyzed by western blot. IR do not increase CAR and integrin levels upon infection.

4.3 IR induces G₂ accumulation and caspase-3 activation: effects of the combined treatment on ATC cell cycle and cell death

It is well known that after exposure to ionising radiations, two distinct G₂/M checkpoints are activated: the early G₂ checkpoint prevents the progression of cells irradiated in G₂ into mitosis; the G₂/M accumulation blocks in G₂ the cells that had been in earlier phases of the cell cycle at the time of irradiation (Metting and Little 1995).

To confirm IR effects on ATC cells, FRO and BHT101-5 were irradiated with different doses (0-4-8-16 Gy) for 24-48-72-96h and by propidium iodide staining, the effects of IR on cell cycle were evaluated. As shown in figure 10, a dose and time dependent increase in polyploid cells was observed. After 24h of treatment, a G₂/M accumulation was observed, and after 48h also an increase in the percentage of cells in subG₁ fraction was observed.



BHT101-5 cells

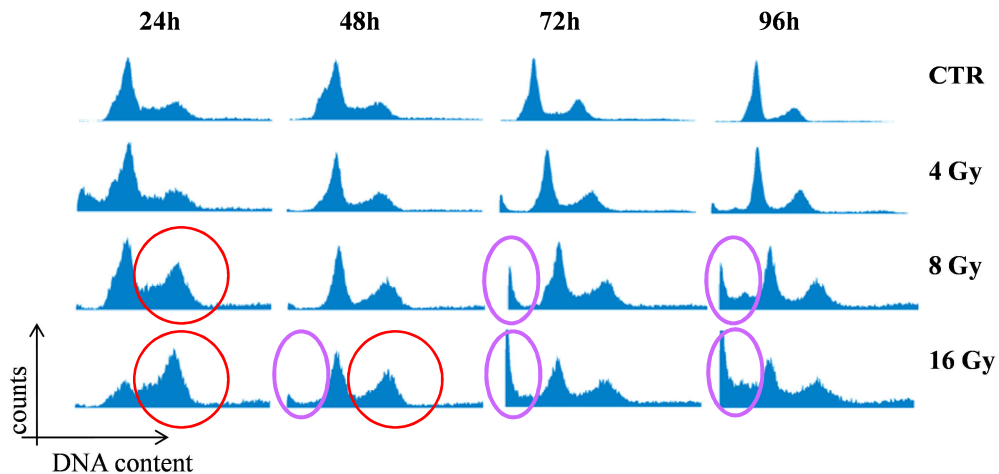


Figure 10. Effects of IR on ATC cell cycle

FRO and BHT101-5 were irradiated with different doses (0-4-8-16 Gy) for different times (24-48-72-96h) and by propidium iodide staining, the effects of IR on cell cycle were evaluated. A dose and time dependent increase in polyploid cells was observed. In particular, after 24h of treatment, a G₂/M accumulation was observed in both cell lines at the higher doses of IR (8-16 Gy), and after 48h of treatment also an increase in the percentage of cells in subG1 fraction was observed.

The increase of cells with >4N DNA content and a subsequent subG1 suggest that IR treated cells could die through mitotic catastrophe, a form of programmed cell death resulting from aberrant mitosis. Caspase-3 activation has been frequently observed in mitotic catastrophe.

I have also analyzed caspase-3 activation in irradiated ATC cells. FRO and BHT101-5 cells were irradiated with increasing doses of IR (0-2-4-8-16 Gy for FRO cells; 0-4-8-16 Gy for BHT101-5 cells) and were collected at different experimental time points (24-48-72-96h) to analyze by western blot the effects of the treatment on caspase-3 activation. As shown in figure 11, a decrease of procaspase-3 was observed 48h after the treatment, followed by caspase-3 cleavage and activation.

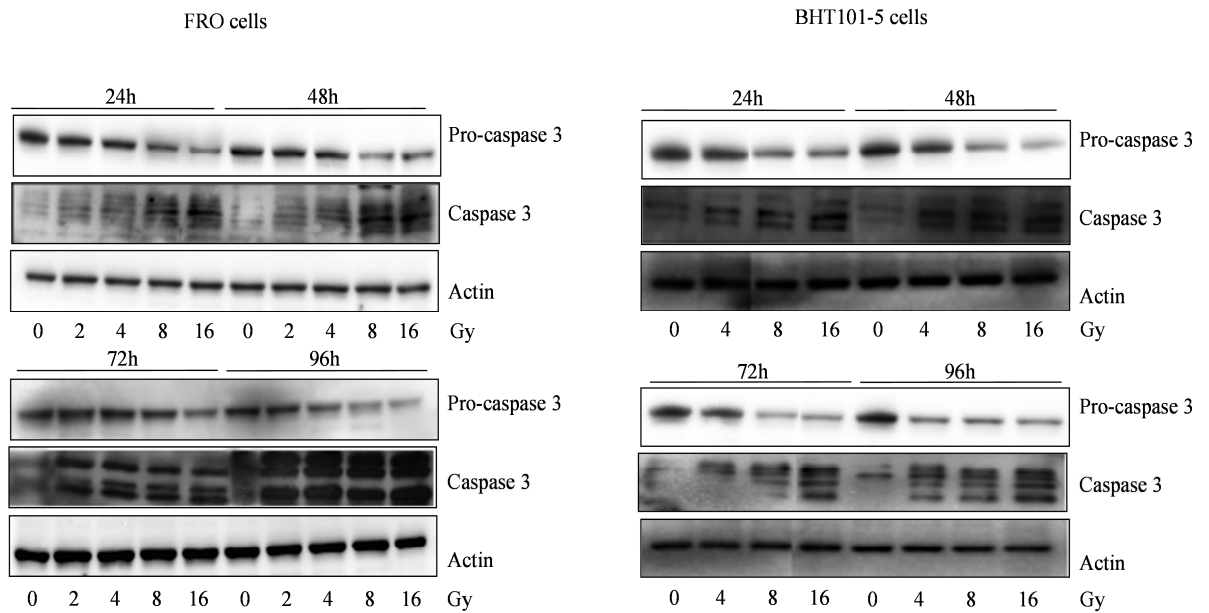


Figure 11. IR activates caspase-3 in ATC treated cells

FRO and BHT101-5 cells were irradiated with increasing doses of IR (0-2-4-8-16 Gy for FRO cells; 0-4-8-16 Gy for BHT101-5 cells) and were collected at different experimental time points (24-48-72-96 h). A decrease of procaspase-3 was observed 48h after the treatment, followed by caspase-3 cleavage and activation.

Mitotic catastrophe is a form of cell death resulting from aberrant mitosis. Such mitosis does not produce proper chromosome segregation and cell division, and leads to the formation of large non-viable cells characterized by micronuclei (Castedo et al. 2004). Micronuclei are nuclear envelopes around clusters of missegregated chromosomes (examples in figure 12).

To verify whether ionising radiation induces the formation of micronuclei, FRO and BHT101-5 cells were irradiated with increasing doses of IR (0-4-8 Gy) and the number of micronucleated cells was quantified by immunofluorescence analysis. As shown in figure 13, a clear dose- and time-dependent increase in the number of micronucleated cells was observed.

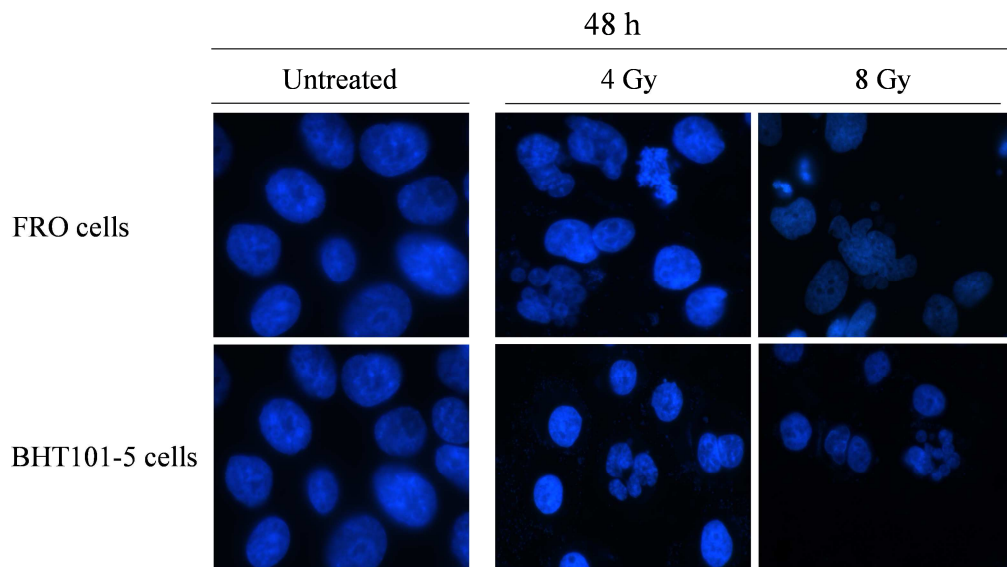


Figure 12. Ionising radiation induces mitotic catastrophe on ATC treated cells
Hoechst staining of FRO and BHT101-5 cells irradiated or not with 4 or 8 Gy. The same magnification (40x) was used in the images.

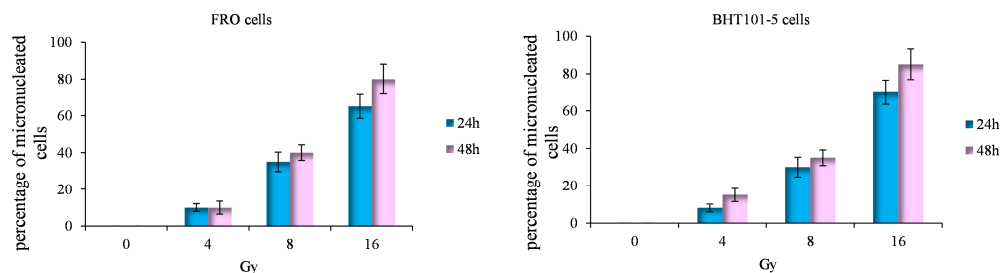


Figure 13. Ionising radiation induces mitotic catastrophe on ATC treated cells
FRO and BHT101-5 cells were irradiated with increasing doses of IR and the number of micronucleated cells was quantified by immunofluorescence analysis. The cells with ≥ 3 micronuclei were counted as positive.

The cell death pathways activated by the infection with OVAs are only partially understood, however several evidences indicate that they are cell type depending. In glioma cells, the infection with *dl922-947* activates an autophagic pathway (Botta et al; under review) while, in ATC cells, *dl922-947* infection does not induce autophagy but rather a programmed cell death, that lacks the features of classical apoptosis, but presents some apoptotic markers such as subG1 accumulation and caspase-3 activation (Libertini et al. 2011). In order to evaluate which type of cell death occurs in ATC cells upon combined treatment, cell cycle profiles in infected/irradiated cells were performed. FRO cells were irradiated (0-4-8 Gy) and then infected with 10 pfu/cell of *dl922-947*. Starting from 24h of treatment, cells were collected and

cell cycle analyzed by PI staining and FACS analysis. The combination between IR and virus increased the percentage of cells in subG1 fraction compared with single treatments (figure 14).

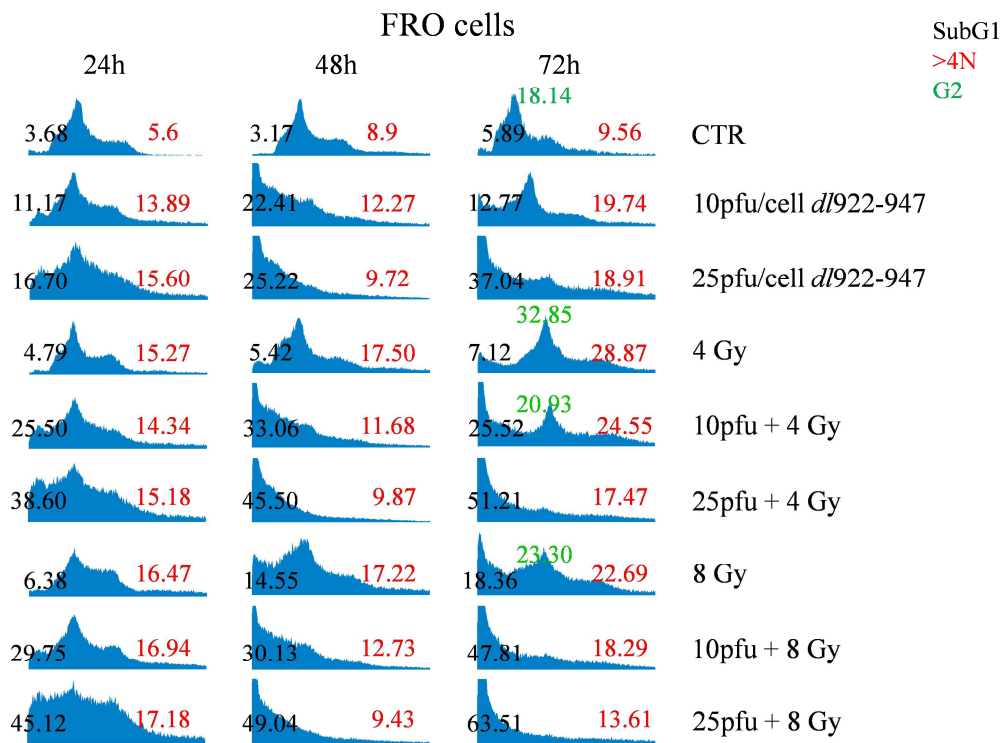


Figure 14. *dl922-947* and IR induce subG1 phase population in treated cells

FRO cells were irradiated and then infected with 10 pfu/cell of *dl922-947*. Cells were collected at different times and cell cycle analyzed by PI staining and FACS analysis. The combination treatment increased the percentage of cells in subG1 fraction compared with single treatments.

Since in ATC cells, *dl922-947* infection leads to programmed cell death lacking the features of classical apoptosis, but showing some apoptotic markers, such as subG₁ accumulation and caspase-3 activation, I have also analyzed caspase-3 activation in cells undergoing the combined treatment.

As shown in figure 15, in the combined treatment, an earlier decrease of procaspase-3 with respect to virus treatment alone was observed. This observation suggests that ionising radiations could enhance viral induced cell death by accelerating the activation of caspase-3 pathway.

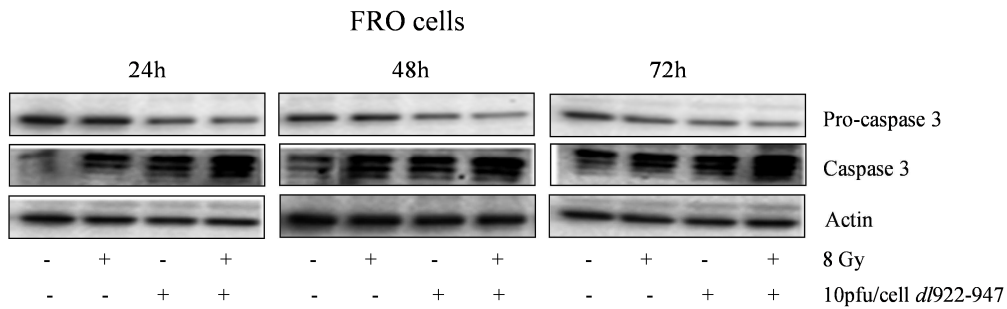


Figure 15. *dI922-947* and IR induce caspase-3 activation

FRO cells were irradiated with 8 Gy and then infected with 10 pfu/cell of the virus. Starting from 24h, cells were collected and caspase-3 levels analyzed by western blot. In the combined treatment, an earlier decrease of procaspase-3 with respect to virus treatment alone was observed.

4.4 Ionising radiation in combination with *dI922-947* reduced the growth of ATC tumor xenografts

In order to demonstrate that the combined treatment ionising radiation and *dI922-947* could potentially yield improved clinical efficacy, I have evaluated the effects of ionising radiation treatment *in vivo*.

Sixty athymic mice were inoculated subcutaneously with FRO cells (8×10^6). After 20 days, when tumors were clearly detectable, the animals were randomized into four groups. Two groups were irradiated with a single radiation dose (10 Gy), on the tumor volume. Virus was administered three times per week by intratumoral injection to avoid first pass effect. A low viral dose (1×10^6 pfu) was used to better evaluate the effects of the combined treatment. The control group was injected with saline solution. As shown in figure 16, a significant difference was observed in the combined treatment group with respect to single treatments.

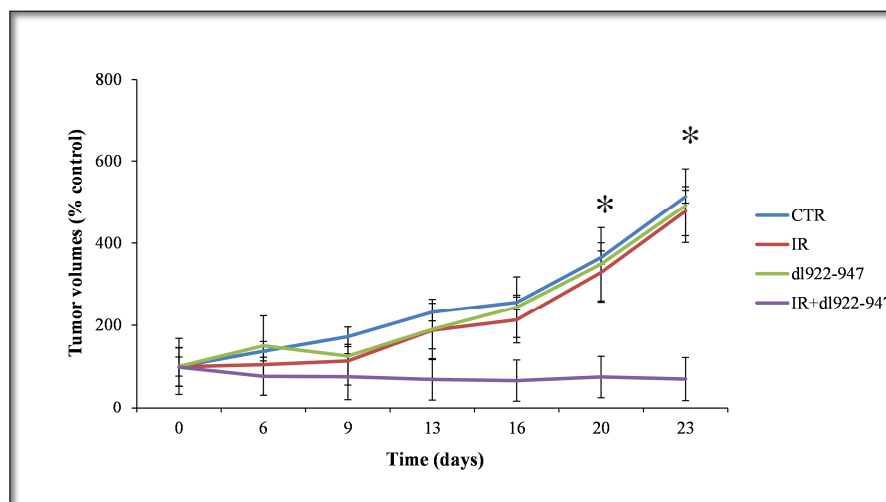


Figure 16. Tumor growth

Two groups were irradiated with a single radiation dose (10 Gy), on the tumor volume; virus was administered three times per week by intratumoral injection to avoid first pass effect. The control group was injected with saline solution. The combined treatment, IR plus *dl922-947*, is able to reduce tumor growth with a higher efficiency with respect to the virus or ionising radiation alone (* $p < 0.05$ up to T=20).

Next, by Real Time PCR, I have evaluated the genome equivalent copies of *dl922-947* in animals treated with IR and *dl922-947*. Figure 17 reports the amount of viral DNA copies in the group treated with *dl922-947* alone and in the group treated with *dl922-947* plus IR. The combined treatment induces a viral replication twenty fold higher with respect to the virus alone.

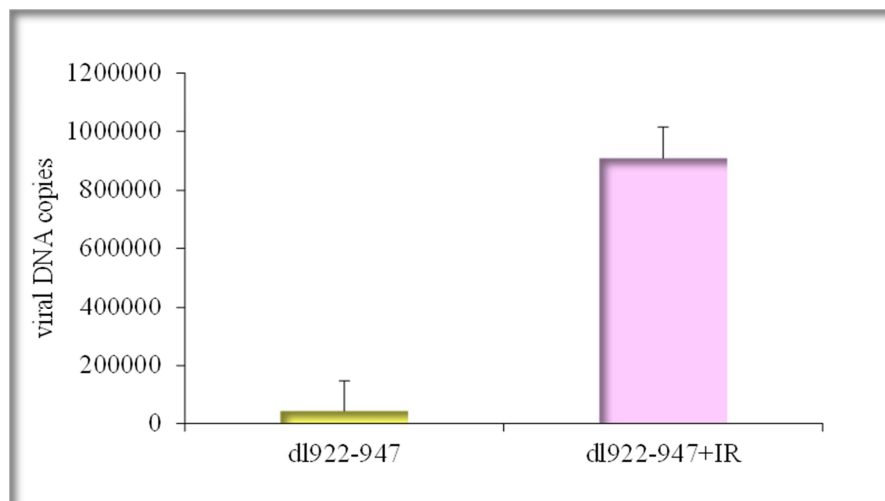


Figure 17. Effects of IR/virus combination

FRO cells were inoculated into the right flank of 10 athymic mice. When tumors were clearly detectable, animals were divided in two groups. One group of animals was irradiated with a single radiation dose (10 Gy) and 24h after the virus was injected intratumorally in both groups. After additional 48h animals were sacrificed, the tumor excised, DNA extracted and viral replication evaluated. The combined treatment induces a viral replication twenty fold higher with respect to the virus alone.

I have then evaluated viral distribution in tumor tissues. Figure 18 reports images of confocal microscopy. Fluorescence is more diffuse and intense in AdGFP injected and irradiated tumors with respect to the AdGFP injected tumors. This observation indicate that together with the effects observed *in vitro*, IR contributes to a better diffusion of the virus within the tumor mass, further confirming the efficacy of this combination.

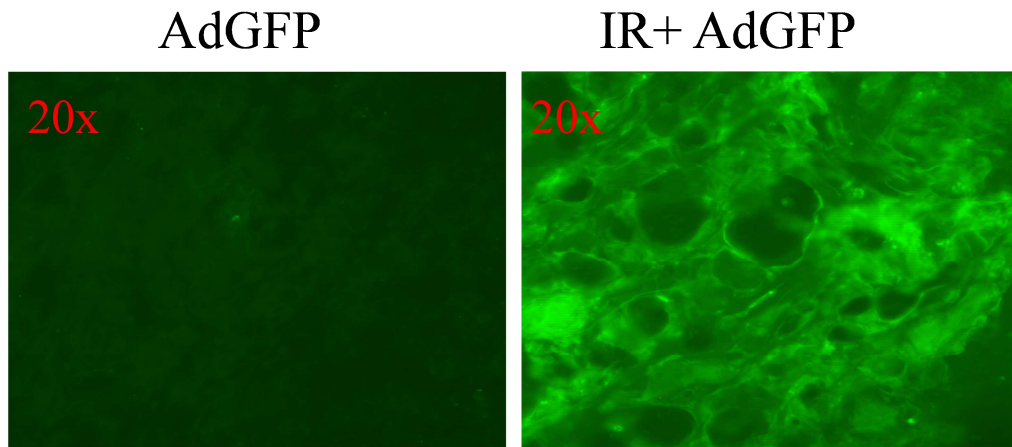


Figure 18. Effects of IR/*dl922-947* combination

FRO cells (8×10^6) were injected into the right flank of 10 athymic mice, and after 20 days, when tumors were clearly detectable, animals were randomized into two groups (5 animals/group). Only one group was irradiated with a single radiation dose (10 Gy). AdGFP (1×10^7 pfu) was injected intratumorally in both groups after 24h. After additional 48h, animals were sacrificed, and tumors were excised. On the left the distribution of AdGFP alone is represented, on the right there is the AdGFP distribution after the pre-treatment with IR. The fluorescence is more diffuse and intense in animal tissues treated with AdGFP plus IR with respect to the tissues treated with the virus alone.

I have also evaluated the activation of caspase-3 in ATC xenografts after the combined treatment. Interestingly, there is a higher activation of caspase-3 in the animals undergoing the combined treatment (figure 19).

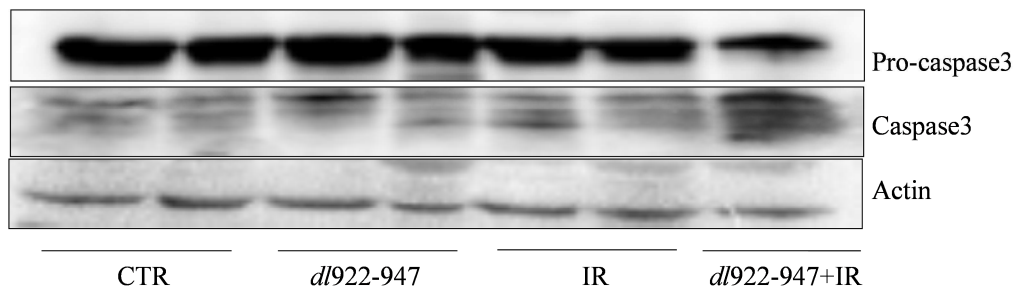


Figure 19. Activation of caspase-3 in ATC xenografts

Proteins were extracted from ATC tumors and caspase-3 activation levels were analyzed by western blot. As shown in the blot, in the animals undergoing the combined treatment there is a higher activation of caspase-3, indicative of a higher tumor cell death.

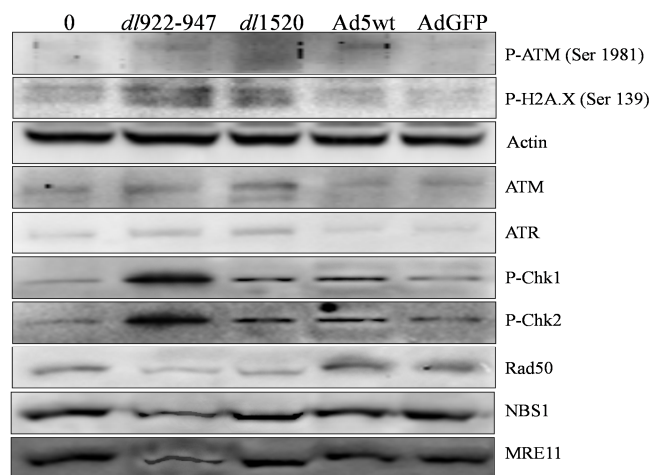
All these results demonstrated that the pre-treatment with IR is able to improve the therapeutic effect of *dl922-947* adenovirus against ATC.

4.5 *dl922-947* modulates the DNA damage signaling pathway to enhance ionising radiation effects

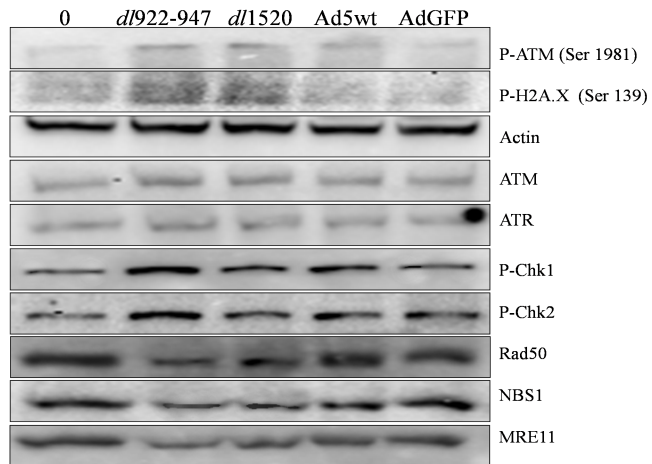
It is well known that ionising radiation induces DNA damage and activates the damage signaling pathway. It has been hypothesized that Ad OVs interact with cellular DNA damage response pathways to avoid the formation of the concatemers and to better replicate in target cells (Evans and Hearing 2005; Stracker et al. 2002; Stracker et al. 2005; Baker et al. 2007).

To verify whether the infection with oncolytic viruses could modify the response to DNA damage IR-induced, FRO cells were infected with a panel of adenoviral mutants: *dl922-947*, *dl1520* bearing a deletion of E1B-55KDa, Ad5wt a non-mutant adenovirus used as control adenovirus, and AdGFP a non replicating E1-deleted adenovirus encoding GFP. After 1-3-6-16h cells were collected and DNA damage pathway proteins levels analyzed by western blot. As shown in figure 20, starting from 1hpi (hours post infection), *dl922-947* and *dl1520* induce the phosphorylation of ATM on Ser1981, an early step of activation of DNA damage signaling pathway. Interestingly, *dl922-947* and *dl1520* also induce the activation by phosphorylation on Ser139 of histone H2A.X, a downstream effector of the activation of ATM. Moreover, *dl922-947* induces the activation of Chk1/2 by phosphorylation on Ser345 and Thr68, respectively. Starting from 3hpi, in cells infected with *dl922-947* I observed a reduction of the MRN proteins, which was more evident after 6 and 16 hours of treatment. It is worth to note that *dl1520*, lacking a functional E1B-55KDa, does not modify MRN protein levels. Ad5wt does not affect MRN protein expression at the time points evaluated. This effect is probably due to the different replication kinetic of Ad5wt with respect to *dl922-947*.

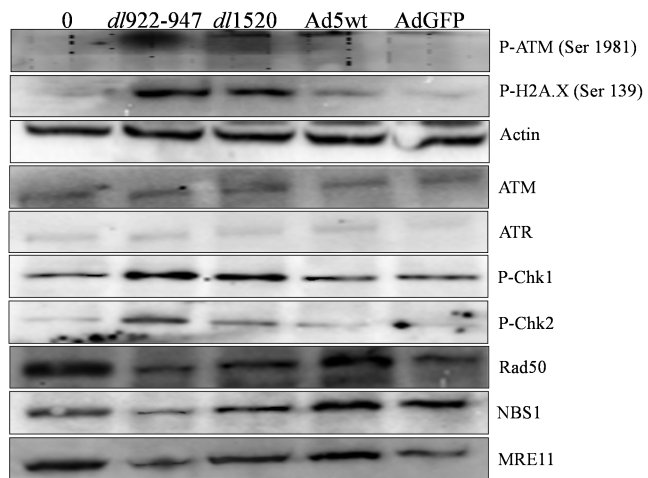
FRO cells 1 hpi



FRO cells 3 hpi



FRO cells 6 hpi



FRO cells 16 hpi

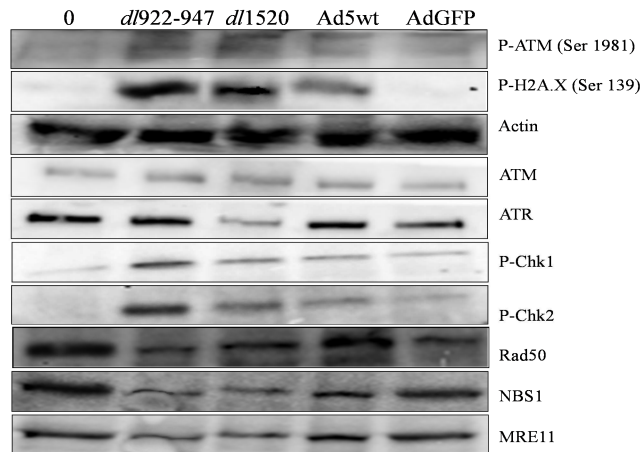


Figure 20. Effects of viral infection on DNA damage signaling pathway

FRO cells were infected with a panel of adenoviral mutants: *dl922-947*, *dl1520*, Ad5wt and AdGFP. Cells were collected at different times (1-3-6-16hpi) and DNA damage pathway protein levels were analyzed by western blot.

To confirm that the infection with *dl922-947* induces a cellular DNA damage in ATC cells, I have also analyzed the activation of histone H2A.X by FACS analysis. FRO cells were infected with two different concentration of the virus (10 and 25 pfu/cell), collected at two different times (6 and 24 hpi) (figure 21). After 6h of treatment the activation of histone H2A.X was observed, as previously demonstrated also by western blot analysis. Interestingly, the activation of the H2A.X persists after 24h of infection, suggesting that the damage was not repaired. The same results were confirmed by western blot (figure 22).

I can conclude that the infection with *dl922-947* induces the activation of the DNA damage signaling pathway, through the activation of the most important sensors of the damage (ATM and histone H2A.X), likely because the host cells recognize the viral genome as a DSB. Moreover, the virus targets the MRN complex proteins, causing its degradation and probably relocalization to avoid the formation of the concatemers.

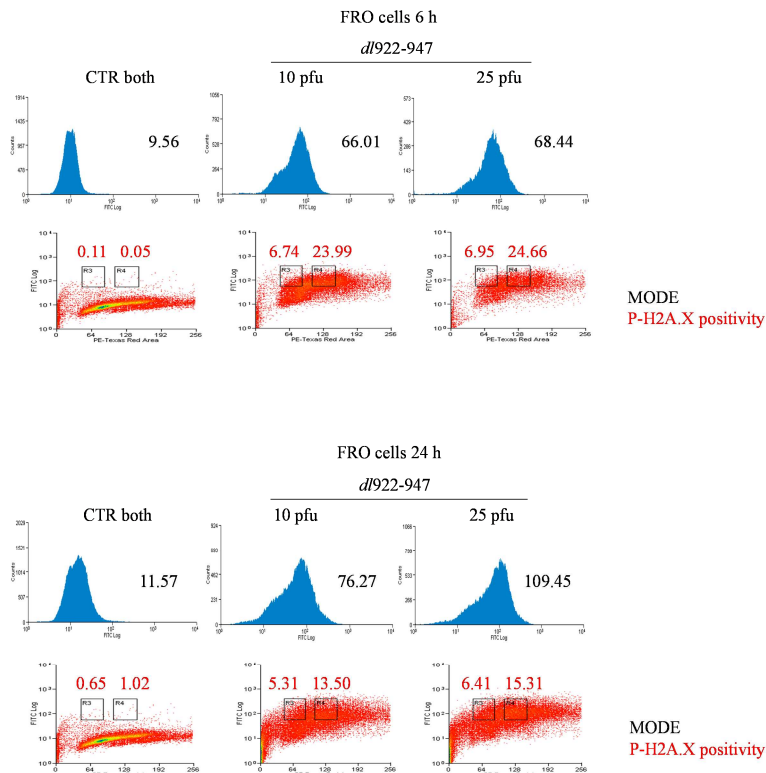


Figure 21. *dl922-947* induces the activation of histone H2A.X

FRO cells were infected with two different concentration of the virus and the P-H2A.X positivity was analyzed by FACS analysis. As shown in the figure, is evident the shift in the FITC channel with respect to the control cells, and also the increasing of the P-H2A.X positivity in cells infected with *dl922-947*.

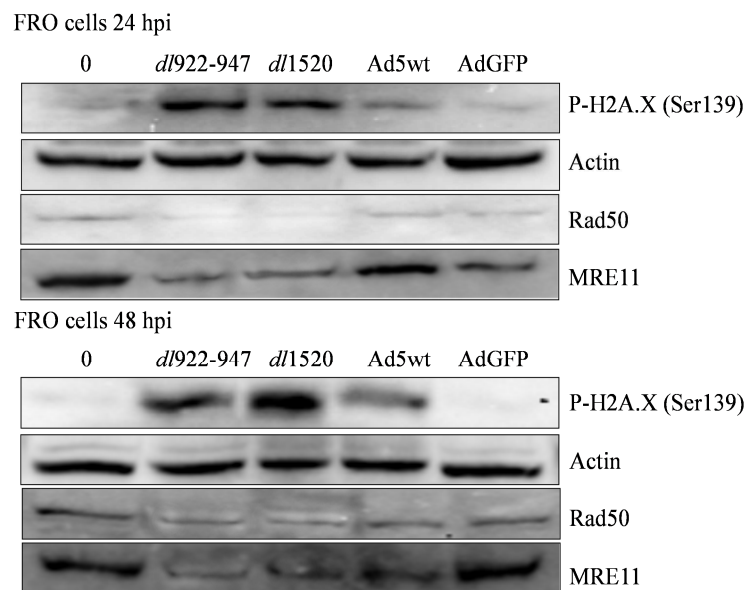


Figure 22. *dl922-947* induces the activation of histone H2A.X

FRO cells were infected with different viral mutants and expression levels of P-H2A.X, Rad50 and MRE11 were evaluated by western blot after 24 and 48h of treatment. Also at 24-48h the virus induces the activation of H2A.X and the reduction of Rad50 and MRE11, suggesting that the damage is not repaired.

It is well known that ionising radiation produces a wide variety of lesions in DNA, including base damage, single- and double-strand breaks. I have also shown that the virus targets the DNA damage signaling pathway. Therefore, I have analyzed the effects of the combined treatment on DNA damage signaling pathway.

FRO cells were infected with *dl922-947* (10 pfu/cell) and then irradiated (0-4 Gy). Cells were collected at different times (3-6-24h) to analyze the effects of the combined treatment on DNA damage signaling pathway proteins (figure 23). Starting from three hours of treatment an increase in the phosphorylation of ATM, histone H2A.X, Chk1 and Chk2 was observed in irradiated cells. This effect is increased in infected cells or in cells undergoing the combined treatment. A decrease of MRN proteins levels was observed only in infected cells or undergoing the combined treatment. This reduction is more evident after 16h and 24h of treatment, suggesting that the DNA damage was not repaired, as also confirmed by the permanent activation of P-H2A.X, P-Chk1 and P-Chk2. In irradiated cells the MRN complex is activated.

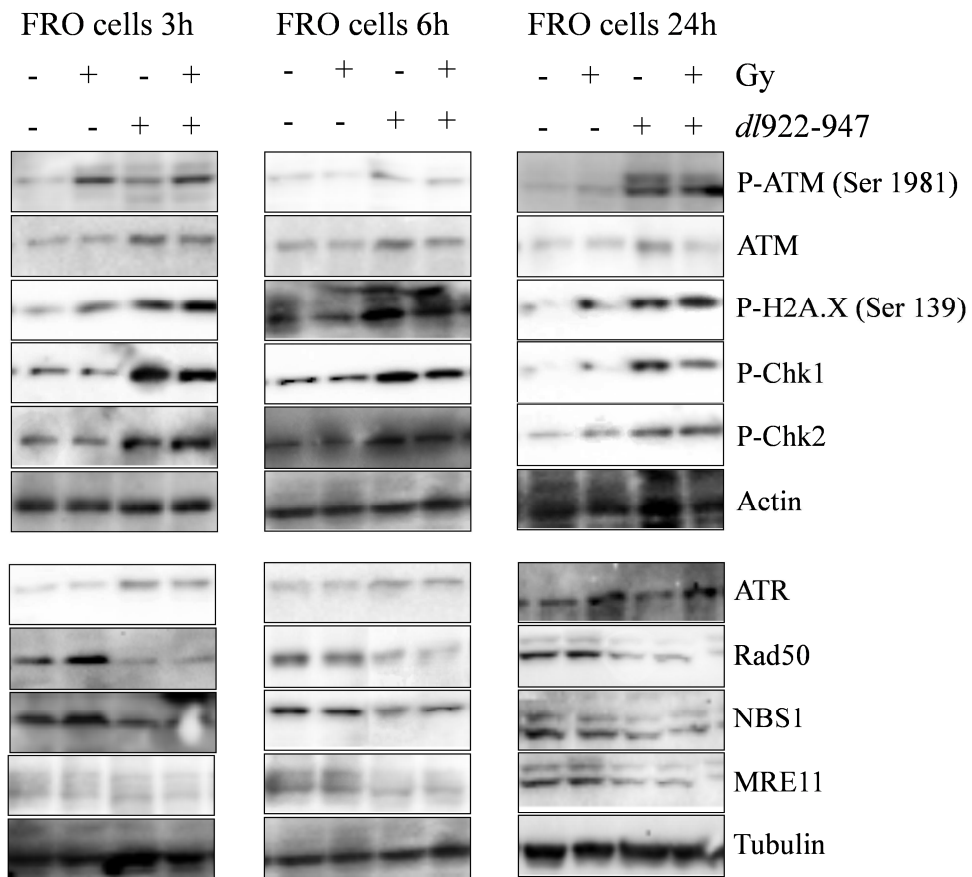
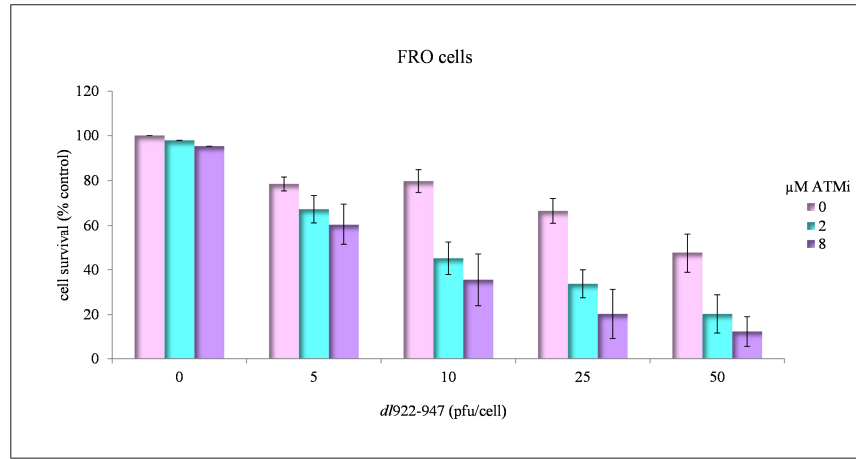


Figure 23. Effects of the combined treatment (virus plus IR) on DNA damage pathway
 FRO cells were infected with *dl922-947* (10 pfu/cell) and then irradiated with two different doses (0-4 Gy). Cells were collected at different times (3-6-24h) to analyze, by western blot, the effects of the combined treatment on DNA damage signaling pathway proteins.

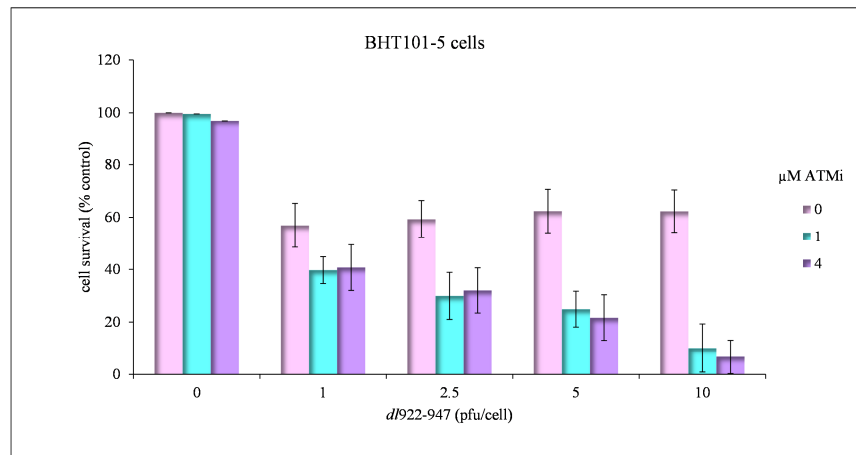
It has been recently published (Connell et al. 2011) that oncolytic virus *dl922-947*, that bears a functional E4 gene, can induce a DNA damage response in ovarian cancer cells, and that Chk1 inhibition can increase the oncolytic potential of *dl922-947*. To evaluate the role of DNA damage pathway on OV's activity and to assess the possible use of drugs affecting DNA damage response in ATC cell lines, FRO and BHT101-5 cells were infected in combination with a specific inhibitor of ATM kinase (KU55933).

FRO and BHT101-5 cell lines were infected with increasing concentration of the virus (0-5-7.5-10-25-50 pfu/cell for FRO cells; 0-1-2.5-5-7.5-10 pfu/cell for BHT101-5 cells) in combination with two different concentrations of the drug (0-2-8 μ M for FRO cells; 0-1-4 μ M for BHT101-5 cells). As shown in figure

24, in both cell lines the combination treatment potentiate the cytotoxic effects of the virus, suggesting that the drug accelerates viral-induced cell death.



| | 0 | 5 | 10 | 25 | 50 |
|-----------------|---------|---------|---------|----------|---------|
| 0 | 0 | 21,5371 | 20,2424 | 33,46809 | 52,4619 |
| 2 μM | 2,12305 | 32,7419 | 54,9519 | 66,2882 | 79,6415 |
| 8 μM | 4,75996 | 39,6 | 64,5109 | 79,70853 | 87,5068 |



| | 0 | 1 | 2.5 | 5 | 10 |
|-----------------|---------|---------|---------|---------|---------|
| 0 | 0 | 43,0784 | 40,7393 | 37,6423 | 37,6744 |
| 1 μM | 0,43875 | 60,2515 | 70,0333 | 75,0648 | 89,8992 |
| 4 μM | 3,11834 | 59,2411 | 67,9683 | 78,3153 | 93,3087 |

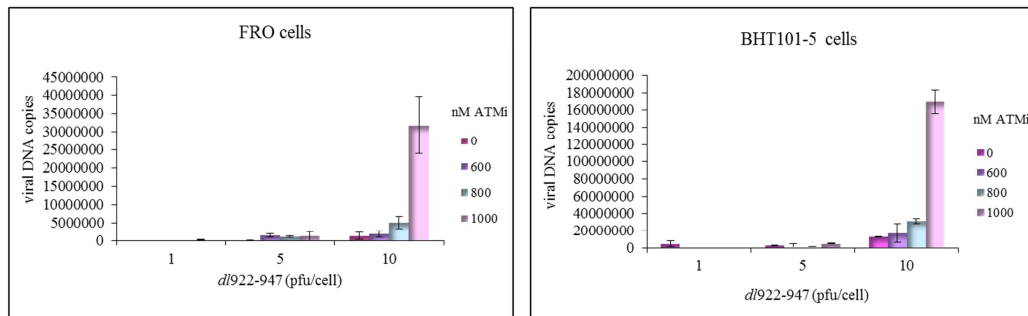
Figure 24. ATM inhibitor potentiates the effects of *dl922-947*

FRO and BHT101-5 cell lines were infected with increasing concentration of the virus (0-5-7.5-10-25-50 pfu/cell for FRO cells; 0-1-2.5-5-7.5-10 pfu/cell for BHT101-5 cells) in combination with two different concentrations of the drug (0-2-8 μM for FRO cells; 0-1-4 μM for BHT101-5 cells). After seven days cells were analyzed for viability assay. In both cell lines ATM inhibitor enhances cytotoxic effects of *dl922-947*. All experimental points, in both cell lines, show a significant difference with respect to the single treatments.

To explore the possibility that the higher cytotoxic effects was due to an increase in viral replication, I have evaluated genome equivalent copies of *dl922-947* in ATC cells undergoing the combined treatment, both in combination or with a 24h pre-treatment with the drug.

A clear increase in viral replication was observed in both cell lines (figure 25), although the combination treatment was more effective with respect to 24h pre-treatment.

A



B

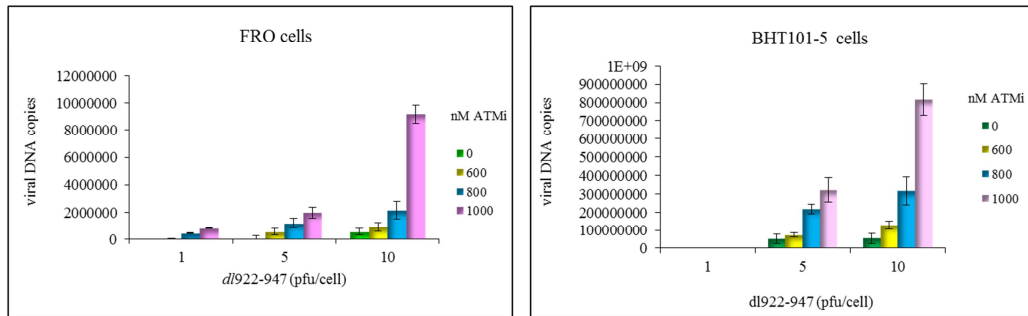


Figure 25. ATM inhibitor increases viral replication

FRO and BHT101-5 cells were infected with increasing concentration of the virus (0-1-5-10 pfu/cell) and treated with different concentration of the drug (0-600-800-1000 nM), in combination (**A**), or with a 24h pre-treatment with the drug (**B**). A clear increase in viral replication was observed in both cell lines, and in both experiments.

Next, I have evaluated the effects of the combined treatment on the activation of ATM kinase, histone H2A.X, Chk1 and Chk2.

The combined treatment reduces P-ATM levels, whereas in infected cells a clear activation was observed. A similar effect was also observed for P-H2A.X, P-Chk1 and P-Chk2.

Interestingly, the MRN complex protein levels were reduced in cells undergoing the combined treatment, indicating that the block of ATM activation does not prevent viral induced degradation of MRN complex.

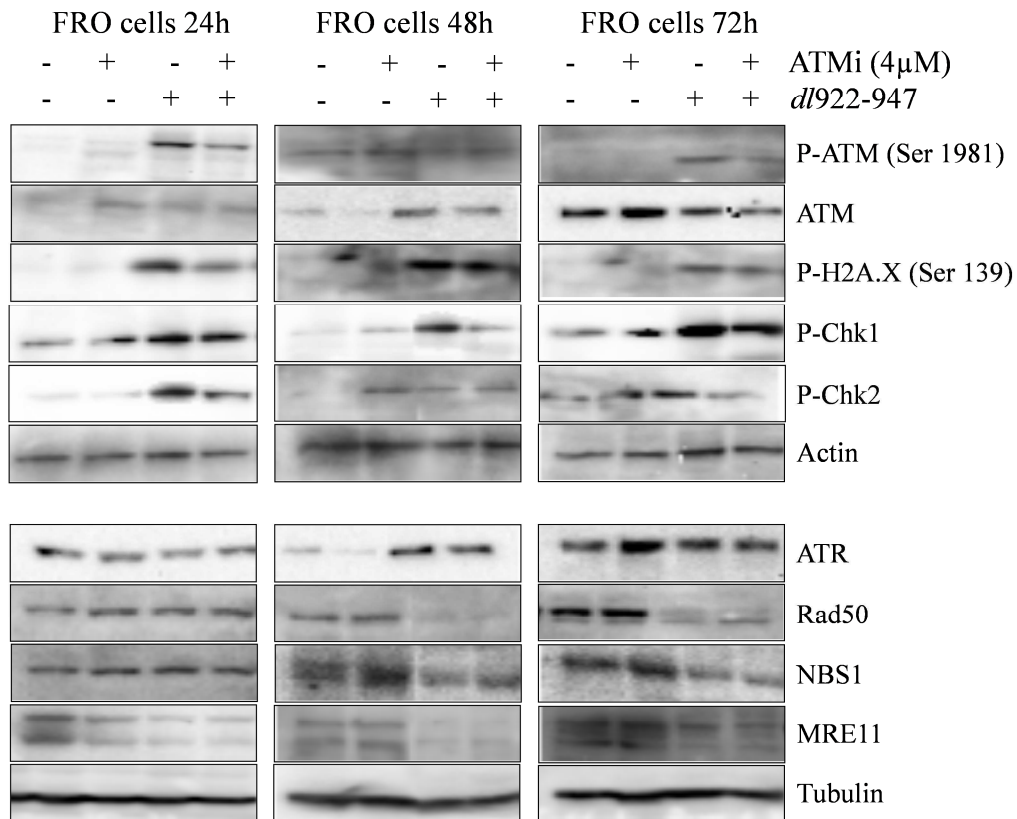


Figure 26. Effects of the combination *dl922-947* plus ATM inhibitor on DNA damage signaling pathway proteins

FRO cells were infected with 10 pfu of *dl922-947* in combination or not with ATM inhibitor at two different concentrations (0-600-800 nM). After 24-48-72h, cells were collected and expression levels of P-ATM, P-H2A.X, P-Chk1, P-Chk2 and MRN complex proteins analyzed by western blot.

I have also monitored cell death mechanisms induced in the combined treatment.

FRO cells were pre-treated for two hours with the drug (10 μ M) and then infected with *dl922-947* (25 pfu/cell). Cells were collected at different times (6-16-24-48-72h) and cell cycle analyzed by FACS analysis. As shown in figure 27, after 6 and 16h of treatment the drug alone does not affect cell cycle profile and the effects in the combined treatment were due only to the virus. Starting from 24h in the cells treated with the drug I can observe an increase in the subG₁ fraction and an increase in the percentage of polyploid cells, while in cells undergoing the combined treatment there is a little increase in the percentage of cells in subG₁ fraction compared to the virus alone. It is also worth noting that, in the combined treatment, the slight increase in subG₁ fraction at later time points is associated with a decrease in polyploidy fractions, as we have already demonstrated (Libertini et al. 2011).

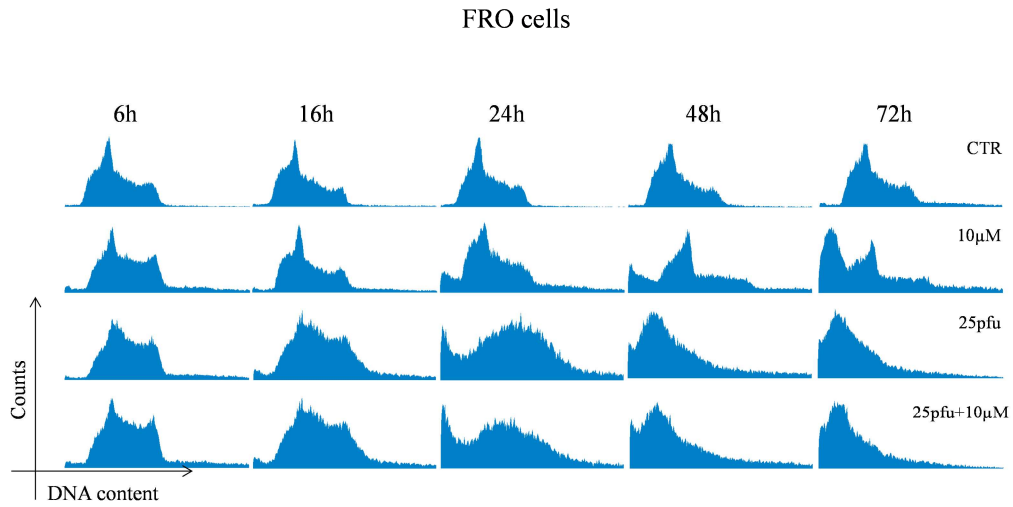


Figure 27. Effects of the combination between *dl922-947* and ATM inhibitor on ATC cell cycle

FRO cells were pre-treated for two hours with the drug (10µM) and then infected with *dl922-947* (25 pfu/cell). Cells were collected at different times (6-16-24-48-72h) and cell cycle analyzed by FACS analysis.

The data obtained treating *in vitro* ATC cells with ATM inhibitor and *dl922-947* demonstrate that the drug enhances the effects of the virus, accelerating viral induced cell death and increasing viral replication, confirming that the inactivation of the DNA damage pathway is important to enhance the cell killing activity of *dl922-947*.

5. DISCUSSION

ATC is one of the most lethal human neoplasia and leads to death in a very short time. Active therapies are not available, making the development of novel therapeutic strategies a necessity (Smallridge et al. 2009).

Oncolytic viruses are emerging as new therapeutic tools for the treatment of cancer, and we have previously demonstrated that the mutants *dl1520* and *dl922-947* are active against ATC *in vitro* and *in vivo* (Libertini et al. 2007; Libertini et al. 2008).

It is increasingly recognized that combining viral therapies with EBRT represents a promising approach. In fact, enhanced antitumor efficacy has been observed with oncolytic adenoviruses when combined with chemotherapeutic agents or radiation in several tumor models (Yoon et al. 2006; DeWeese et al. 2001; Portella et al. 2002). Phase I and II trials investigating combinations of oncolytic viruses and EBRT have been published, paving the way for ongoing phase III trials (Touchefeu et al. 2011).

The previous studies performed with ionising radiation and oncolytic viruses (Portella et al. 2003) and the observation that drugs able to block cells in G₂/M or inhibit cytokinesis could enhance the effects of oncolytic viruses (Seidman et al. 2001), have persuaded me to evaluate whether this combination could positively affect *dl922-947* activity against ATC.

The data presented in this thesis demonstrate the efficacy of this combination. In particular, ionising radiation enhances the effects of the oncolytic adenovirus *dl922-947* both *in vitro* and *in vivo*.

I have identified the most appropriate timing showing that the most effective treatment is infection followed after 24 hours by irradiation. In cells undergoing this treatment, all experimental points show a significant difference with respect to the single treatments. On the contrary, in cells irradiated and then infected a synergistic effect is evident only at the higher concentration of the virus.

A number of potential mechanisms of interaction between viruses and radiation have been described. Radiation can increase viral uptake, probably enhancing the expression of the coxsackie and adenovirus receptor (CAR) on the membrane of infected cells or the expression of $\alpha_v/\beta_3/5$ integrin subunits acting as low affinity coreceptors, viral gene expression and replication.

I monitored viral entry upon radiation treatment. The data obtained show that IR does not affect viral entry in ATC cells.

It has been demonstrated that synchronization or blocks in G₂/M phase led to elevated Ad binding and transgene expression, since expression of high-affinity (coxsackie and adenovirus receptor, CAR) and low-affinity (α_v integrins) Ad receptors showed a significant increase (Seidman et al. 2001). Although IR-treated cells accumulate in G₂/M phase, membrane levels of CAR and its co-receptors integrins $\alpha_v\beta_3$ do not increase after IR treatment in ATC cells. The increase of CAR levels in cells undergoing the combined treatment with

respect to the untreated cells, was due to the viral infection, as previously observed by us (unpublished observation).

This observation is in agreement with Georger et al. (2003) who reported that radiation do not increase CAR or integrin α_v expression in glioma cell lines and Bieler et al. (2008), who showed no increase in CAR expression in glioblastoma cell lines infected with adenoviruses.

In this work I have demonstrated that ionising radiation increases viral replication also in ATC cell lines in a dose-dependent manner. Moreover, IR increases viral gene expression, as demonstrated by the dose-dependent increase of E1A levels.

Some publications report enhanced viral replication following EBRT, both *in vitro* and *in vivo*. This phenomenon has been described with adenoviruses in prostate (Chen et al. 2001; Dilley et al. 2005; Liu et al. 2010), lung (Adusumilli et al. 2005) and glioblastoma models (Bieler et al. 2008). However, in contrast, a smaller number of studies have failed to find evidence that radiation increases viral replication. It is possible that radiation-mediated effects on viral replication may be cell line-dependent.

dl922-947 infection in ATC cells induces a G₂/M accumulation with subsequent polyploidy. It is also well known that after exposure to ionising radiation a G₂/M accumulation blocks in G₂ the cells that had been in earlier phases of the cell cycle at the time of irradiation (Metting and Little 1995). To better understand the effects of the combined treatment on ATC cell death, I have previously analyzed the effects of radiation treatment alone on ATC cell lines.

It has been shown that cells treated with ionising radiation die through mitotic catastrophe (Dodson et al. 2007), a form of cell death resulting from aberrant mitosis. Such mitosis does not produce proper chromosome segregation and cell division, and leads to the formation of large non-viable cells characterized by micronuclei: nuclear envelopes around clusters of missegregated chromosomes (Castedo et al. 2004).

The increase of 4N DNA content and subG₁ accumulation together with caspase-3 activation has been observed in mitotic catastrophe. In ATC cells treated with increasing concentration of IR a decrease of procaspase-3 was observed, followed by caspase-3 cleavage and activation, as well >4N DNA and subG₁ accumulation. Moreover, a clear dose- and time-dependent increase in the number of micronucleated cells was observed, confirming mitotic catastrophe as cell death mechanism activated in irradiated ATC cells.

It has been already demonstrated that *dl922-947* induces in ovarian carcinoma and ATC cells, a non-apoptotic programmed cell death. This type of death shares some features with apoptosis such as caspase-3 activation and subG₁ accumulation (Baird et al. 2008; Libertini et al. 2011).

The association with IR induces a cell death closely resembling the viral non apoptotic programmed cell death. Moreover, the appearance of cleaved caspase-3 and the increase of cells in subG₁ phase is accelerated.

It is possible to exclude death by mitotic catastrophe in the combined treatment since, upon infection, cells detach, a feature not observed in mitotic catastrophe. Moreover, in the few adhering cells, we have not observed the presence of micronuclei (data not shown).

These data indicate that in the combined treatment the viral induced cell death mechanism is dominant.

In order to demonstrate that the combined treatment ionising radiation and *dl922-947* could potentially yield improved clinical efficacy, I have also evaluated the effects of ionising radiation treatment *in vivo*.

The results of *in vivo* experiments showed that the combined treatment enhanced the antineoplastic effects of the virus against ATC xenografts, confirming the data obtained *in vitro*. Accordingly with *in vitro* experiments, *in vivo* I have observed an increase of viral replication and caspase-3 activation. Moreover, the analysis of viral distribution showed that ionising radiation pre-treatment improved viral distribution within the tumor, since a more intense GFP staining was observed in all tumor tissues, indicating that *in vivo* other mechanisms contribute to the enhancement of viral activity, along with those observed in *in vitro* experiments.

Recent data suggest that viruses have evolved with the ability to interact with cellular DNA damage response and repair pathways. A deeper understanding of these interactions could explain the enhanced effect observed in the combined treatment, and should lead to innovative combination strategies involving viral therapy combined with DNA repair inhibitors.

It is well known that ionising radiation induces DNA damage and activates the DNA damage signaling pathway. When a DSB occurs the MRN complex recognizes the lesion and recruits the protein kinases ATM and ATR to the site of the break. Once activated, ATM leads to the direct or indirect phosphorylation of different substrates, such as NBS-1, Chk1, Chk2, BRCA1 and H2AX (Darzynkiewicz et al. 2009; Lavin et al. 2006).

Virus infection presents an assault on the host cell. While the virus tries to commandeer the cellular machinery to aid its own replication, the host cell responds with defense systems that create obstacles for the virus. Viral infection and replication present the host cell with large amounts of exogenous genetic material, much of which may possess unusual DNA secondary structures. It is therefore likely that viral genomes will represent targets for cellular proteins that recognize and respond to abnormal and damaged DNA. Accordingly, viruses have been shown to be capable of interacting with cellular DNA damage response pathway to avoid the formation of the concatemers and to better replicate in target cells (Evans and Hearing 2005; Stracker et al. 2002; Stracker et al. 2005; Baker et al. 2007).

Adenoviruses have evolved different mechanisms to counteract the detrimental effects of NHEJ, two of which specifically target the MRN complex. The E4-ORF3 protein can redistribute Mre11, Rad50, and Nbs1 from their normal diffuse nuclear localization into large nuclear and cytoplasmic accumulations during infections or E4-ORF3 transfection (Evans and Hearing 2005; Stracker

et al. 2002; Stracker et al. 2005). The E4-ORF6 protein interacts with another viral protein, E1B-55KDa, to form an E3 ubiquitin ligase complex with the cellular proteins Rbx1, Cullin 5 (CUL5), and elongins B and C (Harada et al. 2002; Querido et al. 2001). This complex targets specific proteins, such as p53, Mre11, and DNA ligase IV, for proteasome-dependent degradation (Baker et al. 2007; Harada et al. 2002; Querido et al. 2001).

To verify whether the infection with oncolytic adenoviruses could modify the MRN protein levels in our model, FRO cells were infected with a panel of adenoviral mutants: *dl922-947*, bearing a deletion of 24-bp in the CR2 of E1A, *dl1520* an E1B-55KDa deleted virus, Ad5wt a non-mutant adenovirus used as control adenovirus, and AdGFP a non-replicating E1-deleted adenovirus encoding GFP.

Starting from 1 hpi (hour post infection), *dl922-947* and *dl1520* induce the phosphorylation of ATM on Ser1981, an early step of activation of DNA damage signaling pathway. Interestingly, *dl922-947* and *dl1520* also induce the phosphorylation on Ser139 of histone H2A.X, a downstream effector of the activation of ATM. Moreover, *dl922-947* induces the activation of Chk1/2 by phosphorylation on Ser345 and Thr68, respectively. Starting from 3 hpi, in cells infected with *dl922-947* I observed a reduction of the MRN proteins, which was more evident after 6 and 16 hours of treatment.

It is well known that ionising radiation produces a wide variety of lesions in DNA, including base damage, single- and double-strand breaks. Moreover, I have observed that the virus targets the DNA damage signaling pathway to better replicate, therefore I have analyzed the effects of the combined treatment (virus/IR) on the DNA damage signaling pathway.

At three hours *post* treatment an increase in the phosphorylation of ATM, histone H2A.X, Chk1 and Chk2 was observed in irradiated cells; this effect was more evident in infected cells or in cells undergoing the combined treatment.

A decrease of MRN proteins levels in cells undergoing the combined treatment was also observed. This reduction was more evident at longer time (in particular 16h and 24h), suggesting that the DNA damage was not repaired, as confirmed by the permanent activation of histone H2A.X, Chk1 and Chk2. In control irradiated cells no reduction in MRN complex levels were observed.

Our data are in agreement with a recently published study by Connell and colleagues (2011), showing that oncolytic virus *dl922-947* induces a DNA damage response in ovarian cancer cells, and that Chk1 inhibition increases the oncolytic potential of *dl922-947*.

In order to better understand the role of DNA damage pathway on OV's activity and replication as well as to assess the possible use of drugs affecting DNA damage response in ATC cell lines, I have combined *dl922-947* with a specific inhibitor of ATM kinase.

The drug potentiates the cytotoxic effects of the virus; interestingly, an increase in viral replication was observed in both cell lines.

I have then investigated the effects of the combined treatment (*dl922-947*/ATM inhibitor) on the activation of DNA damage pathway, showing in cells undergoing the combined treatment a clear reduction of MRN complex proteins.

These data confirm that the virus needs to target DNA damage pathway for its own replication. Interestingly, despite drug induced block of ATM phosphorylation, MRN complex in cells undergoing the combined treatment is degraded, further confirming the importance of this step for viral life cycle.

In conclusion the data presented here demonstrate that ionising radiation potentiates the oncolytic activity of *dl922-947*. This data could be useful for the development of novel therapeutic strategies for the treatment of ATC.

Moreover, I have shown that the virus targets the DNA damage pathway through the degradation of the MRN repair complex and that this effect is not modified by the combination with ionising radiation or ATM inhibitor, indicating a dominant effect of the virus. The enhancement in viral replication together with an accumulation of unrepaired DNA lesions could explain the increase in cell killing observed in the combined treatment.

This observation suggest that the targeting of DSB repair could represent a novel mechanism to increase the oncolytic activity of *dl922-947*.

6. CONCLUSION

Anaplastic thyroid carcinoma is one of the most lethal human neoplasia, that leads to death in few months. Surgery, radiotherapy and chemotherapy have no effects on its prognosis. Therefore, novel therapeutic approaches are required. Replication selective oncolytic viruses (OVs) are a rapidly expanding therapeutic platform for cancer treatment.

In this study I propose a novel therapeutic approach based on the use of oncolytic adenovirus and in particular of a second generation adenoviral mutant, *dl922-947*. I have demonstrated that ionising radiation enhances the oncolytic activity of *dl922-947* both *in vitro* and *in vivo*. Furthermore, I have shown that ionising radiation acts on viral gene expression, enhancing viral replication, but does not affect membrane CAR or integrin levels and does not increase viral entry.

A single radiation dose of 10 Gy enhances *dl922-947* oncolytic effect and viral replication *in vivo*, and also improves the distribution within the tumor since a more intense GFP staining was observed in all tumor tissues.

I have also shown that *dl922-947* modulates the DNA damage signaling pathway, by inducing the degradation of the MRN complex proteins to avoid the formation of viral concatemers and to better replicate. To evaluate the possible use of such drugs affecting DNA damage response in ATC cell lines, I have decided to combine *dl922-947* with a specific inhibitor of ATM kinase to verify whether the combined treatment could potentiate the cytotoxic effects of the virus, since the drug blocks the ATM pathway. The combination treatment potentiate the cytotoxic effects of the virus, suggesting that the drug increases viral replication.

In conclusion, the results described in this study encourage the use of *dl922-947* for new therapeutic protocols for the treatment of ATC and in particular a combination between the virus and ionising radiation could represent a better option for virotherapy against this aggressive carcinoma. Moreover, also the modulation of the DNA damage signaling pathway, and in particular the inhibition of the ATM kinase could represent a novel therapeutic tool for the enhancement of the oncolytic activity of *dl922-947* in ATC models.

7. ACKNOWLEDGEMENTS

I would like to express my sincere thanks to Prof. Giuseppe Portella for giving me the opportunity to work in his group, for having always confidence in me, for his competent supervision and support over the years. It has been a pleasure working with you, I appreciate your helpfulness, comprehension, wisdom and patience.

Vorrei inoltre ringraziare:

Dott.ssa Silvana Libertini per avermi trasmesso la passione per la ricerca, per l'ammirazione che ha sempre avuto per me "since I was an undergraduated student", per l'amicizia che mi ha sempre dimostrato anche da lontano e per l'infinità di consigli e di insegnamenti che non mi ha mai fatto mancare!!! Grazie perché quel poco che so fare lo devo solo a te!!!

Dott.ssa Carmela Passaro, collega sì, ma soprattutto grande amica, confidente, consigliera, a volte anche sorella e per questo di diritto anche "zia". Grazie per l'allegria, la collaborazione, l'aiuto e l'amicizia che mi hai mostrato e dimostrato ogni giorno!!! Hai reso questi 3 anni più leggeri e divertenti!!!

Dott.ssa Ginevra Botta e dott. Salvatore Iovino (Portellino acquisito) che anche dall'altro capo del mondo non fanno mancare la loro amicizia e il loro sostegno, però quanto mancano i pranzi insieme, le battute e le risate nel "nostro" mitico lab Portella, ma soprattutto quanto mancate voi!!!!

Dott.ssa Sara Barbato per aver alleggerito le giornate di lavoro con chiacchiere, risate, e le sue "perle di saggezza" divisa tra noi e la virologia. Ma in realtà sei sempre solo ed esclusivamente una Portellina.

Il piccolo dott. Max per le meravigliose traversate Policlinico/Stazione centrale accompagnate dai meravigliosi racconti del "Porciello", ma soprattutto per il supporto informatico e in particolare per il grande aiuto manuale che mi ha dato nella fase finale del mio lavoro di tesi.

Ringrazio tutto l'immenso lab Beguinot /Formisano, in particolare Serena che ha condiviso con me questi 3 anni di dottorato dalla preparazione del concorso alla scrittura della tesi; ringrazio Vittoria, Tonia, Federica, Rossella, Francesco, Michele e Cecilia per la sincera amicizia dimostratami ogni giorno, Mimmo per l'immensa ventata di allegria e anche di "serietà" che ha portato nel nostro laboratorio, e Giuseppe per l'affetto che mi ha sempre dimostrato da quando ero una studentessa, sopportando le mie ansie anche durante la preparazione e lo svolgimento del concorso di dottorato.

Il mitico Salvatore Sequino per l'aiuto negli esperimenti in vivo, senza far mai mancare la simpatia, l'allegria, e anche qualche "piccola lamentela".

I miei genitori e tutta la mia famiglia, per essere stati sempre per me guida, sostegno, punto di riferimento sicuro..... Grazie perché tutto quello che ho potuto fare e che ho fatto finora è stato solo merito vostro. Sono onorata di avere una famiglia così!!!!!!

E poi ringrazio te, mio unico e solo amore, mio unico punto di riferimento, mio sostegno nei momenti di sconforto e di scoraggiamento, che non sono mai mancati ma che con te sono diventati sopportabili e superabili.....ti ringrazio per essermi accanto ogni giorno, per accompagnarmi passo dopo passo, per essere sempre presente, attento e premuroso.....e ti ringrazio soprattutto per lui, il nostro dono più grande.....siete tutto quello che di più bello mi potesse capitare nella vita.....

Al mio caro nonnino.....

8. REFERENCES

- Abou El Hassan MA, van der Meulen-Muileman I, Abbas S, Kruyt FA. Conditionally replicating adenoviruses kill tumor cells via a basic apoptotic machinery-independent mechanism that resembles necrosis-like programmed cell death. *J Virol* 2004;78:12243-51.
- Adusumilli PS, Stiles BM, Chan MK, Chou TC, Wong RJ, Rusch VW, Fong Y. Radiation therapy potentiates effective oncolytic viral therapy in the treatment of lung cancer. *Ann Thorac Surg* 2005;80:409-16.
- Alain T, Hirasawa K, Pon KJ, Nishikawa SG, Urbanski SJ, Auer Y, Luidier J, Martin A, Johnston RN, Janowska-Wieczorek A, Lee PW, Kossakowska AE. Reovirus therapy of lymphoid malignancies. *Blood* 2002;100:4146-53.
- Alemany R, Balagué C, Curiel DT. Replicative adenoviruses for cancer therapy. *Nat Biotechnol* 2000;18:723-7.
- Ansardi DC, Porter DC, Jackson CA, Gillespie GY, Morrow CD. RNA replicons derived from poliovirus are directly oncolytic for human tumor cells of diverse origins. *Cancer Res* 2001;61:8470-9.
- Araujo FD, Stracker TH, Carson CT, Lee DV, Weitzman MD. Adenovirus type 5 E4orf3 protein targets the Mre11 complex to cytoplasmic aggresomes. *J Virol* 2005;79:11382-91.
- Asada T. Treatment of human cancer with mumps virus. *Cancer* 1974;34:1907-28.
- Baird SK, Aerts JL, Eddaoudi A, Lockley M, Lemoine NR, McNeish IA. Oncolytic adenoviral mutants induce a novel mode of programmed cell death in ovarian cancer. *Oncogene* 2008;27:3081-90.
- Baker A, Rohleder KJ, Hanakahi LA, Ketner G. Adenovirus E4 34k and E1b 55k oncoproteins target host DNA ligase IV for proteasomal degradation. *J Virol* 2007;81:7034-40.
- Bakkenist CJ, Kastan MB. DNA damage activates ATM through intermolecular autophosphorylation and dimer dissociation. *Nature* 2003;421:499-506.
- Bantel-Schaal U. Growth properties of a human melanoma cell line are altered by adeno-associated parvovirus type 2. *Int J Cancer* 1995;60:269-74.
- Bauerschmidt C, Arrichiello C, Burdak-Rothkamm S, Woodcock M, Hill MA, Stevens DL, Rothkamm K. Cohesin promotes the repair of ionizing radiation-induced DNA double-strand breaks in replicated chromatin. *Nucleic Acids Res* 2010;38:477-87.
- Bhaskara V, Dupré A, Lengsfeld B, Hopkins BB, Chan A, Lee JH, Zhang X, Gautier J, Zakian V, Paull TT. Rad50 adenylate kinase activity regulates DNA tethering by Mre11/Rad50 complexes. *Mol Cell* 2007;25:647-61.
- Bieler A, Mantwill K, Holzmüller R, Jürchott K, Kaszubiak A, Stärk S, Glockzin G, Lage H, Grosu AL, Gansbacher B, Holm PS. Impact of radiation

therapy on the oncolytic adenovirus dl520: implications on the treatment of glioblastoma. *Radiother Oncol* 2008;86:419-27.

- Bischoff JR, Kirn DH, Williams A, Heise C, Horn S, Muna M, Ng L, Nye JA, Sampson-Johannes A, Fattaey A, McCormick F. An adenovirus mutant that replicates selectively in p53-deficient human tumor cells. *Science* 1996;274:373-6.
- Botta G, Passaro C, Libertini S, Abagnale A, Barbato S, Hallden G, Beguinot F, Formisano P, Portella G. Inhibition of autophagy enhances the effects of E1A defective oncolytic adenovirus dl922-947 against glioma cells in vitro and in vivo. *Hum Gene Ther Under Review*.
- Boyer J, Rohleder K, Ketner G. Adenovirus E4 34k and E4 11k inhibit double strand break repair and are physically associated with the cellular DNA-dependent protein kinase. *Virology* 1999;263:307-12.
- Braithwaite AW, Russell IA. Induction of cell death by adenoviruses. *Apoptosis* 2001;6:359-70.
- Breitbach CJ, Burke J, Jonker D, Stephenson J, Haas AR, Chow LQ, Nieva J, Hwang TH, Moon A, Patt R, Pelusio A, Le Boeuf F, Burns J, Evgin L, De Silva N, Cvancic S, Robertson T, Je JE, Lee YS, Parato K, Diallo JS, Fenster A, Daneshmand M, Bell JC, Kirn DH. Intravenous delivery of a multi-mechanistic cancer-targeted oncolytic poxvirus in humans. *Nature* 2011;477:99-102.
- Cahill DP, Kinzler KW, Vogelstein B, Lengauer C. Genetic instability and darwinian selection in tumours. *Trends Cell Biol* 1999;9:M57-60.
- Cassel WA, Garrett RE. Newcastle disease virus as an antineoplastic agent. *Cancer* 1965;18:863-8.
- Castedo M, Perfettini JL, Roumier T, Andreau K, Medema R, Kroemer G. Cell death by mitotic catastrophe: a molecular definition. *Oncogene* 2004;23:2825-37. Review.
- Chakravarti D, Ogryzko V, Kao HY, Nash A, Chen H, Nakatani Y, Evans RM. A viral mechanism for inhibition of p300 and PCAF acetyltransferase activity. *Cell* 1999;96:393-403.
- Chaurushiya MS, Weitzman MD. Viral manipulation of DNA repair and cell cycle checkpoints. *DNA Repair (Amst)* 2009;8:1166-76.
- Chen Y, DeWeese T, Dilley J, Zhang Y, Li Y, Ramesh N, Lee J, Pennathur-Das R, Radzyminski J, Wypych J, Brignetti D, Scott S, Stephens J, Karpf DB, Henderson DR, Yu DC. CV706, a prostate cancer-specific adenovirus variant, in combination with radiotherapy produces synergistic antitumor efficacy without increasing toxicity. *Cancer Res* 2001;61:5453-60.
- Chiocca EA. Oncolytic viruses. *Nat Rev Cancer* 2002;2:938-50.
- Chiou SK, Tseng CC, Rao L, White E. Functional complementation of the adenovirus E1B 19-kilodalton protein with Bcl-2 in the inhibition of apoptosis in infected cells. *J Virol* 1994;68:6553-66.
- Cody JJ, Douglas JT. Armed replicating adenoviruses for cancer virotherapy. *Cancer Gene Ther* 2009;16:473-88.

- Connell CM, Shibata A, Tookman LA, Archibald KM, Flak MB, Pirlo KJ, Lockley M, Wheatley SP, McNeish IA. Genomic DNA damage and ATR-Chk1 signaling determine oncolytic adenoviral efficacy in human ovarian cancer cells. *J Clin Invest* 2011;12:1283-97.
- Cordelier P, Biennu C, Lulka H, Marrache F, Bouisson M, Openheim A, Strayer DS, Vaysse N, Pradayrol L, Buscail L. Replication-deficient rSV40 mediate pancreatic gene transfer and long-term inhibition of tumor growth. *Cancer Gene Ther* 2007;14:19-29.
- Cornelis JJ, Lang SI, Stroh-Dege AY, Balboni G, Dinsart C, Rommelaere J. Cancer gene therapy through autonomous parvovirus-mediated gene transfer. *Curr Gene Ther* 2004;4:249-61.
- Csatory LK, Gosztonyi G, Szeberenyi J, Fabian Z, Liszka V, Bodey B, Csatory CM. TH-68/H oncolytic viral treatment in human high-grade gliomas. *J Neurooncol* 2004;67:83-93.
- Darzynkiewicz Z, Traganos F, Wlodkowic D. Impaired DNA damage response--an Achilles' heel sensitizing cancer to chemotherapy and radiotherapy. *Eur J Pharmacol* 2009;625:143-50.
- de Jager M, van Noort J, van Gent DC, Dekker C, Kanaar R, Wyman C. Human Rad50/Mre11 is a flexible complex that can tether DNA ends. *Mol Cell* 2001;8:1129-35.
- de Jager M, Wyman C, van Gent DC, Kanaar R. DNA end-binding specificity of human Rad50/Mre11 is influenced by ATP. *Nucleic Acids Res* 2002;30:4425-31.
- de Jong RN, van der Vliet PC, Brenkman AB. Adenovirus DNA replication: protein priming, jumping back and the role of the DNA binding protein DBP. *Curr Top Microbiol Immunol* 2003;272:187-211.
- Debbas M, White E. Wild-type p53 mediates apoptosis by E1A, which is inhibited by E1B. *Genes Dev* 1993;7:546-54.
- Desai-Mehta A, Cerosaletti KM, Concannon P. Distinct functional domains of nibrin mediate Mre11 binding, focus formation, and nuclear localization. *Mol Cell Biol* 2001;21:2184-91.
- DeWeese TL, van der Poel H, Li S, Mikhak B, Drew R, Goemann M, Hamper U, DeJong R, Detorie N, Rodriguez R, Haulk T, DeMarzo AM, Piantadosi S, Yu DC, Chen Y, Henderson DR, Carducci MA, Nelson WG, Simons JW. A phase I trial of CV706, a replication-competent, PSA selective oncolytic adenovirus, for the treatment of locally recurrent prostate cancer following radiation therapy. *Cancer Res.* 2001 Oct 15;61(20):7464-72.
- Dilley J, Reddy S, Ko D, Nguyen N, Rojas G, Working P, Yu DC. Oncolytic adenovirus CG7870 in combination with radiation demonstrates synergistic enhancements of antitumor efficacy without loss of specificity. *Cancer Gene Ther* 2005;12:715-22.
- Dmitriev I, Kashentseva E, Rogers BE, Krasnykh V, Curiel DT. Ectodomain of coxsackievirus and adenovirus receptor genetically fused to

epidermal growth factor mediates adenovirus targeting to epidermal growth factor receptor-positive cells. *J Virol* 2000;74:6875-84.

- Dodson H, Wheatley SP, Morrison CG. Involvement of centrosome amplification in radiation-induced mitotic catastrophe. *Cell Cycle* 2007;6:364-70.
- Downs JA, Nussenzweig MC, Nussenzweig A. Chromatin dynamics and the preservation of genetic information. *Nature* 2007;447:951-8.
- el-Deiry WS, Tokino T, Velculescu VE, Levy DB, Parsons R, Trent JM, Lin D, Mercer WE, Kinzler KW, Vogelstein B. WAF1, a potential mediator of p53 tumor suppression. *Cell* 1993;75:817-25.
- Elledge SJ. Cell cycle checkpoints: preventing an identity crisis. *Science* 1996;274:1664-72.
- Evans JD, Hearing P. Relocalization of the Mre11-Rad50-Nbs1 complex by the adenovirus E4 ORF3 protein is required for viral replication. *J Virol* 2005;79:6207-15.
- Falck J, Mailand N, Syljuåsen RG, Bartek J, Lukas J. The ATM-Chk2-Cdc25A checkpoint pathway guards against radioresistant DNA synthesis. *Nature* 2001;410:842-7.
- Fields BN, Knipe DM, Howley PM. *Fields virology*. Philadelphia: Lippincott-Raven, 1996.
- Freeman AI, Zakay-Rones Z, Gomori JM, Linetsky E, Rasooly L, Greenbaum E, Rozenman-Yair S, Panet A, Libson E, Irving CS, Galun E, Siegal T. Phase I/II trial of intravenous NDV-HUJ oncolytic virus in recurrent glioblastoma multiforme. *Mol Ther* 2006;13:221-8.
- Freytag SO, Movsas B, Aref I, Stricker H, Peabody J, Pegg J, Zhang Y, Barton KN, Brown SL, Lu M, Savera A, Kim JH. Phase I trial of replication-competent adenovirus-mediated suicide gene therapy combined with IMRT for prostate cancer. *Mol Ther* 2007;15:1016-23.
- Freytag SO, Stricker H, Pegg J, Paielli D, Pradhan DG, Peabody J, DePeralta-Venturina M, Xia X, Brown S, Lu M, Kim JH. Phase I study of replication-competent adenovirus-mediated double-suicide gene therapy in combination with conventional-dose three-dimensional conformal radiation therapy for the treatment of newly diagnosed, intermediate- to high-risk prostate cancer. *Cancer Res* 2003;63:7497-506.
- Fueyo J, Alemany R, Gomez-Manzano C, Fuller GN, Khan A, Conrad CA, Liu TJ, Jiang H, Lemoine MG, Suzuki K, Sawaya R, Curiel DT, Yung WK, Lang FF. Preclinical characterization of the antiglioma activity of a tropism-enhanced adenovirus targeted to the retinoblastoma pathway. *J Natl Cancer Inst* 2003;95:652-60.
- Fueyo J, Gomez-Manzano C, Alemany R, Lee PS, McDonnell TJ, Mitlianga P, Shi YX, Levin VA, Yung WK, Kyritsis AP. A mutant oncolytic adenovirus targeting the Rb pathway produces anti-glioma effect in vivo. *Oncogene* 2000;19:2-12.

- Georger B, Grill J, Opolon P, Morizet J, Aubert G, Lecluse Y, van Beusechem VW, Gerritsen WR, Kirn DH, Vassal G. Potentiation of radiation therapy by the oncolytic adenovirus dl1520 (ONYX-015) in human malignant glioma xenografts. *Br J Cancer* 2003;89:577-84.
- Goodhead DT. Initial events in the cellular effects of ionizing radiations: clustered damage in DNA. *Int J Radiat Biol* 1994;65:7-17.
- Goodrum FD, Shenk T, Ornelles DA. Adenovirus early region 4 34-kilodalton protein directs the nuclear localization of the early region 1B 55-kilodalton protein in primate cells. *J. Virol* 1996;70:6323-35.
- Gromeier M, Lachmann S, Rosenfeld MR, Gutin PH, Wimmer E. Intergeneric poliovirus recombinants for the treatment of malignant glioma. *Proc Natl Acad Sci U S A* 2000;97:6803-8.
- Guo ZS, Naik A, O'Malley ME, Popovic P, Demarco R, Hu Y, Yin X, Yang S, Zeh HJ, Moss B, Lotze MT, Bartlett DL. The enhanced tumor selectivity of an oncolytic vaccinia lacking the host range and antiapoptosis genes SPI-1 and SPI-2. *Cancer Res* 2005;65:9991-8.
- Halbert DN, Cutt JR, Shenk T. Adenovirus early region 4 encodes functions required for efficient DNA replication, late gene expression, and host cell shutoff. *J Virol* 1985;56:250-7.
- Halicka HD, Zhao H, Podhorecka M, Traganos F, Darzynkiewicz Z. Cytometric detection of chromatin relaxation, an early reporter of DNA damage response. *Cell Cycle* 2009;8:2233-7.
- Hall AR, Dix BR, O'Carroll SJ, Braithwaite AW. p53-dependent cell death/apoptosis is required for a productive adenovirus infection. *Nat Med* 1998;4:1068-72.
- Hallenbeck PL, Chang YN, Hay C, Golightly D, Stewart D, Lin J, Phipps S, Chiang YL. A novel tumor-specific replication-restricted adenoviral vector for gene therapy of hepatocellular carcinoma. *Hum Gene Ther* 1999;10:1721-33.
- Hamamori Y, Sartorelli V, Ogryzko V, Puri PL, Wu HY, Wang JY, Nakatani Y, Keddes L. Regulation of histone acetyltransferases p300 and PCAF by the bHLH protein twist and adenoviral oncoprotein E1A. *Cell* 1999;96:405-13.
- Harada JN, Shevchenko A, Pallas DC, Berk AJ. Analysis of the adenovirus E1B-55K-anchored proteome reveals its link to ubiquitination machinery. *J Virol* 2002;76:9194-206.
- Harlow E, Whyte P, Franza BR Jr, Schley C. Association of adenovirus early-region 1A proteins with cellular polypeptides. *Mol Cell Biol* 1986;6:1579-89.
- Harrington KJ, Hingorani M, Tanay MA, Hickey J, Bhide SA, Clarke PM, Renouf LC, Thway K, Sibtain A, McNeish IA, Newbold KL, Goldsweig H, Coffin R, Nutting CM. Phase I/II study of oncolytic HSV GM-CSF in combination with radiotherapy and cisplatin in untreated stage III/IV squamous cell cancer of the head and neck. *Clin Cancer Res* 2010;16:4005-15.

- Harrington KJ, Karapanagiotou EM, Roulstone V, Twigger KR, White CL, Vidal L, Beirne D, Prestwich R, Newbold K, Ahmed M, Thway K, Nutting CM, Coffey M, Harris D, Vile RG, Pandha HS, Debono JS, Melcher AA. Two-stage phase I dose-escalation study of intratumoral reovirus type 3 dearing and palliative radiotherapy in patients with advanced cancers. *Clin Cancer Res* 2010;16:3067-77.
- Heise C, Hermiston T, Johnson L, Brooks G, Sampson-Johannes A, Williams A, Hawkins L, Kirn D. An adenovirus E1A mutant that demonstrates potent and selective systemic anti-tumoral efficacy. *Nat Med* 2000;6:1134-9.
- Hermann PC, Huber SL, Herrler T, Aicher A, Ellwart JW, Guba M, Bruns CJ, Heeschen C. Distinct populations of cancer stem cells determine tumor growth and metastatic activity in human pancreatic cancer. *Cell Stem Cell* 2007;1:313-23.
- Hingorani M, White CL, Agrawal VK, Vidal L, Melcher A, Harrington KJ. Combining radiation and cancer gene therapy: a potential marriage of physical and biological targeting? *Curr Cancer Drug Targets* 2007;7:389-409.
- Hirasawa K, Nishikawa SG, Norman KL, Coffey MC, Thompson BG, Yoon CS, Waisman DM, Lee PW. Systemic reovirus therapy of metastatic cancer in immune-competent mice. *Cancer Res* 2003;63:348-53.
- Hopfner KP, Karcher A, Shin DS, Craig L, Arthur LM, Carney JP, Tainer JA. Structural biology of Rad50 ATPase: ATP-driven conformational control in DNA double-strand break repair and the ABC-ATPase superfamily. *Cell* 2000;101:789-800.
- Hsieh CL, Yang L, Miao L, Yeung F, Kao C, Yang H, Zhou HE, Chung LW. A novel targeting modality to enhance adenoviral replication by vitamin D(3) in androgen-independent human prostate cancer cells and tumors. *Cancer Res* 2002;62:3084-92.
- Idema S, Lamfers ML, van Beusechem VW, Noske DP, Heukelom S, Moeniralm S, Gerritsen WR, Vandertop WP, Dirven CM. AdDelta24 and the p53-expressing variant AdDelta24-p53 achieve potent anti-tumor activity in glioma when combined with radiotherapy. *J Gene Med* 2007;9:1046-56.
- Iliakis G, Wang Y, Guan J, Wang H. DNA damage checkpoint control in cells exposed to ionizing radiation. *Oncogene* 2003;22:5834-47.
- Immonen A, Vapalahti M, Tyynelä K, Hurskainen H, Sandmair A, Vanninen R, Langford G, Murray N, Ylä-Herttuala S. AdvHSV-tk gene therapy with intravenous ganciclovir improves survival in human malignant glioma: a randomised, controlled study. *Mol Ther* 2004;10:967-72.
- Ishii H, Iwatsuki M, Ieta K, Ohta D, Haraguchi N, Mimori K, Mori M. Cancer stem cells and chemoradiation resistance. *Cancer Sci* 2008;99:1871-7.
- Ito H, Aoki H, Kühnel F, Kondo Y, Kubicka S, Wirth T, Iwado E, Iwamaru A, Fujiwara K, Hess KR, Lang FF, Sawaya R, Kondo S. Autophagic cell death of malignant glioma cells induced by a conditionally replicating adenovirus. *J Natl Cancer Inst* 2006;98:625-36.

- Jackson SP. Sensing and repairing DNA double-strand breaks. *Carcinogenesis* 2002;23:687-96.
- Kao CC, Yew PR, Berk AJ. Domains required for in vitro association between the cellular p53 and the adenovirus 2 E1B 55K proteins. *Virology* 1990;179:806-14.
- Kim JH, Oh JY, Park BH, Lee DE, Kim JS, Park HE, Roh MS, Je JE, Yoon JH, Thorne SH, Kirn D, Hwang TH. Systemic armed oncolytic and immunologic therapy for cancer with JX-594, a targeted poxvirus expressing GM-CSF. *Mol Ther* 2006;14:361-70.
- Kim YC, Gerlitz G, Furusawa T, Catez F, Nussenzweig A, Oh KS, Kraemer KH, Shiloh Y, Bustin M. Activation of ATM depends on chromatin interactions occurring before induction of DNA damage. *Nat Cell Biol.* 2009;11:92-6.
- Kirn D. Oncolytic virotherapy for cancer with the adenovirus dl1520 (Onyx-015): results of phase I and II trials. *Expert Opin Biol Ther* 2001;1:525-38. Review.
- Kobayashi J, Antoccia A, Tauchi H, Matsuura S, Komatsu K. NBS1 and its functional role in the DNA damage response. *DNA Repair (Amst)* 2004;3:855-61.
- Kruyt FA, Curiel DT. Toward a new generation of conditionally replicating adenoviruses: pairing tumor selectivity with maximal oncolysis. *Hum Gene Ther* 2002;13:485-95.
- Kumar S, Gao L, Yeagy B, Reid T. Virus combinations and chemotherapy for the treatment of human cancers. *Curr Opin Mol Ther* 2008;10:371-9.
- Lamfers ML, Grill J, Dirven CM, Van Beusechem VW, Georger B, Van Den Berg J, Alemany R, Fueyo J, Curiel DT, Vassal G, Pinedo HM, Vandertop WP, Gerritsen WR. Potential of the conditionally replicative adenovirus Ad5-Delta24RGD in the treatment of malignant gliomas and its enhanced effect with radiotherapy. *Cancer Res* 2002;62:5736-42.
- Lavin MF, Delia D, Chessa L. ATM and the DNA damage response. Workshop on ataxia-telangiectasia and related syndromes. *EMBO Rep* 2006;7:154-60.
- Li C, Heidt DG, Dalerba P, Burant CF, Zhang L, Adsay V, Wicha M, Clarke MF, Simeone DM. Identification of pancreatic cancer stem cells. *Cancer Res* 2007;67:1030-7.
- Libertini S, Abagnale A, Passaro C, Botta G, Barbato S, Chieffi P, Portella G. AZD1152 negatively affects the growth of anaplastic thyroid carcinoma cells and enhances the effects of oncolytic virus dl922-947. *Endocr Relat Cancer* 2011;18:129-41.
- Libertini S, Iacuzzo I, Ferraro A, Vitale M, Bifulco M, Fusco A, Portella G. Lovastatin enhances the replication of the oncolytic adenovirus dl1520 and its antineoplastic activity against anaplastic thyroid carcinoma cells. *Endocrinology* 2007;148:5186-94.

- Libertini S, Iacuzzo I, Perruolo G, Scala S, Ieranò C, Franco R, Hallden G, Portella G. Bevacizumab increases viral distribution in human anaplastic thyroid carcinoma xenografts and enhances the effects of E1A-defective adenovirus dl922-947. *Clin Cancer Res* 2008;14:6505-14.
- Lieber MR. The mechanism of human nonhomologous DNA end joining. *J Biol Chem* 2008;283:1-5.
- Lilley CE, Schwartz RA, Weitzman MD. Using or abusing: viruses and the cellular DNA damage response. *Trends Microbiol* 2007;15:119-26.
- Lisby M, Barlow JH, Burgess RC, Rothstein R. Choreography of the DNA damage response: spatiotemporal relationships among checkpoint and repair proteins. *Cell* 2004;118:699-713.
- Liu C, Zhang Y, Liu MM, Zhou H, Chowdhury W, Lupold SE, Dewese TL, Rodriguez R. Evaluation of continuous low dose rate versus acute single high dose rate radiation combined with oncolytic viral therapy for prostate cancer. *Int J Radiat Biol.* 2010;86:220-9.
- Liu Y, Shevchenko A, Shevchenko A, Berk AJ. Adenovirus exploits the cellular aggresome response to accelerate inactivation of the MRN complex. *J Virol* 2005;79:14004-16.
- Lockley M, Fernandez M, Wang Y, Li NF, Conroy S, Lemoine N, McNeish I. Activity of the adenoviral E1A deletion mutant dl922-947 in ovarian cancer: comparison with E1A wild-type viruses, bioluminescence monitoring, and intraperitoneal delivery in icodextrin. *Cancer Res* 2006;66:989-98.
- Lorence RM, Pecora AL, Major PP, Hotte SJ, Laurie SA, Roberts MS, Groene WS, Bamat MK. Overview of phase I studies of intravenous administration of PV701, an oncolytic virus. *Curr Opin Mol Ther* 2003;5:618-24.
- Martuza RL. Molecular neurosurgery for glial and neuronal disorders. *Stereotact Funct Neurosurg* 1992;59:92-9.
- Maser RS, Monsen KJ, Nelms BE, Petrini JH. hMre11 and hRad50 nuclear foci are induced during the normal cellular response to DNA double-strand breaks. *Mol Cell Biol* 1997;17:6087-96.
- Matsubara S, Wada Y, Gardner TA, Egawa M, Park MS, Hsieh CL, Zhau HE, Kao C, Kamidono S, Gillenwater JY, Chung LW. A conditional replication-competent adenoviral vector, Ad-OC-E1a, to cotarget prostate cancer and bone stroma in an experimental model of androgen-independent prostate cancer bone metastasis. *Cancer Res* 2001;61:6012-9.
- Matsuoka S, Huang M, Elledge SJ. Linkage of ATM to cell cycle regulation by the Chk2 protein kinase. *Science* 1998;282:1893-7.
- McCart JA, Ward JM, Lee J, Hu Y, Alexander HR, Libutti SK, Moss B, Bartlett DL. Systemic cancer therapy with a tumor-selective vaccinia virus mutant lacking thymidine kinase and vaccinia growth factor genes. *Cancer Res* 2001;61:8751-7.

- Metting NF, Little JB. Transient failure to dephosphorylate the cdc2-cyclin B1 complex accompanies radiation-induced G2-phase arrest in HeLa cells. *Radiat Res* 1995;143:286-92.
- Mineta T, Rabkin SD, Yazaki T, Hunter WD, Martuza RL. Attenuated multi-mutated herpes simplex virus-1 for the treatment of malignant gliomas. *Nat Med* 1995;1:938-43.
- Miyashita T, Reed JC. Tumor suppressor p53 is a direct transcriptional activator of the human bax gene. *Cell* 1995;80:293-9.
- Moran E. DNA tumor virus transforming proteins and the cell cycle. *Curr Opin Genet Dev* 1993;3:63-70.
- Moreno-Herrero F, de Jager M, Dekker NH, Kanaar R, Wyman C, Dekker C. Mesoscale conformational changes in the DNA-repair complex Rad50/Mre11/Nbs1 upon binding DNA. *Nature* 2005;437:440-3.
- Mousset S, Rommelaere J. Minute virus of mice inhibits cell transformation by simian virus 40. *Nature* 1982;300:537-9.
- Mundt AJ, Vijayakumar S, Nemunaitis J, Sandler A, Schwartz H, Hanna N, Peabody T, Senzer N, Chu K, Rasmussen CS, Kessler PD, Rasmussen HS, Warso M, Kufe DW, Gupta TD, Weichselbaum RR. A Phase I trial of TNFerade biologic in patients with soft tissue sarcoma in the extremities. *Clin Cancer Res* 2004;10:5747-53.
- Nandi S, Ulasov IV, Tyler MA, Sugihara AQ, Molinero L, Han Y, Zhu ZB, Lesniak MS. Low-dose radiation enhances survivin-mediated virotherapy against malignant glioma stem cells. *Cancer Res* 2008;68:5778-84.
- Nemunaitis J, Ganly I, Khuri F, Arseneau J, Kuhn J, McCarty T, Landers S, Maples P, Romel L, Randlev B, Reid T, Kaye S, Kirn D. Selective replication and oncolysis in p53 mutant tumors with ONYX-015, an E1B-55kD gene-deleted adenovirus, in patients with advanced head and neck cancer: a phase II trial. *Cancer Res* 2000;60:6359-66.
- Nevins JR. Adenovirus E1A: transcription regulation and alteration of cell growth control. *Curr Top Microbiol Immunol* 1995;199:25-32.
- Norman KL, Coffey MC, Hirasawa K, Demetrick DJ, Nishikawa SG, DiFrancesco LM, Strong JE, Lee PW. Reovirus oncolysis of human breast cancer. *Hum Gene Ther* 2002;13:641-52.
- Nyberg KA, Michelson RJ, Putnam CW, Weinert TA. Toward maintaining the genome: DNA damage and replication checkpoints. *Annu Rev Genet* 2002;36:617-56.
- Okuno Y, Asada T, Yamanishi K, Otsuka T, Takahashi M, Tanioka T, Aoyama H, Fukui O, Matsumoto K, Uemura F, Wada A. Studies on the use of mumps virus for treatment of human cancer. *Biken J* 1978;21:37-49.
- O'Shea CC, Soria C, Bagus B, McCormick F. Heat shock phenocopies E1B-55K late functions and selectively sensitizes refractory tumor cells to ONYX-015 oncolytic viral therapy. *Cancer Cell* 2005;8:61-74.
- Ottolino-Perry K, Diallo JS, Lichty BD, Bell JC, McCart JA. Intelligent design: combination therapy with oncolytic viruses. *Mol Ther* 2010;18:251-63.

- Pack GT. Note on the experimental use of rabies vaccine for melanomatosis. *AMA Arch Derm Syphilol* 1950;62:694-5.
- Parato KA, Senger D, Forsyth PA, Bell JC. Recent progress in the battle between oncolytic viruses and tumours. *Nat Rev Cancer* 2005;5:965-76.
- Parreño M, Garriga J, Limón A, Albrecht JH, Graña X. E1A modulates phosphorylation of p130 and p107 by differentially regulating the activity of G1/S cyclin/CDK complexes. *Oncogene* 2001;20:4793-806.
- Paull TT, Gellert M. A mechanistic basis for Mre11-directed DNA joining at microhomologies. *Proc Natl Acad Sci U S A* 2000;97:6409-14.
- Pilder S, Moore M, Logan J, Shenk T. The adenovirus E1B-55K transforming polypeptide modulates transport or cytoplasmic stabilization of viral and host cell mRNAs. *Mol Cell Biol* 1986;6:470-6.
- Portella G, Pacelli R, Libertini S, Cella L, Vecchio G, Salvatore M, Fusco A. ONYX-015 enhances radiation-induced death of human anaplastic thyroid carcinoma cells. *J Clin Endocrinol Metab.* 2003 Oct;88(10):5027-32.
- Portella G, Scala S, Vitagliano D, Vecchio G, Fusco A. ONYX-015, an E1B gene-defective adenovirus, induces cell death in human anaplastic thyroid carcinoma cell lines. *J Clin Endocrinol Metab* 2002;87:2525-31.
- Post DE, Khuri FR, Simons JW, Van Meir EG. Replicative oncolytic adenoviruses in multimodal cancer regimens. *Hum Gene Ther* 2003;14:933-46.
- Powers JT, Hong S, Mayhew CN, Rogers PM, Knudsen ES, Johnson DG. E2F1 uses the ATM signaling pathway to induce p53 and Chk2 phosphorylation and apoptosis. *Mol Cancer Res* 2004;2:203-14.
- Prise KM, Schettino G, Folkard M, Held KD. New insights on cell death from radiation exposure. *Lancet Oncol* 2005;6:520-8.
- Querido E, Blanchette P, Yan Q, Kamura T, Morrison M, Boivin D, Kaelin WG, Conaway RC, Conaway JW, Branton PE. Degradation of p53 by adenovirus E4orf6 and E1B55K proteins occurs via a novel mechanism involving a Cullin-containing complex. *Genes Dev* 2001;15:3104-17.
- Rajecki M, af Hällström T, Hakkarainen T, Nokisalmi P, Hautaniemi S, Nieminen AI, Tenhunen M, Rantanen V, Desmond RA, Chen DT, Guse K, Stenman UH, Gargini R, Kapanen M, Klefström J, Kanerva A, Pesonen S, Ahtiainen L, Hemminki A. Mre11 inhibition by oncolytic adenovirus associates with autophagy and underlies synergy with ionizing radiation. *Int J Cancer* 2009;125:2441-9.
- Rao L, Debbas M, Sabbatini P, Hockenbery D, Korsmeyer S, White E. The adenovirus E1A proteins induce apoptosis, which is inhibited by the E1B 19-kDa and Bcl-2 proteins. *Proc Natl Acad Sci U S A* 1992;89:7742-6.
- Reid T, Galanis E, Abbruzzese J, Sze D, Andrews J, Romel L, Hatfield M, Rubin J, Kirn D. Intra-arterial administration of a replication-selective adenovirus (dl1520) in patients with colorectal carcinoma metastatic to the liver: a phase I trial. *Gene Ther* 2001;8:1618-26.
- Reid T, Galanis E, Abbruzzese J, Sze D, Wein LM, Andrews J, Randlev B, Heise C, Uprichard M, Hatfield M, Rome L, Rubin J, Kirn D. Hepatic

arterial infusion of a replication-selective oncolytic adenovirus (dl1520): phase II viral, immunologic, and clinical endpoints. *Cancer Res* 2002;62:6070-9.

- Ries SJ, Brandts CH, Chung AS, Biederer CH, Hann BC, Lipner EM, McCormick F, Korn WM. Loss of p14ARF in tumor cells facilitates replication of the adenovirus mutant dl1520 (ONYX-015). *Nat Med* 2000;6:1128-33.
- Robert A, Miron MJ, Champagne C, Gingras MC, Branton PE, Lavoie JN. Distinct cell death pathways triggered by the adenovirus early region 4 ORF 4 protein. *J Cell Biol* 2002;158:519-28.
- Rodriguez R, Schuur ER, Lim HY, Henderson GA, Simons JW, Henderson DR. Prostate attenuated replication competent adenovirus (ARCA) CN706: a selective cytotoxic for prostate-specific antigen-positive prostate cancer cells. *Cancer Res* 1997;57:2559-63.
- Roussel MF. The INK4 family of cell cycle inhibitors in cancer. *Oncogene* 1999;18:5311-7.
- Rowe WP, Huebner RJ, Gilmore LK, Parrott RH, Ward TG. Isolation of a cytopathogenic agent from human adenoids undergoing spontaneous degeneration in tissue culture. *Proc Soc Exp Biol Med* 1953;84:570-3
- Schweppe RE, Klopper JP, Korch C, Pugazhenti U, Benezra M, Knauf JA, Fagin JA, Marlow LA, Copland JA, Smallridge RC, Haugen BR. Deoxyribonucleic acid profiling analysis of 40 human thyroid cancer cell lines reveals cross-contamination resulting in cell line redundancy and misidentification. *J Clin Endocrinol Metab* 2008;93:4331-41.
- Seidman MA, Hogan SM, Wendland RL, Worgall S, Crystal RG, Leopold PL. Variation in adenovirus receptor expression and adenovirus vector-mediated transgene expression at defined stages of the cell cycle. *Mol Ther* 2001;4:13-21.
- Senzer N, Mani S, Rosemurgy A, Nemunaitis J, Cunningham C, Guha C, Bayol N, Gillen M, Chu K, Rasmussen C, Rasmussen H, Kufe D, Weichselbaum R, Hanna N. TNFerade biologic, an adenovector with a radiation-inducible promoter, carrying the human tumor necrosis factor alpha gene: a phase I study in patients with solid tumors. *J Clin Oncol* 2004;22:592-601.
- Shah AC, Benos D, Gillespie GY, Markert JM. Oncolytic viruses: clinical applications as vectors for the treatment of malignant gliomas. *J Neurooncol* 2003;65:203-26.
- Shah AN, Summy JM, Zhang J, Park SI, Parikh NU, Gallick GE. Development and characterization of gemcitabine-resistant pancreatic tumor cells. *Ann Surg Oncol* 2007;14:3629-37.
- Shenk T. Adenoviridae: The viruses and their replication. In *Virology* 1996. B.N. Fields, D.M. Knipe, and P.M. Howley, eds. (Lippincott-Raven, New York) pp. 2111-2148.
- Sherr CJ. The Pezcoller lecture: cancer cell cycles revisited. *Cancer Res* 2000;60:3689-95.

- Sinkovics J, Horvath J. New developments in the virus therapy of cancer: a historical review. *Intervirology* 1993;36:193-214.
- Sinkovics JG, Horvath JC. Newcastle disease virus (NDV): brief history of its oncolytic strains. *J Clin Virol* 2000;16:1-15.
- Smallridge RC, Marlow LA, Copland JA. Anaplastic thyroid cancer: molecular pathogenesis and emerging therapies. *Endocr Relat Cancer* 2009;16:17-44.
- Southam CM, Hilleman CM, Hilleman MR, Werner JH. Pathogenicity and oncolytic capacity of RI virus strain RI-67 in man. *J Lab Clin Med* 1956;47:573-82
- Southam CM, Moore AE. Clinical studies of viruses as antineoplastic agents with particular reference to Egypt 101 virus. *Cancer* 1952;5:1025-34.
- Stanziale SF, Petrowsky H, Joe JK, Roberts GD, Zager JS, Gusani NJ, Ben-Porat L, Gonen M, Fong Y. Ionizing radiation potentiates the antitumor efficacy of oncolytic herpes simplex virus G207 by upregulating ribonucleotide reductase. *Surgery* 2002;132:353-9.
- Steegenga WT, Riteco N, Jochemsen AG, Fallaux FJ, Bos JL. The large E1B protein together with the E4orf6 protein target p53 for active degradation in adenovirus infected cells. *Oncogene* 1998;16:349-57.
- Stracker TH, Carson CT, Weitzman MD. Adenovirus oncoproteins inactivate the Mre11-Rad50-NBS1 DNA repair complex. *Nature* 2002;418:348-52.
- Stracker TH, Lee DV, Carson CT, Araujo FD, Ornelles DA, Weitzman MD. Serotype-specific reorganization of the Mre11 complex by adenoviral E4orf3 proteins. *J Virol* 2005;79:6664-73.
- Strayer DS, Cordelier P, Kondo R, Liu B, Matskevich AA, McKee HJ, Nichols CN, Mitchell CB, Geverd DA, White MK, Strayer MS. What they are, how they work and why they do what they do? The story of SV40-derived gene therapy vectors and what they have to offer. *Curr Gene Ther* 2005;5:151-65.
- Stucki M, Jackson SP. gammaH2AX and MDC1: anchoring the DNA-damage-response machinery to broken chromosomes. *DNA Repair (Amst)* 2006;5:534-43.
- Swisher SG, Roth JA, Komaki R, Gu J, Lee JJ, Hicks M, Ro JY, Hong WK, Merritt JA, Ahrar K, Atkinson NE, Correa AM, Dolormente M, Dreiling L, El-Naggar AK, Fossella F, Francisco R, Glisson B, Grammer S, Herbst R, Huaranga A, Kemp B, Khuri FR, Kurie JM, Liao Z, McDonnell TJ, Morice R, Morello F, Munden R, Papadimitrakopoulou V, Pisters KM, Putnam JB Jr, Sarabia AJ, Shelton T, Stevens C, Shin DM, Smythe WR, Vaporciyan AA, Walsh GL, Yin M. Induction of p53-regulated genes and tumor regression in lung cancer patients after intratumoral delivery of adenoviral p53 (INGN 201) and radiation therapy. *Clin Cancer Res* 2003;9:93-101.
- Tauber B, Dobner T. Molecular regulation and biological function of adenovirus early region: the E4 ORFs. *Gene* 2001;278:1-23.

- Taylor MW, Cordell B, Souhrada M, Prather S. Viruses as an aid to cancer therapy: regression of solid and ascites tumors in rodents after treatment with bovine enterovirus. *Proc Natl Acad Sci U S A* 1971;68:836-40.
- Teh BS, Ayala G, Aguilar L, Mai WY, Timme TL, Vlachaki MT, Miles B, Kadmon D, Wheeler T, Caillouet J, Davis M, Carpenter LS, Lu HH, Chiu JK, Woo SY, Thompson T, Aguilar-Cordova E, Butler EB. Phase I-II trial evaluating combined intensity-modulated radiotherapy and in situ gene therapy with or without hormonal therapy in treatment of prostate cancer-interim report on PSA response and biopsy data. *Int J Radiat Oncol Biol Phys* 2004;58:1520-9.
- Todo T, Rabkin SD, Sundaresan P, Wu A, Meehan KR, Herscowitz HB, Martuza RL. Systemic antitumor immunity in experimental brain tumor therapy using a multimutated, replication-competent herpes simplex virus. *Hum Gene Ther* 1999;10:2741-55.
- Touchefeu Y, Vassaux G, Harrington KJ. Oncolytic viruses in radiation oncology. *Radiother Oncol* 2011;99:262-70.
- Toyoda H, Ido M, Hayashi T, Gabazza EC, Suzuki K, Kisenge RR, Kang J, Hori H, Komada Y. Experimental treatment of human neuroblastoma using live-attenuated poliovirus. *Int J Oncol* 2004;24:49-58.
- Uziel T, Lerenthal Y, Moyal L, Andegeko Y, Mittelman L, Shiloh Y. Requirement of the MRN complex for ATM activation by DNA damage. *EMBO J* 2003;22:5612-21.
- Vähä-Koskela MJ, Kallio JP, Jansson LC, Heikkilä JE, Zakhartchenko VA, Kallajoki MA, Kähäri VM, Hinkkanen AE. Oncolytic capacity of attenuated replicative semliki forest virus in human melanoma xenografts in severe combined immunodeficient mice. *Cancer Res* 2006;66:7185-94.
- Wakimoto H, Fulci G, Tyminski E, Chiocca EA. Altered expression of antiviral cytokine mRNAs associated with cyclophosphamide's enhancement of viral oncolysis. *Gene Ther* 2004;11:214-23.
- Watrin E, Peters JM. Cohesin and DNA damage repair. *Exp Cell Res* 2006;312:2687-93.
- Weiden MD, Ginsberg HS. Deletion of the E4 region of the genome produces adenovirus DNA concatemers. *Proc. Natl. Acad. Sci. USA* 1994;91:153-7.
- Weinberg DH, Ketner G. Adenoviral early region 4 is required for efficient viral DNA replication and for late gene expression. *J Virol* 1986;57:833-8.
- Weitzman MD, Ornelles DA. Inactivating intracellular antiviral responses during adenovirus infection. *Oncogene* 2005;24:7686-96.
- Xia ZJ, Chang JH, Zhang L, Jiang WQ, Guan ZZ, Liu JW, Zhang Y, Hu XH, Wu GH, Wang HQ, Chen ZC, Chen JC, Zhou QH, Lu JW, Fan QX, Huang JJ, Zheng X. Phase III randomized clinical trial of intratumoral injection of E1B gene-deleted adenovirus (H101) combined with cisplatin-based

chemotherapy in treating squamous cell cancer of head and neck or esophagus. *Ai Zheng* 2004;23:1666-70.

- Xiao Z, Chen Z, Gunasekera AH, Sowin TJ, Rosenberg SH, Fesik S, Zhang H. Chk1 mediates S and G2 arrests through Cdc25A degradation in response to DNA-damaging agents. *J Biol Chem* 2003;278:21767-73.
- Xiong Y, Hannon GJ, Zhang H, Casso D, Kobayashi R, Beach D. p21 is a universal inhibitor of cyclin kinases. *Nature* 1993;366:701-4.
- Yang WQ, Senger D, Muzik H, Shi ZQ, Johnson D, Brasher PM, Rewcastle NB, Hamilton M, Rutka J, Wolff J, Wetmore C, Curran T, Lee PW, Forsyth PA. Reovirus prolongs survival and reduces the frequency of spinal and leptomeningeal metastases from medulloblastoma. *Cancer Res* 2003;63:3162-72.
- Yang WQ, Senger DL, Lun XQ, Muzik H, Shi ZQ, Dyck RH, Norman K, Brasher PM, Rewcastle NB, George D, Stewart D, Lee PW, Forsyth PA. Reovirus as an experimental therapeutic for brain and leptomeningeal metastases from breast cancer. *Gene Ther* 2004;11:1579-89.
- Yew PR, Berk AJ. Inhibition of p53 transactivation required for transformation by adenovirus early 1B protein. *Nature* 1992;357:82-5.
- Yew PR, Liu X, Berk AJ. Adenovirus E1B oncoprotein tethers a transcriptional repression domain to p53. *Genes Dev* 1994;8:190-202.
- Yoon AR, Kim JH, Lee YS, Kim H, Yoo JY, Sohn JH, Park BW, Yun CO. Markedly enhanced cytolysis by E1B-19kD-deleted oncolytic adenovirus in combination with cisplatin. *Hum Gene Ther* 2006;17:379-90.
- Zhang J, Powell SN. The role of the BRCA1 tumor suppressor in DNA double-strand break repair. *Mol Cancer Res* 2005;3:531-9.
- Zhang XP, Liu F, Wang W. Coordination between cell cycle progression and cell fate decision by the p53 and E2F1 pathways in response to DNA damage. *J Biol Chem* 2010;285:31571-80.
- Zhou BB, Elledge SJ. The DNA damage response: putting checkpoints in perspective. *Nature* 2000;408:433-9.
- Zhou PK, Sun Y, An J. Interaction between viral proteins and hosts and its disturbance in the cellular responses to ionising radiation. *Int J Radiat Biol* 2009;85:587-97.

Aurora B Expression in Post-Puberal Testicular Germ Cell Tumours

FRANCESCO ESPOSITO,¹ SILVANA LIBERTINI,¹ RENATO FRANCO,² ANTONELLA ABAGNALE,¹ LUIGI MARRA,² GIUSEPPE PORTELLA,¹ AND PAOLO CHIEFFI^{1,3*}

¹Dipartimento di Biologia e Patologia Cellulare e Molecolare, Università di Napoli "Federico II", Naples, Italy

²Istituto Nazionale dei Tumori "Fondazione G. Pascale", Naples, Italy

³Dipartimento di Medicina Sperimentale, II Università di Napoli, Naples, Italy

Aurora/lplI-related kinases are a conserved family of proteins that are essential for the regulation of chromosome segregation and cytokinesis during mitosis. Aberrant expression and activity of these kinases occur in a wide range of human tumours and have been implicated in mechanisms leading to mitotic spindle aberrations, aneuploidy, and genomic instability. Previous studies of our group have shown that Aurora B expression is restricted to specific germinal cells. In this study, we have evaluated by immunohistochemical analysis Aurora B expression in post-puberal testicular germ cell tumours (22 seminomas, 2 teratomas, 15 embryonal carcinomas, 5 mixed germinal tumours with a prominent yolk sac tumour component and 1 choriocarcinoma). The Aurora B protein expression was detected in all intratubular germ cell tumours, seminomas and embryonal carcinomas analysed but not in teratomas and yolk sac carcinomas. The immunohistochemical data were further confirmed by Western blot analysis. In addition, the kinase Aurora B was vigorously expressed in GC-1 cells line derived from murine spermatogonia. The block of Aurora B function induced by a pharmacological inhibitor significantly reduced the growth of GC-1 cells suggesting that Aurora B is a potential therapeutic target.

J. Cell. Physiol. 221: 435–439, 2009. © 2009 Wiley-Liss, Inc.

Post-puberal testicular germ cell tumours (TGCTs) represent the most common malignancy in males between 15 and 34 years of age, and represent a major cause of death attributable to cancer in this age group (Oosterhuis and Looijenga, 2005). TGCTs can be subdivided into seminoma and non-seminoma germ cell tumours (NSGCTs) including embryonal cell carcinoma, choriocarcinoma, yolk sac tumour and teratoma, both recognizing a unique histological precursor, the intratubular testicular germ cell tumour (ITGCT).

Neoplasms containing more than one tumour history are referred to as mixed germ cell tumours. Seminomas and NSGCTs do not only present distinctive clinical features, but they also show significant differences as far as therapy and prognosis are concerned (Chieffi, 2007).

Mitosis, the process by which a complete copy of the duplicated genome is precisely segregated by the microtubule spindle apparatus into two daughter cells, is an extraordinarily complex biological process. Serine threonine kinases of Aurora family (Aurora A, Aurora B and Aurora C) are key mitotic regulators required for genome stability and for the progression through the M phase and it is well known that the products of the Aurora genes are expressed in proliferating cells and are overexpressed in neoplastic cells (Tanaka et al., 1999). Expression and activity of Aurora B in proliferating tissues are cell cycle regulated: its expression peaks at G2-M transition and the kinase activity is maximal during mitosis.

Aurora B is a one of the component of the chromosomal passenger complex (CPC). CPC contains three non-enzymatic subunits, all of which are essential for the activity, localization, stability and substrate specificity of Aurora B. In human cells, these non-enzymatic subunits are Survivin, the inner centromere protein (INCENP), and Borealin. Aurora B is involved in chromosome segregation, spindle-checkpoint and cytokinesis, and alteration of each of these steps could induce aneuploidy, that is commonly found feature of cancer cells (Adams et al., 2001; Carmena and Earnshaw, 2003).

Aurora B expression has been studied in different human cancer and it has been shown that its expression directly correlates with malignancy in several human lesions such as non-small cell lung carcinoma (Smith et al., 2005; Vischioni et al., 2006), mesothelioma (López-Ríos et al., 2006), glioblastoma (Araki et al., 2004; Zeng et al., 2007), oral cancer (Qi et al., 2007), hepatocellular carcinoma (Kurai et al., 2005), and thyroid carcinomas (Sorrentino et al., 2005). High expression levels of Aurora B were detected in primary human colorectal cancers at various pathologic stages with a tendency to group in higher grades of malignancy (Katayama et al., 1999), and Aurora B expression directly correlates with Gleason grade in prostate cancer (Chieffi et al., 2006). However, it is not clear whether the observed overexpression of Aurora B is a mere reflection of the high proliferative index of cancerous cells or whether it is indeed causally related to tumorigenesis. It has been reported a direct link between Aurora B and carcinogenesis (Ota et al., 2002) and Aurora B kinase activity augments Ras-mediated cell

Francesco Esposito and Silvana Libertini contributed equally to this work.

Contract grant sponsor: Italian Ministry of Education;

Contract grant number: MIUR-PRIN 2007.

Contract grant sponsor: Second University of Naples;

Contract grant number: Ateneo 2008.

Contract grant sponsor: Associazione Italiana per la Ricerca sul Cancro (AIRC).

*Correspondence to: Paolo Chieffi, Dipartimento di Medicina

Sperimentale, Via Costantinopoli 16, 80138 Naples, Italy.

E-mail: Paolo.Chieffi@unina2.it

Received 2 April 2009; Accepted 8 June 2009

Published online in Wiley InterScience

(www.interscience.wiley.com.), 22 July 2009.

DOI: 10.1002/jcp.21875

transformation, suggesting that the overexpression of Aurora B may contribute to the generation of a transformed phenotype (Kanda et al., 2005).

It has been previously shown that Aurora B is present, among germ cells, in mitotic cells (spermatogonia and primary spermatocytes) (Chieffi et al., 2004; Kimmins et al., 2007); the aim of the present study is to evaluate Aurora B expression in TGCTs to assess correlation with differential histological diagnosis and to validate Aurora B as a potential therapeutic target.

Materials and Methods

Tissue samples and cell culture

As source of neoplastic tissues, the tissue Bank of National Cancer Institute "G. Pascale" provided 45 cases of cryopreserved tissue from 22 seminomas, 2 teratomas, 15 pure embryonal carcinomas, 5 mixed tumours with a prevalent component of yolk sac tumour and 1 choriocarcinoma. To analyse the intratubular germ cell tumours (ITGCTs) we evaluated ITGCTs carcinomas areas in 15 of 22 examined seminomas. Ethical Committee approval was given in all instances. The GC-1 cell line were cultured in Dulbecco's modified Eagle's Medium (D-MEM) supplemented with 10% foetal bovine serum (FBS) (Gibco BRL, Milan, Italy), and grown in a 37°C humidified atmosphere of 5% CO₂ (Hofmann et al., 1992). Tcam-2 cells were grown at 37°C in a 5% CO₂ atmosphere in RPMI 1640 (LONZA, Milan, Italy) supplemented with 10% FBS (de Jong et al., 2008).

Antibodies

Antibodies were purchased from the following sources: (1) polyclonal rabbit antibody anti-Aurora B (#611082; BD Transduction Laboratories, San Diego, CA); (2) polyclonal rabbit antibody anti-Aurora B (#36-5200, Invitrogen, Carlsbad, CA); (3) mouse monoclonal antibody against recombinant PCNA (#M-0879, Dako Corp., Glostrup, Denmark); (4) polyclonal goat antibody anti-vinculin (#sc-7649, Santa Cruz Biotechnology Inc., Santa Cruz, CA); (5) polyclonal rabbit antibody anti-β-actin (Sigma, Milan, Italy); (6) polyclonal rabbit anti-P-H3 histone (#06-570, Upstate, Lake Placid); (7) polyclonal rabbit anti-histone H3 (#06-755, Upstate); (8) mouse monoclonal antibody anti-Ki-67 (#sc56319, Santa Cruz Biotechnology Inc.).

Histologic analysis and immunohistochemistry

For light microscopy, tissues were fixed in 10% formalin and embedded in paraffin by standard procedures. Four-micrometer sections were stained with haematoxylin and eosin or processed for immunohistochemistry. For each paraffin-embedded sample a 4-μm serial section mounted on slides pretreated for immunohistochemistry were dewaxed in xylene and brought through ethanols to deionized distilled water. Before staining for immunohistochemistry, sections were incubated in a 750 W microwave oven for 15 min in 10 mM, pH 6.0 buffered citrate to complete antigen unmasking. The classical Avidin-Biotin peroxidase Complex (ABC) procedure was used for immunohistochemistry. In the ABC system, endogenous peroxidase was quenched by incubation of the sections in 0.1% sodium azide with 0.3% hydrogen peroxide for 30 min at room temperature. Non-specific binding was blocked by incubation with non-immune serum (1% TRIS-bovine albumin for 15 min at room temperature). Sections were incubated overnight with antibodies against Aurora B (diluted 1:200), 2) against ki-67 (diluted 1:200). For Aurora B detection additional antibody was used which gave similar results (not shown). The following controls were performed: (1) omission of the primary antibody; (2) substitution of the primary antiserum with non-immune serum diluted 1:500 in blocking buffer, (3) addition of the target peptide used to produce the antibody (10⁻⁶ M); no immunostaining was observed after any

of the control procedures. Peroxidase activity was developed with the use of a filtered solution of 5 mg of 3-3'-diaminobenzidine tetrahydrochloride (dissolved in 10 ml of 0.05 M Tris buffer, pH 7.6) and 0.03% H₂O₂. We used Mayer's haematoxylin for nuclear counterstaining. Sections were mounted with a synthetic medium. Cases were scored as negative when non-neoplastic cell expressed Aurora B, at low and high expression when respectively less and more than 20% of neoplastic cells expressed Aurora B.

Protein extraction and Western blot analysis

Total cell extracts (TCE) were prepared with lysis buffer (50 mM Tris HCl pH 7.5, 5 mM EDTA, 300 mM NaCl, 150 mM KCl, 1 mM dithiothreitol, 1% Nonidet P40, and a mix of protease inhibitors). Protein concentration was estimated by a modified Bradford assay (Bio-Rad, Melville, NY). The protein extracts were boiled in Laemmli sample buffer, separated by sodium dodecyl sulphate-polyacrylamide gel electrophoresis (SDS-PAGE) and transferred to Immobilon-P transfer membranes (Immobilon Millipore Corporation, Bedford, MA). Membranes were blocked with 5% nonfat milk proteins and incubated with the primary antibody: (1) against Aurora B (diluted 1:500), (2) against PCNA (diluted 1:1,000), (3) anti-vinculin (diluted 1:1,000), (4) anti-β-actin (diluted 1:500). Also, for Western blot analyses a additional antibody was used for Aurora B which gave the same results (not shown). Bound antibodies were detected by the horseradish peroxidase-conjugated secondary antibodies followed by enhanced chemiluminescence (Amersham, Life Science, Bucks, UK). As a control for equal loading of protein lysates, the blotted proteins were probed with antibodies against vinculin and β-actin proteins.

FACS analysis

GC1 cells treated for 24 h with different amounts of Aurora B inhibitor were harvested by trypsinization, washed with PBS and fixed in 70% cold-ethanol over night. The fixed cells were washed with PBS and permeabilized 15 min in 10% FBS/TBStween 0.1%. PBS washed pellet was incubated 2 h in 50 μl of anti-phosphohistone H3 antibody diluted 1:130 in 4% FBS/TBStween 0.1%. After washing with PBS, cells were incubated 45 min in anti-rabbit IgG FITC conjugated antibody diluted 1:50 in 4% FBS/TBStween 0.1%. The immunostained cells were then washed with PBS and stained 20 min with 5 ng/μl propidium iodide plus 2 ng/μl RNase A in 300 μl PBS. All incubations were performed at room temperature, the last two ones were also performed in the dark. Incubation with H3 and without primary antibody was performed to assess the specificity of the observed signal. Samples were acquired with a CYAN flow cytometer (DAKO Corporation, San Jose, CA) and analysed using SUMMIT[®] software.

Results and Discussion

We evaluated the expression of Aurora B protein in normal and TGCTs by immunohistochemistry using two commercially available polyclonal antibodies. These antibodies are specific for Aurora B protein without cross-reactivity. Immunohistochemical assays were first performed on sections of normal human testis (data not shown), in agreement with our previous results a specific nuclear positivity for Aurora B was observed in spermatogonia and primary spermatocytes (Chieffi et al., 2004).

Aurora B expression was examined in a series of post-puberal TGCTs including 22 seminomas, 15 pure embryonal carcinomas, 5 yolk sac tumours in mixed tumours, 2 teratoma component in mixed tumours and 1 choriocarcinoma. Aurora B expression was also evaluated in 15 ITGCTs areas out of 22 examined seminoma. The results of this analysis, summarized in the Table 1, showed Aurora B immunoreactivity in ITGCTs, seminomas, and embryonal carcinomas, ranging from low to high expression. Conversely, in epithelial and mesenchymal

TABLE 1. Aurora B immunohistochemical data in post-puberal TGCTs

| | Number of cases (45) | Mean age, years (range years) | Aurora B | |
|----------|----------------------|-------------------------------|----------------|-----------------|
| | | | Low expression | High expression |
| Seminoma | 22 | 34 (20–52) | 9 | 13 |
| EC | 15 | 28 (20–40) | 3 | 12 |
| Teratoma | 2 | 30 (26–35) | 2 | 0 |
| YST | 5 | 31 (22–34) | 4 | 1 |
| CC | 1 | 30 | 0 | 1 |
| ITGCT | — | — | 0 | 15 |

EC, embryonal carcinoma; YST, yolk sac tumour; CC, choriocarcinoma; ITGCT = intratubular germ cell tumour = associated areas in 15 cases out of 22 examined seminoma. High expression, >20% of neoplastic cells; Low expression, <20% expression.

areas of teratomas and in yolk sac carcinomas, Aurora B immunoreactivity was not observed or low. Representative immunohistochemical data are shown in Figure 1. Mainly in seminomas Aurora B expression correlates to the proliferative index, evaluated through Ki-67 expression (Fig. 2). Reflecting the role of this kinase in mitosis, seminomas with high proliferative index showed high expression of Aurora B (Fig. 2).

Western blot analysis was performed on the same samples used showing that Aurora B levels correlates with PCNA levels, thus confirming immunohistochemical data (Fig. 3).

Aurora B expression has been analysed in GCI and TCam-2 cell lines, respectively derived from immortalized type B murine spermatogonia and human seminoma (Hofmann et al., 1992; de Jong et al., 2008). As shown in Figure 4A, higher Aurora B and PCNA protein levels were observed in the fast growing GCI cells, whereas TCam-2 cells, characterized by a slow growth kinetic, showed lower levels of Aurora B and PCNA expression. Therefore, we have evaluated on GCI cells the

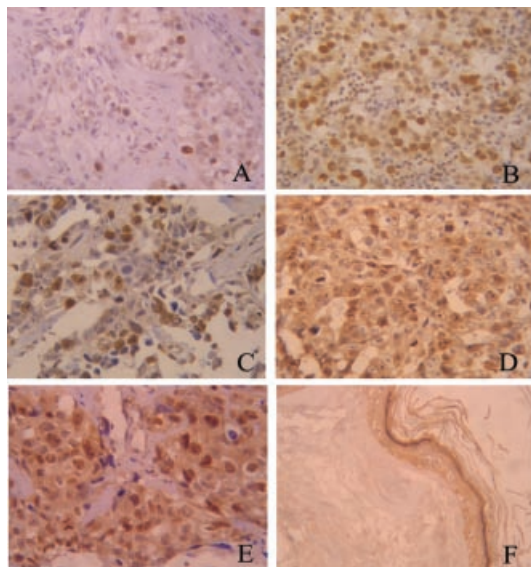


Fig. 1. Immunohistochemistry analysis of Aurora B expression in TGCTs. A: Aurora B expression in intratubular germ cells tumour in which an intense nuclear positivity were observed (case #3); (B) classic seminoma with an intense and diffuse nuclear Aurora B positivity (case #3); (C) high expression of Aurora B in embryonal carcinoma (case #23); (D) low expression of Aurora B in yolk sac tumours (case #40); (E) high nuclear expression of Aurora B in choriocarcinoma (case #45); (F) absent expression of Aurora B in mature teratoma (case #38) (magnification 40 \times).

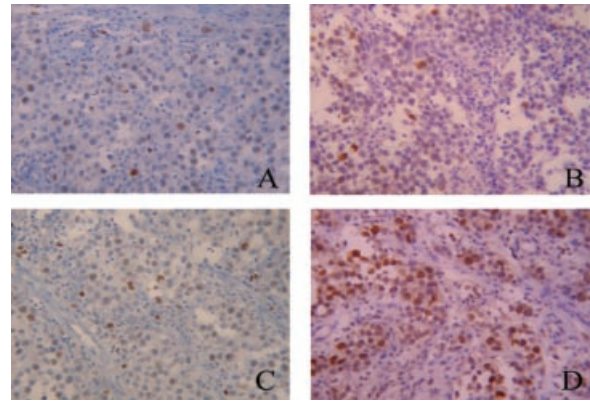


Fig. 2. Immunohistochemistry analysis of Aurora B and Ki-67 expression on serial sections of seminomas. A: Seminoma with low nuclear positivity of ki-67 (B) and Aurora B (case #2); (C) seminoma with an intense and diffuse nuclear ki-67 (D) and Aurora B (case #4) positivity (magnification 40 \times).

effects of Aurora B block induced by a specific inhibitor, a small molecule similar to the quinazoline derivative: N-[4-(6,7-dimethoxy-quinazolin-4-ylamino)-phenyl]-benzamide (Sorrentino et al., 2005). The treatment with Aurora B inhibitor induced a significant ($P < 0.001$) decrease in cell growth at all concentration used (Fig. 4B).

Aurora B is responsible for the mitotic phosphorylation of Ser10 residue in the tail of H3 histone and of Ser28 in H3 and of Ser7 in CENP-A. To confirm the specific effects of the inhibitor, cells were treated for 24 h and then analysed by FACS using a specific antibody anti-phospho-Ser-10 H3 histone. To quantify H3 histone phosphorylation (P-H3) with respect to cell cycle phase, cells were also stained with propidium iodide.

Control cells showed about $3 \pm 0.1\%$ of staining with anti-P-H3 antibody (Fig. 4C lower part). At 5 μM , a slight decrease in P-H3 levels staining was observed (about 2.7 ± 0.1). At higher concentrations, a more pronounced decrease in P-H3 levels was observed. Cell cycle analysis (Fig. 4C upper part and Fig. 4D) showed that Aurora B inhibitor induces an accumulation in G2/M phase, already after 24 h. Interestingly, at

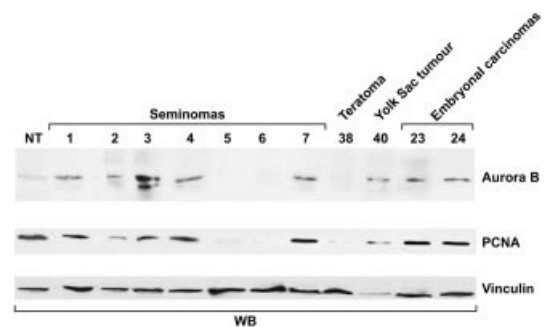


Fig. 3. Western blot analysis of Aurora B expression in normal testis and TGCTs. 40 μg of total tissue lysates were resolved on 12% SDS-PAGE, transferred onto nitrocellulose filters and Western blotted with anti-Aurora B and anti-PCNA antibodies. Lane NT: normal testis; Lanes 2–8: seminomas (cases #1–7); lane 9: teratoma (cases #38); lane 10: yolk sac tumour (case #40); lanes 11–12: embryonal carcinomas (cases #23, 24). Antibodies to α -vinculin served as loading control.

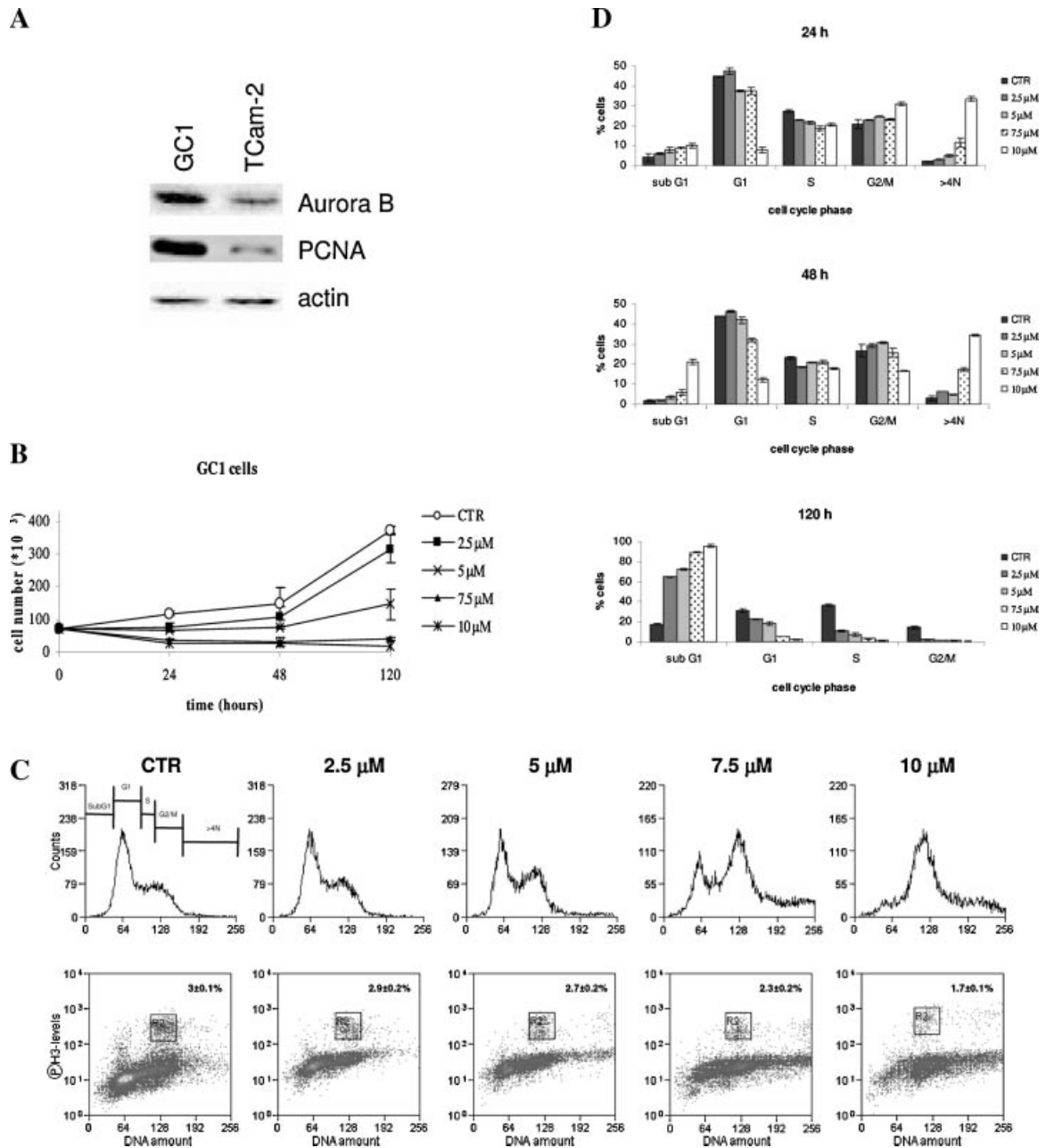


Fig. 4. **A:** Western blot analysis of Aurora B expression in GC1 and Tcam-2 cells. Lysates from Tcam-2 and GC1 cells (50 μg) were analysed for Aurora B and PCNA expression. GC1 cells express higher Aurora B and PCNA levels. Actin was used as loading control. **B:** Growth curve of GC1 cells treated with Aurora B inhibitor. GC1 (50,000 cells/well) were plated in 12 wells plates and the day after treated with different concentrations (2.5, 5, 7.5, 10 μM) of Aurora B inhibitor. Cell number was evaluated in the following days by counting. The bar represents the standard deviation of experiments performed twice in triplicate. **C:** FACS analysis after 2 h of Aurora B inhibitor treatment. GC1 (50,000 cells/well) were plated in 12 wells plates and the day after treated with different concentrations (2.5, 5, 7.5, 10 μM) of Aurora B inhibitor. DNA content and P-H3 amount were evaluated by FACS analysis. The percentages represent the number of P-H3 positive cells (lower part). The accumulation of tetraploid cells and the decrease in P-H3 levels became evident starting from 7.5 μM . The bars (upper part) represent the gates used to quantify cell cycle phases shown in (D). **D:** Quantification of cell cycle changes after 24, 48 and 120 h of treatment with Aurora B inhibitor. G2/M accumulation, polyploidy and subG1 phase increase in dose- and time-dependent manner.

this concentration, cells start to show a decrease in P-H3 staining levels. At 7.5 μM , was also observed polyploidy (see also Fig. 4D) in parallel with a strong decrease in P-H3 positivity. As shown in Figure 4D, more than 50% of the cells were in sub-G1 phase after 120 h of treatment. Sub-G1 phase is indicative of cell death and can be due to the activation of the apoptotic

pathway or by necrosis, therefore the block of Aurora B activity induced cell death.

Testicular tumours are rare, comprising 2% of all cancers in men; however, post-pubertal testicular cancer is the most common malignancy affecting males aged 15–34 years (Senturia, 1987; Looijenga and Oosterhuis, 1999). Because the molecular

basis of these cancers needs to be elucidated, identification of cellular genes involved in testicular tumourigenesis could increase our understanding of the development of testicular tumours, thus providing the basis for new targeted therapies. There are at least three Aurora-related kinases in mammals, Aurora A (STK-15), Aurora B (AIM-1), and Aurora C (STK-13). All three mammalian members of this family are overexpressed in human cancer cells. In the present study, we show that Aurora B expression is a consistent feature of human seminomas, where its topological staining pattern is lost, and in embryonal carcinomas. Aurora B expression levels are regulated at both mRNA and protein levels, with maximal mRNA and protein levels occurring during the G2/M phases (Terada et al., 1998). This cyclical pattern of regulation is conserved in cancer cells (Tatsuka et al., 1998). This indicates that the effects of Aurora B overexpression may be of critical importance during the G2/M phases of the cell cycle. The sequence of these events is essential for normal mitotic cell division in spermatogenesis and clearly overexpression of Aurora B may have implications for the abnormalities in germ cell maturation, such as those that occur in testicular cancer. Taken together, our data support a role for Aurora B in the initiation and/or progression of testicular cancers.

The identification of Aurora B inhibitors is an important discovery, considering the role of the corresponding gene in human cancers small molecules can selectively target the enzymatic activity of kinases by occupying the catalytic ATP-binding site. Several Aurora kinase inhibitors have been described, including ZM447439 (Ditchfield et al., 2003; Gadea and Ruderman, 2005), Hesperadin (Hauf et al. 2003), VX-680 (Harrington et al., 2004), and AZD1152 (Wilkinson et al., 2007). These inhibitor have already be shown to be specific for Aurora B, although it has been observed that pharmacological inhibition and disruption of Aurora B by other means such as RNA interference (RNAi) are not completely identical, since residual phosphorylation of histone H3 has been observed upon specific Aurora B RNAi (Keen and Taylor, 2004).

Preclinical and clinical studies show that these drugs are usually well tolerated, being the most common adverse effect neutropenia. The use of a specific Aurora B inhibitor demonstrates that the block of kinase activity induces the death of germ cells with a high proliferative rate suggesting its potential therapeutic role for the treatment of TGCTs.

In conclusion, we have shown that Aurora B is a consistent feature of human seminomas and embryonal carcinomas. Although germinal cell tumours are highly responsive to commonly used chemotherapeutic treatment, cases of acute toxicity and chronic collateral effects, such as sterility, are recorded. Therefore, the availability of novel drugs such as Aurora B inhibitor(s) could represent an escape from chemotherapy early and late effects.

Acknowledgments

This work was supported by grants to Paolo Chieffi from Italian Ministry of Education (MIUR-PRIN 2007), and from Second University of Naples (Ateneo 2008) and to Giuseppe Portella from Associazione Italiana per la Ricerca sul Cancro (AIRC). Francesco Esposito and Silvana Libertini are supported by fellowships from Fondazione Italiana per la Ricerca sul Cancro (FIRC).

We are indebted to Drs Sohei Kitazawa and Leendert Looijenga for the providing of Tcam-2 cells and to Dr. Claudio Sette for GCI cells. We thank Dr. S. Linaropoulos for the gift of Aurora B inhibitor and Fabrizio Fiorbianco (www.studiocitolita.it) for skilful technical assistance with the artwork.

Literature Cited

- Adams RR, Carmena M, Earnshaw WC. 2001. Chromosomal passengers and the (aurora) ABCs of mitosis. *Trends Cell Biol* 11:49–54.
- Araki K, Nozaki K, Ueba T, Tatsuka M, Hashimoto N. 2004. High expression of Aurora-B/Aurora and Ipl1-like midbody-associated protein (AIM-1) in astrocytomas. *J Neurooncol* 67:53–64.
- Carmena M, Earnshaw WC. 2003. The cellular geography of aurora kinases. *Nat Rev Mol Cell Biol* 4:842–854.
- Chieffi P. 2007. Molecular targets for the treatment of testicular germ cell tumors. *Mini-Rev Med Chem* 7:755–759.
- Chieffi P, Troncone G, Caleo A, Libertini S, Linaropoulos S, Tramontano D, Portella G. 2004. Aurora B expression in normal testis and seminomas. *J Endocrinol* 181:263–270.
- Chieffi P, Cozzolino L, Kisslinger A, Libertini S, Staibano S, Mansueti G, De Rosa G, Villacci A, Vitale M, Linaropoulos S, Portella G, Tramontano D. 2006. Aurora B expression directly correlates with prostate cancer malignancy and influence prostate cell proliferation. *Prostate* 66:326–333.
- de Jong J, Stoop H, Gillis AJ, Hersmus R, van Gurp RJ, van de Geijn GJ, van Drunen E, Beverloo HB, Schneider DT, Sherlock JK, Baeten J, Kitazawa S, van Zoelen EJ, van Roozendaal K, Oosterhuis JW, Looijenga LH. 2008. Further characterization of the first seminoma cell line Tcam-2. *Genes Chromosomes Cancer* 47:185–196.
- Ditchfield C, Johnson VL, Tighe A, Ellston R, Haworth C, Johnson T, Mortlock A, Keen N, Taylor SS. 2003. Aurora B couples chromosome alignment with anaphase by targeting BubR1, Mad2, and Cenp-E to kinetochores. *J Cell Biol* 161:267–280.
- Gadea BB, Ruderman JV. 2005. Aurora kinase inhibitor ZM447439 blocks chromosome-induced spindle assembly, the completion on chromosome condensation, and the establishment of the spindle integrity checkpoint in *Xenopus* egg extracts. *Mol Biol Cell* 16:1305–1318.
- Harrington EA, Bebbington D, Moore J, Rasmussen RK, Ajose-Adeogun AO, Nakayama T, Graham JA, Demur C, Hercend T, Diu-Hercend A, Su M, Golec JM, Miller KM. 2004. VX-680, a potent and selective small-molecule inhibitor of the Aurora kinases, suppresses tumor growth in vivo. *Nat Med* 10:262–267.
- Hauf S, Cole RW, LaTerra S, Zimmer C, Schnapp G, Walter R, Heckel A, van Meel J, Rieder CL, Peters JM. 2003. The small molecule Hesperadin reveals a role for Aurora B in correcting kinetochore-microtubule attachment and in maintaining the spindle assembly checkpoint. *J Cell Biol* 161:281–294.
- Hofmann MC, Narisava S, Hess RA, Millan JL. 1992. Immortalization of germ cells and somatic testicular cells using the SV40 large T antigen. *Exp Cell Res* 201:417–435.
- Kanda A, Kawai H, Suto S, Kitajima S, Sato S, Takata T, Tatsuka M. 2005. Aurora-B/AIM-1 kinase activity is involved in Ras-mediated cell transformation. *Oncogene* 10:7266–7272.
- Katayama H, Ota T, Jisaki F, Ueda Y, Tanaka T, Odashima S, Suzuki F, Terada Y, Tatsuka M. 1999. Mitotic kinase expression and colorectal cancer progression. *J Natl Cancer Inst* 91:1160–1162.
- Keen N, Taylor S. 2004. Aurora-kinase inhibitors as anticancer agents. *Nat Rev Cancer* 4:927–936.
- Kimmins S, Crosio C, Kotaja N, Hirayama J, Monaco L, Höög C, van Duin M, Gossen JA, Sassone Corsi P. 2007. Differential functions of the Aurora-B and Aurora-C kinases in mammalian spermatogenesis. *Mol Endocrinol* 21:726–739.
- Kurai M, Shiozawa T, Shih HC, Miyamoto T, Feng YZ, Kashima H, Suzuki A, Konishi I. 2005. Expression of Aurora kinases A and B in normal, hyperplastic, and malignant human endometrium: Aurora B as a predictor for poor prognosis in endometrial carcinoma. *Hum Pathol* 36:1281–1288.
- Looijenga LH, Oosterhuis WJ. 1999. Pathogenesis of testicular germ cell tumours. *J Reprod Fert* 4:90–100.
- López-Ríos F, Chuai S, Flores R, Shimizu S, Ohno T, Wakahara K, Illei PB, Hussain S, Krug L, Zakowski MF, Rusch V, Olshen AB, Ladanyi M. 2006. Global gene expression profiling of pleural mesotheliomas: Overexpression of aurora kinases and P16/CDKN2A deletion as prognostic factors and critical evaluation of microarray-based prognostic prediction. *Cancer Res* 66:2970–2979.
- Oosterhuis JW, Looijenga LH. 2005. Testicular germ-cell tumors in a broader perspective. *Nat Rev Cancer* 5:210–222.
- Ota T, Suto S, Katayama H, Han ZB, Suzuki F, Maeda M, Tanino M, Terada Y, Tatsuka M. 2002. Increased mitotic phosphorylation of histone H3 attributable to AIM-1/Aurora B overexpression contributes to chromosome number instability. *Cancer Res* 62:5168–5177.
- Qi G, Ogawa I, Kudo Y, Miyauchi M, Siriwardena BS, Shimamoto F, Tatsuka M, Takata T. 2007. Aurora-B expression and its correlation with cell proliferation and metastasis in oral cancer. *Virchows Arch* 450:297–302.
- Senturia YD. 1987. The epidemiology of testicular cancer. *Br J Urol* 60:285–291.
- Smith SL, Bowers NL, Betticher DC, Gautschi O, Ratschiller D, Hoban PR, Botton R, Santibáñez-Koref MF, Heighway J. 2005. Overexpression of aurora B kinase (AURKB) in primary non-small cell lung carcinoma is frequent, generally driven from one allele, and correlates with the level of genetic instability. *Br J Cancer* 93:719–729.
- Sorrentino R, Libertini S, Pallante P, Troncone G, Palombini L, Bavetsias V, Spalletti Cernia D, Laccetti P, Linaropoulos S, Chieffi P, Fusco A, Portella G. 2005. Aurora B overexpression associates with the thyroid carcinoma undifferentiated phenotype and is required for thyroid carcinoma cell proliferation. *J Clin Endocrinol Metab* 90:928–935.
- Tanaka T, Kimura M, Matsunaga K, Fukada D, Mori K, Okano Y. 1999. Centrosomal kinase AIK1 is overexpressed in invasive ductal carcinoma. *Cancer Res* 59:2041–2044.
- Tatsuka M, Katayama H, Ota T, Tanaka T, Odashima S, Suzuki F, Terada Y. 1998. Multinuclearity and increased ploidy caused by overexpression of the aurora- and Ipl1-like midbody-associated protein mitotic kinase in human cancer cells. *Cancer Res* 58:4811–4816.
- Terada Y, Tatsuka M, Suzuki F, Yasuda Y, Fujita S, Otsu MA. 1998. AIM-1: A mammalian midbody-associated protein required for cytokinesis. *EMBO J* 17:667–676.
- Vischioni B, Oudejans JJ, Vos W, Rodriguez JA, Giaccone G. 2006. Frequent overexpression of aurora B kinase, a novel drug target, in non-small cell lung carcinoma patients. *Mol Cancer Ther* 5:2905–2913.
- Wilkinson RW, Odedra R, Heaton SP, Wedge SR, Keen NJ, Crafter C, Foster JR, Brady MC, Bigley A, Brown E, Byth KF, Barrass NC, Mundt KE, Foote KM, Heron NM, Jung FH, Mortlock AA, Boyle FT, Green S. 2007. AZD1152, a selective inhibitor of Aurora B Kinase, inhibits human tumor xenograft growth by inducing apoptosis. *Clin Cancer Res* 13:3682–3688.
- Zeng WF, Navaratnek K, Prayson RA, Weil RJ. 2007. Aurora B expression correlates with aggressive behaviour in glioblastoma multiforme. *J Clin Pathol* 60:218–221.

PED/PEA-15 Modulates Coxsackievirus–Adenovirus Receptor Expression and Adenoviral Infectivity via ERK-Mediated Signals in Glioma Cells

Ginevra Botta,^{1,*} Giuseppe Perruolo,^{1,2,*} Silvana Libertini,¹ Angela Cassese,^{1,2} Antonella Abagnale,¹ Francesco Beguinot,¹ Pietro Formisano,¹ and Giuseppe Portella¹

Abstract

Glioblastoma multiforme (GBM) is the most aggressive human brain tumor, and is highly resistant to chemo- and radiotherapy. Selectively replicating oncolytic viruses represent a novel approach for the treatment of neoplastic diseases. Coxsackievirus–adenovirus receptor (CAR) is the primary receptor for adenoviruses, and loss or reduction of CAR greatly decreases adenoviral entry. Understanding the mechanisms regulating CAR expression and localization will contribute to increase the efficacy of oncolytic adenoviruses. Two glioma cell lines (U343MG and U373MG) were infected with the oncolytic adenovirus *dl922-947*. U373MG cells were more susceptible to cell death after viral infection, compared with U343MG cells. The enhanced sensitivity was paralleled by increased adenoviral entry and CAR mRNA and protein levels in U373MG cells. In addition, U373MG cells displayed a decreased ERK1/2 (extracellular signal-regulated kinase-1/2) nuclear-to-cytosolic ratio, compared with U343MG cells. Intracellular content of PED/PEA-15, an ERK1/2-interacting protein, was also augmented in these cells. Both ERK2 overexpression and genetic silencing of PED/PEA-15 by antisense oligonucleotides increased ERK nuclear accumulation and reduced CAR expression and adenoviral entry. Our data indicate that *dl922-947* could represent an useful tool for the treatment of GBM and that PED/PEA-15 modulates CAR expression and adenoviral entry, by sequestering ERK1/2.

Introduction

MALIGNANT GLIOMA of astrocytic origin, or glioblastoma multiforme (GBM), is the most common primary brain tumor in adults and the most aggressive human brain tumor (Furnari *et al.*, 2007; Brandes *et al.*, 2008).

Treatment normally includes tumor resection, radiation, and chemotherapy; however, GBM cells are largely resistant to chemo- and radiotherapy. Consequently, only a small minority of patients with GBM achieve long-term survival (Furnari *et al.*, 2007; Brandes *et al.*, 2008). Novel treatment strategies are therefore required in order to increase the therapeutic options.

Selectively replicating oncolytic viruses represent a novel platform for the treatment of neoplastic diseases and several studies have been performed showing the feasibility of this therapeutic strategy in patients with glioblastoma (Haseley *et al.*, 2009).

dl922-947 is a selectively replicating oncolytic adenoviral mutant bearing a 24-bp deletion in E1A-conserved region-2

(CR2), necessary for binding and inactivation of the pRb family of proteins (Heise *et al.*, 2000); *dl922-947* mutant is unable to induce progression from G₁ into the S phase of normal cells, but replicates with high efficiency in cells with an abnormal G₁–S checkpoint.

The G₁–S checkpoint is critical for cell growth progression (Sherr, 2000) and is abnormal in GBM (Solomon *et al.*, 2008); therefore mutant E1A adenoviruses have been proposed for the therapy of gliomas and are now in preclinical development as antiglioma therapy (Vecil and Lang, 2003).

The efficacy of adenoviral vectors as therapeutic agents depends on the ability of neoplastic cells to bind and internalize adenoviruses. Adenoviral infection involves two distinct virus–cell interactions. First, cell surface attachment is mediated by binding of the viral fiber protein to the cellular coxsackievirus–adenovirus receptor (CAR) (Bergelson *et al.*, 1997; Tomko *et al.*, 2000). CAR is a 46-kDa integral membrane protein and variant isoforms, which differ only at the C terminus and that most likely result from alternative

¹Dipartimento di Biologia e Patologia Cellulare e Molecolare, Università Federico II, 80131 Naples, Italy.

²Istituto di Endocrinologia e Oncologia Sperimentale, Consiglio Nazionale delle Ricerche (CNR), 80131 Naples, Italy.

*G. Botta and G. Perruolo contributed equally to this study.

splicing, have also been identified in mice, humans, and rats (Fechner *et al.*, 1999; Coyne and Bergelson, 2005).

Internalization, via receptor-mediated endocytosis, involves interactions between the viral penton protein and cellular integrins, such as $\alpha_v\beta_3$, $\alpha_v\beta_5$, $\alpha_5\beta_1$, and $\alpha_3\beta_1$, that act as coreceptors (Nemerow, 2000). Low or absent expression of CAR is seen in many primary tumor tissues (Rein *et al.*, 2006) and low expression of CAR has been observed in grade IV gliomas (Fuxe *et al.*, 2003).

However, the molecular mechanisms by which CAR expression is regulated have been only partially elucidated. Interestingly, inhibition of ERK (extracellular signal-regulated kinase)/MAPK (mitogen-activated protein kinase) pathway has been reported to upregulate CAR expression (Anders *et al.*, 2003).

Here we show that, in two glioblastoma cell lines (Hao *et al.*, 2001; Xiao *et al.*, 2002), the expression of PED/PEA (phosphoprotein enriched in diabetes/phosphoprotein enriched in astrocytes)-15, a protein that binds ERK and prevents its nuclear accumulation (Formstecher *et al.*, 2001; Hill *et al.*, 2002; Renault *et al.*, 2003; Whitehurst *et al.*, 2004; Renganathan *et al.*, 2005), correlates with CAR mRNA levels as well as with the sensitivity to adenoviral infection and dl922-947 killing activity. Indeed, silencing of PED/PEA-15 promotes ERK nuclear translocation and simultaneously reduces CAR expression and adenoviral entry into glioblastoma cells.

Materials and Methods

Cell lines, plasmids, and transfections

Glioma cell lines U343MG and U373MG were purchased from the American Type Culture Collection (Manassas, VA). All cell lines were cultured in Dulbecco's modified Eagle's medium (DMEM) supplemented with 10% fetal bovine serum, penicillin (100 IU/ml), streptomycin (100 IU/ml), and 2% L-glutamine in a humidified CO₂ incubator.

The pcDNA3 vector carrying PED/PEA-15 cDNA was obtained as previously described (Condorelli *et al.*, 1998).

Sequences of scramble and antisense oligonucleotides (Sigma-Aldrich, St. Louis, MO) are as follows:

AS-PED/PEA-15 human: 5'-TGACGCCCTCTGGAGCTGA GA-3'

Scr-PED/PEA-15 human: 5'-GGCAATTCGAGCGGCAC GT-3'

The plasmid pcDNA3-HA carrying ERK2 cDNA (pcDNA3-HA-pMAPK2) was kindly provided by M. Chiarillo (Istituto di Endocrinologia e Oncologia Sperimentale, CNR, Naples, Italy).

Transfection of a pcDNA3 vector carrying PED/PEA-15 cDNA, PED antisense and scramble oligonucleotides, or pcDNA3-HA carrying ERK2 cDNA, was accomplished by the Lipofectamine (Invitrogen, Carlsbad, CA) method as previously described (Condorelli *et al.*, 1998).

Preparation of adenoviruses, infection, and viability assay

dl922-947 is a second-generation adenoviral mutant that has a 24-bp deletion in E1A conserved region-2 (CR2). AdGFP is a nonreplicating E1A-deleted adenovirus encoding

green fluorescent protein. Viral stocks were expanded in the human embryonic kidney cell line HEK-293, and purified, as previously reported (Portella *et al.*, 2002).

Stocks were stored at -70°C after the addition of glycerol to a concentration of 50% (v/v). Virus titer was determined by plaque-forming units (pfu) on the HEK-293 cells.

For evaluation of the cytotoxic effects of the dl922-947 virus, 1×10^3 cells were seeded in the wells of 96-well plates, and 24 hr later cells were infected with various multiplicities of infection (MOIs). After 10 days cells were fixed with 10% trichloroacetic acid (TCA) and stained with 0.4% sulforhodamine B in 1% acetic acid (Skehan *et al.*, 1990). The bound dye was solubilized in 200 μl of 10 mM unbuffered Tris solution and the optical density was determined at 490 nm in a microplate reader (Bio-Rad, Munich, Germany). The percent survival rates of treated cells were calculated by assuming the survival rate of untreated cells to be 100%.

For the evaluation of infectivity cells were detached, counted, and plated in 6-well plates at 70% cell density. After 24 hr cells were infected with AdGFP diluted in growth medium at various MOIs; medium was replaced after 2 hr. Cells were washed 24 hr postinfection and then trypsinized and analyzed for GFP expression with a flow cytometer (Dako, Carpinteria, CA) and Summit version 4.3 software (Dako).

Quantitative PCR of dl922-947

To quantify the amount of dl922-947 viral genome, cells were infected with dl922-947 at various MOIs (0.1, 1, and 10 pfu/cell). At 48 hr postinfection, cell supernatant was collected and viral DNA was extracted with a QIAamp DNA mini kit (Qiagen, Valencia, CA) and then quantified by real-time PCR, using assay-specific primer and probe. A real time-based assay was developed with primers 5'-GCCACCGAGACGTACTTCAGCCTG-3' (upstream primer) and 5'-TTGTACGAGTACGGGTATCCT-3' (downstream primer) for amplification of a 143-bp sequence of the viral hexon gene (from bp 99 to 242). For quantification, a standard curve was constructed by assaying serial dilutions of dl922-947 virus ranging from 0.1 to 100 pfu/cell to quantify the input dose.

Detection of cell surface CAR and mRNA quantification

Cells were grown in 6-well plates. After 48 hr cells were detached in phosphate-buffered saline (PBS)-10 mM EDTA, washed with PBS, and then incubated with mouse anti-CAR monoclonal antibody RmC (Hsu *et al.*, 1988) and a secondary antibody (polyclonal rabbit anti-mouse antibody conjugated to fluorescein isothiocyanate [FITC]; Sigma-Aldrich), and analyzed for CAR expression with a flow cytometer (Dako) and Summit version 4.3 software (Dako). Background emission was subtracted and FITC emission was normalized to control emission.

To block CAR, cells were pretreated with increasing concentrations of the mouse anti-CAR monoclonal antibody RmC, anti-insulin-like growth factor-1 receptor β subunit (IGF-1R) (Upstate Cell Signaling Solutions/Millipore, Lake Placid, NY), and anti-actin (Santa Cruz Biotechnology, Santa Cruz, CA) antibodies (diluted 1:100, 1:250, and 1:500), for 1 hr at room temperature before addition of virus. Cells were harvested and analyzed as previously described.

To analyze CAR mRNA levels cells were harvested and total RNA was isolated and digested with DNase, using an RNeasy mini kit (Qiagen) according to the manufacturer's recommendations. One microgram of tissue or cell RNA from each sample was reverse transcribed, using SuperScript II reverse transcriptase (Invitrogen). PCR products were analyzed with SYBR green mix (Invitrogen). Reactions were performed with Platinum SYBR green qPCR SuperMix-UDG, using an iCycler iQ multicolor real-time PCR detection system (Bio-Rad). All reactions were performed in triplicate, and β -actin was used as an internal standard.

The primer sequences were as follows: Cxadr forward (5'-ATGAAAAGGAAGTTCATCAACGTA-3') and Cxadr reverse (5'-AATGATTACTGCCGATGTAGCTT-3'), generating an amplicon of 93 nucleotides scattered among exons 6 and 7; and β -actin forward (5'-GCGTGACATCAAAGAGAAG-3') and β -actin reverse (5'-ACTGTGTTGGCATAGAGG-3').

The conditions used for PCR were 10 min at 95°C and then 45 cycles of 20 sec at 95°C and 1 min at 60°C. To calculate the relative expression levels, we used the $2^{-\Delta\Delta C_t}$ method, where $\Delta\Delta C_t = \Delta C_{t, \text{sample}} - \Delta C_{t, \text{reference}}$.

Protein extraction, cell subfractionation, and Western blot analysis

In all experiments, 70% confluent cells were used. Subcellular fractionation was performed by a previously described method (Ruvolo *et al.*, 1998). Briefly, cells were broken in ice-cold hypotonic HEPES buffer (10 mM HEPES [pH 7.4], 5 mM MgCl₂, 40 mM KCl, 1 mM phenylmethylsulfonyl fluoride, aprotinin [10 g/ml], leupeptin [10 g/ml]). Broken cells were centrifuged at 200×g to pellet the nuclei. The resulting supernatants were centrifuged at 10,000×g to pellet the heavy membrane fraction. The last supernatant represented the cytosolic fraction. The nuclear membranes were isolated by centrifugation of the nuclei through a 2 M sucrose cushion at 150,000×g. For protein extraction cells were homogenized directly into lysis buffer (50 mM HEPES, 150 mM NaCl, 1 mM EDTA, 1 mM EGTA, 10% glycerol, 1% Triton X-100, 1 mM phenylmethylsulfonyl fluoride, aprotinin [1 g/ml], 0.5 mM sodium orthovanadate, 20 mM sodium pyrophosphate). The lysates were clarified by 20 min of centrifugation at 14,000×g. Protein concentrations were estimated by a Bio-Rad assay, and then proteins were boiled in Laemmli buffer for 5 min before electrophoresis. Proteins were subjected to sodium dodecyl sulfate-polyacrylamide gel electrophoresis (SDS-PAGE) (10% polyacrylamide) under reducing conditions. After electrophoresis, proteins were transferred to nitrocellulose membranes (Immobilon; Millipore). After blocking with Tris-buffered saline-bovine serum albumin (TBS-BSA), the membrane was incubated with primary antibody: polyclonal rabbit antibody against CAR (SC-15-405, diluted 1:250; Santa Cruz Biotechnology), rabbit anti-PED serum (diluted 1:2000; previously described [Condorelli *et al.*, 1998]), rabbit antibody against ERK1 and ERK2 (diluted 1:1000), rabbit anti-IGF-1R (diluted 1:1000; Upstate Cell Signaling Solutions/Millipore), or rabbit anti-H1 histone (diluted 1:1000; Upstate Cell Signaling Solutions/Millipore), or with the rabbit antibody against actin (diluted 1:2000; Santa Cruz Biotechnology) for an overnight incubation.

Membranes were then incubated with horseradish peroxidase-conjugated secondary antibody (diluted 1:2000) for

45 min (at room temperature) and the reaction was detected with an enhanced chemiluminescence (ECL) system (GE Healthcare Life Sciences, Chalfont St Giles, UK).

Densitometric analysis was performed with Scion Image (Scion, Frederick, MD). All data were expressed as means \pm SD.

Results

U373MG and U343MG cells show different sensitivities to adenoviral infection

First, we evaluated the antineoplastic activity of the selectively replicating oncolytic adenovirus *dl922-947* against U373MG and U343MG glioma cell lines (Fig. 1A).

Cells were infected with various MOIs of *dl922-947* and cell survival was evaluated after 7 days. The U373MG cell line displayed higher sensitivity to *dl922-947*, with a 50% inhibitory concentration (IC₅₀) at an MOI of 0.0001 pfu/cell, whereas for U343MG the IC₅₀ was observed at an MOI of 0.1 pfu/cell (Fig. 1A).

Our data indicate that both glioma cell lines are sensitive to *dl922-947*, although displaying different sensitivities to its oncolytic activity. Genome equivalent copies analysis showed that both cell lines sustain the replication of *dl922-947* (Fig. 1B).

To study whether this difference could be due to dissimilar infection efficiency, we used a nonreplicating reporter adenovirus encoding the green fluorescent protein (AdGFP), as previously reported (Watanabe *et al.*, 2006). Cells were infected with various MOIs of AdGFP and 24 hr postinfection the amount of GFP-positive cells was quantified by flow cytometric analysis.

At 1 pfu/cell of AdGFP 80% of U373MG cells showed positivity for GFP expression, whereas a higher viral dose (10 pfu/cell) was required to obtain the same percentage of GFP-positive U343MG cells. Starting from 10 pfu/cell no further increase in GFP-positive cells was observed in either cell line.

These differences in infection efficiency could explain the differences in viral replication, because at 0.1 and 1 pfu/cell a highly significant difference ($p < 0.001$) in genome copies of *dl922-947* was detected in U373MG compared with U343MG.

Conversely, at 10 pfu/cell the differences in genome equivalent copies of *dl922-947* were less evident ($p < 0.05$).

Infectivity of U343MG and U373MG cells is mediated by coxsackievirus-adenovirus receptor

It has been reported that CAR is the main mediator of adenoviral entry (Bergelson *et al.*, 1997; Nemerow, 2000; Tomko *et al.*, 2000; Arnberg, 2009). Therefore, we analyzed CAR expression by Western blot and cytofluorimetric analysis in U343MG and U373MG cell lines. Two CAR-specific bands of 44 and 46 kDa, respectively, were detected in all samples (Fig. 2A), as previously reported (Cohen *et al.*, 2001; Libertini *et al.*, 2007).

U373MG cells displayed higher total levels (Fig. 2A) and membrane levels (Fig. 2B) of CAR, compared with U343MG cells; this observation parallels the higher viral entry and sensitivity to the oncolytic activity of *dl922-947*. To evaluate whether CAR may play a direct role in infection efficiency, U343MG and U373MG cells were pretreated for 1 hr with increasing amounts of the blocking anti-CAR monoclonal

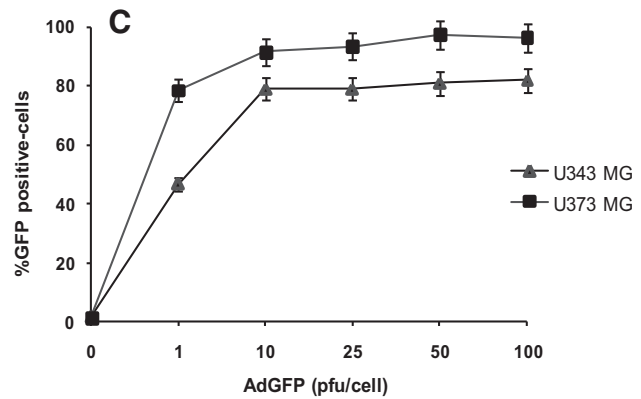
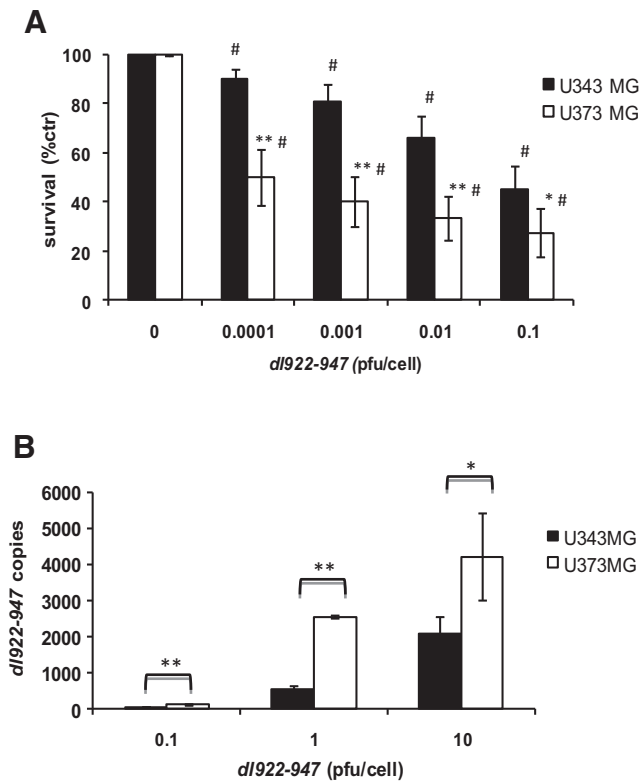


FIG. 1. Comparison of the cell-killing activity, replication of *dl922-947*, and infectivity in U343MG and U373MG glioblastoma cell lines. **(A)** Cytotoxic effects of the oncolytic adenovirus *dl922-947* were evaluated on U343MG and U373MG glioma cells. The percent survival rates of cells exposed to adenovirus were calculated by assuming the survival rate of untreated cells to be 100%. *dl922-947*-infected U373MG cells showed significant or highly significant differences in viral sensitivity compared with U343MG cells. A highly significant difference ($p < 0.001$) in cell survival was observed at all points with respect to the control for both cell lines: *significance compared with equally infected U343MG cells; #significance compared with uninfected cells. The differences observed were at least significant ($*p < 0.05$; $**p < 0.001$). Shown are mean percentages of untreated cells and SD from three different experiments. **(B)** Replication was assessed by real-time PCR genome equivalent analysis. Cells were infected with *dl922-947* at various MOIs (0.1, 1, and 10 pfu/cell). At 48 hr postinfection, cell medium was collected and viral DNA was extracted and quantified. At an MOI of 0.1 and 1 pfu/cell the difference in *dl922-947* replication between U343MG and U373MG levels was highly significant ($**p < 0.001$), whereas at an MOI of 10 pfu/cell the difference was significant ($*p < 0.05$). Shown are mean percentages of untreated cells and SD from three different experiments. Standard deviations (error bars) were calculated. **(C)** Cells were seeded in 6-well plates and infected with AdGFP at various MOIs (1, 10, 25, 50, and 100 pfu/cell). At 24 hr postinfection, cells were collected and the percentage of GFP-positive cells was quantified by FACS analysis. Data represent the mean of three different experiments.

antibody RmcB and infected with AdGFP at 25 pfu/cell. We also pretreated cells with two control antibodies: anti-IGF-1R and anti-actin. Significant decreases in GFP emission were observed in U373MG cells ($p < 0.005$) and U343MG cells ($p < 0.001$), upon treatment with RmcB, but not upon treatment with anti-IGF-1R or anti-actin antibodies (Fig. 2C and D). These data confirm that CAR plays a crucial role in infection efficiency in both cell lines.

ERK modulates U373MG cell line infectivity by regulating CAR expression

It has been described that ERK signaling regulates CAR levels in cancer cell lines (Anders *et al.*, 2003). Therefore, we evaluated ERK1/2 phosphorylation and subcellular localization in U373MG and U343MG cells. No difference in ERK1/2 phosphorylation was detected in the two cell lines (Fig. 3A). However, in U373MG cells, ERK1/2 cytosolic content was higher than in U343MG cells. Conversely, U343MG cells displayed higher levels of ERK1/2 in the nucleus than did U373MG cells (Fig. 3B), suggesting that ERK1/2 nuclear localization might contribute to downregulate CAR expression.

Next, a plasmid carrying ERK2 cDNA (pcDNA3-HA-pERK2) was transiently transfected into U373MG cells, in order to force ERK into the nucleus. Transfection efficiency was evaluated by Western blot (Fig. 3C). ERK2 overexpression

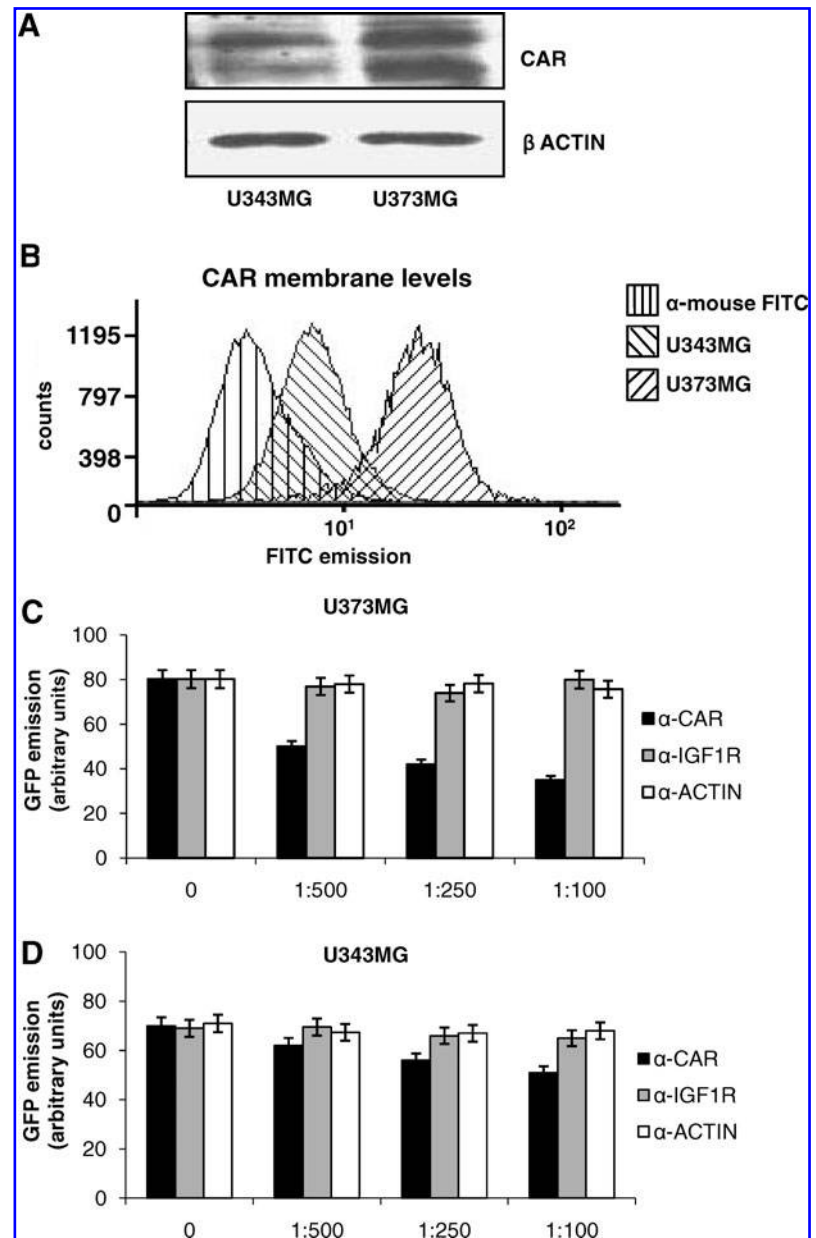
was paralleled by increased detection of ERK2 in the nuclei and by a reduction of CAR total and membrane levels (Fig. 3C). CAR mRNA levels, evaluated by reverse transcription (RT) real-time PCR, also showed a reduction of about 80% (Fig. 3D), thus suggesting that an ERK nuclear shift downregulates CAR gene expression. Accordingly, a significant reduction in GFP emission was observed in ERK2-transfected U373MG cells, after infection with AdGFP (Fig. 3E).

PED/PEA-15 modulates ERK localization and CAR expression

PED/PEA-15 is a death effector domain-containing protein, which is involved in the regulation of apoptotic cell death (Hao *et al.*, 2001; Xiao *et al.*, 2002). PED/PEA-15 is highly expressed in cells of glial origin (Hao *et al.*, 2001; Xiao *et al.*, 2002; Sharif *et al.*, 2004). Moreover, it has been reported that PED/PEA-15 inhibits nuclear translocation and activity of ERK1/2 (Formstecher *et al.*, 2001; Hill *et al.*, 2002; Renault *et al.*, 2003; Whitehurst *et al.*, 2004; Renganathan *et al.*, 2005).

As previously reported (Hao *et al.*, 2001), PED/PEA-15 levels were higher in U373MG cells than in U343MG cells (Fig. 4A). To assess whether PED/PEA-15 may control ERK localization and CAR expression, a PED/PEA-15 antisense oligonucleotide (PED-As) was transfected into U373MG cells, using a scrambled oligonucleotide (PED-Scr) as control,

FIG. 2. Coxsackievirus-adenovirus receptor (CAR) in U343MG and U373MG cells. **(A)** Western blot analysis of CAR expression in glioma cells. β -Actin was used as loading control. U373MG cells displayed higher levels of total CAR expression. **(B)** Cytofluorimetric analysis of CAR expression on the membrane of glioma cell lines. U343MG and U373MG cells were harvested and incubated with an anti-CAR (RmcB) monoclonal antibody or fluorescein isothiocyanate (FITC)-labeled mouse antibody alone. FITC-labeled cells were used as basal fluorescence control. The first curve represents FITC-labeled secondary antibody in the absence of primary antibody. U373MG cells showed about 60% CAR-positive cells, whereas only 8% of U343MG cells stained positive with anti-CAR antibody. In all experiments, 70% confluent cells were used. **(C)** U343MG and U373MG cells were pretreated for 1 hr with increasing concentrations (1:100, 1:250, and 1:500) of the mouse anti-CAR monoclonal antibody RmcB, using anti-insulin-like growth factor-1 receptor β subunit (IGF-1R) and anti-actin antibodies as controls, and then infected with AdGFP (25 pfu/cell). At 24 hr postinfection GFP emission was analyzed by cytofluorimetric analysis. Standard deviations (error bars) of three different experiments were calculated. GFP emission decreased in a dose-dependent manner (>50%) after preincubation with RmcB, but not with anti-IGF-1R or anti-actin antibodies, in both cell lines. Data represent the mean of three different experiments.



and PED/PEA-15 levels in transfected cells were evaluated by Western blot.

After PED-As transfection, a decrease in CAR total levels was observed (Fig. 4B) and the nuclear-to-cytosolic ratio of ERK distribution was shifted toward the nucleus (Fig. 4C).

To further confirm the role of PED/PEA-15 in the expression of CAR, U343MG cells were transfected with a plasmid carrying PED/PEA-15 cDNA, showing an increase in CAR total levels (Fig. 4D).

Downregulation of PED/PEA-15 decreases CAR levels, adenoviral infectivity, and sensitivity to dl922-947 in U373MG cells

Downregulation of PED/PEA-15 was accompanied by a reduction in total (Fig. 4B) and membrane (Fig. 5A) CAR levels, respectively. Transfection of U373MG cells with the scrambled oligonucleotide (PED-Scr) led to a slight reduction

(about 30%) of CAR membrane levels, compared with untransfected cells. However, PED-As-transfected cells showed a significant decrease in CAR membrane levels with respect to PED-Scr-transfected cells ($p < 0.05$).

RT real-time PCR experiments showed an approximately 50% reduction of CAR mRNA levels ($p < 0.05$) (Fig. 5B) after transfection with PED-As and a significant decrease in GFP emission was observed in PED-As-transfected cells after infection with AdGFP at 25 pfu/cell ($p < 0.05$) (Fig. 5C).

These data indicate that PED/PEA-15 plays a role in controlling the regulation of CAR expression and in adenoviral infectivity in glioma cells. To confirm that the downregulation of PED/PEA-15 reduces sensitivity to the oncolytic virus *dl922-947*, U373MG cells were transfected with PED-As or PED-Scr.

U373MG cells were also transfected with pcDNA3-HA pERK2 or pcDNA3-HA plasmid as controls. Forty-eight hours after transfection cells were infected with *dl922-947*

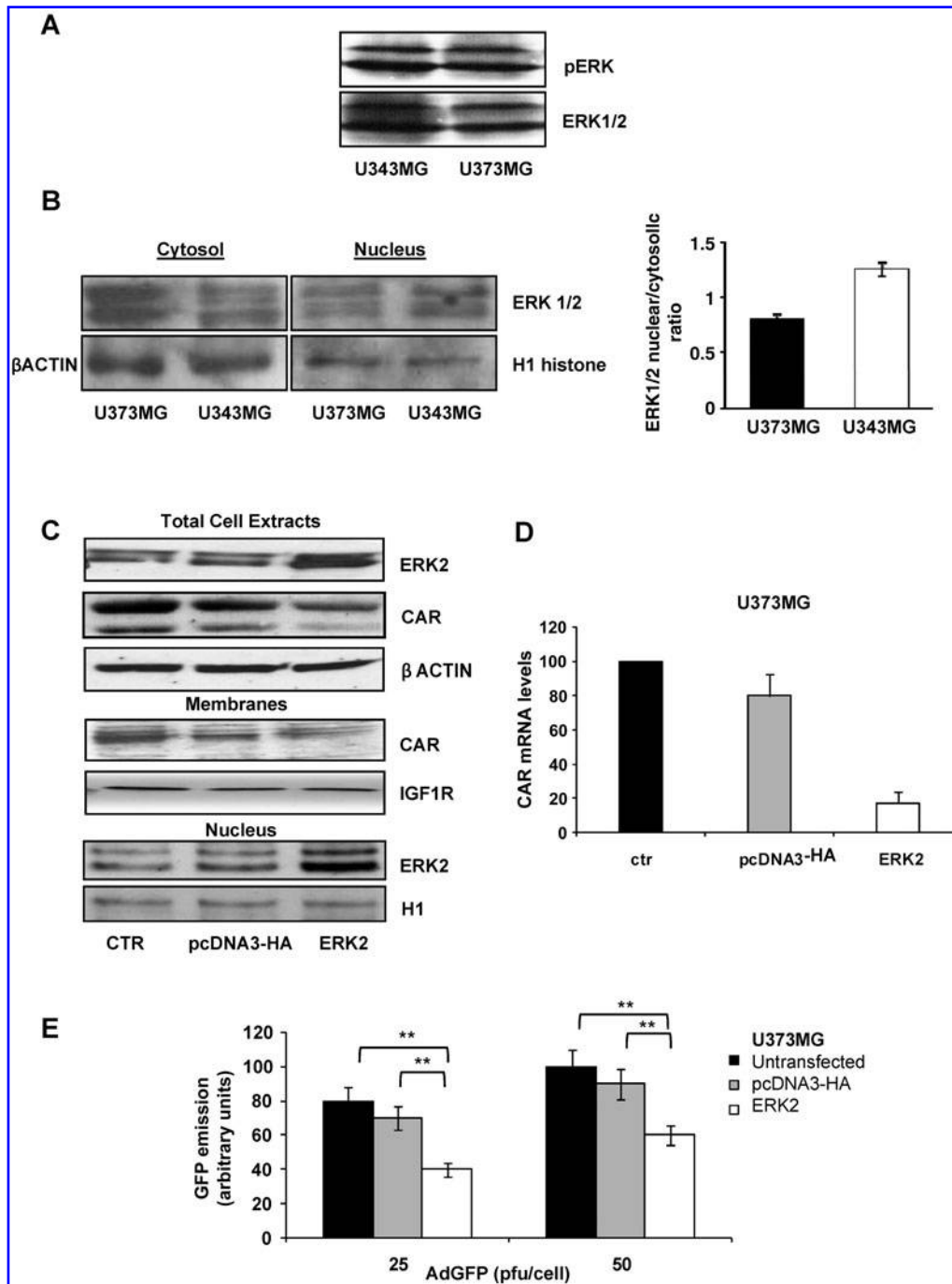


FIG. 3. ERK pathway regulates CAR expression in glioma cells. (A) U343MG and U373MG cells were analyzed for the expression of phospho-ERK1/2 by Western blot, using ERK1/2 total levels as loading control. (B) Subcellular fractionation (nuclear and cytoplasmic) of U343MG and U373MG cells was performed as described in Materials and Methods, and proteins were extracted and subjected to SDS-PAGE and immunoblotted with anti-ERK1/2 antibody. β -Actin and H1 histone were used as loading control for the cytosolic and nuclear fractions, respectively. Blots were revealed by ECL and autoradiography (left). Autoradiographs of the experiment were subjected to densitometric analysis. The graph on the right represents the ratio of the values obtained for nuclear and cytosolic ERK immunodetection, after normalizing each fraction for H1 histone and β -actin levels, respectively. Standard deviations (error bars) of three different experiments were calculated. (C) U373MG cells were transiently transfected with the plasmid pcDNA3-HA carrying ERK2 cDNA (ERK2) or pcDNA3-HA plasmid as a control. Total lysates, membrane enrichments, and nuclear fractions were obtained 48 hr after transfection. β -Actin, IGF-1R, and H1 histone levels were used as loading control and as markers for total, membrane and nuclear lysates, respectively. (D) CAR mRNA levels were quantified in U373MG cells by RT real-time PCR 24 hr after transfection with 5 μ g of ERK2 plasmid or pcDNA3-HA control plasmid. Expression levels were normalized to the expression of β -actin. Data represent the mean of three experiments. ERK2 overexpression greatly reduced CAR mRNA levels. (E) Effect of ERK2 transfection on infectivity of glioma cells. U373MG cells were transfected with 5 μ g of ERK2 plasmid or pcDNA3-HA control plasmid, and 48 hr post-transfection were infected with AdGFP (25 and 50 pfu/cell). GFP expression was analyzed by cytofluorimetric analysis. Data represent the mean of three experiments. Standard deviations (error bars) of three different experiments were calculated. The differences observed were highly significant (** $p < 0.001$).

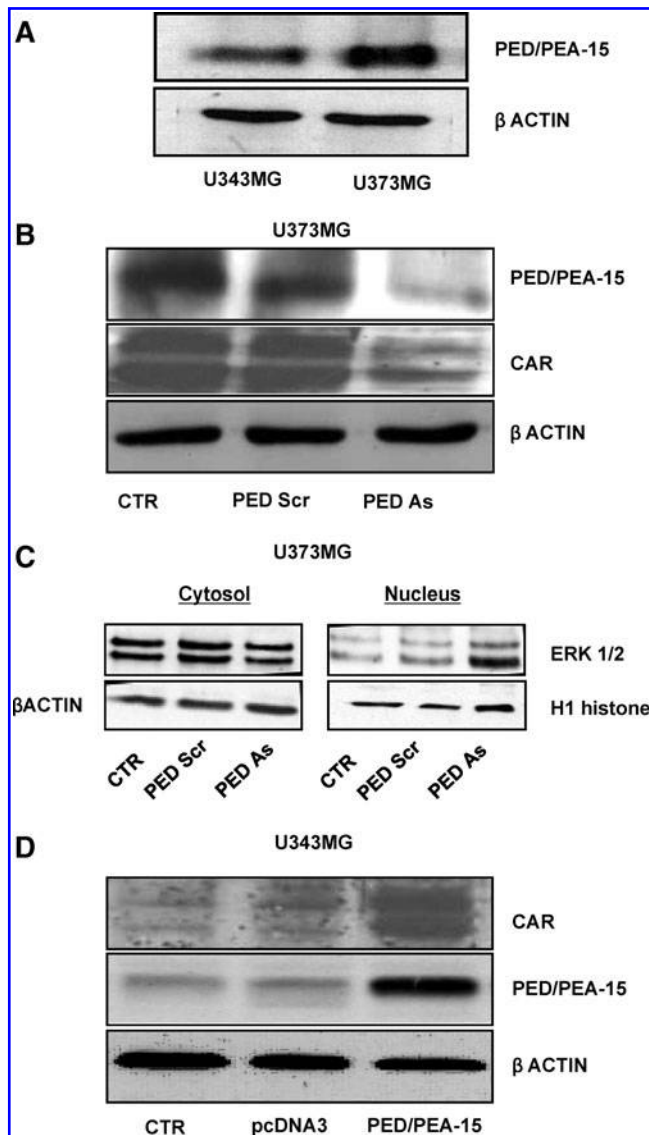


FIG. 4. PED/PEA-15 antisense (PED As) transfection. (A) Differential expression of PED/PEA-15 in glioma cell lines. U343MG and U373MG cells were analyzed for the expression of the antiapoptotic protein PED/PEA-15 on Western blot, using β -actin levels as loading control. (B) Effect of PED/PEA-15 downregulation on CAR. U373MG cells were transiently transfected with PED/PEA-15 antisense oligonucleotides (PED As) and PED/PEA-15 scrambled oligonucleotides (PED Scr). PED/PEA-15 and CAR total levels were analyzed 48 hr after transfection. (C) Effect of PED/PEA-15 downregulation on ERK1/2 localization. U373MG cells were transiently transfected with PED/PEA-15 antisense (PED As), or with a scrambled oligonucleotide (PED Scr) as control. Subcellular fractionation (nuclear and cytoplasmic) of PED As-transfected U373MG cells was performed, and ERK1/2 expression was analyzed in both fractions. β -actin and H1 histone were used as a loading control for cytosolic and nuclear fractions, respectively. (D) Effect of PED/PEA-15 upregulation on CAR expression. U343MG cells were transiently transfected with 5 μ g of the plasmid pcDNA3 carrying PED/PEA-15 cDNA (PED/PEA-15) or pcDNA3 plasmid as a control. PED/PEA-15 and CAR total levels were analyzed 48 hr after transfection, using β -actin levels as loading control.

(10 pfu/cell) and after 48 hr cell survival was analyzed (Fig. 5D). A highly significant ($p < 0.001$) increase in cell survival after infection was observed in PED As- and ERK2-transfected cells with respect to untransfected or transfected controls ($p < 0.001$).

Discussion

GBM is surgically incurable in the vast majority of patients (Brandes *et al.*, 2008), with median survival duration of about 9–15 months (Furnari *et al.*, 2007). The protocol of adjuvant therapy, radiation followed by chemotherapy, administered after surgery, has demonstrated only a moderate increase in survival (Argyriou *et al.*, 2009). Therefore novel therapeutic approaches are required. Genetically engineered, conditionally replicating viruses are promising therapeutic agents for cancer and several oncolytic viruses have already been tested in preclinical or clinical studies for the treatment of gliomas (Jiang *et al.*, 2007).

In the present study, we have observed that *dl922-947* is active against two glioblastoma cell lines, U343MG and U373MG, reinforcing the concept that the therapy of glioblastoma could benefit from the use of oncolytic viruses. However, a differential sensitivity to the oncolytic activity of *dl922-947* was evidenced in the two cell lines, with U343MG cells being more resistant to the virus.

This difference could potentially be due to factors affecting the viral life cycle (such as attachment, entry, viral gene expression, etc.). It is generally accepted that poor adenoviral entry in neoplastic cells represents the most important obstacle for an effective therapy based on replicating oncolytic adenoviruses (Vähä-Koskela *et al.*, 2007).

Coxsackievirus–adenovirus receptor (CAR) is the primary receptor for adenoviruses, and loss or reduction of CAR greatly decreases adenoviral entry (Bergelson *et al.*, 1997; Nemerow, 2000; Tomko *et al.*, 2000; Rein *et al.*, 2006). Higher levels of CAR expression were observed in U373MG cells, as compared with U343MG cells, and this was paralleled by increased infection efficiency. However, a significant reduction was observed in both cell lines blocking the receptor with an anti-CAR antibody.

Although complete abrogation of adenoviral entry was not obtained, possibly because of residual entry via alternative pathways (Arnberg *et al.*, 2009) or subtotal blockade with the antibody, our data are consistent with the hypothesis that CAR-mediated internalization plays a major role in both cell lines.

It has been demonstrated that disruption of signaling through the Raf/MEK (MAPK/ERK kinase)/ERK pathway by MEK inhibitors (U0126 and PD184352) upregulates CAR expression (Anders *et al.*, 2003). Interestingly, U373MG cells displayed higher ERK1/2 cytosolic localization, compared with U343MG cells, in which ERK1/2 was mostly nuclear. Because nuclear translocation is a crucial step for ERK-mediated regulation of gene expression, we hypothesized that ERK nuclear activity could control CAR expression. Indeed, overexpression of ERK2 in U373MG cells was accompanied by forced nuclear localization and decreased CAR mRNA and protein levels, leading to a reduction in infection efficiency.

PED/PEA-15 is a death effector domain-containing protein involved in the regulation of apoptotic cell death and highly expressed in cells of glial origin (Hao *et al.*, 2001;

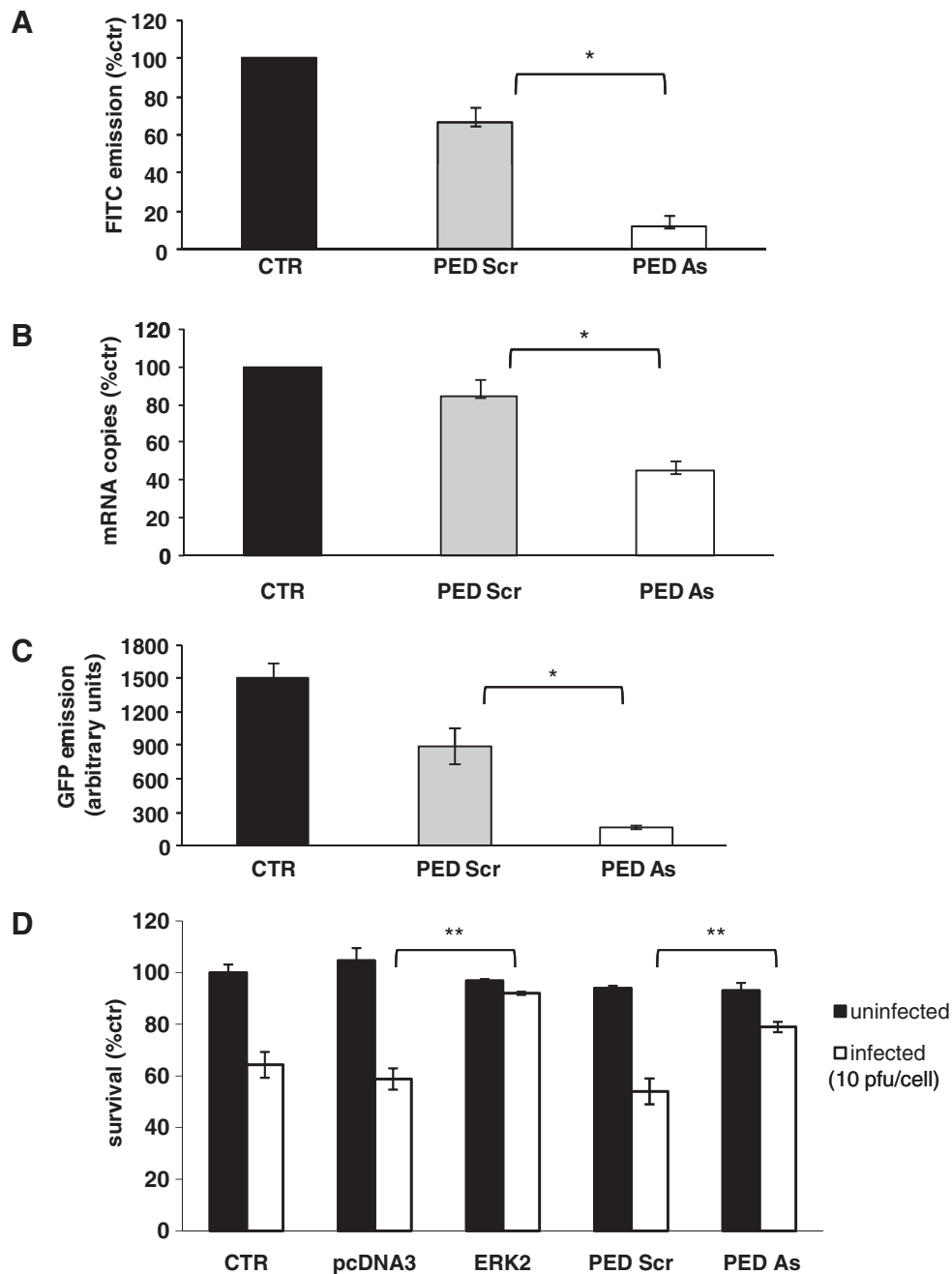


FIG. 5. Transfection with PED/PEA-15 antisense (PED As) reduces CAR levels, infectivity, and sensitivity in U373MG cells. (A) U373MG cells transfected with PED As or PED Scr oligonucleotides were analyzed for expression of CAR by surface labeling. Forty-eight hours after transfection, cells were harvested and incubated with anti-CAR or secondary FITC-labeled anti-mouse antibody alone. Labeled cells were analyzed for CAR expression by cytofluorimetric analysis. A strong reduction in CAR membrane levels was observed in PED As-transfected cells. The difference observed was significant ($*p < 0.05$). Standard deviations (error bars) of three different experiments were calculated. (B) CAR mRNA levels were quantified on U373MG cells by real-time PCR 24 hr after transfection. Expression levels were normalized to the expression of β -actin. PED As-transfected cells displayed lower CAR mRNA levels. The difference observed was significant ($*p < 0.05$). Standard deviations (error bars) of three different experiments were calculated. (C) U373MG cells were transfected with PED/PEA-15 antisense or scrambled sequence and 48 hr post-transfection were infected with AdGFP (25 pfu/cell). GFP expression was analyzed by cytofluorimetric analysis; PED As transfection significantly reduced GFP emission ($*p < 0.05$). Standard deviations (error bars) of three different experiments were calculated. (D) U373MG cells were transfected with PED/PEA-15 antisense (PED As), scrambled sequence (PED Scr), ERK2 plasmid, or pcDNA3-HA control plasmid. Forty-eight hours after transfection cells were infected with *dI922-947* (10 pfu/cell). Cell survival was analyzed 48 hr postinfection. ERK2- and PED As-transfected cells displayed lower sensitivity to the virus compared with cells transfected with control plasmids. The differences observed were highly significant ($**p < 0.001$). Standard deviations (error bars) of three different experiments were calculated.

Xiao *et al.*, 2002). PED/PEA-15 regulates the ERK/MAPK pathway by binding ERK1/2 and preventing its nuclear accumulation and activity (Formstecher *et al.*, 2001; Hill *et al.*, 2002; Renault *et al.*, 2003; Whitehurst *et al.*, 2004; Renganathan *et al.*, 2005). Moreover, abrogation of ERK1/2 binding as a result of point mutations in PED/PEA-15 restores normal ERK1/2 function (Whitehurst *et al.*, 2004). We have hypothesized that PED/PEA-15 could be involved in CAR regulation and adenoviral infectivity by controlling ERK subcellular distribution. Indeed, PED/PEA-15 levels are higher in U373MG cells than in U343MG cells and positively correlate with the relative ERK cytosolic abundance, CAR levels, adenoviral infectivity, and *dl922-947* killing capacity.

In U373MG cells genetic silencing of PED/PEA-15 with a specific antisense oligonucleotide enhanced ERK1/2 nuclear distribution and led to a reduction of CAR levels and sensitivity to the oncolytic adenovirus *dl922-947*. Conversely, overexpression of PED/PEA-15 increased CAR total levels in U343MG cells.

Our data show that PED/PEA-15 levels correlate with infectivity and sensitivity to oncolytic adenoviruses and suggested that, in association with CAR, the evaluation of PED/PEA-15 levels could represent a useful tool to guide patients with glioblastoma toward specific therapeutic options.

It is important to note that PED/PEA-15 is involved in the regulation of apoptotic cell death (Hao *et al.*, 2001; Condorelli *et al.*, 2002; Xiao *et al.*, 2002) and it has been demonstrated that, in glioma cell lines, the apoptotic cascade activated by tumor necrosis factor-related apoptosis-inducing ligand (TRAIL) is negatively regulated by PED/PEA-15 (Hao *et al.*, 2001; Xiao *et al.*, 2002; Song *et al.*, 2006). Moreover, overexpression of PED/PEA-15 induces a marked resistance against glucose deprivation-induced apoptosis in glioma cells (Eckert *et al.*, 2008). Glioma cells overexpressing PED/PEA-15 also show a marked resistance to radiotherapy (G. Perruolo, G. Botta, and G. Portella, unpublished data) and it has been reported that PED/PEA-15 may contribute to the resistance to chemotherapeutic agents in breast cancer cells (Stassi *et al.*, 2005) and B-cell chronic lymphocytic leukemia cells (Garofalo *et al.*, 2007), and in human non-small cell lung cancer (Zanca *et al.*, 2008).

These findings indicate that PED/PEA-15 increases the resistance to apoptotic agents, and that PED/PEA-15 expression could predict resistance to apoptosis. It is possible to hypothesize that patients with high PED/PEA-15 levels should not benefit from therapy based on these agents, whereas our data indicate that these patients could benefit from adenovirus-based therapy.

Therefore, PED/PEA-15 expression levels could play a dual predictive role: as a marker of resistance to chemo- and radiotherapy for its antiapoptotic activity and as a marker of sensitivity to adenovirus-based therapies, for its role on CAR expression.

In conclusion, our data show that adenoviral infectivity is mostly CAR-mediated in glioblastoma cells and that PED/PEA-15 upregulates CAR expression, by preventing ERK nuclear translocation. Further studies are required to clearly assess the role of PED/PEA-15 as a predictive marker in glioblastoma.

Acknowledgments

The authors thank Dr. G. Hallden for kindly providing RmcB antibody and Dr. M. Chiariello for the gift of plasmid

pcDNA3-HA-pERK2. This study was supported by the Associazione Italiana per la Ricerca sul Cancro (AIRC) and by the Italian Ministry of Instruction, University and Research. S.L. is the recipient of a grant from the Fondazione Italiana per la Ricerca sul Cancro (FIRC).

Author Disclosure Statement

No competing financial interests exist.

References

- Anders, M., Christian, C., McMahon, M., McCormick, F., and Korn, W.M. (2003). Inhibition of the Raf/MEK/ERK pathway up-regulates expression of the coxsackievirus and adenovirus receptor in cancer cells. *Cancer Res.* 63, 2088–2095.
- Argyriou, A.A., Antonacopoulou, A., Iconomou, G., and Kalofonos, H.P. (2009). Treatment options for malignant gliomas, emphasizing towards new molecularly targeted therapies. *Crit. Rev. Oncol. Hematol.* 69, 199–210.
- Arnberg, N. (2009). Adenovirus receptors: Implications for tropism, treatment and targeting. *Rev. Med. Virol.* 19, 165–178.
- Bergelson, J.M., Cunningham, J.A., Droguett, G., Kurt-Jones, E.A., Krithivas, A., Hong, J.S., Horwitz, M.S., Crowell, R.L., and Finberg, R.W. (1997). Isolation of a common receptor for coxsackie B viruses and adenoviruses 2 and 5. *Science* 275, 1320–1323.
- Brandes, A.A., Tosoni, A., Franceschi, E., Reni, M., Gatta, G., and Vecht, C. (2008). Glioblastoma in adults. *Crit. Rev. Oncol. Hematol.* 67, 139–152.
- Cohen, C.J., Shieh, J.T., Pickles, R.J., Okegawa, T., Hsieh, J.T., and Bergelson, J.M. (2001). The coxsackievirus and adenovirus receptor is a transmembrane component of the tight junction. *Proc. Natl. Acad. Sci. U.S.A.* 98, 15191–15196.
- Condorelli, G., Vigliotta, G., Iavarone, C., Caruso, M., Tocchetti, C.G., Andreozzi, F., Cafieri, A., Tecce, M.F., Formisano, P., Beguinot, L., and Beguinot, F. (1998). PED/PEA-15 gene controls glucose transport and is overexpressed in type 2 diabetes mellitus. *EMBO J.* 17, 3858–3866.
- Condorelli, G., Trencia, A., Vigliotta, G., Perfetti, A., Goglia, U., Cassese, A., Musti, A.M., Miele, C., Santopietro, S., Formisano, P., and Beguinot, F. (2002). Multiple members of the mitogen-activated protein kinase family are necessary for PED/PEA-15 anti-apoptotic function. *J. Biol. Chem.* 277, 11013–11018.
- Coyne, C.B., and Bergelson, J.M. (2005). CAR: A virus receptor within the tight junction. *Adv. Drug Deliv. Rev.* 57, 869–882.
- Eckert, A., Böck, B.C., Tagscherer, K.E., Haas, T.L., Grund, K., Sykora, J., Herold-Mende, C., Ehemann, V., Hollstein, M., Chneiweiss, H., Wiestler, O.D., Walczak, H., and Roth, W. (2008). The PEA-15/PED protein protects glioblastoma cells from glucose deprivation-induced apoptosis via the ERK/MAP kinase pathway. *Oncogene* 27, 1155–1166.
- Fechner, H., Haack, A., Wang, H., Wang, X., Eizema, K., Pauschinger, M., Schoemaker, R., Veghel, R., Houtsmuller, A., Schultheiss, H.P., Lamers, J., and Poller, W. (1999). Expression of coxsackie adenovirus receptor and α_v -integrin does not correlate with adenovector targeting *in vivo* indicating anatomical vector barriers. *Gene Ther.* 6, 1520–1535.
- Formstecher, E., Ramos, J.W., Fauquet, M., Calderwood, D.A., Hsieh, J.C., Canton, B., Nguyen, X.T., Barnier, J.V., Camonis, J., Ginsberg, M.H., and Chneiweiss, H. (2001). PEA-15 mediates cytoplasmic sequestration of ERK MAP kinase. *Dev. Cell* 1, 239–250.
- Furnari, F.B., Fenton, T., Bachoo, R.M., Mukasa, A., Stommel, J.M., Stegh, A., Hahn, W.C., Ligon, K.L., Louis, D.N., Brennan,

- C., Chin, L., DePinho, R.A., and Cavenee, W.K. (2007). Malignant astrocytic glioma: Genetics, biology, and paths to treatment. *Genes Dev.* 21, 2683–2710.
- Fuxe, J., Liu, L., Malin, S., Philipson, L., Collins, V.P., and Pettersson, R.F. (2003). Expression of the coxsackie and adenovirus receptor in human astrocytic tumors and xenografts. *Int. J. Cancer* 103, 723–729.
- Garofalo, M., Romano, G., Quintavalle, C., Romano, M.F., Chiurazzi, F., Zanca, C., and Condorelli, G. (2007). Selective inhibition of PED protein expression sensitizes B-cell chronic lymphocytic leukaemia cells to TRAIL-induced apoptosis. *Int. J. Cancer* 120, 1215–1222.
- Hao, C., Beguinot, F., Condorelli, G., Trecia, A., Van Meir, E.G., Yong, V.W., Parney, I.F., Roa, W.H., and Petruk, K.C. (2001). Induction and intracellular regulation of tumor necrosis factor-related apoptosis-inducing ligand (TRAIL) mediated apoptosis in human malignant glioma cells. *Cancer Res.* 61, 1162–1170.
- Haseley, A., Alvarez-Breckenridge, C., Chaudhury, A.R., and Kaur, B. (2009). Advances in oncolytic virus therapy for glioma. *Recent Pat. CNS Drug Discov.* 4, 1–13.
- Heise, C., Hermiston, T., Johnson, L., Brooks, G., Sampson-Johannes, A., Williams, A., Hawkins, L., and Kirn, D. (2000). An adenovirus E1A mutant that demonstrates potent and selective systemic anti-tumoral efficacy. *Nat. Med.* 6, 1134–1139.
- Hill, J.M., Vaidyanathan, H., Ramos, J.W., Ginsberg, M.H., and Werner, M.H. (2002). Recognition of ERK MAP kinase by PEA-15 reveals a common docking site within the death domain and death effector domain. *EMBO J.* 21, 6494–6504.
- Hsu, K.L., Lonberg-Holm, K., Alstein, B., and Crowell, R.L. (1988). A monoclonal antibody specific for the cellular receptor for the group B coxsackieviruses. *J. Virol.* 62, 1647–1652.
- Jiang, H., Gomez-Manzano, C., Aoki, H., Alonso, M.M., Kondo, S., McCormick, F., Xu, J., Kondo, Y., Bekele, B.N., Colman, H., Lang, F.F., and Fueyo, J. (2007). Examination of the therapeutic potential of Delta-24-RGD in brain tumor stem cells: Role of autophagic cell death. *J. Natl. Cancer Inst.* 99, 1410–1414.
- Libertini, S., Iacuzzo, I., Ferraro, A., Vitale, M., Bifulco, M., Fusco, A., and Portella, G. (2007). Lovastatin enhances the replication of the oncolytic adenovirus *d11520* and its anti-neoplastic activity against anaplastic thyroid carcinoma cells. *Endocrinology* 148, 5186–5194.
- Nemerow, G.R. (2000). Cell receptors involved in adenovirus entry. *Virology* 274, 1–4.
- Portella, G., Scala, S., Vitagliano, D., Vecchio, G., and Fusco, A. (2002). ONYX-015, an E1B gene-defective adenovirus, induces cell death in human anaplastic thyroid carcinoma cell lines. *J. Clin. Endocrinol. Metab.* 8, 2525–2531.
- Rein, D.T., Breidenbach, M., and Curiel, D.T. (2006). Current developments in adenovirus-based cancer gene therapy. *Future Oncol.* 2, 137–143.
- Renault, F., Formstecher, E., Callebaut, I., Junier, M.P., and Chneiweiss, H. (2003). The multifunctional protein PEA-15 is involved in the control of apoptosis and cell cycle in astrocytes. *Biochem. Pharmacol.* 66, 1581–1588.
- Renganathan, H., Vaidyanathan, H., Knapinska, A., and Ramos, J.W. (2005). Phosphorylation of PEA-15 switches its binding specificity from ERK/MAPK to FADD. *Biochem. J.* 390, 729–735.
- Ruvolo, P.P., Deng, X., Carr, B.K., and May, W.S. (1998). A functional role for mitochondrial protein kinase C α in Bcl2 phosphorylation and suppression of apoptosis. *J. Biol. Chem.* 273, 25436–25442.
- Sharif, A., Renault, F., Beuvon, F., Castellanos, R., Canton, B., Barbeito, L., Junier, M.P., and Chneiweiss, H. (2004). The expression of PEA-15 (phosphoprotein enriched in astrocytes of 15 kDa) defines subpopulations of astrocytes and neurons throughout the adult mouse brain. *Neuroscience* 126, 263–275.
- Sherr, C.J. (2000). The Pezcoller Lecture: Cancer cell cycle revisited. *Cancer Res.* 60, 3689–3695.
- Skehan, P., Storeng, R., Scudiero, D., Monks, A., McMahon, J., Vistica, D., Warren, J.T., Bokesch, H., Kenney, S., and Boyd, M.R. (1990). New colorimetric cytotoxicity assay for anticancer-drug screening. *J. Natl. Cancer Inst.* 82, 1107–1112.
- Solomon, D.A., Kim, J.S., Jean, W., and Waldman, T. (2008). Conspirators in a capital crime: Co-deletion of p18^{INK4c} and p16^{INK4a}/p14^{ARF}/p15^{INK4b} in glioblastoma multiforme. *Cancer Res.* 68, 8657–8660.
- Song, J.H., Bellail, A., Tse, M.C., Yong, V.W., and Hao, C. (2006). Human astrocytes are resistant to Fas ligand and tumor necrosis factor-related apoptosis-inducing ligand-induced apoptosis. *J. Neurosci.* 26, 3299–3308.
- Stassi, G., Garofalo, M., Zerilli, M., Ricci-Vitiani, L., Zanca, C., Todaro, M., Aragona, F., Limite, G., Petrella, G., and Condorelli, G. (2005). PED mediates AKT-dependent chemoresistance in human breast cancer cells. *Cancer Res.* 65, 6668–6675.
- Tomko, R.P., Johansson, C.B., Totrov, M., Abagyan, R., Frisén, J., and Philipson, L. (2000). Expression of the adenovirus receptor and its interaction with the fiber knob. *Exp. Cell Res.* 255, 47–55.
- Vähä-Koskela, M.J., Heikkilä, J.E., and Hinkkanen, A.E. (2007). Oncolytic viruses in cancer therapy. *Cancer Lett.* 254, 178–216.
- Vecil, G.G., and Lang, F.F. (2003). Clinical trials of adenoviruses in brain tumors: A review of Ad-p53 and oncolytic adenoviruses. *J. Neurooncol.* 65, 237–246.
- Watanabe, T., Hioki, M., Fujiwara, T., Nishizaki, M., Kagawa, S., Taki, M., Kishimoto, H., Endo, Y., Urata, Y., Tanaka, N., and Fujiwara, T. (2006). Histone deacetylase inhibitor FR901228 enhances the antitumor effect of telomerase-specific replication-selective adenoviral agent OBP-301 in human lung cancer cells. *Exp. Cell Res.* 312, 256–265.
- Whitehurst, A.W., Robinson, F.L., Moore, M.S., and Cobb, M.H. (2004). The death effector domain protein PEA-15 prevents nuclear entry of ERK2 by inhibiting required interactions. *J. Biol. Chem.* 279, 12840–12847.
- Xiao, C., Yang, B.F., Asadi, N., Beguinot, F., and Hao, C. (2002). Tumor necrosis factor-related apoptosis-inducing ligand-induced death-inducing signaling complex and its modulation by c-FLIP and PED/PEA-15 in glioma cells. *J. Biol. Chem.* 277, 25020–25025.
- Zanca, C., Garofalo, M., Quintavalle, C., Romano, G., Acunzo, M., Ragno, P., Montuori, N., Incoronato, M., Tornillo, L., Baumhoer, D., Briguori, C., Terracciano, L., and Condorelli, G. (2008). PED is overexpressed and mediates TRAIL resistance in human non-small cell lung cancer. *J. Cell. Mol. Med.* 12, 2416–2426.

Address correspondence to:

Dr. Giuseppe Portella
 Dipartimento di Biologia e Patologia Cellulare e Molecolare
 Facoltà di Medicina e Chirurgia
 Università di Napoli Federico II
 via S. Pansini 5
 80131 Naples, Italy

E-mail: Portella@unina.it

Received for publication September 28, 2009;
 accepted after revision April 12, 2010.

Published online: July 16, 2010.

Aurora A and B Kinases - Targets of Novel Anticancer Drugs

Silvana Libertini[§], Antonella Abagnale[§], Carmela Passaro, Ginevra Botta and Giuseppe Portella*

Dipartimento of Biology and Cellular and Molecular Pathology, School of Medicine, University of Naples Federico II, via s. Pansini 5, 80131 Napoli, Italy

Received: November 11, 2009; Accepted: January 16, 2010; Revised: May 6, 2010

Abstract: The Aurora Kinases are highly related serine-threonine kinases, essential for accurate and equal segregation of genomic material during mitosis. A large number of studies have linked the aberrant expression of Aurora kinases to cancer, leading to the development of specific Aurora kinases inhibitors. Several small molecules inhibit with a similar efficacy both Aurora A and Aurora B, however, in most cases the effects resemble Aurora B disruption by genetic methods, indicating that Aurora B represents an effective therapeutic target. These drugs are currently under preclinical or clinical evaluation and are reviewed in this article. The relevant patents are discussed.

Keywords: Aurora kinase, Aurora B, serine-threonine kinase, mitosis, cytokinesis, cancer, inhibitors.

INTRODUCTION

Aurora Kinases

Mitosis is an extraordinarily complex biological process, by which a complete copy of the duplicated genome is precisely segregated into two daughter cells. All mitotic phases are strictly controlled by phosphorylation events performed by several evolutionary conserved serine-threonine kinases, known as mitotic kinases, such as cyclin-dependent kinases, NIMA-related kinases and Aurora-Ipl1 related kinases [1].

Mammalian genomes contain three genes encoding Aurora kinases, denoted Aurora A, Aurora B, and Aurora C [2]. The three Aurora kinases are serine-threonine protein kinases that together form a small kinase family phylogenetically related to the branch of the AGC (protein kinase A/protein kinase G/protein kinase C family) protein kinases [3]. The founding member of the Aurora kinases is the *Drosophila* Aurora kinase that was discovered in a screen to identify genes involved in mitotic spindle function [4]. Fungi have only one Aurora kinase (Ipl1 in *S. cerevisiae* [5, 6] and Ark1 in *S. pombe* [7]) that is functionally more related to the Aurora B kinases in higher organisms. Mammals have a third Aurora gene called Aurora C. Aurora kinase function is controlled by several mechanisms. Firstly, gene transcription of the Aurora kinases is cell cycle regulated. The promoters of Aurora B and Aurora A contain specific sequences (CDE/CHR sequences) required for transcription in G2 [8-10]. Several transcription factors, such as E2F-1, E2F-4, DP-2 and FoxM1 have been implicated in cell cycle regulated transcription of Aurora B [8-11]. The Aurora C gene seems to be mainly expressed in meiotically dividing cells, and its transcription is at least in part controlled by a testis-specific transcription factor called Testis Zinc Finger Protein (Tzfp)

[12]. Aurora C, like Aurora B, is capable of binding to the IN-box of INCENP. This binding also results in activation of Aurora C, in a manner that is most likely similar to the mode of activation of Aurora B [13, 14]. Aurora C is the least studied of the three mammalian Aurora kinases [15]. It was initially discovered in mice as a testis-specific serine/threonine kinase named Aie1 [16]. Protein kinase A (PKA) is able to phosphorylate Aurora C on Thr¹⁷¹, which is the threonine residue that must be phosphorylated for kinase activity. When Thr¹⁷¹ and Thr¹⁷⁵ were both mutated to alanines, Aurora C showed impaired kinase activity toward an as yet undefined 16kDa protein named Aurora C substrate 1 (ACS-1) [17]. Interestingly, Aurora C appears to share its cellular localization and some functions with Aurora B. Both Aurora B and C are chromosomal passenger proteins and both form complexes with INCENP [14] and survivin [18]. INCENP was also found to stimulate the ability of Aurora C to phosphorylate histone 3 (H3) [14]. The Aurora C gene is expressed at low levels in several tissues and is over-expressed in some cancer cell lines [13] such as those derived from thyroid cancer [19]. Protein expression of Aurora C is similar to the two other mammalian Aurora kinases in that it peaks during G2/M phases, but it does so later in mitosis than Aurora A or B [13]. Either over-expression of kinase dead Aurora C or knockdown of Aurora C causes cells to become multinucleated; this phenotype is reminiscent of knockdown of Aurora B. Interestingly, Aurora C can rescue Aurora B knockdown and the same is true of the reverse scenario [14, 18]. Taken together, the similar cellular localization and common knockdown phenotypes of Aurora B and C suggest that these two kinases may have redundant cellular functions.

Both Aurora A and Aurora B are targets of a multi-subunit E3-ubiquitin ligase called the Anaphase Promoting Complex/Cyclosome (APC/C) [20-25]. The APC/C, in conjunction with its specificity factor Cdh1, targets these proteins for destruction during mitotic exit and as such ensures that G1 cells contain low levels of these proteins. The cellular consequences of misregulated degradation of the

*Address correspondence to this author at the Dipartimento of Biology and Cellular and Molecular Pathology, School of Medicine, University of Naples Federico II, via s. Pansini 5, 80131 Napoli, Italy;

Tel: ++39 081 7463052; Fax: 39 081 7463846; E-mail: portella@unina.it

[§]Equal contribution.

Aurora kinases are unknown, although non-degradable Aurora B was shown to be more potent in promoting anchorage-independent growth than wild type Aurora B [21]. Besides the APC/C, also a Cullin 3(Cul3)-based E3 ligase was shown to ubiquitinate Aurora B *in vitro* and *in vivo* [26]. Ubiquitination was shown to promote dissociation of Aurora B from metaphase chromosomes, and recent data indicate that degradation-independent ubiquitination of Aurora B triggers Cdc48/p97 ATPase-dependent extraction of Aurora B from mitotic chromosomes, an event required for timely chromosome decondensation during mitotic exit. In addition, removal of Aurora B from mitotic chromosomes is required for nuclear membrane assembly in telophase. Human Aurora A is turned over through the anaphase promoting complex/cyclosome (APC/C)-ubiquitin-proteasome pathway [27]. Aurora A degradation is dependent on hCdh1 *in vivo*, not on hCdc20 [20] and involves two different degradation motifs. The first corresponds to a N-terminal, D-Box-activating motif (RxLxPS). This motif confers functionality to a second motif, a D-Box, consisting of the sequence RxxLxxG. The D-box is located at the C-terminus of the kinase domain and is the target of Fizzy-related proteins [28]. Although Aurora B possesses the same D-Box as Aurora A, it is not degraded by the same ubiquitin ligase. Instead, Aurora B undergoes degradation by binding to the human proteasome α -subunit C8 (HC8) in a proteasome-dependent manner [29]. In contrast with Aurora A and B, the mechanism(s) involved in Aurora C degradation remain obscure. Certainly, the detailed study of Aurora C regulation constitutes an interesting area of research [30].

Regulation of Aurora A is complex and involves both phosphorylation/dephosphorylation and degradation. Phosphorylation stimulates kinase activity. Three phosphorylation sites have been identified in *Xenopus* Aurora A by mass spectrometry [31]. Phosphorylation of Thr²⁹⁵ (Thr²⁸⁸ in human Aurora A) in the activation loop is essential for kinase activity [27]. This residue is in a protein kinase A (PKA) consensus motif, and PKA can phosphorylate and activate Aurora A *in vitro* [27]. However, this site also fits the consensus phosphorylation sequence that has been defined for *S. cerevisiae* Ip11 (R/K)X(T/S)(I/L/V) [32]; and the equivalent residue (Thr²⁶⁰) in yeast Aurora has indeed been identified as an autophosphorylation site [32]. Ser⁵³ in the N-terminal A-box is phosphorylated during M phase and might have a role in the regulation of Aurora A degradation. Although the third phosphorylation site to be identified - Ser³⁴⁹ - is not essential for catalytic activity, S349D mutants block kinase activation, which indicates a possible structural or regulatory role for this modification [31]. The phosphatase PP1 negatively regulates the Aurora kinases. The counteracting effect of PP1, which was first described for yeast Ip11, has also been shown in *Xenopus* and human cell lines [27, 33-36]. The activation of Aurora A by TPX2 is at least partly due to antagonism of PP1 [37, 38]. Aurora A is degraded in late mitosis/early G1 by the Cdh1/Fizzy-related form of the anaphase-promoting complex/cyclosome (APC/C; the APC/C with Cdh1/Fizzy-related as a substrate recognition subunit) [6, 28]. Aurora A has a silent C-terminal D-box (destruction box), which is also present in Aurora B [24, 38], but which is only functional in the presence of a N-terminal A-box (also called the D-box-activating-domain

(DAD)) [38]. The A-box/DAD is absent from Aurora B and C, and their D-boxes are not targeted by the APC/C during mitotic exit. Phosphorylation of the A-box seems to make the Aurora A resistant to APC/C mediated degradation. Interestingly, the D-box is recognized by both the Cdh1/Fizzy-related and Cdc20/Fizzy forms of the APC/C, but Aurora A is only targeted by the former. The recently identified Aurora A-kinase-interacting protein (AIP), a negative regulator of Aurora A, is a conserved nuclear protein that interacts with the kinase *in vivo* [39]. AIP was isolated as a dosage-dependent suppressor of Aurora A that was ectopically overexpressed in budding yeast. In mammalian cells, AIP might downregulate Aurora through proteasome-dependent degradation [39]. Its normal function is not known [40].

Aurora kinases are involved in multiple facets of mitosis and cell division, including centrosome duplication, mitotic spindle formation, chromosome alignment upon the spindle, mitotic checkpoint activation, and cytokinesis. Errors in these processes ultimately lead to aneuploidy or cell death [41]. Aberrant expression of Aurora Kinases may disturb checkpoint functions, particularly in mitosis, and this may lead to genetic instability and trigger the development of tumours [42]. The Aurora A and B have emerged as essential regulators of cell division. Aurora A is involved in the regulation of mitotic entry, centrosome maturation, and spindle assembly. Aurora B is required for correct chromosome segregation and cytokinesis; Aurora C plays a role in the regulation of cilia and flagella, localizes to centrosomes from anaphase to cytokinesis and it is predominantly expressed in testis [43, 44].

The protein encoded by the Aurora A, B, and C genes are 403, 343, and 275 amino acids long, respectively. These kinases present a similar domain organization: a N-terminal regulatory domain of 39-129 residues in length, a protein kinase domain and a short C-terminal catalytic domain of 15-20 residues. The catalytic domain of these three proteins is highly homologous, sharing greater than 70% homology among the three Aurora proteins [40, 45-47]. In all three kinases ATP binding active site are lined by 26 residues and three variants: Leu²¹⁵, Thr²¹⁷, Arg²²⁰ are specific to Aurora A. A PEST-like motif has been identified in Aurora C, and a mutation of this motif significantly abrogates Aurora C kinase activity [17]. Each Aurora kinase domain contains a threonine residue (Thr²⁸⁸) within the protein's activation loop that must be phosphorylated for the kinase to be active. The N-terminal domain of the Aurora kinases shares low sequence conservation, which determines selectivity during protein-protein interactions. Additionally, the Aurora proteins all contain a destruction box, or D-box, at the C-terminal, which is a sequence typically recognized by APC/C, mediating the proteasomal degradation of a D-box containing protein. The alignment of Aurora A and B allows the identification of one distantly conserved KEN motif, spanning 11-18 residues. The KEN motif acts as a Cdh1-dependent anaphase-promoting complex (APC) recognition signal. Destruction also requires a short region in the N-terminal, which contains a newly identified recognition signal, the A-box. The A-box is conserved in vertebrate Aurora kinases and contains a Ser⁵³, which is phosphorylated during M phase. Mutation of Ser⁵³ to aspartic acid, which can mimic the effects of phosphorylation, completely blocks

Cdh1-dependent destruction of Aurora A. The N-terminal domain varies widely among the Aurora proteins, and this domain is believed to be involved in substrate binding and cellular localization Fig. (1) [15, 24, 30, 40, 46].

Despite significant sequence homology, the localization and functions of these three Kinases are largely distinct from one another. Aurora A is ubiquitously expressed and regulates cell cycle events occurring from late S phase through M phase, including centrosome maturation [48], mitotic entry [49, 50], centrosome separation [51], bipolar-spindle assembly [38, 52], cytokinesis [53], chromosome alignment on the metaphase plate [53-56], and mitotic exit. Aurora B is essential for chromosome biorientation, accurate chromosomal segregation, correct functioning of the spindle assembly checkpoint and cytokinesis [57-61]. Aurora C exhibits similar functions to those assigned to Aurora B and is required for cytokinesis. A study of 2004 found that direct association with INCEP activates Aurora C, suggesting the cooperation of Aurora A and B in the regulation of mitotic events. Recently, it has been shown that Aurora C can complement the functions of Aurora B [44].

The genes encoding the three human Aurora kinases map to regions that are affected by chromosomal abnormalities in different cancer types, and overexpression of each of the human Aurora kinases has been detected in human tumours [42].

Aurora B

The Aurora B gene lies on human chromosome 17p13 and codifies for a 41KDa serine-threonine kinase. Aurora B expression and activity in proliferating tissues are cell cycle regulated: expression peaks at G2-M transition and kinase

activity is maximal during mitosis. At the end of mitosis, the D-box region of Aurora B is recognized by the anaphase-promoting complex/cyclosome (APC/C), leading to Aurora B ubiquitination and degradation [46].

Aurora B is the enzymatic component of a bigger complex called Chromosomal Passenger Complex (CPC) [62]. The CPC shows a very dynamic localization during mitosis hence its name: it covers the entire chromatin during the onset of mitosis, moves from the chromosome arms toward the kinetochores during prometaphase, relocates to the microtubules of the central spindle at the metaphase-anaphase transition, and finally concentrates at the midbody during telophase/cytokinesis. This localization parallels the diverse functions of the CPC during mitosis: modifying histones at the chromatin, correcting misattachments while at the centromere, and regulating cytokinesis at the central spindle. The CPC contains three non enzymatic subunits, all of which are essential for the activity, localization, stability, and substrate specificity of Aurora B. In human cells, these non enzymatic subunits are Survivin, the Inner Centromere Protein (INCENP), and Borealin [63, 64]. It is believed that, during mitosis, two distinct passenger complexes exist: one consisting of INCENP and Aurora B, responsible for histone H3 phosphorylation and another containing all four CPC members, responsible for chromosome alignment and cytokinesis [63, 65]. As such, Aurora B can be considered as a histone kinase, a spindle checkpoint kinase and a cytokinesis kinase Fig. (2) [62].

Histone kinase -Aurora B kinases are responsible for one of the classic modifications of chromatin in mitosis: phosphorylation of histone H3 on Ser¹⁰ [66]. This modification, which is conserved from yeast to vertebrates, is carried out

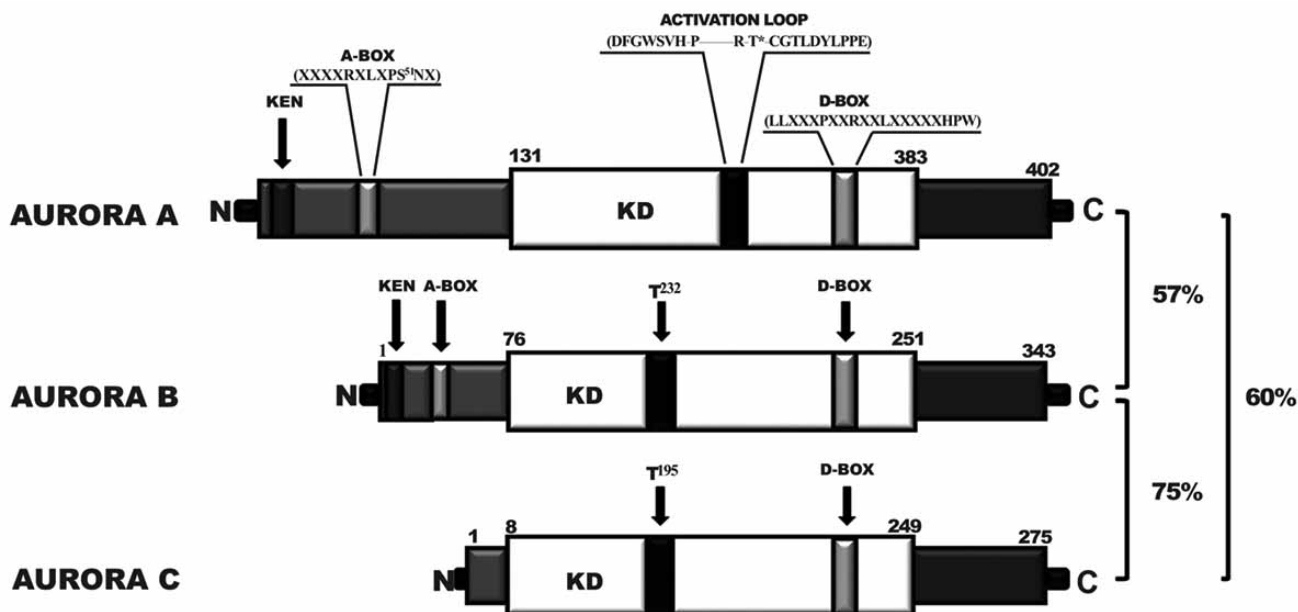


Fig. (1). Human Aurora kinase structure. The Aurora kinases are largely composed of two domains, the N-terminal regulatory domain and the C-terminal catalytic domain. In the regulatory domain, Aurora A and B contain an activation domain (A-box) that regulates their degradation. Aurora A contains a KEN box similar to that found on cdc20 ubiquitinated in response to APC/C^{Cdh1}. In the C-terminal domain all three Aurora kinases contain the kinase domain (KD) and a destruction box (D-box).

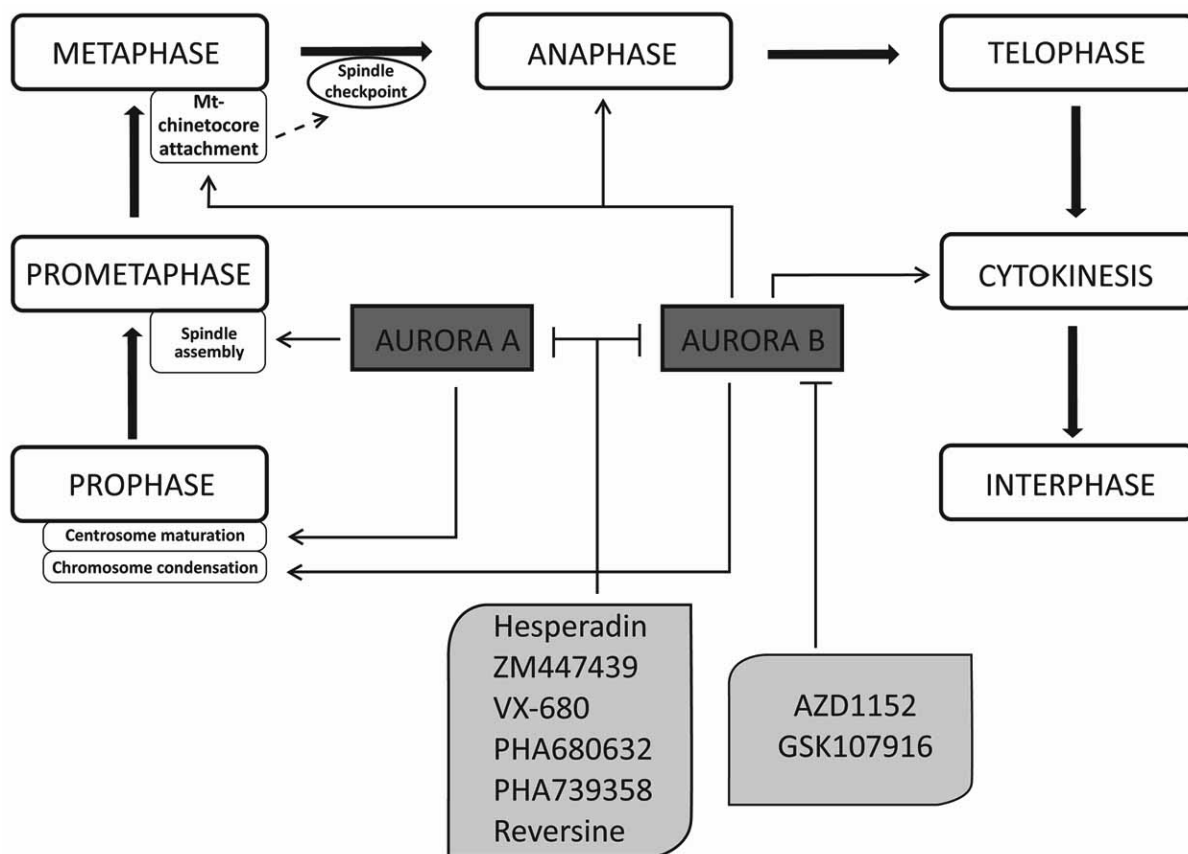


Fig. (2). Localization and function of human Aurora kinases during mitosis and their inhibitors.

by Ipl1 in budding yeast [67] and Aurora B in metazoans [35, 67, 68-72]. Aurora B is also responsible for histone H3 phosphorylation on Ser²⁸ from prophase to metaphase [64, 73] and for the mitotic phosphorylation of Ser⁷ of the kinetochore-specific histone H3 variant centromere protein A (CENP-A) [58]. Condensation of chromosomes into compact structures is essential for error-free sister chromatid segregation and is driven by the action of Condensin complexes (Condensin I and II in human cells) [74, 75]. Aurora B contributes to proper condensation and chromosomal association of the Condensin I complex in several organisms, potentially via direct phosphorylation of the three non-SMC subunits [70, 76-80]. It must be noted that Condensin loading and condensation show a different dependency on Aurora B in different organisms [70, 76-79, 81]. Phosphorylation of histone H3 at Ser¹⁰ during late G2/prophase by Aurora B has also been linked with chromosome condensation, also because mutation of this phosphorylation site in *Tetrahymena thermophila* and *S. pombe* caused chromosome condensation and subsequent segregation defects [70, 72, 82-84]. However, a similar mutation did not cause any mitotic defects in the budding yeast *Saccharomyces cerevisiae* [82]. These differences might be explained by differences in chromosome structure between these species. In human cells, phosphorylation of Ser¹⁰ histone H3 was suggested to displace the HP-1 family of proteins from heterochromatin in mitosis [85, 86], but whether this displacement has consequences for chromosome condensation is unknown. Defects in chromosome structure and compaction are observed in Aurora B depleted *Drosophila* cells [68, 87], but the

underlying mechanism is not known. One possibility is that Aurora activity might be required for condensin function. However, the relationship between the kinase and condensin is unclear. The condensin complex [88] does not localize properly to chromosomes in *Drosophila* cells that lack active Aurora B [87] or in *S. pombe* that lacks Ark1 [89]. In *C. elegans*, condensin activity is independent of Aurora B in prometaphase, but becomes dependent on the kinase in metaphase [90, 91]; in *Xenopus* extracts, Aurora B is not required for condensin binding or chromosome condensation [72]. Furthermore, in cells treated with the Aurora B inhibitor hesperadin [92], in which Aurora B localizes properly but is enzymatically inactive, the condensin complex localizes normally. There is no evidence so far that any of the condensin subunits is a substrate of Aurora B [40].

Spindle checkpoint kinase -Aurora B also controls chromosome cohesion. Cohesion is brought about by a ring-like Cohesin complex, which is related to the Condensin complexes. Cohesion persists between sister chromatids until the metaphase to anaphase transition [93]. In vertebrate cells, Cohesin is removed in mitosis through two distinct mechanisms [94]. The first, referred to as the prophase pathway, removes Cohesin from chromosome arms in a fashion that depends on Plk-1 and Aurora B [79, 95, 96]. Aurora B functions in this prophase pathway through control of the Shugoshin family of centromeric proteins. These proteins were identified as regulators of meiotic chromosome segregation in *Drosophila* and budding yeast [97, 98]. The human counterpart of these proteins (Sgo1) protects centromeric Cohesin during mitosis *via* recruitment of a PP2A-

phosphatase complex to the centromere [99-104]. Aurora B activity confines Sgo1 localisation to centromeric regions and upon inhibition or depletion of Aurora B, Sgo1 fails to concentrate on centromeres and instead localises diffusely along chromosome arms [77, 105, 106]. Displacement of Sgo1 from centromeres causes protection of chromosome arm-localised Cohesin complexes against removal [99, 100, 102]. Alternatively, since HP-1 influences Cohesin recruitment to chromatin [107, 108], Aurora B-dependent regulation of HP-1-chromatin retention might be an alternative way by which it influences chromosome cohesion.

Recently, Aurora B has also been put forward as an important regulator of chromatin-induced spindle assembly in a pathway functioning in parallel to the Ran-dependent pathway. Aurora B is activated on chromatin and depletion or inhibition of Aurora B severely perturbs spindle assembly in *Xenopus* extracts [109-111]. Two different Aurora B substrates were suggested as downstream targets in this pathway. The first is the microtubule-depolymerising kinesin MCAK (Mitotic Centromere-Associated Kinesin), since depletion of MCAK in Aurora B depleted cells or extracts restored the chromosome-driven spindle pathway [110, 112, 113]. The second is the microtubule-destabilizing protein Stathmin/Op18, whose activity is inhibited by Aurora B phosphorylation in the vicinity of chromosomes [109, 114]. Kinetochore capture by the mitotic spindle is a stochastic process that will give rise to intermediate states of attachment. Non-bipolar attachments in which both kinetochores bind microtubules emanating from the same pole (also called syntelic attachments) occur during every mitosis and need to be corrected to eventually produce biorientation [115-117]. These attachments are actively destabilized through the activity of Aurora B [116, 118, 119]. Unattached kinetochores can now enter a new cycle of microtubule attachment until bipolar attachment is obtained. Two important kinetochore microtubule-capture factors (the Ndc80/Hec1- and Dam1-complexes) are subject to phosphoregulation by Aurora B [118]. In addition, Aurora B phosphorylates MCAK, and this also contributes to the correction of defective attachments [120-122]. Phosphorylation of Ndc80/Hec1 by Aurora B reduces its affinity for microtubules *in vitro* [123] and mutation of the putative Aurora B phosphorylation-sites in Ndc80/Hec1 stabilises microtubule-kinetochore interactions *in vivo* [124]. Additionally, several subunits of the Dam1-complex are also substrates of the budding yeast Aurora B (Ipl1) and mutation of phosphorylation-sites within the Dam1-subunit of this complex causes chromosome segregation defects similar to those occurring in Ipl1-mutants [118]. In summary, Aurora B influences the stability of microtubule kinetochore interactions by controlling the function of key microtubule-capture factors on the kinetochore. It is capable of destabilizing defective non-bipolar attachments and as such functions as an error correction factor that ensures faithful segregation of sister chromatids.

Aurora B becomes enriched at centromeres of merotelically attached kinetochores where it promotes kinetochore microtubule turnover [125, 126] most likely via regulation of MCAK. Aurora B influences the function of MCAK at different levels. First, Aurora B activity is required for the concentration of MCAK on centromeres [120, 121, 126]. Second, phosphorylation of MCAK within its neck

region inhibits its microtubule-destabilising activity *in vitro* and expression of phosphodeficient MCAK mutants (containing serine/threonine to alanine mutations on all Aurora B sites) causes clear chromosome alignment defects [111, 120]. Third, Aurora B also indirectly influences MCAK function. Aurora B interacts with ICIS (inner centromere Kin-I simulator), a centromeric protein that can stimulate MCAK activity *in vitro* [127] and Aurora B is also required to target Sgo2 to centromeres. Interestingly, Sgo2 depletion caused a displacement of MCAK from centromeres and an increase in the amount of merotelic attachments [128]. Clearly, regulation of MCAK by Aurora B is complex and has an effect on multiple important processes that influence chromosome segregation.

Aurora B also plays an essential role in the mitotic checkpoint by recruiting BubR1 (Budding Uninhibited by Benzimidazoles 1 homolog (yeast)-related kinase or MAD3/Bub1b), Mad2 (Mitotic Arrest Deficient 2) and Cenp-E (Centromere Protein E) to unattached kinetochores, thus coupling chromosome alignment with anaphase [129]. The mitotic checkpoint is compromised by the lack of Aurora B activity [130].

Cytokinesis kinase -From anaphase onwards, Aurora B localises to both the central spindle/midbody and to the cell cortex, to which it is transported *via* microtubules. Aurora B activity is required for efficient execution of anaphase and cytokinesis in several organisms [68, 70, 92, 129, 131-133]. Localisation of Aurora B to the central spindle contributes to the rapid switch in microtubule dynamics during anaphase [134] and Aurora B is also required for efficient disassembly of the mitotic spindle during telophase [135]. During cytokinesis, the cytoplasm is divided into two new daughter cells each containing a single nucleus. A cleavage furrow is generated by contraction of an actomyosin ring that encircles the cell equator and eventually divides the cytoplasm into two [136]. It is important that the cleavage furrow only forms after chromosome segregation and that it is positioned correctly between the two daughter nuclei. An essential determinant of contractile ring function is the GTPase RhoA [137]. Active (GTP-bound) RhoA controls several downstream effectors involved in cytokinesis [137]. RhoA function during cytokinesis is controlled in part by a central spindle-localised complex called centralspindlin. This complex, consisting of a GTPase activating protein (GAP) (MgcRacGAP/Cyk4) and a kinesin (Mklp-1/ZEN-4), influences RhoA by controlling localisation of Ect2, an essential Rho-GEF [138-142]. Correct function and localisation of centralspindlin depends on Aurora B activity [143-145]. Aurora B phosphorylates several other proteins involved in cytokinesis, like Vimentin [146], Myosin II regulatory light chain [147], Desmin, and GFAP [148]. In budding yeast, Ipl1 plays an additional role during cytokinesis by controlling the NoCut pathway that prevents abscission (the final step of cytokinesis) when chromosomes are present in the direct vicinity of the site of abscission [149]. Ipl1 controls the localization of the anillin-related proteins Boi1 and Boi2 to the site of cleavage ingression where they can function as abscission inhibitors and prevent premature abscission and concomitant chromosome breakage [149].

Aurora Kinases and Cancer

In the last decade, a large number of studies have linked the aberrant expression of Aurora kinases to cancer and this has led to a great effort on the development of Aurora kinase inhibitors.

The role of Aurora A in the development of neoplastic lesions was established first, and therefore the search for anticancer therapeutic targets was initially centred on Aurora A inhibitors. However, most of them react with both Aurora A and Aurora B. The studies performed with dual Aurora kinase inhibitors have shown that treated cells display aberrant mitosis, increase in DNA content (>4N) and cell death. These effects closely resemble that of Aurora B disruption by genetic methods, suggesting that Aurora B represents an effective therapeutic target despite its uncertain role in the development or progression of neoplastic lesions.

A large number of dual activity Aurora inhibitors are currently under clinical evaluation. Therefore, we will also discuss the role of Aurora A in cancer.

Aurora A and Cancer

Aurora A is ubiquitously expressed and regulates cell cycle events occurring from late S phase through M phase, including centrosome maturation, mitotic entry, centrosome separation, bipolar-spindle assembly, chromosome alignment on the metaphase plate, cytokinesis and mitotic exit [1, 40]. Different proteins, TPX2, Ajuba, Bora, HEF1 are known to play a role in Aurora A activation and function, however it is not been fully understood how these activators relate to each other and how their signaling cooperates during cell cycle progression [46].

The role of Aurora A in cancer development has been largely studied and clarified. Aurora A gene is located on chromosome 20q13.2, a known hotspot of amplification in tumours [150]. The gene was first named BTAK (Breast Tumor Activated Kinase), since its mRNA was found to be overexpressed in breast tumours and to play a critical role in breast tumour cell transformation [151, 152]. Several studies have shown amplification of the Aurora A locus and concomitant overexpression of Aurora A kinase in a multitude of tumours, such as gliomas, breast, endometrial and others [151-166]. Accumulating evidences have demonstrated that gene amplification and overexpression of Aurora A are linked to tumorigenesis, suggesting that Aurora A is an oncogene [161, 167-175]. In addition, Aurora A overexpression has been used as a negative prognostic marker, being associated with resistance to anti-mitotic agents commonly used for cancer therapy [161, 169, 171, 172, 176-184]. Aurora A has been identified as a low-penetrance tumour-susceptibility gene [185-187]. A T-to-A polymorphism, resulting in a change from phenylalanine 31 (Phe³¹) to isoleucine (Ile³¹), has been observed in the Aurora A gene and reported to be associated with the degree of aneuploidy in human colon tumours [185, 186]. The Phe31Ile variant is also preferentially amplified in esophageal squamous cell carcinomas, and also in this case correlates with an increase in aneuploidy. In particular, the Ile/Ile genotype was significantly associated with increased risk of oesophageal squamous cell carcinoma occurrence compared with the Phe/Phe genotype [186]. Aurora A polymorphisms have

been associated with increased risk of breast [186, 188-190], oesophageal [170, 186], lung [186, 191] and gastric cancer [192].

Aurora A overexpression alone is insufficient to induce carcinogenesis, and other molecular alterations need to be associated with Aurora A amplification/overexpression to induce oncogenicity [154, 169, 173, 193]. This hypothesis is supported by the observation that transgenic mice overexpressing Aurora A in an inducible manner in the mammary glands do not develop tumours; in mammary epithelium tetraploid cells and apoptotic features are observed [194, 195]. Consistent with this data, the conditional expression of Phe31Ile variant in mouse skin alone or treated with the co-carcinogenetic agent TPA did not result in squamous cell carcinoma. However, Phe31Ile transgenic animals presented accelerated squamous cell carcinoma (SCC) development with greater metastatic activity compared to wild type animals, upon skin carcinogenesis treatment. These observations indicate that Aurora A cannot initiate skin carcinogenesis but rather promotes the malignant conversion of skin papillomas [175].

Aurora B and Cancer

Aurora B is involved in chromosome segregation, spindle-checkpoint and cytokinesis, and alteration of each of these steps could induce aneuploidy, one of main features and driving force of cancer cells. However, the role of Aurora B in cancer development and/or progression has not been fully clarified.

In vitro studies performed with several Aurora B inhibitors, dominant negative mutants or RNAi, show that Aurora B deficiency interferes with cell cycle. Treated cells cannot divide after mitosis and become tetraploid, with two couples of centrosomes. Moreover, cells expressing catalytically inactive Aurora B do not arrest in mitosis in the presence of nocodazole or taxol. These observations concur with Aurora B presumed roles: spindle checkpoint suppression allows cells to go through mitosis, despite a number of chromosomes being oriented in a syntelic manner (both kinetocore attached to the same pole), while the lack of phosphorylation of cleavage furrow components prevents cytokinesis. The effects of longer depletion of Aurora B seem to be cell line dependent. Some cells either enter additional cell cycles but, because of cell division failure, they become massively polyploid, whereas other cell lines undergo apoptosis or arrest in a pseudo G1 state. These differences are probably due to the p53-dependent post-mitotic checkpoint.

Ota *et al.* [196] strongly suggest a direct link between Aurora B and carcinogenesis. In this report, Chinese hamster embryo (CHE) cells, carrying wild type p53 (CHEp53^{wt}) or an inactivating mutation (CHEp53^{-/-}), were transfected with Aurora B. The mutation in p53 abrogates the p53-dependent G1 checkpoint. Stable clones overexpressing Aurora B were isolated and injected in nude mice. Notably, the authors could use only CHEp53^{-/-} transfected cells, since they could not isolate any stable clone from CHEp53^{wt}. Untransfected CHE cells induce tumours when injected in nude mice, but they do not metastasize, whereas mice injected with Aurora B overexpressing CHEp53^{-/-} cells formed more aggressive

tumours that also gave distant metastases [196]. In a recent paper, Kanda *et al.* [197] showed that, although Aurora B overexpression is not oncogenic in BALB/c 3T3 A31-1-1 cells, Aurora B kinase activity augments Ras-mediated cell transformation, suggesting that the overexpression of Aurora B may contribute to the generation of a transformed phenotype, by potentiating oncogene activity during carcinogenesis.

Aurora B is located on chromosome 17p13.1, a chromosomal region that has not been frequently associated with amplification in tumours, with the exception of glioblastomas [198].

Aurora B gene is dramatically up-regulated in highly proliferating compared with non-proliferating cells. Although Aurora B overexpression has been shown in many tumours types, this is not the result of gene amplification, and it is still under debate whether the observed overexpression of Aurora B is a reflection of the high proliferative rate of neoplastic cells or whether it is causally related to tumorigenesis.

Aurora B is overexpressed in several human cancers, such as non small cell lung carcinoma [199, 200], mesothelioma [201], glioblastoma [198, 202], oral cancer [203], malignant endometrium [159], hepatocellular carcinoma [204-206], testicular germ cell tumours [207, 208], ovarian [187], thyroid [209], colon [210] and prostate [211]. Aurora B expression is positively correlated with poor prognosis and displays a tendency to group in higher grade of malignancy in different neoplastic lesions. Aurora B expression directly correlates with Gleason grade in prostate cancer [212], Duke's grade in colorectal cancer [40] and dedifferentiation in ovary and thyroid carcinoma [209]. In thyroid tumours, an increase of Aurora B expression has been observed in papillary and anaplastic thyroid carcinomas. In the late stages of thyroid tumour progression a further increase of Aurora B expression was observed indicating that Aurora B overexpression might confer a growth advantage to neoplastic cells [19, 209].

In all lesions overexpressing Aurora B, phosphorylation of the histone H3 was clearly detectable.

Several studies have suggested that commonly occurring gene polymorphisms of Aurora B are associated with cancer risk see Table 1. Recently, an alternative splicing variant of Aurora B (Aurora B-Sv2) has been found frequently associated with advanced stages of hepatocellular carcinoma; this variant appears to be more frequently associated with tumour recurrence and poor prognosis [206]. The inhibition of Aurora B kinase has an anti-proliferative effects and causes regression in several animal models of human cancers, including breast, colon, lung, leukemia, prostate and thyroid [46, 130, 208, 209, 211, 213-217]. These observations strongly suggest Aurora B as a potential therapeutic target.

Aurora Inhibitors

To target the enzymatic activity of Aurora kinases, small molecules able to occupy the catalytic binding site have been identified. In contrast to antimetabolic drugs, Aurora(s) inhibitors do not bind to microtubules but, acting on proteins required for proper mitosis, induce mitotic arrest followed, in

most cases, by cell death. The number of Aurora inhibitors is rapidly increasing: approximately 15 Aurora inhibitors are under Phase I/II evaluation and others are in preclinical testing [218, 219].

The mechanism of action suggests a potentially high therapeutic index. Indeed, Aurora kinases are only expressed and active during mitosis, therefore non-proliferating cells would not be adversely affected by these drugs. Furthermore, cells lacking a p53-mediated post-mitotic checkpoint are highly responsive to Aurora(s) inhibition and alteration in p53 pathways are common in human cancers [220, 221]. Last but not least, since Aurora inhibitors do not bind to tubulin, they do not induce neuropathy, that is one of the main side effects on classical antimetabolic drugs, such as nocodazole.

Although Aurora A has received most of the attention in terms of a link with human cancer, so far few molecules capable to selectively inhibit Aurora A activity have been identified.

MLN8054 presents an IC_{50} of 4 and 172nM for Aurora A and Aurora B, respectively [222, 223]. This drug induces abnormal spindles, often with unseparated centrosomes, and delays progression through mitosis. However, MLN8054-treated cells are able to exit from mitosis, although with segregation errors due to the formation of ectopic poles. The long term administration of MLM8054 *in vitro* and *in vivo* models of human neoplasia induces cell death and tumour growth arrest [222, 223]. Preliminary data of a phase I trial have shown no profound myelosuppression [224].

MLN8237 inhibits Aurora A with an IC_{50} value of 1 nM. It inhibits growth of various cancer cell lines and treatments of animal models induced significant tumor growth inhibition. A recent *in vivo* study shows that MLN8237 exhibits potent anticancer activity in CML and Philadelphia chromosome positive acute lymphoblastic leukemia models. Phase I clinical trials are ongoing in patients with advanced solid tumours and advanced hematological malignancies [219].

Inhibition of Aurora B by specific inhibitors interferes with normal chromosome alignment during mitosis and overrides the mitotic spindle checkpoint inducing endoreduplication. Aurora A and Aurora B specific inhibitors exert different effects in treated cells suggesting that the pathways leading to the mitotic block in response to inhibitors are distinct. Moreover, Aurora B seems to be more suitable as anticancer drug target, since inhibition of Aurora B rapidly results in a catastrophic mitosis, leading to cell death.

Being the number of Auroras inhibitors rapidly increasing, in Table 2 are summarised the results of the most relevant clinical trials with Aurora A and B kinase inhibitors.

Dual Inhibitors of Aurora Kinases

In order to block Aurora B functions, several anti-cancer drugs targeting its catalytic binding site have been developed. However, given the high homology of the catalytic domain of Aurora kinases, small molecules do not differentiate between them [225]. The first three small-molecule inhibitors of Aurora(s) described include Hesperadin [212], VX-680 [226], and ZM447439 [130]. These three drugs have similar potency versus Aurora A, Aurora B and Aurora C.

Table 1. Aurora Kinases A and B Molecular Alterations in Human Cancer

| Alteration | Cancer Type | Aurora Kinase | Study |
|-------------------------|----------------------|---------------|---|
| Overexpression | Breast | A | Miyoshi <i>et al.</i> ; Tanaka <i>et al.</i> ; Hoque <i>et al.</i> ; Royce <i>et al.</i> [161, 166, 169, 180] |
| | Lung | A-B | Xu <i>et al.</i> ; Smith <i>et al.</i> ; Vischioni <i>et al.</i> [182, 199, 200]. |
| | Pancreas | A | Li <i>et al.</i> [160]. |
| | Prostate | B | Chieffi <i>et al.</i> [168, 176, 211]. |
| | Bladder | A | Fraizer <i>et al.</i> ; Comperat <i>et al.</i> [168, 176]. |
| | Esophagus | A | Yang <i>et al.</i> ; Tong <i>et al.</i> [162, 174]. |
| | Brain | B | Zeng <i>et al.</i> ; Araki <i>et al.</i> [198, 202]. |
| | Liver | A | Jeng <i>et al.</i> [157]. |
| | Head/Neck | A-B | Reiter <i>et al.</i> ; Qi <i>et al.</i> ; Zhao <i>et al.</i> ; Li <i>et al.</i> ; [172, 203, 214, 215]. |
| | Thyroid | B | Sorrentino <i>et al.</i> [209] |
| | Ovarian | A | Lassman <i>et al.</i> ; Landen <i>et al.</i> [178, 183]. |
| | Renal | A | Kurahashi <i>et al.</i> [158]. |
| | Amplification | Breast | A |
| Colon | | A | Bischoff <i>et al.</i> ; Nishida <i>et al.</i> [151, 171]. |
| Brain | | A | Klein <i>et al.</i> ; Reichardt <i>et al.</i> ; Neben <i>et al.</i> [163, 164, 216]. |
| Bladder | | A | Sen <i>et al.</i> [153]. |
| Head/Neck | | A | Tatsuka <i>et al.</i> [173]. |
| Endometrium | | A | Moreno-Bueno <i>et al.</i> [165]. |
| Polymorphisms | Colon | A | Hienonen <i>et al.</i> ; Ewart-Toland <i>et al.</i> ; Chen <i>et al.</i> [156, 185, 217]. |
| | Breast | A-B | Cox <i>et al.</i> ; Lo <i>et al.</i> ; Tchatchou <i>et al.</i> ; Vidarsdottir <i>et al.</i> ; [188-190, 193] |
| | Esophagus | A | Kimura <i>et al.</i> [170]. |
| | Lung | A | Gu <i>et al.</i> [191]. |
| | Gastric | A | Ju <i>et al.</i> [192]. |
| | Multiple | A | Ewart-Toland <i>et al.</i> [186]. |
| Splicing Variant | Liver | B | Yasen <i>et al.</i> [206] |

Each induces a similar phenotype in cell-based assays, characterized by inhibition of phosphorylation of histone H3 on Ser¹⁰ and Ser²⁸, inhibition of cytokinesis, and development of polyploidy.

Other drugs such as PHA-680632 [227], PHA-739358 [228] and Reversine [229] are potent inhibitors of all three Aurora kinases. Also in this case, the phenotypic effects closely resemble those achieved by selective inhibition of Aurora B.

The general chemical structures of dual inhibitors are shown in Fig. (3).

The IC₅₀s values of Aurora kinases inhibitors are shown in Table 3.

HESPERADIN

Hesperadin (Boehringer Ingelheim) is a novel indolinone that inhibits immunoprecipitated Aurora B with an IC₅₀ of 250nmol/L. Hesperadin has IC₅₀s values in the range of 1.2μM to A > 10μM for cdk1/cyclin B or cdk2/cyclin E, respectively. The inhibitor inserts into the ATP binding pocket of both Aurora A and Aurora B [212, 218, 219].

HeLa cells treated with 20-100nM of Hesperadin show polyploidy and loss of mitotic phosphorylation of histone H3 on Ser¹⁰ [212]. Moreover, HeLa cells treated with 50nM of Hesperadin stop proliferating although do not stop the growth, showing an increase in nuclear size that correlates

Table 2. Clinical trials with Aurora Kinases Inhibitors

| Drug | Tumour Type | Title of The Study | Phase | Sponsored by | Clinicaltrials.Gov Identifier |
|-----------------|--|---|------------|--------------|-------------------------------|
| VX-680 (MK0457) | ADVANCED CANCER | A Phase I Dose Escalation Study of MK0457 Evaluating the Safety, Tolerability, Pharmacokinetics and Pharmacodynamics of a 24-Hour Continuous Infusion Given Every 21 Days in Patients with Advanced Cancer | PHASE I | MERCK | NCT00104351 |
| VX-680 (MK0457) | LEUKEMIA | A Phase I/II Dose Escalation Study of MK0457 in Patients with Leukemia | PHASE I | MERCK | NCT00111683 |
| VX-680 (MK0457) | CARCINOMA, NON-SMALL-CELL LUNG | A Phase IIA Study Evaluating the Efficacy of MK0457 as a 5-Day Continuous Infusion in Patients with Advanced Non-Small Cell Lung Cancer (NSCLC) | PHASE II | MERCK | NCT00290550 |
| VX-680 (MK0457) | LEUKEMIA | A Phase II Study of MK0457 in Patients with T315I Mutant Chronic Myelogenous Leukemia and Philadelphia Chromosome-Positive Acute Lymphoblastic Leukemia | PHASE II | MERCK | NCT00405054 |
| VX-680 (MK0457) | CHRONIC MYELOGENOUS LEUKEMIA, LEUKEMIA LYMPHOBLASTIC ACUTE PHILADELPHIA-POSITIVE | A Phase I Dose Escalation of MK0457 in Combination with Dasatinib in Patients with Chronic Myelogenous Leukemia and Philadelphia Chromosome-Positive Acute Lymphoblastic Leukemia | PHASE I | MERCK | NCT00500006 |
| AZD1152 | ACUTE MYELOID LEUKEMIA | A Phase I, Open Label, Multi-centre Study to assess the Safety, Tolerability, and Pharmacokinetics of AZD1152 in Japanese Patients with Acute Myeloid Leukaemia | PHASE I | AstraZeneca | NCT00530699 |
| AZD1152 | MYELOID LEUKEMIA | A Phase I/II, Open Label, Multi-Centre Study to assess the Safety, Tolerability, Pharmacokinetics and Efficacy of AZD1152 in Patients with Acute Myeloid Leukaemia | PHASE I/II | AstraZeneca | NCT00497991 |
| AZD1152 + LDAC | ACUTE MYELOID LEUKEMIA | A Randomised, Open-label, Multi-centre, 2-stage, Parallel Group Study to Assess the Efficacy, Safety and Tolerability of AZD1152 Alone and in Combination with Low Dose Cytosine Arabinoside (LDAC) in Comparison with LDAC Alone in Patients Aged ≥ 60 with Newly Diagnosed Acute Myeloid Leukaemia (AML) | PHASE II | AstraZeneca | NCT00952588 |
| AZD1152 + LDAC | ACUTE MYELOID LEUKEMIA | A Phase I, Open-Label, Multi-Centre, Multiple Ascending Dose Study to assess the Safety and Tolerability of AZD1152 in Combination with Low Dose Cytosine Arabinoside (LDAC) in Patients with Acute Myeloid Leukaemia (AML) | PHASE I | AstraZeneca | NCT00926731 |
| AZD1152 | TUMOURS | A Phase I, Open-Label, Multi-Centre Study to Assess the Safety, Tolerability and Pharmacokinetics of AZD1152 Given as a Continuous 48-Hour Intravenous Infusion in Patients with Advanced Solid Malignancies | PHASE I | AstraZeneca | NCT00338182 |

(Table 2) Contd....

| Drug | Tumour Type | Title of The Study | Phase | Sponsored by | Clinical Trials. Gov Identifier |
|------------|---|--|----------|-------------------------------------|---------------------------------|
| AZD1152 | SOLID TUMOURS | A Phase I, Open-Label, Multi-Centre Study to Assess the Safety, Tolerability and Pharmacokinetics of AZD1152 Given as a Continuous 7-Day Intravenous Infusion in Patients with Advanced Solid Malignancies | PHASE I | AstraZeneca | NCT00497679 |
| AZD1152 | SOLID TUMOURS | A Phase I, Open-Label, Multi-Centre Study to Assess the Safety, Tolerability and Pharmacokinetics of AZD1152 Given as a 2 Hour Intravenous Infusion on Two Dose Schedules in Patients with Advanced Solid Malignancies | PHASE I | AstraZeneca | NCT00497731 |
| PHA-739358 | LEUKEMIA | A Pilot Phase II Study of PHA-739358 in Patients with Chronic Myeloid Leukemia Relapsing on Gleevec or c-ABL Therapy | PHASE II | Jonsson Comprehensive Cancer Center | NCT00335868 |
| PHA-739358 | METASTATIC HORMONE REFRACTORY PROSTATE CANCER | A Phase II Study of PHA-739358 in Patients with Metastatic Hormone Refractory Prostate Cancer | PHASE II | Nerviano Medical Sciences | NCT00766324 |
| PHA-739358 | MULTIPLE MYELOMA | An Exploratory Phase II Study of PHA-739358 in Patients with Multiple Myeloma Harboring the t(4;14) Translocation with or without FGFR3 Expression | PHASE II | Nerviano Medical Sciences | NCT00872300 |

Website: clinicaltrials.gov

Table 3. IC₅₀s Values of Aurora Kinases Inhibitors

| Compound | K _i Aurora A (nmol/L) | K _i Aurora B (nmol/L) | K _i Aurora C (nmol/L) | Selectivity |
|---------------|----------------------------------|----------------------------------|----------------------------------|--|
| Hesperadin | Not tested | 250 | Not tested | Inhibits other kinases <i>in vitro</i> (AMPK, LcK, MKK1, MAPKAP-K1, CHK1, PHK with a K of 1 ?mol/L |
| ZM1 | 1000 | 50 | 250 | Do not seems to inhibit other kinases <i>in vitro</i> |
| ZM2 | 800 | 7,5 | Not tested | Do not seems to inhibit other kinases <i>in vitro</i> |
| ZM3 | 50 | 15 | Not tested | Do not seems to inhibit other kinases <i>in vitro</i> |
| VX-680 | 0,6 | 18 | 4,6 | Inhibits FLT3 with a K _i of 30 nmol/L |
| PHA680632 | 27 | 135 | 120 | Inhibits other kinases <i>in vitro</i> , including FLT3, LcK, PLK1, STK2, VEGFR2, VEGFR3 |
| PHA739358 | 13 | 79 | 61 | Inhibits several other kinases <i>in vitro</i> , including ABL, Ret, TRK-A, FGFR |
| Reversine | 150-400 | 500 | 400 | Not tested |
| CYC116 | 44 | 19 | 65 | Inhibits VEGFR2 with a K _i of 69 nmol/L |
| SNS-314 | 9 | 31 | 3,4 | Not tested |
| PF-03814735 | 5 | 0,8 | Not tested | Not tested |
| ENMD-2076 | 14 | 290 | Not tested | Inhibits Src, cKit, FAK and VEGFR2 with K _i of 100, 40, 5, and 80 nmol/L |
| AT9283 | 3 | 3 | <10 | Inhibits JAK-2 and -3, Tyk2, RSK2 with K _i values less than 10 nmol/L |
| R763(AS70316) | 4 | 4,8 | 6,8 | Inhibits FMS-related tyrosine kinase 3 (FLT3) with a K _i of 100nmol/L |
| MP529 | 110 | >10000 | Not tested | Not tested |
| GSK1070916 | 100 | 3,5 | 6,5 | Do not seems to inhibit other kinases <i>in vitro</i> |
| AZD1152 | 1,369 | 0,36 | Not tested | Less activity against a panel of 50 other kinases including FLT3, JAK2 and Abl |

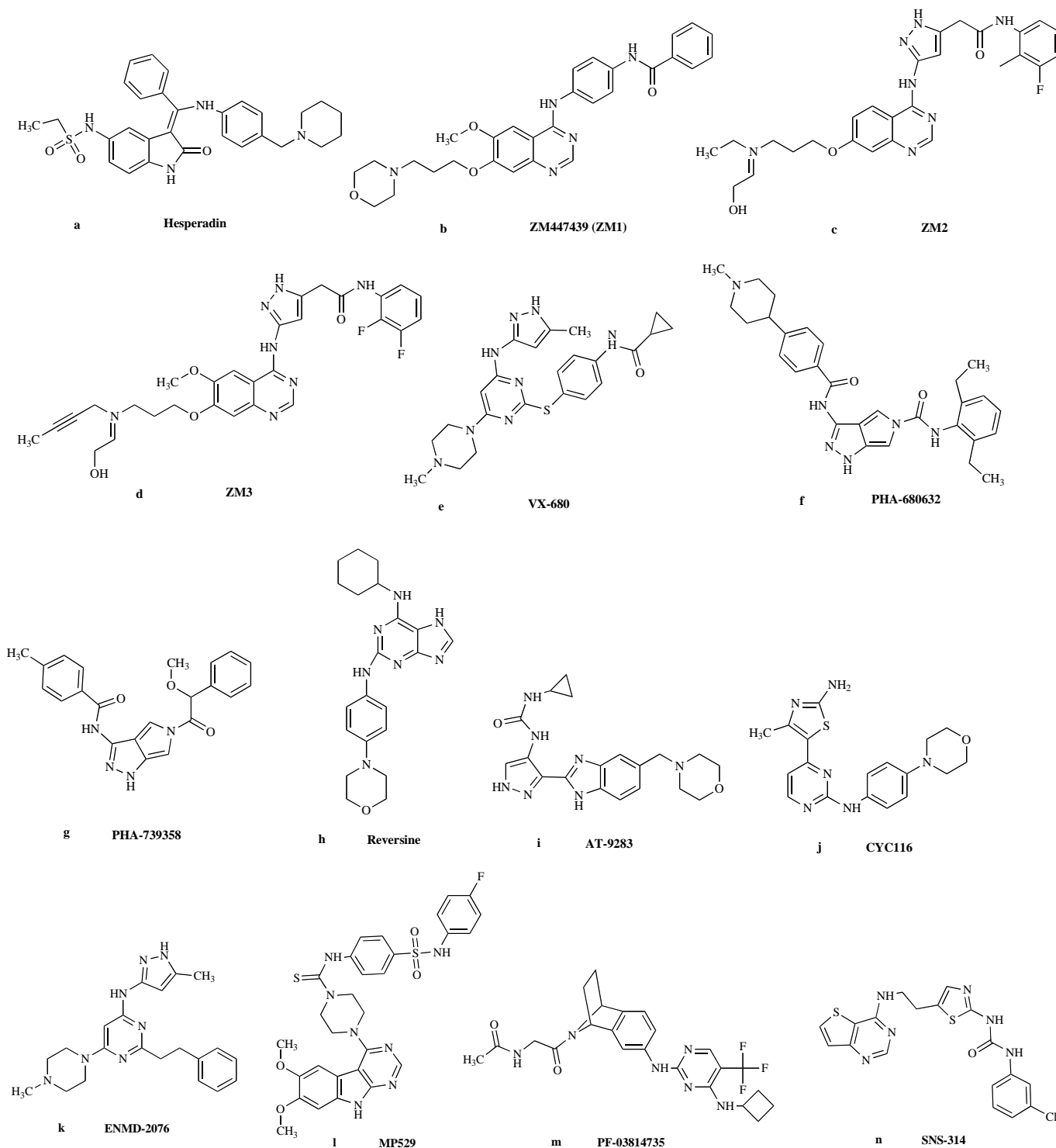


Fig. (3). Aurora kinase inhibitors. Dual inhibitors of Aurora kinases. Chemical structures of (a) Hesperadin, (b) ZM447439, (c) ZM2, (d) ZM3, (e) VX-680, (f) PHA-680632, (g) PHA-739358, (h) Reversine, (i) AT-9283, (j) CYC116, (k) ENMD-2076, (l) MP529, (m) PF-03814735, (n) SNS-314.

with polyploidization. The phenotypes induced by knocking down Aurora B by RNAi and inhibiting its function by Hesperadin are highly similar. It is demonstrated that $1\mu\text{M}$ of Hesperadin markedly reduced the activity of other six kinases (AMPK, LcK, MKK1, MAPKAP-K1, CHK1, and PHK). It has been reported that MKK1 inhibition blocks

cells in G2 phase, however *in vivo* experiments show that, at the concentration used, inhibition of MKK1 activity was not observed [212]. Moreover, it seems that the CDKs are not inhibited *in vivo*, because it is required a high concentration of Hesperadin to inhibit them [230].

ZM447439

ZM447439 (also known as ZM1), is a quinazoline derivative developed by AstraZeneca. It binds both the ATP-binding site and the adjacent cleft, that it is not present in other kinases, thus giving this inhibitor its specificity for Aurora Kinases [130]. ZM447439 does not inhibit most other kinases tested, including the mitotic regulators CDK1 and PLK1 ($IC_{50} > 10\mu M$). ZM1 inhibits Aurora A, B and C with an IC_{50} of 1000, 50 and 250nM respectively [130].

ZM1 induces incorrect microtubule-kinetochore attachments, failure of chromosome biorientation, abrogation of the mitotic checkpoint, failure of cytokinesis, and the development of tetraploidy. Cells treated with ZM1 shows cell cycle arrest at G₂/M with subsequent accumulation of cells with 4N/8N DNA content, a common defect in cells with impaired Aurora B activity. Cells later either underwent apoptosis via activation of caspase-3 and PARP cleavage, or a G₁ arrest possibly induced by a p53-dependent G₁ tetraploidy checkpoint [231]. ZM447439 suppressed the phosphorylation at Ser¹⁰ of histone H3. Although ZM447239 inhibits both Aurora A and Aurora B *in vitro*, the phenotype observed in treated cells suggests a greater inhibition of Aurora B, missing the centrosome separation defect or the delayed mitotic entry characteristic of Aurora A inhibition [130].

ZM2 and ZM3 are two compounds structurally related to ZM1, which also inhibit Aurora kinase activity *in vitro*. ZM2 inhibits Aurora A and B with IC_{50} s values of 800nM and 7.5nM respectively and it is ~100 times more selective against Aurora B than Aurora A. In addition, *in vitro*, ZM2 is 5-10 times more potent against Aurora B than ZM1 and induces similar mitotic phenotypes and similar biological effects to ZM1 but at lower concentrations. ZM2 significantly reduces phosphorylation of histone H3 at 0.1 μM , whereas 3 μM ZM1 is required for extensive inhibition. ZM3 does appear to be a potent Aurora A inhibitor with an IC_{50} value of 50nM, but ZM3 also inhibits Aurora B *in vitro* with an IC_{50} of 15nM. ZM3 is more potent against both Aurora A (20-fold) and Aurora B (~3.3-fold) compared with ZM1 [130].

VX-680 (MK0457)

VX-680 is a 4,6 di-amino pyrimidine developed by Vertex. It has been reported to be a potent *in vitro* inhibitor of Aurora A, B and C with inhibition constants (K_i) of 0.6, 18 and 4.6nM respectively [226].

VX-680 shows selectivity for the Aurora kinases over 55 other kinases tested, the only exception is Fms-related tyrosine kinase-3 (FLT-3), that it is inhibited with a K_i of 30 nM. However, the phenotype described after exposing cells to this compound are consistent with the inhibition of Aurora B [226]. In fact, the treatment of a variety of tumor cell types with VX-680 generates polyploidy through defects in cytokinesis and inhibits the phosphorylation of the Aurora B substrate histone H3 [231]. Harrington *et al.* have shown that the treatment with VX-680 induces the accumulation of cells with 4N DNA content, suggesting DNA replication in the absence of cytokinesis [232]. Whether cells arrest with 4N DNA content in pseudo-G₁ or endoreduplicate with the

accumulation of >4N DNA content likely depends on the integrity of the p53-dependent postmitotic checkpoint; in fact the integrity of the p53-p21^{Waf1/Cip1} pathway in the G₁ postmitotic checkpoint governs the response to VX-680, and cells with compromised checkpoint function are most likely to undergo apoptosis [233].

It is also reported that VX-680 is able to inhibit the proliferation of phytohemagglutinin-stimulated primary human lymphocytes ($IC_{50}=79nM$), but has no effect on the viability of noncycling primary human cells at concentration as high as 10 μM . This lack of toxicity in resting cells is consistent with the fact that expression and activity of Aurora proteins are low or undetectable in noncycling cells.

In vivo, VX-680 is able to suppress the growth of human cancer cell xenografts in nude animals. VX-680 causes a marked reduction in tumour size in human acute myelocytic leukemia (HL60 cells) xenograft model. VX-680 is well tolerated, with a small decrease in body weight observed only at the highest doses. This small molecule also induces tumour regression in pancreatic and colon xenograft models [232]. Moreover, VX-680 has a potent antitumor activity when infused *i.v.* in nude rats bearing established colon (HCT116 cells) tumours. In this model, a fall in neutrophil counts, that recovers to normal levels at the end of the treatment, was observed. The inhibition of tumour growth is paralleled by a reduction in histone H3 phosphorylation and a significant increase in apoptosis [231].

VX-680 also binds to wild-type Abl kinase and Abl mutants and reduces cell proliferation of cells with Bcr-Abl mutations, with an IC_{50} value ranging from 100 to 200nM [193]. A phase I clinical trials in patients with chronic myeloid leukemia (CML) or acute lymphocytic leukemia (ALL(Ph⁺)) with T315I Bcr-Abl mutation has been performed [194-196]. Positive effects were observed with no major side effects; grade 1 nausea in one patient and grade 1 alopecia in four patients were reported. Enrollment in Phase I/II clinical trials of VX-680 has been suspended, on the base of preliminary safety data, due to the observation of QTc prolongation in one patient [219].

Compared to ZM447439, much lower concentrations of VX-680 are required to significantly suppress histone H3 phosphorylation, inhibit mitotic progression and the spindle assembly checkpoint (0.5 μM for VX-680 with respect to 5 μM for ZM1). These differences could be explained in part by the increased potency of Aurora inhibition by VX-680, but in some cases are also due to additional Aurora A inhibitory effects. However, VX-680 is significantly more cytotoxic than ZM447439 when compared side-by-side in the human colon carcinoma cell line DLD-1, in fact the LD₅₀ for VX-680 is some 30-fold lower than that for ZM447439 [226, 232].

VE-465 is a low molecular weight pan-Aurora kinase inhibitor. It is an analog of VX-680 that has been evaluated against multiple myeloma cell lines [234].

PHA-680632

PHA-680632 was developed by Nerviano Medical Sciences as an ATP competitive compound and is a derivative of a 1,4,5,6-tetrahydropyrrrolo [3,4-*c*] pyrazole

scaffold [227]. It was shown to be a potent inhibitor of all three Aurora kinases with IC_{50} s of 27, 135, and 120nmol/L for Aurora A, B and C respectively [227]. This compound has been tested over a panel of 29 additional kinases and it has been found to be active against 6 of these kinases including FLT3, LCK, PLK1, STK2, VEGFR2 and VEGFR3, whose IC_{50} s are much higher than that of Aurora A (30 to 200 fold). PHA-680632 has potent antiproliferative activity in a wide range of cell types with an IC_{50} in the range of 0.06 to 7.15 μ mol/L. PHA-680632 induces a biological response consistent with an Aurora B inhibition, such as decreased histone H3 phosphorylation, endoreduplication and polyploidy [227]. It has been also demonstrated that PHA-680632 can suppress tumor growth in human tumor cell xenografts model and syngenic models in mouse and rat [235]. After i.v. administration, a significant tumor growth inhibition is observed. A more prolonged exposure to PHA-680632 has been tested in HCT116 colon carcinoma xenograft, administering the compound i.p. for 12 days. The treatment was well tolerated and tumour growth inhibition was 75% compared with controls [235]. *In vivo* xenografts (p53^{-/-} HCT116) of a mice study showed enhanced tumour growth delay after the PHA-680632-IR combinatorial treatment compared with IR alone. PHA-680632 in association with radiation leads to an additive effect in cancer cells, especially in the p53-deficient cells, but does not act as a radiosensitiser *in vitro* or *in vivo* [235].

PHA-739358

PHA-739358 is a small-molecule 3-aminopyrazole derivative developed by Nerviano Medical Sciences, that exhibits activity in nanomolar range against all Aurora Kinases [228]. In a biochemical assay, it inhibits Aurora A, B and C with an IC_{50} s of 13, 79 and 61 nmol/L respectively. It also acts on other relevant cancer tyrosine kinases, such as wild type and mutated ABL, RET, TRK-A and FGFRs [228]. After treatment with this inhibitor, cells fail to divide, resulting in polyploidy without a strong impact on the timing of mitosis and finally leading to a reduction in viability. In some cell lines, an increased apoptosis was observed. Overall, most of the effects of the drug are related to the inhibition of Aurora B [233]. During a phase I clinical trial grade 3/4 of neutropenia were reported, no tumour responses were observed but 8 out of 40 patients has stable disease for at least 4 months [219]. PHA-739358 is currently in phase II clinical trial and have a favorable preclinical profile.

REVERSINE

Reversine [2-(4-morpholinoanilino)-N⁶-cyclohexyladenine] is a substituted purine analogue, that occupies the ATP-binding pocket at the interface between small and large lobes [229, 236]. It was originally shown to promote the dedifferentiation of myotubes derived from the murine myoblast cell line C20 [236]. To provide a molecular explanation for the function of reversine, its activity was tested on a broad panel of protein kinases and it was found that reversine specifically inhibits the function of Aurora kinases, both *in vitro* and in cell-based assay. It has been demonstrated that reversine inhibits Aurora B kinase, causing inhibition of cytokinesis and induction of polyploidy. How-

ever, the IC_{50} of reversine on Aurora A is 400nmol/L, whereas Aurora B and C IC_{50} s were 500 and 400nmol/L respectively [229, 236]. After 12 hours treatment with reversine, the majority (~80%) of HCT116 human colon carcinoma cells had doubled their DNA content (4N). Longer reversine treatments resulted in DNA endo-reduplication and in the accumulation of polyploid cells. It was demonstrated that reversine was less potent on normal cells than VX-680 [229].

CYC116

CYC116, developed by Cyclacel, inhibits Aurora A, Aurora B and Aurora C with IC_{50} s values of 44nM, 19nM and 65nM, respectively. In comparison to pan-Aurora kinase inhibitor VX-680, treatment of CYC116 showed similar molecular alteration to Aurora A and Aurora B in A549 lung carcinoma cells. In addition, 0.5-1 μ M of CYC116 induced mitotic arrest and delayed cell cycle entry in HeLa cells. Multinucleation of HeLa cells was shown in CYC116 treatment group *in vitro*. In NCI-H460 NSCLC xenograft mice, orally administrated CYC116 at doses of 75mg/kg and 100mg/kg reduced tumor growth by 42% and 79% respectively. Further, CYC116 reduces phosphorylation on Ser¹⁰ of histone H3 in tumor. In combination therapies, CYC116 shows a synergistic effect with several chemotherapeutic agents such as cisplatin and gemcitabine when CYC116 is given before the other drug. Besides Aurora kinase, this compound also inhibits VEGFR2 with an IC_{50} value of 69nM. *In vivo* investigation shows that CYC116 exhibits anti-angiogenic properties [219, 237-244].

SNS-314

A recent paper discusses the discovery and development of SNS-314, which is in Phase I clinical trials. SNS-314 inhibits Aurora A, Aurora B and Aurora C with IC_{50} s values of 9nM, 31nM and 3.4nM, respectively. At molecular and cellular level, SNS-314 inhibits phosphorylation of histone H3 and disrupts mitosis. SNS-314 blocks proliferation in various human tumor cell lines such as HT-29, PC3, HeLa and A375 with a BrdU IC_{50} value ranging from 1.8 to 9.3nM. In human HCT116 colon xenograft mice, administration of SNS-314 at doses of 100, 125 and 150mg/kg once daily or twice weekly for 5 days with a 9-day treatment-free interval significantly reduced tumor volume. In addition, it has potent anti-tumor activity in mouse xenograft models, such as A375 (melanoma), PC3 (prostate) and CALU6 (NSCLC).

In the clinical study, SNS-314 was given as a 3-h i.v. infusion with a treatment schedule once a week for 4 weeks continuously. The initial dose of the treatment was 30mg/m². Serum-drug concentrations have exceeded preclinical target thresholds at the 120mg/m² dose level. Dose-limiting toxicity or grade 3 or higher related adverse events have not been observed so far. SNS-314 is now undergoing another Phase I clinical trial in patients with advanced solid tumors [219, 245-250].

PF-03814735

PF-03814735 is an ATP-competitive, reversible inhibitor of Aurora A and Aurora B with IC_{50} s values of 5nM and

0.8nM respectively. In addition, it inhibits autophosphorylation of Aurora A at submicromolar concentrations. Phenotypically, PF-03814735 inhibits cytokinesis, and induces formation of multinucleated cells. In animal models, treatments of PF-03814735 inhibited tumor growth in HCT-116, Colo-205 and HL-60 tumor xenograft mice. This compound is now undergoing Phase I clinical trial evaluation. Twenty patients with colorectal, breast, bladder, ovarian, renal and head and neck cancers and melanoma, NSCLC and SCLC received PF-03814735 with dosages of 5-100 mg/day for 5 days. Mild-to-moderate diarrhea, vomiting, anorexia, fatigue and nausea were observed in 16 patients. Dose-limiting febrile neutropenia was observed in two out of seven patients treated at 100mg/day [219, 251-253].

ENMD-2076

ENMD-2076 [L-(+)-Lactic acid salt of ENMD-981693] is an orally active, vinyl-pyrimidine-based compound and selectively inhibits Aurora A with an IC_{50} value of 14nM, instead of Aurora B kinase (290nM). It also inhibits molecules such as Src, cKit, FAK and VEGFR2 with IC_{50} s values of 100, 40, 5 and 80 nM respectively. Molecular studies on human HCT-116 and U937 cells show that incubation of ENMD-2076 induced cell cycle arrest at G2/M phase and subsequent apoptosis. In a preclinical animal model, ENMD-2076 increased proportion of phosphohistone H3 positive 1A9 ovarian cancer cells by 80%. Fifty-one percent of tumor growth inhibition was observed in human MDA-MB-231 breast-cancer-injected SCID mice at a dosage of 50mg/kg p.o. q.d. Moreover, 70% of tumor regression was observed at a dosage of 200mg/kg p.o. b.i.d.. These data show that ENMD-2076 has a unique combination of anti-angiogenic, cell cycle and antiproliferative activities and support clinical rationale for this compounds utility in hematological cancers, including multiple myeloma. A Phase I clinical study of ENMD-2076 was initiated in March 2008 in patients with solid tumors, and there are plans to initiate a second Phase I study in patients with hematological malignances [219, 254-256].

AT9283

AT9283, by Astex Therapeutics, is a multitargeted kinase inhibitor that inhibits tyrosine and serine/threonine kinases such as Aurora A and B, JAK-2 and -3, Tyk2, RSK2 with IC_{50} s values less than 10nM *in vitro*. AT9283 has potent anti-proliferative activity against human cell lines expressing the wild-type BCR-ABL or mutated-BCR-ABL. AT9283 has potential antiproliferative activity in a panel of BAF3 and human cell lines expressing the BCR-ABL or its mutant forms. Series of Phase I/II clinical studies of this compound are in progress to investigate it in patients with advanced solid tumors and leukemia. In a Phase I study of AT9283 in patients with refractory solid tumors, 72h of intravenous infusion every 3 weeks with dose escalation was used. Maximum tolerated dose was determined at 9mg/m²/day. Results from another Phase I clinical study in patients with refractory leukemia were disclosed at the 2008 ASCO meeting. AT9283 was administered by 72h *i.v.* continuous infusion in patients with refractory AML, ALL, high-risk myelodys-

plastic syndromes (MDS) and imatinib- and dasatinib-refractory CML [219, 257-261].

R763 (AS703569)

R763 (AS703569), by Rigel, is an orally available inhibitor of Aurora A, Aurora B and several other kinases. AS703569 induced dose-dependent and time-dependent antiproliferative effects in SCC61 and Miapaca-2 cancer cell lines with IC_{50} s of 5 μ M and 2 μ M respectively. AS703569 also inhibited the phosphorylation of a tyrosine kinase receptor, FGFR1. *In vitro* study reveals that combination of AS703569 with imatinib displayed synergistic effects, when SCC61 cancer cells were pre-exposed to AS703569 before imatinib. In 2006, Merck Serono initiated a Phase I study of AS703569 in patients with solid tumor. The starting dose level was 6mg/m² p.o. per 21-day cycle divided in two or three doses. A total of 15 patients, comprising three cases of uterine/cervical cancer and two cases of breast cancer, have been included in the study so far. No severe adverse effect has been observed in drug-treated patients. Two patients were withdrawn from the study because of disease progression. Rigel has announced an initiation of a Phase I combination therapy study of R763 with gemcitabine in cancer patients with advanced malignancies [219, 262-264].

VX-689/MK-5108

In February 2008, Merck initiated a Phase I clinical trial of MK-5108 in patients with advanced and refractory solid tumors, dosed orally as monotherapy and also in combination with *i.v.* docetaxel. However, the chemical structure and *in vitro* data related to this compound are not available [219, 265].

MP529

MP529 shows selective inhibition on Aurora A kinase with an IC_{50} value of 110nM, where as IC_{50} value of Aurora B inhibition is > 10,000nM. MP529 is in late-stage preclinical development, the details of which were revealed at the 2008 AACR meeting [218].

MK615

MK615, an extract from the Japanese apricot, contains several triterpenoids and has been shown to exert an anti-neoplastic effect against human cancers. This is not a classical Aurora kinase inhibitor (small molecules), being able to inhibit Aurora A and B gene expression. However, the entire mechanisms of the anti-neoplastic effects of MK615 have not been elucidated. MK615 had an anti-neoplastic effect that was exerted by dual inhibition of Aurora A and B kinases. Previous studies have revealed that this drug has anti-neoplastic effects against gastric cancer [266], breast cancer [267], hepatocellular carcinoma [268], and colon cancer [269]. The mechanisms responsible for the anti-neoplastic effect of MK615 include induction of apoptosis [266, 267] and autophagy [269], and suppression of Aurora A kinase [268] in cancer cells. A previous study showed that MK615 induced cell cycle arrest at the end of G2 phase in hepatocellular carcinoma [268]. MK615 treatment increased the cell population in G2-M phase,

inhibits Aurora A and Aurora B kinases and may induce cancer cell death at the G2-arrest checkpoint [270, 271]. Although further investigation is needed, MK615 seems to have the property anti-Aurora kinase compound [272].

Selective Aurora B inhibitors

Selective inhibitors of Aurora B have also been developed, including AZD1152 [222] (highly potent and selective inhibitor of Aurora B), and GSK1070916 (a potent and selective inhibitor of Aurora B and Aurora C kinases) [273]. The general chemical structures of selective Aurora B inhibitors are shown in Fig. (4).

AZD1152

AZD1152 (AstraZeneca) is a novel acetanilide-substitute pyrazole-aminoquinazoline prodrug that is converted rapidly to the active drug AZD1152 hydroxy-QPA (AZD1152-HQPA) [213].

It is a highly potent and selective inhibitor of Aurora B (K_i , 0.36nmol/L), compared with Aurora A (K_i , 1,369 nmol/L), and has less activity against a panel of 50 other kinases including FLT3, JAK2 and Abl [213].

In vitro treatment of human tumor cell lines with AZD1152-HQPA suppresses the phosphorylation of the Aurora B substrate histone H3. In acute myeloid leukemia cell lines and primary acute myeloid leukemia cultures, AZD1152-HQPA induces growth arrest and the accumulation of polyploid cells in a dose- and time-dependent manner (almost identical to the mode of action of ZM1) [274]. Leukemia cells exposed to AD1152-HQPA exit mitosis and subsequently proceed through S phase in the absence of cytokinesis, with an increased population of cells with 4N/8N DNA content. Treatment with AZD1152 (1-10nM) for 24 and 48 hours in these cells induces apoptosis in a dose-dependent manner [274].

Administering AZD1152 to animals bearing human tumor xenografts resulted in profound antitumor effects in colorectal, lung and acute myeloid leukemia human tumor xenograft models [213, 274, 275]. AZD1152 was well tolerated within the dose range required to elicit a potent and durable antitumor effect, with animals showing only tran-

sient loss of body weight. Bone marrow analyses revealed reversible myelosuppression in AZD1152-treated animals, with full recovery occurring within a week of cessation of dosing. Analysis of peripheral blood cells also indicated a neutropenia followed by full recovery [213, 274].

It was also demonstrated that AZD1152 enhances the effect of radiation on p53-deficient cancer cells, in particular it is observed an enhanced cell killing when cells were irradiated 24h after exposure to AZD1152 [276, 277]. Apoptosis and DNA repair play a minor role in the response of tumor cells exposed to ADZ1152. In contrast, mitotic death is the major cell death mechanism following AZD1152 exposure, both *in vitro* and *in vivo* [276, 277].

AZD1152 is currently being studied in phase I-II clinical trials in solid tumor patients Table 2. In early results, the drug is reported to be well tolerated when administered by i.v. infusion at doses up to 300mg with significant disease stabilization in five of eight reported patients; transient neutropenia being the only noteworthy toxicity. No significant anemia, thrombocytopenia or neuropathy was observed. Melanoma, nasopharyngeal carcinoma and adenocystic carcinoma patients achieved prolonged stable disease lasting more than 25 weeks [275].

GSK1070916

GSK1070916 is a highly potent and selective Aurora B/Aurora C kinase inhibitor [273, 278]. This inhibition results in antiproliferative activity in multiple cancer cell lines and in mouse xenograft models of human tumors. Anderson *et al.* evaluated the selectivity of the drug and in this study they have demonstrated that GSK10700916 is an ATP competitive inhibitor of the Aurora B/INCENP enzyme. GSK1070916 inhibits Aurora A, Aurora B/INCENP and Aurora C/INCENP with IC_{50} s values of 1100, 3.5, and 6.5nM respectively. The selectivity may be partly due to the differences in the ATP-binding pockets of Aurora B/Aurora C versus Aurora A induced upon different cofactor binding. Moreover, GSK1070916 inhibitory activity became more potent over time, suggesting that the drug inhibits Aurora B/INCENP in a time-dependent fashion. At molecular level, GSK1070916 inhibits phosphorylation of histone H3 and shows potent antiproliferative activity against various human

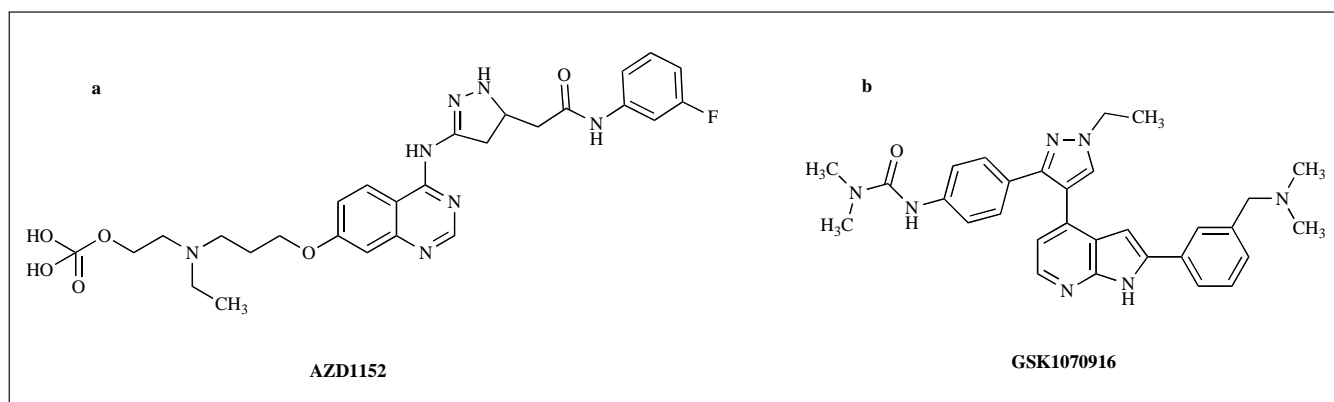


Fig. (4). Selective Aurora B inhibitors. Chemical structures of (a) AZD1152, (b) GSK1070916.

tumor cell lines *in vitro* [278]. In animal models, administration of GSK1070916 at a dose of 25 mg/kg induced complete inhibition of histone H3 in human Colo205 colon tumor xenograft mice. In addition, intraperitoneal administration of GSK1070916 at a dose of 100mg/kg (maximum tolerated dose) for 5 consecutive days with two cycles induced tumor regression [279]. Furthermore, human-leukemia-cell-implanted SCID-NOD mice were sensitive to GSK1070916 treatment at a dose of 25mg/kg with the same schedule of administration [279]. This compound is being progressed to Phase I clinical trials in patients with advanced solid tumors. This inhibitor may represent an “ultimate physiological inhibitor” that exerts a constant inhibition of Aurora B until the enzyme is degraded and replaced by new protein synthesis [273, 278]. Patents references [218, 280-286].

CURRENT & DEVELOPMENTS

Evidences suggest that deregulation of Aurora kinases contributes to the development of human neoplasia. The role of Aurora A in cancer has been clarified, being the gene frequently amplified in human tumours. On the other hand, the role of Aurora B in human tumourigenesis remains to be fully clarified.

The efficacy of Aurora inhibitors for the treatment of human neoplasia remains to be defined, and it is still not clear if these drugs present a better therapeutic index compared to antimetabolic drugs, which include taxol and vinka alkaloids, all proved successful in the clinic. However, antimetabolic drugs frequently show the appearance of drug resistance, adverse side effects (neurotoxicity) and their clinical effects are not predictable. Aurora inhibitors lacks neurotoxicity and could contribute to the treatment of human neoplasia [287, 288].

A large number of Aurora inhibitors have been obtained; most of them yield activity against both Aurora A and Aurora B. As expected by their mechanisms of action, clinical trials have shown that, compared to classical antimetabolic drugs, these inhibitors do not induce irreversible neutropenia, but consistent with their activity on proliferating cells-induce bone marrow suppression, alopecia, nausea, vomiting and diarrhoea. Several Aurora B and dual A/B inhibitors are currently under clinical trials, but little information about the clinical outcome is available. The dual A/B inhibitor PHA-739358 has resulted in partial/complete response in chronic myeloid leukemia (CML) and stabilization of the disease in solid tumours. Other clinical trials are ongoing to evaluate the clinical benefit of PHA-739358. Less encouraging data have been obtained with VX-680, that has been suspended on the base of preliminary safety data.

Overexpression of Aurora B and hyper-phosphorylation of histone H3 could be used to select patients likely to benefit of a treatment with dual or specific Aurora B kinase inhibitors, and the reduction of H3 phosphorylation in target tissues could help in monitoring the efficacy of these treatments. Furthermore, accumulating preclinical data are predicting that the association of these inhibitors with conventional chemotherapy and radiotherapy display additive or even synergistic anticancer effect. Emerging data suggest that spindle checkpoint inhibitors, in combination

with DNA damaging agents, may be valid tools for the treatment of human neoplasia [279]. The rationale is that, in normal cells, these agents would arrest the cells mostly in G1 in a p53-dependent manner, whereas p53-deficient cells, accounting for over half of all tumor-types, have to rely on S or G2-M checkpoint -although weaker than in healthy cells-to arrest cell cycle and repair the DNA. Therefore, combining a G2 checkpoint inhibitor with a DNA damaging agent should kill tumor cells, but most importantly spare the normal ones. Recent data demonstrates the efficacy of this association [177, 235, 277, 289, 290], thus opening new avenues towards the cure of certain cancers.

ACKNOWLEDGEMENTS

We thank Dr Formisano P and Dr Chieffi P for the critical review of the manuscript. We also thank the Associazione Italiana per la Ricerca sul Cancro (AIRC) for supporting our study.

CONFLICT OF INTEREST

The authors declare any conflict of interest.

REFERENCES

- [1] Nigg EA. Mitotic kinases as regulators of cell division and its checkpoints. *Nat Rev Mol Cell Biol* 2001; 2(1): 21-32.
- [2] Vader G, Lens SM. The Aurora kinase family in cell division and cancer. *Biochim Biophys Acta* 2008; 1786(1): 60-72.
- [3] Gold MG, Barford D, Komander D. Lining the pockets of kinases and phosphatases. *Curr Opin Struct Biol* 2006; 16(6): 693-701.
- [4] Glover DM, Leibowitz MH, McLean DA, Parry H. Mutations in aurora prevent centrosome separation leading to the formation of monopolar spindles. *Cell* 1995; 81(1): 95-105.
- [5] Chan CS, Botstein D. Isolation and characterization of chromosome-gain and increase-in-ploidy mutants in yeast. *Genetics* 1993; 135(3): 677-91.
- [6] Francisco L, Wang W, Chan CS. Type 1 protein phosphatase acts in opposition to Ipl1 protein kinase in regulating yeast chromosome segregation. *Mol Cell Biol* 1994; 14(7): 4731-40.
- [7] Petersen J, Paris J, Willer M, Philippe M, Hagan IM. The *S. pombe* aurora-related kinase Ark1 associates with mitotic structures in a stage dependent manner and is required for chromosome segregation. *J Cell Sci* 2001; 114(Pt 24): 4371-84.
- [8] Kimura M, Kotani S, Hattori T, Sumi N, Yoshioka T, Todokoro K, et al. Cell cycle-dependent expression and spindle pole localization of a novel human protein kinase, Aik, related to Aurora of *Drosophila* and yeast Ipl1. *J Biol Chem* 1997; 272(21): 13766-71.
- [9] Tanaka M, Ueda A, Kanamori H, Ideguchi H, Yang J, Kitajima S, et al. Cell-cycle-dependent regulation of human aurora A transcription is mediated by periodic repression of E4TF1. *J Biol Chem* 2002; 277(12): 10719-26.
- [10] Kimura M, Uchida C, Takano Y, Kitagawa M, Okano Y. Cell cycle-dependent regulation of the human aurora B promoter. *Biochem Biophys Res Commun* 2004; 316(3): 930-6.
- [11] Wang IC, Chen YJ, Hughes D, Petrovic V, Major ML, Park HJ, et al. Forkhead box M1 regulates the transcriptional network of genes essential for mitotic progression and genes encoding the SCF (Skp2-Cks1) ubiquitin ligase. *Mol Cell Biol* 2005; 25(24): 10875-94.
- [12] Tang CJ, Chuang CK, Hu HM, Tang TK. The zinc finger domain of Tzfp binds to the tbs motif located at the upstream flanking region of the Aie1 (Aurora-C) kinase gene. *J Biol Chem* 2001; 276(22): 19631-9.
- [13] Sasai K, Katayama H, Stenoien DL, Fujii S, Honda R, Kimura M, et al. Aurora-C kinase is a novel chromosomal passenger protein that can complement Aurora-B kinase function in mitotic cells. *Cell Motil Cytoskeleton* 2004; 59(4): 249-63.
- [14] Li X, Sakashita G, Matsuzaki H, Sugimoto K, Kimura K, Hanaoka F, et al. Direct association with inner centromere protein (INCENP)

- activates the novel chromosomal passenger protein, Aurora-C. *J Biol Chem* 2004; 279(45): 47201-211.
- [15] Lukasiewicz KB, Lingle WL. Aurora A, centrosome structure, and the centrosome cycle. *Environ Mol Mutagen* 2009; 50(8): 602-19.
- [16] Tseng TC, Chen SH, Hsu YP, Tang TK. Protein kinase profile of sperm and eggs: Cloning and characterization of two novel testis-specific protein kinases (AIE1, AIE2) related to yeast and fly chromosome segregation regulators. *DNA Cell Biol* 1998; 17(10): 823-33.
- [17] Chen SH, Tang TK. Mutational analysis of the phosphorylation sites of the Aie1 (Aurora-C) kinase *in vitro*. *DNA Cell Biol* 2002; 21(1): 41-6.
- [18] Lo YL, Yu JC, Chen ST, Yang HC, Fann CS, Mau YC, *et al*. Breast cancer risk associated with genotypic polymorphism of the mitosis-regulating gene Aurora-A/STK15/BTAK. *Int J Cancer* 2005; 115(2): 276-283.
- [19] Ulisse S, Delcros JG, Baldini E, Toller M, Curcio F, Giacomelli L, *et al*. Expression of Aurora kinases in human thyroid carcinoma cell lines and tissues. *Int J Cancer* 2006; 119(2): 275-82.
- [20] Taguchi S, Honda K, Sugiura K, Yamaguchi A, Furukawa K, Urano T. Degradation of human Aurora-A protein kinase is mediated by hCdh1. *FEBS Lett* 2002; 519(1-3): 59-65.
- [21] Nguyen HG, Chinnappan D, Urano T, Ravid K. Mechanism of Aurora-B degradation and its dependency on intact KEN and A-boxes: Identification of an aneuploidy-promoting property. *Mol Cell Biol* 2005; 25(12): 4977-92.
- [22] Arlot-Bonnemains Y, Klotzbucher A, Giet R, Uzbekov R, Bihan R, Prigent C. Identification of a functional destruction box in the *Xenopus laevis* aurora-A kinase pEg2. *FEBS Lett* 2001; 508(1): 149-52.
- [23] Crane R, Kloepfer A, Ruderman JV. Requirements for the destruction of human Aurora-A. *J Cell Sci* 2004; 117(Pt 25): 5975-83.
- [24] Littlepage LE, Ruderman JV. Identification of a new APC/C recognition domain, the A box, which is required for the Cdh1-dependent destruction of the kinase Aurora-A during mitotic exit. *Genes Dev* 2002; 16(17): 2274-85.
- [25] Stewart S, Fang G. Destruction box-dependent degradation of aurora B is mediated by the anaphase-promoting complex/cyclosome and Cdh1. *Cancer Res* 2005; 65(19): 8730-5.
- [26] Sumara I, Quadroni M, Frei C, Olma MH, Sumara G, Ricci R, *et al*. A Cul3-based E3 ligase removes Aurora B from mitotic chromosomes, regulating mitotic progression and completion of cytokinesis in human cells. *Dev Cell* 2007; 12(6): 887-900.
- [27] Walter AO, Seghezzi W, Korver W, Sheung J, Lees E. The mitotic serine/threonine kinase Aurora2/AIK is regulated by phosphorylation and degradation. *Oncogene* 2000; 19(42): 4906-16.
- [28] Castro A, Arlot-Bonnemains Y, Vigneron S, Labbé JC, Prigent C, Lorca T. APC/Fizzy-Related targets Aurora-A kinase for proteolysis. *EMBO Rep* 2002; 3(5): 457-62.
- [29] Shu F, Guo S, Dang Y, Qi M, Zhou G, Guo Z, *et al*. Human aurora-B binds to a proteasome alpha-subunit HC8 and undergoes degradation in a proteasome-dependent manner. *Mol Cell Biochem* 2003; 254(1-2): 157-62.
- [30] Bolanos-Garcia VM. Aurora kinases. *Int J Biochem Cell Biol* 2005; 37(8): 1572-7.
- [31] Littlepage LE, Wu H, Andresson T, Deanehan JK, Amundadottir LT, Ruderman JV. Identification of phosphorylated residues that affect the activity of the mitotic kinase Aurora-A. *Proc Natl Acad Sci USA* 2002; 99(24): 15440-5.
- [32] Cheeseman IM, Anderson S, Jwa M, Green EM, Kang J, Yates JR 3rd, *et al*. Phospho-regulation of kinetochore-microtubule attachments by the Aurora kinase Ipl1p. *Cell* 2002; 111(2): 163-72.
- [33] Andrésson T, Ruderman JV. The kinase Eg2 is a component of the *Xenopus* oocyte progesterone-activated signaling pathway. *EMBO J* 1998; 17(19): 5627-37.
- [34] Katayama H, Zhou H, Li Q, Tatsuka M, Sen S. Interaction and feedback regulation between STK15/BTAK/Aurora-A kinase and protein phosphatase 1 through mitotic cell division cycle. *J Biol Chem* 2001; 276(49): 46219-24.
- [35] Murnion ME, Adams RR, Callister DM, Allis CD, Earnshaw WC, Swedlow JR. Chromatin-associated protein phosphatase 1 regulates aurora-B and histone H3 phosphorylation. *J Biol Chem* 2001; 276(28): 26656-65.
- [36] Tsai MY, Wiese C, Cao K, Martin O, Donovan P, Ruderman J, *et al*. A Ran signalling pathway mediated by the mitotic kinase Aurora A in spindle assembly. *Nat Cell Biol* 2003; 5(3): 242-8.
- [37] Eyers PA, Erikson E, Chen LG, Maller JL. A novel mechanism for activation of the protein kinase Aurora A. *Curr Biol* 2003; 13(8): 691-7.
- [38] Castro A, Vigneron S, Bernis C, Labbé JC, Prigent C, Lorca T. The D-Box-activating domain (DAD) is a new proteolysis signal that stimulates the silent D-Box sequence of Aurora-A. *EMBO Rep* 2002; 3(12): 1209-14.
- [39] Kiat LS, Hui KM, Gopalan G. Aurora-A kinase interacting protein (AIP), a novel negative regulator of human Aurora-A kinase. *J Biol Chem* 2002; 277(47): 45558-65.
- [40] Carmena M, Earnshaw WC. The cellular geography of aurora kinases. *Nat Rev Mol Cell Biol* 2003; 4(11): 842-54.
- [41] Carvajal RD, Tse A, Schwartz GK. Aurora kinases: New targets for cancer therapy. *Clin Cancer Res* 2006; 12(23): 6869-75.
- [42] Kollareddy M, Dzubak P, Zheleva D, Hajdich M. Aurora kinases: Structure, functions and their association with cancer. *Biomed Pap Med Fac Univ Palacky Olomouc Czech Repub* 2008; 152(1): 27-33.
- [43] Ducat D, Zheng Y. Aurora kinases in spindle assembly and chromosome segregation. *Exp Cell Res* 2004; 301(1): 60-7.
- [44] Zhou H, Kuang J, Zhong L, Kuo WL, Gray JW, Sahin A, *et al*. Tumour amplified kinase STK15/BTAK induces centrosome amplification, aneuploidy and transformation. *Nat Genet* 1998; 20(2): 189-93.
- [45] Giet R, Prigent C. Aurora/Ipl1p-related kinases, a new oncogenic family of mitotic serine-threonine kinases. *J Cell Sci* 1999; 112(Pt 21): 3591-601.
- [46] Vader G, Lens SM. The Aurora kinase family in cell division and cancer. *Biochim Biophys Acta* 2008; 1786(1): 60-72.
- [47] Slattery SD, Mancini MA, Brinkley BR, Hall RM. Aurora-C kinase supports mitotic progression in the absence of Aurora-B. *Cell Cycle* 2009; 8(18): 2984-94.
- [48] Berdnik D, Knoblich JA. *Drosophila* Aurora-A is required for centrosome maturation and actin-dependent asymmetric protein localization during mitosis. *Curr Biol* 2002; 12(8): 640-7.
- [49] Hirota T, Kunitoku N, Sasayama T, Marumoto T, Zhang D, Nitta M, *et al*. Aurora-A and an interacting activator, the LIM protein Ajuba, are required for mitotic commitment in human cells. *Cell* 2003; 114(5): 585-98.
- [50] Dutertre S, Cazales M, Quaranta M, Froment C, Trabut V, Dozier C, *et al*. Phosphorylation of CDC25B by Aurora-A at the centrosome contributes to the G2-M transition. *J Cell Sci* 2004; 117: 2523-31.
- [51] Marumoto T, Honda S, Hara T, Nitta M, Hirota T, Kohmura E, *et al*. Aurora-A kinase maintains the fidelity of early and late mitotic events in HeLa cells. *J Biol Chem* 2003; 278: 51786-95.
- [52] Kufer TA, Sillje HH, Korner R, Gruss OJ, Meraldi P, Nigg EA. Human TPX2 is required for targeting Aurora-A kinase to the spindle. *J Cell Biol* 2002; 158: 617-23.
- [53] Kunitoku N, Sasayama T, Marumoto T, Zhang D, Honda S, Kobayashi O, *et al*. CENP-A phosphorylation by Aurora-A in prophase is required for enrichment of Aurora-B at inner centromeres and for Kinetochore function. *Dev Cell* 2003; 5: 242-8.
- [54] Liu Q, Kaneko S, Yang L, Feldman RI, Nicosia SV, Chen J, *et al*. Aurora-A abrogation of p53 DNA binding and trasactivation activity by phosphorylation of serine 215. *J Biol Chem* 2004; 279: 52175-82.
- [55] Sakai H, Urano T, Ookata K, Kim MH, Hirai Y, Saito M, *et al*. MBD3 and HDAC1, two components of the NuRD complex, are localized at Aurora-A-positive centrosomes in M phase. *J Biol Chem* 2002; 277: 48714-23.
- [56] Ouchi M, Fujiuchi N, Sasai K, Katayama H, Minamishima YA, Ongusaha PP, *et al*. BRCA1 phosphorylation by Aurora-A in the regulation of G2 to M transition. *J Biol Chem* 2004; 279: 19643-8.
- [57] Murata-Hori M, Wang YL. The Kinase activity of Aurora B is require for Kinetochore-microtubule interactions during mitosis. *Curr Biol* 2002; 12: 894-9.
- [58] Zeitlin SG, Shelby RD, Sullivan KF. CENP_A is phosphorylated by Aurora B Kinase and plays an unexpected role in completion of cytokinesis. *J Cell Biol* 2001; 155: 1147-57.
- [59] Honda R, Korner R, Nigg EA. Exploring the functional interactions between Aurora B, INCEP, and survivin in mitosis. *Mol Biol Cell* 2003; 14: 3325-41.

- [60] Sessa F, Mapelli M, Ciferri C, Tarricone C, Areces LB, Schneider TR, *et al.* Mechanism of Aurora B activation by INCEP and inhibition by hesperadin. *Mol Cell* 2005; 18: 379-91.
- [61] Adams RR, Carmena M, Earnshaw WC. Chromosomal passengers and the Aurora ABCs of mitosis. *Trends Cell Biol* 2001; 11: 49-54.
- [62] Ruchaud S, Carmena M, Earnshaw WC. Chromosomal passengers: Conducting cell division. *Nat Rev Mol Cell Biol* 2007; 8(10): 798-812.
- [63] Vader G, Medema RH, Lens SM. The chromosomal passenger complex: Guiding Aurora-B through mitosis. *J Cell Biol* 2006; 173(6): 833-7.
- [64] Goto H, Yasui Y, Nigg EA, Inagaki M. Aurora-B phosphorylates Histone H3 at serine28 with regard to the mitotic chromosome condensation. *Genes Cells* 2002; 7(1): 11-7.
- [65] Gassmann R, Carvalho A, Henzing AJ, Ruchaud S, Hudson DF, Honda R, *et al.* Borealin: A novel chromosomal passenger required for stability of the bipolar mitotic spindle. *J Cell Biol* 2004; 166(2): 179-91.
- [66] Gurley LR, D'Anna JA, Barham SS, Deaven LL, Tobey RA. Histone phosphorylation and chromatin structure during mitosis in Chinese hamster cells. *Eur J Biochem* 1978; 84(1): 1-15.
- [67] Hsu JY, Sun ZW, Li X, Reuben M, Tatchell K, Bishop DK, *et al.* Mitotic phosphorylation of histone H3 is governed by Ipl1/aurora kinase and Glc7/PP1 phosphatase in budding yeast and nematodes. *Cell* 2000; 102(3): 279-91.
- [68] Adams RR, Maiato H, Earnshaw WC, Carmena M. Essential roles of *Drosophila* inner centromere protein (INCENP) and aurora B in histone H3 phosphorylation, metaphase chromosome alignment, kinetochore disjunction, and chromosome segregation. *J Cell Biol* 2001; 153(4): 865-80.
- [69] Speliotes EK, Uren A, Vaux D, Horvitz HR. The survivin-like *C. elegans* BIR-1 protein acts with the Aurora-like kinase AIR-2 to affect chromosomes and the spindle midzone. *Mol Cell* 2000; 6(2): 211-23.
- [70] Giet R, Glover DM. *Drosophila* aurora B kinase is required for histone H3 phosphorylation and condensin recruitment during chromosome condensation and to organize the central spindle during cytokinesis. *J Cell Biol* 2001; 152(4): 669-82.
- [71] Crosio C, Fimia GM, Loury R, Kimura M, Okano Y, Zhou H, *et al.* Mitotic phosphorylation of histone H3: Spatio-temporal regulation by mammalian Aurora kinases. *Mol Cell Biol* 2002; 22(3): 874-85.
- [72] MacCallum DE, Losada A, Kobayashi R, Hirano T. ISWI remodeling complexes in *Xenopus* egg extracts: Identification as major chromosomal components that are regulated by INCENP-aurora B. *Mol Biol Cell* 2002; 13(1): 25-39.
- [73] Goto H, Tomono Y, Ajiro K, Kosako H, Fujita M, Sakurai M, *et al.* Identification of a novel phosphorylation site on histone H3 coupled with mitotic chromosome condensation. *J Biol Chem* 1999; 274(36): 25543-9.
- [74] Swedlow JR, Hirano T. The making of the mitotic chromosome: modern insights into classical questions. *Mol Cell* 2003; 11(3): 557-69.
- [75] Hirano T. At the heart of the chromosome: SMC proteins in action. *Nat Rev Mol Cell Biol* 2006; 7(5): 311-22.
- [76] Maddox PS, Portier N, Desai A, Oegema K. Molecular analysis of mitotic chromosome condensation using a quantitative time-resolved fluorescence microscopy assay. *Proc Natl Acad Sci USA* 2006; 103(41): 15097-102.
- [77] Lipp JJ, Hirota T, Poser I, Peters JM. Aurora B controls the association of condensin I but not condensin II with mitotic chromosomes. *J Cell Sci* 2007; 120(Pt 7): 1245-55.
- [78] Takemoto A, Murayama A, Katano M, Urano T, Furukawa K, Yokoyama S, *et al.* Analysis of the role of Aurora B on the chromosomal targeting of condensin I. *Nucleic Acids Res* 2007; 35(7): 2403-12.
- [79] Losada A, Hirano M, Hirano T. Cohesin release is required for sister chromatid resolution, but not for condensin-mediated compaction, at the onset of mitosis. *Genes Dev* 2002; 16(23): 3004-16.
- [80] Morishita J, Matsusaka T, Goshima G, Nakamura T, Tatebe H, Yanagida M. Bir1/Cut17 moving from chromosome to spindle upon the loss of cohesion is required for condensation, spindle elongation and repair. *Genes Cells* 2001; 6(9): 743-63.
- [81] Ono T, Fang Y, Spector DL, Hirano T. Spatial and temporal regulation of Condensins I and II in mitotic chromosome assembly in human cells. *Mol Biol Cell* 2004; 15(7): 3296-308.
- [82] Hsu JY, Sun ZW, Li X, Reuben M, Tatchell K, Bishop DK, *et al.* Mitotic phosphorylation of histone H3 is governed by Ipl1/aurora kinase and Glc7/PP1 phosphatase in budding yeast and nematodes. *Cell* 2000; 102: 279-91.
- [83] Wei Y, Mizzen CA, Cook RG, Gorovsky MA, Allis CD. Phosphorylation of histone H3 at serine 10 is correlated with chromosome condensation during mitosis and meiosis in *Tetrahymena*. *Proc Natl Acad Sci USA* 1998; 95: 7480-4.
- [84] Mellone BG, Ball L, Suka N, Grunstein MR, Partridge JF, Allshire RC. Centromere silencing and function in fission yeast is governed by the amino terminus of histone H3. *Curr Biol* 2003; 13: 1748-57.
- [85] Hirota T, Lipp JJ, Toh BH, Peters JM. Histone H3 serine 10 phosphorylation by Aurora B causes HP1 dissociation from heterochromatin. *Nature* 2005; 438: 1176-80.
- [86] Fischle W, Tseng BS, Dormann HL, Ueberheide BM, Garcia BA, Shabanowitz J, *et al.* Regulation of HP1-chromatin binding by histone H3 methylation and phosphorylation. *Nature* 2005; 438: 1116-22.
- [87] Giet R, Prigent C. The *Xenopus laevis* aurora/Ipl1p-related kinase pEg2 participates in the stability of the bipolar mitotic spindle. *Exp Cell Res* 2000; 258(1): 145-51.
- [88] Hirano T. The ABCs of SMC proteins: Two-armed ATPases for chromosome condensation, cohesion, and repair. *Genes Dev* 2002; 16(4): 399-414.
- [89] Petersen J, Hagan IM. *S. pombe* aurora kinase/survivin is required for chromosome condensation and the spindle checkpoint attachment response. *Curr Biol* 2003; 13(7): 590-7.
- [90] Kaitna S, Pasierbek P, Jantsch M, Loidl J, Glotzer M. The aurora B kinase AIR-2 regulates kinetochores during mitosis and is required for separation of homologous chromosomes during meiosis. *Curr Biol* 2002; 12(10): 798-812.
- [91] Hagstrom KA, Holmes VF, Cozzarelli NR, Meyer BJ. *C. elegans* condensin promotes mitotic chromosome architecture, centromere organization, and sister chromatid segregation during mitosis and meiosis. *Genes Dev* 2002; 16(6): 729-42.
- [92] Hauf S, Cole RW, LaTerra S, Zimmer C, Schnapp G, Walter R, *et al.* The small molecule Hesperadin reveals a role for Aurora B in correcting kinetochore-microtubule attachment and in maintaining the spindle assembly checkpoint. *J Cell Biol* 2003; 161(2): 281-94.
- [93] Nasmyth K, Peters JM, Uhlmann F. Splitting the chromosome: cutting the ties that bind sister chromatids. *Novartis Found Symp* 2001; 237: 113-33; discussion 133-138, 158-63.
- [94] Waizenegger IC, Hauf S, Meinke A, Peters JM. Two distinct pathways remove mammalian cohesin from chromosome arms in prophase and from centromeres in anaphase. *Cell* 2000; 103(3): 399-410.
- [95] Sumara I, Vorlaufer E, Stukenberg PT, Kelm O, Redemann N, Nigg EA, *et al.* The dissociation of cohesin from chromosomes in prophase is regulated by Polo-like kinase. *Mol Cell* 2002; 9(3): 515-25.
- [96] Giménez-Abián JF, Sumara I, Hirota T, Hauf S, Gerlich D, de la Torre C, *et al.* Regulation of sister chromatid cohesion between chromosome arms. *Curr Biol* 2004; 14(13): 1187-93.
- [97] Kerrebrock AW, Moore DP, Wu JS, Orr-Weaver TL. Mei-S332, a *Drosophila* protein required for sister-chromatid cohesion, can localize to meiotic centromere regions. *Cell* 1995; 83(2): 247-56.
- [98] Kitajima TS, Kawashima SA, Watanabe Y. The conserved kinetochore protein shugoshin protects centromeric cohesion during meiosis. *Nature* 2004; 427(6974): 510-17.
- [99] Riedel CG, Katis VL, Katou Y, Mori S, Itoh T, Helmhart W, *et al.* Protein phosphatase 2A protects centromeric sister chromatid cohesion during meiosis I. *Nature* 2006; 441: 53-61.
- [100] Kitajima TS, Sakuno T, Ishiguro K, Iemura S, Natsume T, Kawashima SA, *et al.* Shugoshin collaborates with protein phosphatase 2A to protect Cohesin. *Nature* 2006; 441: 46-52.
- [101] Hauf S, Roitinger E, Koch B, Dittrich CM, Mechtler K, Peters JM. Dissociation of Cohesin from chromosome arms and loss of arm cohesion during early mitosis depends on phosphorylation of SA2. *PLoS Biol* 2005; 3: e69.
- [102] Tang Z, Shu H, Qi W, Mahmood NA, Mumby MC, Yu H. PP2A is required for centromeric localization of Sgol and proper chromosome segregation. *Dev Cell* 2006; 10: 575-85.

- [103] Salic A, Waters JC, Mitchison TJ. Vertebrate Shugoshin links sister centromere cohesion and kinetochore-microtubule stability in mitosis. *Cell* 2004; 118: 567-78.
- [104] McGuinness BE, Hirota T, Kudo NR, Peters JM, Nasmyth K. Shugoshin prevents dissociation of Cohesin from centromeres during mitosis in vertebrate cells. *PLoS Biol* 2005; 3: e86.
- [105] Dai J, Sullivan BA, Higgins JM. Regulation of mitotic chromosome cohesion by Haspin and Aurora B. *Dev Cell* 2006; 11: 741-50.
- [106] Resnick TD, Satinover DL, MacIsaac F, Stukenberg PT, Earnshaw WC, Orr-Weaver TL, *et al.* INCENP and Aurora B promote meiotic sister chromatid cohesion through localization of the Shugoshin MEI-S332 in *Drosophila*. *Dev Cell* 2006; 11: 57-68.
- [107] Nonaka N, Kitajima T, Yokobayashi S, Xiao G, Yamamoto M, Grewal SI, *et al.* Recruitment of Cohesin to heterochromatic regions by Swi6/HP1 in fission yeast. *Nat Cell Biol* 2002; 4: 89-93.
- [108] Bernard P, Maure JF, Partridge JF, Genier S, Javerzat JP, Allshire RC. Requirement of heterochromatin for cohesion at centromeres. *Science* 2001; 294: 2539-42.
- [109] Kelly AE, Sampath SC, Maniar TA, Woo EM, Chait BT, Funabiki H. Chromosomal enrichment and activation of the Aurora B pathway are coupled to spatially regulate spindle assembly. *Dev Cell* 2007; 12: 31-43.
- [110] Sampath SC, Ohi R, Leismann O, Salic A, Pozniakovski A, Funabiki H. The chromosomal passenger complex is required for chromatin-induced microtubule stabilization and spindle assembly. *Cell* 2004; 118: 187-202.
- [111] Zhang X, Lan W, Ems-McClung SC, Stukenberg PT, Walczak CE. Aurora B phosphorylates multiple sites on MCAK to spatially and temporally regulate its function. *Mol Biol Cell* 2008; 3264-76.
- [112] Tulu US, Fagerstrom C, Ferenz NP, Wadsworth P. Molecular requirements for kinetochore-associated microtubule formation in mammalian cells. *Curr Biol* 2006; 16(5): 536-41.
- [113] Bakhom SF, Thompson SL, Manning AL, Compton DA. Genome stability is ensured by temporal control of kinetochore-microtubule dynamics. *Nat Cell Biol* 2009; 11(1): 27-35.
- [114] Gadea BB, Ruderman JV. Aurora B is required for mitotic chromatin-induced phosphorylation of Op18/Stathmin. *Proc Natl Acad Sci USA* 2006; 103(12): 4493-8.
- [115] Roos UP. Light and electron microscopy of rat kangaroo cells in mitosis. III. Patterns of chromosome behavior during prometaphase. *Chromosoma* 1976; 54(4): 363-85.
- [116] Tanaka TU, Rachidi N, Janke C, Pereira G, Galova M, Schiebel E, *et al.* Evidence that the Ipl1-Sli15 (Aurora kinase-INCENP) complex promotes chromosome bi-orientation by altering kinetochore-spindle pole connections. *Cell* 2002; 108(3): 317-29.
- [117] Tanaka TU. Chromosome bi-orientation on the mitotic spindle. *Philos Trans R Soc Lond B Biol Sci* 2005; 360(1455): 581-9.
- [118] Cheeseman IM, Anderson S, Jwa M, Green EM, Kang J, Yates JR 3rd, *et al.* Phospho-regulation of kinetochore-microtubule attachments by the Aurora kinase Ipl1p. *Cell* 2002; 111(2): 163-72.
- [119] Lampson MA, Renduchitala K, Khodjakov A, Kapoor TM. Correcting improper chromosome-spindle attachments during cell division. *Nat Cell Biol* 2004; 6(3): 232-7.
- [120] Andrews PD, Ovechkina Y, Morrice N, Wagenbach M, Duncan K, Wordeman L, *et al.* Aurora B regulates MCAK at the mitotic centromere. *Dev Cell* 2004; 6(2): 253-68.
- [121] Lan W, Zhang X, Kline-Smith SL, Rosasco SE, Barrett-Wilt GA, Shabanowitz J, *et al.* Aurora B phosphorylates centromeric MCAK and regulates its localization and microtubule depolymerization activity. *Curr Biol* 2004; 14(4): 273-86.
- [122] Ohi R, Sapra T, Howard J, Mitchison TJ. Differentiation of cytoplasmic and meiotic spindle assembly MCAK functions by Aurora B-dependent phosphorylation. *Mol Biol Cell* 2004; 15(6): 2895-906.
- [123] Cheeseman IM, Chappie JS, Wilson-Kubalek EM, Desai A. The conserved KMN network constitutes the core microtubule-binding site of the kinetochore. *Cell* 2006; 127(5): 983-97.
- [124] DeLuca JG, Gall WE, Ciferri C, Cimini D, Musacchio A, Salmon ED. Kinetochore microtubule dynamics and attachment stability are regulated by Hec1. *Cell* 2006; 127(5): 969-82.
- [125] Cimini D, Wan X, Hirel CB, Salmon ED. Aurora kinase promotes turnover of kinetochore microtubules to reduce chromosome segregation errors. *Curr Biol* 2006; 16(17): 1711-8.
- [126] Knowlton AL, Lan W, Stukenberg PT. Aurora B is enriched at merotelic attachment sites, where it regulates MCAK. *Curr Biol* 2006; 16(17): 1705-10.
- [127] Ohi R, Coughlin ML, Lane WS, Mitchison TJ. An inner centromere protein that stimulates the microtubule depolymerizing activity of a KinI kinesin. *Dev Cell* 2003; 5(2): 309-21.
- [128] Huang H, Feng J, Famulski J, Rattner JB, Liu ST, Kao GD, *et al.* Tripin/hSgo2 recruits MCAK to the inner centromere to correct defective kinetochore attachments. *J Cell Biol* 2007; 177(3): 413-24.
- [129] Ditchfield C, Johnson VL, Tighe A, Ellston R, Haworth C, Johnson T, *et al.* Aurora B couples chromosome alignment with anaphase by targeting BubR1, Mad2, and Cenp-E to kinetochores. *J Cell Biol* 2003; 161(2): 267-80.
- [130] Girdler F, Gascoigne KE, Evers PA, Hartmuth S, Crafter C, Foote KM, *et al.* Validating Aurora B as an anti-cancer drug target. *J Cell Sci* 2006; 119(Pt 17): 3664-75.
- [131] Terada Y, Tatsuka M, Suzuki F, Yasuda Y, Fujita S, Otsu M. AIM-1: A mammalian midbody-associated protein required for cytokinesis. *EMBO J* 1998; 17(3): 667-76.
- [132] Kaitna S, Pasierbek P, Jantsch M, Loidl J, Glotzer M. The aurora B kinase AIR-2 regulates kinetochores during mitosis and is required for separation of homologous chromosomes during meiosis. *Curr Biol* 2002; 12(10): 798-812.
- [133] Severson AF, Hamill DR, Carter JC, Schumacher J, Bowerman B. The aurora-related kinase AIR-2 recruits ZEN-4/CeMKLP1 to the mitotic spindle at metaphase and is required for cytokinesis. *Curr Biol* 2000; 10(19): 1162-71.
- [134] Higuchi T, Uhlmann F. Stabilization of microtubule dynamics at anaphase onset promotes chromosome segregation. *Nature* 2005; 433(7022): 171-6.
- [135] Buvelot S, Tatsutani SY, Vermaak D, Biggins S. The budding yeast Ipl1/Aurora protein kinase regulates mitotic spindle disassembly. *J Cell Biol* 2003; 160(3): 329-39.
- [136] Glotzer M. The molecular requirements for cytokinesis. *Science* 2005; 307(5716): 1735-9.
- [137] Piekny A, Werner M, Glotzer M. Cytokinesis: Welcome to the Rho zone. *Trends Cell Biol* 2005; 15(12): 651-8.
- [138] Yüce O, Piekny A, Glotzer M. An ECT2-centralspindlin complex regulates the localization and function of RhoA. *J Cell Biol* 2005; 170(4): 571-82.
- [139] Nishimura Y, Yonemura S. Centralspindlin regulates ECT2 and RhoA accumulation at the equatorial cortex during cytokinesis. *J Cell Sci* 2006; 119(Pt 1): 104-14.
- [140] Zhao WM, Fang G. MgcRacGAP controls the assembly of the contractile ring and the initiation of cytokinesis. *Proc Natl Acad Sci USA* 2005; 102(37): 13158-63.
- [141] Lehner CF. The pebble gene is required for cytokinesis in *Drosophila*. *J Cell Sci* 1992; 103 (Pt 4): 1021-30.
- [142] Tatsumoto T, Xie X, Blumenthal R, Okamoto I, Miki T. Human ECT2 is an exchange factor for Rho GTPases, phosphorylated in G2/M phases, and involved in cytokinesis. *J Cell Biol* 1999; 147(5): 921-8.
- [143] Kaitna S, Mendoza M, Jantsch-Plunger V, Glotzer M. Incenp and an aurora-like kinase form a complex essential for chromosome segregation and efficient completion of cytokinesis. *Curr Biol* 2000; 10(19): 1172-81.
- [144] Guse A, Mishima M, Glotzer M. Phosphorylation of ZEN-4/MKLP1 by aurora B regulates completion of cytokinesis. *Curr Biol* 2005; 15(8): 778-786.
- [145] Minoshima Y, Kawashima T, Hirose K, Tonzuka Y, Kawajiri A, Bao YC, *et al.* Phosphorylation by aurora B converts MgcRacGAP to a RhoGAP during cytokinesis. *Dev Cell* 2003; 4(4): 549-60.
- [146] Goto H, Yasui Y, Kawajiri A, Nigg EA, Terada Y, Tatsuka M, *et al.* Aurora-B regulates the cleavage furrow-specific vimentin phosphorylation in the cytokinetic process. *J Biol Chem* 2003; 278(10): 8526-30.
- [147] Murata-Hori M, Fumoto K, Fukuta Y, Iwasaki T, Kikuchi A, Tatsuka M, *et al.* Myosin II regulatory light chain as a novel substrate for AIM-1, an aurora/Ipl1-related kinase from rat. *J Biochem* 2000; 128(6): 903-7.
- [148] Kawajiri A, Yasui Y, Goto H, Tatsuka M, Takahashi M, Nagata K, *et al.* Functional significance of the specific sites phosphorylated in desmin at cleavage furrow: Aurora-B may phosphorylate and regulate type III intermediate filaments during cytokinesis coordinately with Rho-kinase. *Mol Biol Cell* 2003; 14(4): 1489-500.
- [149] Norden C, Mendoza M, Dobbelaere J, Kotwaliwale CV, Biggins S, Barral Y. The NoCut pathway links completion of cytokinesis to

- spindle midzone function to prevent chromosome breakage. *Cell* 2006; 125(1): 85-98.
- [150] Marumoto T, Zhang D, Saya H. Aurora-A - A guardian of poles. *Nat Rev Cancer* 2005; 5(1): 42-50.
- [151] Bischoff JR, Anderson L, Zhu Y, Mossie K, Ng L, Souza B, et al. A homologue of *Drosophila* aurora kinase is oncogenic and amplified in human colorectal cancers. *EMBO J* 1998; 17(11): 3052-65.
- [152] Sen S, Zhou H, White RA. A putative serine/threonine kinase encoding gene BTAK on chromosome 20q13 is amplified and overexpressed in human breast cancer cell lines. *Oncogene* 1997; 14(18): 2195-200.
- [153] Sen S, Zhou H, Zhang RD, Yoon DS, Vakar-Lopez F, Ito S, et al. Amplification/overexpression of a mitotic kinase gene in human bladder cancer. *J Natl Cancer Inst* 2002; 94(17): 1320-9.
- [154] Bodvarsdottir SK, Hilmarsdottir H, Birgisdottir V, Steinarsdottir M, Jonasson JG, Eyfjord JE. Aurora-A amplification associated with BRCA2 mutation in breast tumours. *Cancer Lett* 2007; 248(1): 96-102.
- [155] Gritsko TM, Coppola D, Paciga JE, Yang L, Sun M, Shelley SA, et al. Activation and overexpression of centrosome kinase BTAK/Aurora-A in human ovarian cancer. *Clin Cancer Res* 2003; 9(4): 1420-6.
- [156] Hienonen T, Salovaara R, Mecklin JP, Järvinen H, Karhu A, Aaltonen LA. Preferential amplification of AURKA 91A (Ile31) in familial colorectal cancers. *Int J Cancer* 2006; 118(2): 505-8.
- [157] Jeng YM, Peng SY, Lin CY, Hsu HC. Overexpression and amplification of Aurora-A in hepatocellular carcinoma. *Clin Cancer Res* 2004; 10(6): 2065-71.
- [158] Kurahashi T, Miyake H, Hara I, Fujisawa M. Significance of Aurora-A expression in renal cell carcinoma. *Urol Oncol* 2007; 25(2): 128-33.
- [159] Kurai M, Shiozawa T, Shih HC, Miyamoto T, Feng YZ, Kashima H, et al. Expression of Aurora kinases A and B in normal, hyperplastic, and malignant human endometrium: Aurora B as a predictor for poor prognosis in endometrial carcinoma. *Hum Pathol* 2005; 36(12): 1281-8.
- [160] Li D, Zhu J, Firozi PF, Abbruzzese JL, Evans DB, Cleary K, et al. Overexpression of oncogenic STK15/BTAK/Aurora A kinase in human pancreatic cancer. *Clin Cancer Res* 2003; 9(3): 991-7.
- [161] Miyoshi Y, Iwao K, Egawa C, Noguchi S. Association of centrosomal kinase STK15/BTAK mRNA expression with chromosomal instability in human breast cancers. *Int J Cancer* 2001; 92(3): 370-3.
- [162] Yang SB, Zhou XB, Zhu HX, Quan LP, Bai JF, He J, et al. Amplification and overexpression of Aurora-A in esophageal squamous cell carcinoma. *Oncol Rep* 2007; 17(5): 1083-8.
- [163] Klein A, Reichardt W, Jung V, Zang KD, Meese E, Urbschat S. Overexpression and amplification of STK15 in human gliomas. *Int J Oncol* 2004; 25(6): 1789-94.
- [164] Reichardt W, Jung V, Brunner C, Klein A, Wemmer S, Romeike BF, et al. The putative serine/threonine kinase gene STK15 on chromosome 20q13.2 is amplified in human gliomas. *Oncol Rep* 2003; 10(5): 1275-9.
- [165] Moreno-Bueno G, Sánchez-Estévez C, Cassia R, Rodríguez-Perales S, Díaz-Uriarte R, Domínguez O, et al. Differential gene expression profile in endometrioid and nonendometrioid endometrial carcinoma: STK15 is frequently overexpressed and amplified in nonendometrioid carcinomas. *Cancer Res* 2003; 63(18): 5697-702.
- [166] Tanaka T, Kimura M, Matsunaga K, Fukada D, Mori H, Okano Y. Centrosomal kinase AIK1 is overexpressed in invasive ductal carcinoma of the breast. *Cancer Res* 1999; 59(9): 2041-4.
- [167] Baba Y, Noshio K, Shima K, Irahara N, Kure S, Toyoda S, et al. Aurora-A expression is independently associated with chromosomal instability in colorectal cancer. *Neoplasia* 2009; 11(5): 418-25.
- [168] Fraizer GC, Diaz MF, Lee IL, Grossman HB, Sen S. Aurora-A/STK15/BTAK enhances chromosomal instability in bladder cancer cells. *Int J Oncol* 2004; 25(6): 1631-9.
- [169] Hoque A, Carter J, Xia W, Hung MC, Sahin AA, Sen S, et al. Loss of aurora A/STK15/BTAK overexpression correlates with transition of *in situ* to invasive ductal carcinoma of the breast. *Cancer Epidemiol Biomarkers Prev* 2003; 12(12): 1518-22.
- [170] Kimura MT, Mori T, Conroy J, Nowak NJ, Satomi S, Tamai K, et al. Two functional coding single nucleotide polymorphisms in STK15 (Aurora-A) coordinately increase esophageal cancer risk. *Cancer Res* 2005; 65(9): 3548-54.
- [171] Nishida N, Nagasaka T, Kashiwagi K, Boland CR, Goel A. High copy amplification of the Aurora-A gene is associated with chromosomal instability phenotype in human colorectal cancers. *Cancer Biol Ther* 2007; 6(4): 525-33.
- [172] Reiter R, Gais P, Jütting U, Steuer-Vogt MK, Pickhard A, Bink K, et al. Aurora kinase A messenger RNA overexpression is correlated with tumor progression and shortened survival in head and neck squamous cell carcinoma. *Clin Cancer Res* 2006; 12(17): 5136-41.
- [173] Tatsuka M, Sato S, Kitajima S, Suto S, Kawai H, Miyauchi M, et al. Overexpression of Aurora-A potentiates HRAS-mediated oncogenic transformation and is implicated in oral carcinogenesis. *Oncogene* 2005; 24(6): 1122-7.
- [174] Tong T, Zhong Y, Kong J, Dong L, Song Y, Fu M, et al. Overexpression of Aurora-A contributes to malignant development of human esophageal squamous cell carcinoma. *Clin Cancer Res* 2004; 10(21): 7304-10.
- [175] Torchia EC, Chen Y, Sheng H, Katayama H, Fitzpatrick J, Brinkley WR, et al. A genetic variant of Aurora kinase A promotes genomic instability leading to highly malignant skin tumors. *Cancer Res* 2009; 69(18): 7207-15.
- [176] Compérat E, Camparo P, Haus R, Chartier-Kastler E, Radenen B, Richard F, et al. Aurora-A/STK-15 is a predictive factor for recurrent behaviour in non-invasive bladder carcinoma: A study of 128 cases of non-invasive neoplasms. *Virchows Arch* 2007; 450(4): 419-24.
- [177] Guan Z, Wang XR, Zhu XF, Huang XF, Xu J, Wang LH, et al. Aurora-A, a negative prognostic marker, increases migration and decreases radiosensitivity in cancer cells. *Cancer Res* 2007; 67(21): 10436-44.
- [178] Lassmann S, Shen Y, Jütting U, Wiehle P, Walch A, Gitsch G, et al. Predictive value of Aurora-A/STK15 expression for late stage epithelial ovarian cancer patients treated by adjuvant chemotherapy. *Clin Cancer Res* 2007; 13(14): 4083-91.
- [179] Ogawa E, Takenaka K, Katakura H, Adachi M, Otake Y, Toda Y, et al. Perimembrane Aurora-A expression is a significant prognostic factor in correlation with proliferative activity in non-small-cell lung cancer (NSCLC). *Ann Surg Oncol* 2008; 15(2): 547-54.
- [180] Royce ME, Xia W, Sahin AA, Katayama H, Johnston DA, Hortobagyi G, et al. STK15/Aurora-A expression in primary breast tumors is correlated with nuclear grade but not with prognosis. *Cancer* 2004; 100(1): 12-9.
- [181] Sakakura C, Hagiwara A, Yasuoka R, Fujita Y, Nakanishi M, Masuda K, et al. Tumour-amplified kinase BTAK is amplified and overexpressed in gastric cancers with possible involvement in aneuploid formation. *Br J Cancer* 2001; 84(6): 824-31.
- [182] Xu HT, Ma L, Qi FJ, Liu Y, Yu JH, Dai SD, et al. Expression of serine threonine kinase 15 is associated with poor differentiation in lung squamous cell carcinoma and adenocarcinoma. *Pathol Int* 2006; 56(7): 375-80.
- [183] Landen CN Jr, Lin YG, Immaneni A, Deavers MT, Merritt WM, Spannuth WA, et al. Overexpression of the centrosomal protein Aurora-A kinase is associated with poor prognosis in epithelial ovarian cancer patients. *Clin Cancer Res* 2007; 13(14): 4098-104.
- [184] Shang X, Burlingame SM, Okcu MF, Ge N, Russell HV, Egler RA, et al. Aurora A is a negative prognostic factor and a new therapeutic target in human neuroblastoma. *Mol Cancer Ther* 2009; 8(8): 2461-9.
- [185] Ewart-Toland A, Briassouli P, de Koning JP, Mao JH, Yuan J, Chan F, et al. Identification of Stk6/STK15 as a candidate low-penetrance tumor-susceptibility gene in mouse and human. *Nat Genet* 2003; 34(4): 403-12.
- [186] Ewart-Toland A, Dai Q, Gao YT, Nagase H, Dunlop MG, Farrington SM, et al. Aurora-A/STK15 T+91A is a general low penetrance cancer susceptibility gene: a meta-analysis of multiple cancer types. *Carcinogenesis* 2005; 26(8): 1368-73.
- [187] Chen YJ, Chen CM, Twu NF, Yen MS, Lai CR, Wu HH, et al. Overexpression of Aurora B is associated with poor prognosis in epithelial ovarian cancer patients. *Virchows Arch* 2009; 455(5): 431-40.
- [188] Cox DG, Hankinson SE, Hunter DJ. Polymorphisms of the AURKA (STK15/Aurora Kinase) gene and breast cancer risk (United States). *Cancer Causes Control* 2006; 17(1): 81-3.

- [189] Lo YL, Yu JC, Chen ST, Yang HC, Fann CS, Mau YC, *et al.* Breast cancer risk associated with genotypic polymorphism of the mitosis-regulating gene Aurora-A/STK15/BTAK. *Int J Cancer* 2005; 115(2): 276-83.
- [190] Tchatchou S, Wirtenberger M, Hemminki K, Sutter C, Meindl A, Wappenschmidt B, *et al.* Aurora kinases A and B and familial breast cancer risk. *Cancer Lett* 2007; 247(2): 266-72.
- [191] Gu J, Gong Y, Huang M, Lu C, Spitz MR, Wu X. Polymorphisms of STK15 (Aurora-A) gene and lung cancer risk in Caucasians. *Carcinogenesis* 2007; 28(2): 350-5.
- [192] Ju H, Cho H, Kim YS, Kim WH, Ihm C, Noh SM, *et al.* Functional polymorphism 57Val>Ile of aurora kinase A associated with increased risk of gastric cancer progression. *Cancer Lett* 2006; 242(2): 273-9.
- [193] Vidarsdottir L, Bodvarsdottir SK, Hilmarsdottir H, Tryggvadottir L, Eyfjord JE. Breast cancer risk associated with AURKA 91T -->A polymorphism in relation to BRCA mutations. *Cancer Lett* 2007; 250(2): 206-12.
- [194] Fukuda T, Mishina Y, Walker MP, DiAugustine RP. Conditional transgenic system for mouse aurora kinase: Degradation by the ubiquitin proteasome pathway controls the level of the transgenic protein. *Mol Cell Biol* 2005; 25(12): 5270-81.
- [195] Zhang D, Hirota T, Marumoto T, Shimizu M, Kunitoku N, Sasayama T, *et al.* Cre-loxP-controlled periodic Aurora-A overexpression induces mitotic abnormalities and hyperplasia in mammary glands of mouse models. *Oncogene* 2004; 23(54): 8720-30.
- [196] Ota T, Suto S, Katayama H, Han ZB, Suzuki F, Maeda M, *et al.* Increased mitotic phosphorylation of histone H3 attributable to AIM-1/Aurora-B overexpression contributes to chromosome number instability. *Cancer Res* 2002; 62(18): 5168-77.
- [197] Kanda A, Kawai H, Suto S, Kitajima S, Sato S, Takata T, *et al.* Aurora-B/AIM-1 kinase activity is involved in Ras-mediated cell transformation. *Oncogene* 2005; 24(49): 7266-72.
- [198] Zeng WF, Navaratne K, Prayson RA, Weil RJ. Aurora B expression correlates with aggressive behaviour in glioblastoma multiforme. *J Clin Pathol* 2007; 60(2): 218-21.
- [199] Smith SL, Bowers NL, Betticher DC, Gautschi O, Ratschiller D, Hoban PR, *et al.* Overexpression of aurora B kinase (AURKB) in primary non-small cell lung carcinoma is frequent, generally driven from one allele, and correlates with the level of genetic instability. *Br J Cancer* 2005; 93(6): 719-29.
- [200] Vischioni B, Oudejans JJ, Vos W, Rodriguez JA, Giaccone G. Frequent overexpression of aurora B kinase, a novel drug target, in non-small cell lung carcinoma patients. *Mol Cancer Ther* 2006; 5(11): 2905-13.
- [201] López-Ríos F, Chuai S, Flores R, Shimizu S, Ohno T, Wakahara K, *et al.* Global gene expression profiling of pleural mesotheliomas: Overexpression of aurora kinases and P16/CDKN2A deletion as prognostic factors and critical evaluation of microarray-based prognostic prediction. *Cancer Res* 2006; 66(6): 2970-9.
- [202] Araki K, Nozaki K, Ueba T, Tatsuka M, Hashimoto N. High expression of Aurora-B/Aurora and Ipl1-like midbody-associated protein (AIM-1) in astrocytomas. *J Neurooncol* 2004; 67(1-2): 53-64.
- [203] Qi G, Ogawa I, Kudo Y, Miyachi M, Siriwardena BS, Shimamoto F, *et al.* Aurora-B expression and its correlation with cell proliferation and metastasis in oral cancer. *Virchows Arch* 2007; 450(3): 297-302.
- [204] Sistayanarain A, Tsuneyama K, Zheng H, Takahashi H, Nomoto K, Cheng C, *et al.* Expression of Aurora-B kinase and phosphorylated histone H3 in hepatocellular carcinoma. *Anticancer Res* 2006; 26(5A): 3585-93.
- [205] Tanaka S, Arai S, Yasen M, Mogushi K, Su NT, Zhao C, *et al.* Aurora kinase B is a predictive factor for the aggressive recurrence of hepatocellular carcinoma after curative hepatectomy. *Br J Surg* 2008; 95(5): 611-9.
- [206] Yasen M, Mizushima H, Mogushi K, Obulhasim G, Miyaguchi K, Inoue K, *et al.* Expression of Aurora B and alternative variant forms in hepatocellular carcinoma and adjacent tissue. *Cancer Sci* 2009; 100(3): 472-80.
- [207] Chieffi P, Troncone G, Caleo A, Libertini S, Linardopoulos S, Tramontano D, *et al.* Aurora B expression in normal testis and seminomas. *J Endocrinol* 2004; 181(2): 263-70.
- [208] Esposito F, Libertini S, Franco R, Abagnale A, Marra L, Portella G, *et al.* Aurora B expression in post-puberal testicular germ cell tumours. *J Cell Physiol* 2009; 221(2): 435-9.
- [209] Sorrentino R, Libertini S, Pallante PL, Troncone G, Palombini L, Bavetsias V, *et al.* Aurora B overexpression associates with the thyroid carcinoma undifferentiated phenotype and is required for thyroid carcinoma cell proliferation. *J Clin Endocrinol Metab* 2005; 90(2): 928-35.
- [210] Tatsuka M, Katayama H, Ota T, Tanaka T, Odashima S, Suzuki F, *et al.* Multinuclearity and increased ploidy caused by overexpression of the aurora- and Ipl1-like midbody-associated protein mitotic kinase in human cancer cells. *Cancer Res* 1998; 58(21): 4811-6.
- [211] Chieffi P, Cozzolino L, Kisslinger A, Libertini S, Staibano S, Mansueto G, *et al.* Aurora B expression directly correlates with prostate cancer malignancy and influence prostate cell proliferation. *Prostate* 2006; 66(3): 326-33.
- [212] Hauf S, Cole RW, LaTerra S, Zimmer C, Schnapp G, Walter R, *et al.* The small molecule Hesperadin reveals a role for Aurora B in correcting kinetochore-microtubule attachment and in maintaining the spindle assembly checkpoint. *J Cell Biol* 2003; 161(2): 281-94.
- [213] Wilkinson RW, Odedra R, Heaton SP, Wedge SR, Keen NJ, Crafter C, *et al.* AZD1152, a selective inhibitor of Aurora B kinase, inhibits human tumor xenograft growth by inducing apoptosis. *Clin Cancer Res* 2007; 13(12): 3682-8.
- [214] Zhao X, Li FC, Li YH, Fu WN, Huang DF, Ye Y, *et al.* Mutation of p53 and overexpression of STK15 in laryngeal squamous-cell carcinoma. *Zhonghua Zhong Liu Za Zhi* 2005; 27: 134-7.
- [215] Li FC, Li YH, Zhao X, Kang N, Fu WN, Xu ZM, *et al.* Deletion of p15 and p16 genes and overexpression of STK15 gene in human laryngeal squamous cell carcinoma. *Zhonghua Yi Xue Za Zhi* 2003; 83: 316-9.
- [216] Neben K, Korshunov A, Benner A, Wrobel G, Hahn M, Kokocinski F, *et al.* Microarray-based screening for molecular markers in medulloblastoma revealed STK15 as independent predictor for survival. *Cancer Res* 2004; 64: 3103-11.
- [217] Chen J, Sen S, Amos CI, Wei C, Jones JS, Lynch P, *et al.* Association between Aurora-A kinase polymorphisms and age of onset of hereditary nonpolyposis colorectal cancer in a Caucasian population. *Mol Carcinog* 2007; 46: 249-56.
- [218] Coumar MS, Cheung CH, Chang JY, Hsieh HP. Advances in Aurora kinase inhibitor patents. *Expert Opin Ther Pat* 2009; 19(3): 321-56.
- [219] Cheung CH, Coumar MS, Hsieh HP, Chang JY. Aurora kinase inhibitors in preclinical and clinical testing. *Expert Opin Investig Drugs* 2009; 18(4): 379-98.
- [220] Tomita M, Tanaka Y, Mori N. Aurora kinase inhibitor AZD1152 negatively affects the growth and survival of HTLV-1-infected T lymphocytes *in vitro*. *Int J Cancer* 2010 [Epub ahead of print].
- [221] Tomita M, Mori N. Aurora A selective inhibitor MLN8237 suppresses the growth and survival of HTLV-1-infected T-cells *in vitro*. *Cancer Sci* 2010 [Epub ahead of print].
- [222] Hoar K, Chakravarty A, Rabino C, Wyson D, Bowman D, Roy N, *et al.* MLN8054, a small-molecule inhibitor of Aurora A, causes spindle pole and chromosome congression defects leading to aneuploidy. *Mol Cell Biol* 2007; 27(12): 4513-25.
- [223] Manfredi MG, Ecsedy JA, Meetze KA, Balani SK, Burenkova O, Chen W, *et al.* Antitumor activity of MLN8054, an orally active small-molecule inhibitor of Aurora A kinase. *Proc Natl Acad Sci USA* 2007; 104(10): 4106-11.
- [224] Gautschi O, Heighway J, Mack PC, Purnell PR, Lara PN Jr, Gandara DR. Aurora kinases as anticancer drug targets. *Clin Cancer Res* 2008; 14(6): 1639-48.
- [225] Carvajal RD, Tse A, Schwartz GK. Aurora kinases: New targets for cancer therapy. *Clin Cancer Res* 2006; 12(23): 6869-75.
- [226] Tyler RK, Shpiro N, Marquez R, Eyers PA. VX-680 inhibits Aurora A and Aurora B kinase activity in human cells. *Cell Cycle* 2007; 6(22): 2846-54.
- [227] Soncini C, Carpinelli P, Gianellini L, Fancelli D, Vianello P, Rusconi L, *et al.* PHA-680632, a novel Aurora kinase inhibitor with potent antitumoral activity. *Clin Cancer Res* 2006; 12(13): 4080-9.
- [228] Carpinelli P, Ceruti R, Giorgini ML, Cappella P, Gianellini L, Croci V, *et al.* PHA-739358, a potent inhibitor of Aurora kinases with a selective target inhibition profile relevant to cancer. *Mol Cancer Ther* 2007; 6(12 Pt 1): 3158-68.

- [229] D'Alise AM, Amabile G, Iovino M, Di Giorgio FP, Bartiromo M, Sessa F, *et al.* Reversine, a novel Aurora kinases inhibitor, inhibits colony formation of human acute myeloid leukemia cells. *Mol Cancer Ther* 2008; 7(5): 1140-9.
- [230] Sessa F, Mapelli M, Ciferri C, Tarricone C, Areces LB, Schneider TR, *et al.* Mechanism of Aurora B activation by INCENP and inhibition by hesperadin. *Mol Cell* 2005; 18(3): 379-91.
- [231] Li M, Jung A, Ganswindt U, Marini P, Friedl A, Daniel PT, *et al.* Aurora kinase inhibitor ZM447439 induces apoptosis via mitochondrial pathways. *Biochem Pharmacol* 2010; 79(2): 122-9.
- [232] Harrington EA, Bebbington D, Moore J, Rasmussen RK, Ajose-Adeogun AO, Nakayama T, *et al.* VX-680, a potent and selective small-molecule inhibitor of the Aurora kinases, suppresses tumor growth *in vivo*. *Nat Med* 2004; 10(3): 262-7.
- [233] Gizatullin F, Yao Y, Kung V, Harding MW, Loda M, Shapiro GI. The Aurora kinase inhibitor VX-680 induces endoreduplication and apoptosis preferentially in cells with compromised p53-dependent postmitotic checkpoint function. *Cancer Res* 2006; 66(15): 7668-77.
- [234] Negri JM, McMillin DW, Delmore J, Mitsiades N, Hayden P, Klippel S, *et al.* *In vitro* anti-myeloma activity of the Aurora kinase inhibitor VE-465. *Br J Haematol* 2009; 147(5): 672-6.
- [235] Tao Y, Zhang P, Frascogna V, Lecluse Y, Auperin A, Bourhis J, *et al.* Enhancement of radiation response by inhibition of Aurora-A kinase using siRNA or a selective Aurora kinase inhibitor PHA680632 in p53-deficient cancer cells. *Br J Cancer* 2007; 97(12): 1664-72.
- [236] Chen S, Zhang Q, Wu X, Schultz PG, Ding S. Dedifferentiation of lineage-committed cells by a small molecule. *J Am Chem Soc* 2004; 126(2): 410-411.
- [237] Griffiths G, Scaerou F, Midgley C, McClue S, Tosh C, Jackson W, *et al.* Anti-tumor activity of CYC116, a novel small molecule inhibition of Aurora kinases and VEGFR2. AACR Annual Meeting. San Francisco, CA, USA 12-16 April 2008.
- [238] Hajduch M, Vydra D, Dzubak P, Dziechciarkova M, Stuart I, Zheleva D. *In vivo* mode of action of CYC116, a novel small molecule inhibitor of Aurora kinases and VEGFR2. AACR Annual Meeting. San Francisco, CA, USA 12-16 April 2008.
- [239] MacCallum D, Green, S. Combined anticancer pyrimidine-thiazole aurora kinase inhibitors. WO2007132221 (2007)
- [240] MacCallum D, Melville J, Watt K, Green SR. Combination studies with the oral Aurora kinase inhibitor CYC116 and chemotherapeutic agents. AACR Annual Meeting. San Francisco, CA, USA 12-16 April 2008.
- [241] Fernandez E, Hardy A, Orrell D, Ramsell L, Fell D, Chassagnole C. Optimal cancer chronotherapeutic schedules of Seliciclib revealed by a system biology approach. ACCR Annual Meeting. San Francisco, CA, USA 12-16 April 2008.
- [242] Chassagnole C, Fernandez E, Scaerou F, Snell C, Zheleva D, Glover D, *et al.* System biology analysis of CYC116, a novel aurora kinase inhibitor. AACR Annual Meeting. San Francisco, CA, USA 12-16 April 2008.
- [243] NCT00560716. A Phase I pharmacologic study of CYC116, an oral aurora kinase inhibitor, in patients with advanced solid tumors. 16 November 2007. Available from: www.ClinicalTrials.gov (Accessed on: Aug 1, 2008).
- [244] NCT00530465. CYC116 in treating patients with advanced solid tumors. 23 May 2008. Available from: www.ClinicalTrials.gov (Accessed on: Aug 1, 2008).
- [245] Oslob JD, Romanowski MJ, Allen DA, Baskaran S, Bui M, Elling RA, *et al.* Discovery of a potent and selective Aurora kinase inhibitor. *Bioorg Med Chem Lett* 2008; 18(17): 4880-4.
- [246] Gamo K, Belmont B, Tangonan B. SNS-314, a novel small-molecule Aurora kinase inhibitor, induces cell-cycle defects and potently suppresses tumor growth. AACR Annual Meeting. San Francisco, CA, USA 12-16 April 2008.
- [247] Evanchik M, Hogan J, Arbitrario J, Kumer J, Hoch U, Howlett A, *et al.* SNS-314, a potent inhibitor of aurora kinases, has preclinical anti-tumour activity and induces apoptosis. AACR Annual Meeting. San Francisco, CA, USA 12-16 April 2008.
- [248] Hogan J, Kumer J, Arbitrario J. SNS-314, a potent inhibitor of aurora kinases, shows broad anti-tumor activity and dosing flexibility *in vivo*. AACR Annual Meeting. San Francisco, CA, USA 12-16 April 2008.
- [249] Robert F, Verschraegen C, Hurwitz H, Uronis H, Advani R, Chen A, *et al.* Phase 1 trial of SNS-314, a novel selective inhibitor of aurora kinases A, B, and C, in advanced solid tumor patients. ASCO Annual Meeting. Chicago, IL, USA 30 May-3 June 2008.
- [250] NCT00519662. Safety and tolerability study of SNS-314 for advanced solid tumors. 12 June 2008. Available from: www.ClinicalTrials.gov (Accessed on: Jun 12, 2008).
- [251] Bhattacharya S, Wishka D, Luzzio M, Arcari J, Bernardo V, Briere D, *et al.* SAR and chemistry of Aurora kinase inhibitors: discovery of PF-3814735, an oral clinical candidate. AACR Annual Meeting. San Francisco, CA, USA 12-16 April 2008.
- [252] Jani J, Jakubczak J, Arcari J, Bernardo V, Bhattacharya S, Boyden T, *et al.* Identification and characterization of PF-03814735, an oral aurora inhibitor for cancer therapy. AACR Annual Meeting. San Francisco, CA, USA 12-16 April 2008.
- [253] Jones SF, Burris HA, Dumez H, Infante JR, Fowst C, Gerletti P, *et al.* Phase I accelerated dose-escalation, pharmacokinetic (PK) and pharmacodynamic study of PF-03814735, an oral aurora kinase inhibitor, in patients with advanced solid tumors: preliminary results. ASCO Annual Meeting. Chicago, IL, USA 30 May-3 June 2008.
- [254] Bray MR. ENMD-981693: An oral, aurora kinase-angiogenesis inhibitor. Drug Discovery and Development of Innovative Therapeutics. Boston, MA, USA 6-9 August 2007.
- [255] Bray MR. ENMD-2076, an oral Aurora A and angiogenesis kinase inhibitor. AACR Annual Meeting. San Francisco, CA, USA 12-16 April 2008.
- [256] NCT00658671. A dose-escalation study of ENMD-2076; administered orally to patients with advanced cancer. 9 July 2008. Available from: www.ClinicalTrials.gov (Accessed on: Aug 1, 2008).
- [257] Howard S, Berdini V, Boulstridge JA, Carr MG, Cross DM, Curry J, *et al.* Fragment-based discovery of the pyrazol-4-yl urea (AT9283), a multitargeted kinase inhibitor with potent aurora kinase activity. *J Med Chem* 2009; 52(2): 379-88.
- [258] Tanaka R, Squires MS, Kimura S, Yokota A, Mallett K, Smyth T, *et al.* Activity of the multi-targeted kinase inhibitor, AT9283 on Imatinib-resistant CML models. ASH Annual Meeting. San Francisco, CA, USA 12-16 April 2008.
- [259] NCT00443976. Aurora kinase inhibitor AT9283 in treating patients with advanced or metastatic solid tumors or non-Hodgkin's lymphoma. 23 July 2008. Available from: www.ClinicalTrials.gov (Accessed on: Dec 30, 2008).
- [260] NCT00522990. Study to assess the safety of escalating doses of AT9283, in Patients with leukemias. 23 April 2008. Available from: www.ClinicalTrials.gov (Accessed on: Dec 30, 2008).
- [261] Plummer ER, Calvert H, Arkenau H. A dose-escalation and pharmacodynamic study of AT9283 in patients with refractory solid tumours. *J Clin Oncol (Meeting Abstracts)* 2008; 26(15 Suppl): 2519.
- [262] Aissat N, Serova M, Ghoul A, Le Tourneau C, Romanelli A, Gianella-Boradorri A, *et al.* Cellular and molecular mechanisms of action of AS703569, a novel aurora kinase inhibitor, in human cancer cell lines. AACR-NCI-EORTC International Conference. San Francisco, CA, USA 22-26 October 2007.
- [263] Serova M, Aissat N, Ghoul A, Le Tourneau C, Romanelli A, Gianella-Boradorri A, *et al.* AS703569, a novel aurora kinase inhibitor, enhances the antiproliferative effects of other targeted therapies in human cancer cell lines. AACR-NCI-EORTC International Conference. San Francisco, CA, USA 22-26 October 2007.
- [264] Renshaw JS, Patnaik A, Gordon M, Beeram M, Fischer D, Gianella-Boradorri A, *et al.* A phase I two arm trial of AS703569 (R763), an orally available aurora kinase inhibitor, in subjects with solid tumors: preliminary results. ASCO Annual Meeting. Chicago, IL, USA 30 May-3 June 2007.
- [265] NCT00543387. Treatment of patients with advanced and/or refractory solid tumors. 5 November 2008. Available from: www.ClinicalTrials.gov (Accessed on: Aug 1, 2008).
- [266] Adachi M, Suzuki Y, Mizuta T, Osawa T, Adachi T, Osaka K, *et al.* The Japanese apricot *Prunus mume* Sieb. et Zucc. (*ume*) is a rich natural source of novel anti-cancer substance. *Int J Food Prop* 2007; 10: 375-84.
- [267] Nakagawa A, Sawada T, Okada T, Ohsawa T, Adachi M, Kubota K. New antineoplastic agent, MK615, from UME (a Variety of) Japanese apricot inhibits growth of breast cancer cells *in vitro*. *Breast J* 2007; 13: 44-9.

- [268] Okada T, Sawada T, Osawa T, Adachi M, Kubota K. A novel anti-cancer substance, MK615, from ume, a variety of Japanese apricot, inhibits growth of hepatocellular carcinoma cells by suppressing Aurora A kinase activity. *Hepatogastroenterology* 2007; 54: 1770-4.
- [269] Mori S, Sawada T, Okada T, Ohsawa T, Adachi M, Keiichi K. New anti-proliferative agent, MK615, from Japanese apricot "Prunus mume" induces striking autophagy in colon cancer cells *in vitro*. *World J Gastroenterol* 2007; 13: 6512-7.
- [270] Marumoto T, Hirota T, Morisaki T, Kunitoku N, Zhang D, Ichikawa Y, *et al.* Roles of aurora-A kinase in mitotic entry and G2 checkpoint in mammalian cells. *Genes Cells* 2002; 7: 1173-82.
- [271] Vogel C, Hager C, Bastians H. Mechanisms of mitotic cell death induced by chemotherapy-mediated G2 checkpoint abrogation. *Cancer Res* 2007; 67: 339-45.
- [272] Okada T, Sawada T, Osawa T, Adachi M, Kubota K. MK615 inhibits pancreatic cancer cell growth by dual inhibition of Aurora A and B kinases. *World J Gastroenterol* 2008; 14(9): 1378-82.
- [273] Anderson K, Lai Z, McDonald OB, Stuart JD, Nartey EN, Hardwicke MA, *et al.* Biochemical characterization of GSK-1070916, a potent and selective inhibitor of Aurora B and Aurora C kinases with an extremely long residence time. *Biochem J* 2009; 420(2): 259-65.
- [274] Walsby E, Walsh V, Pepper C, Burnett A, Mills K. Effects of the aurora kinase inhibitors AZD1152-HQPA and ZM447439 on growth arrest and polyploidy in acute myeloid leukemia cell lines and primary blasts. *Haematologica* 2008; 93(5): 662-9.
- [275] Evans RP, Naber C, Steffler T, Checkland T, Maxwell CA, Keats JJ, *et al.* The selective Aurora B kinase inhibitor AZD1152 is a potential new treatment for multiple myeloma. *Br J Haematol* 2008; 140(3): 295-302.
- [276] Tao Y, Leteur C, Calderaro J, Girdler F, Zhang P, Frascogna V, *et al.* The aurora B kinase inhibitor AZD1152 sensitizes cancer cells to fractionated irradiation and induces mitotic catastrophe. *Cell Cycle* 2009; 8(19): 3172-81.
- [277] Tao Y, Zhang P, Girdler F, Frascogna V, Castedo M, Bourhis J, *et al.* Enhancement of radiation response in p53-deficient cancer cells by the Aurora-B kinase inhibitor AZD1152. *Oncogene* 2008; 27(23): 3244-55.
- [278] Hardwicke MA, Oleykowski CA, Plant R, Wang J, Liao Q, Moss K, *et al.* GSK1070916, a potent Aurora B/C kinase inhibitor with broad antitumor activity in tissue culture cells and human tumor xenograft models. *Mol Cancer Ther* 2009; 8(7): 1808-17.
- [279] Wang X, Cheung HW, Chun AC, Jin DY, Wong YC. Mitotic checkpoint defects in human cancers and their implications to chemotherapy. *Front Biosci* 2008; 13: 2103-14.
- [280] Cheetham, G., Knegtel, R., Swenson, L., Coll, J. T., Renwick, S., Weber, P. Crystal structure of Aurora-2 protein and binding pockets thereof. WO03092607 (2003).
- [281] Binch, H., Mortimore, M., Fraysse, D., Rutherford, A. Aminopyrimidines useful as kinase inhibitors. WO2007056163 (2007).
- [282] Binch, H., Mortimore, M., Fraysse, D., Davis, C., O'Donnell, M., Everitt, S., Robinson, D., Pinder, J., Miller, A. Aminopyrimidines useful as kinase inhibitors. WO2007056164 (2007).
- [283] Claiborne, C., Sells, T., Stroud, S. Pyridobenzazepine compounds and methods for inhibiting mitotic progression. WO2008021038 (2008).
- [284] Bearss, D., Grand, C., Liu, X., Vankayalapati, H. Protein kinase inhibitors. WO2008055233 (2008).
- [285] Curry, J., Gallagher, N.J., Lyons, J.F., Thompson, N.T. Pharmaceutical combinations. WO2008001115 (2008).
- [286] Bossenmaier, B., Engh, R., Georges, G., Hoffmann, E., Koerner, M., Voelger, H. Tricyclic lactam derivatives, their manufacture and use as pharmaceutical agents. WO2008022747 (2008).
- [287] Gascoigne KE, Taylor SS. How do anti-mitotic drugs kill cancer cells? *J Cell Sci* 2009; 122(Pt 15): 2579-85.
- [288] Gascoigne KE, Taylor SS. Cancer cells display profound intra- and interline variation following prolonged exposure to antimitotic drugs. *Cancer Cell* 2008; 14(2): 111-22.
- [289] Wan XB, Fan XJ, Chen MY, Xu J, Long ZJ, Hua YJ, *et al.* Inhibition of Aurora-A results in increased cell death in 3-dimensional culture microenvironment, reduced migration and is associated with enhanced radiosensitivity in human nasopharyngeal carcinoma. *Cancer Biol Ther* 2009; 8(15): 1500-6.
- [290] Olsen CC, Schefter TE, Chen H, Kane M, Leong S, McCarter MD, *et al.* Results of a phase I trial of 12 patients with locally advanced pancreatic carcinoma combining gefitinib, paclitaxel, and 3-dimensional conformal radiation: report of toxicity and evaluation of circulating K-ras as a potential biomarker of response to therapy. *Am J Clin Oncol* 2009; 32(2): 115-21.

AZD1152 negatively affects the growth of anaplastic thyroid carcinoma cells and enhances the effects of oncolytic virus *dl922-947*

Silvana Libertini*, Antonella Abagnale, Carmela Passaro, Ginevra Botta, Sara Barbato, Paolo Chieffi¹ and Giuseppe Portella

Dipartimento di Biologia e Patologia Cellulare e Molecolare, Facoltà di Medicina e Chirurgia, Università di Napoli Federico II, Via S. Pansini 5, 80131 Napoli, Italy

¹Dipartimento di Medicina Sperimentale, II Università di Napoli, Via Costantinopoli 16, 80138 Napoli, Italy

(Correspondence should be addressed to G Portella; Email: portella@unina.it)

*S Libertini is now at The Beatson Institute for Cancer Research, Switchback Road, Bearsden, Glasgow G61 1BD, UK)

Abstract

Novel therapeutic approaches are required for the treatment of anaplastic thyroid carcinoma (ATC), an incurable disease resistant to current available therapies. Aurora B is an important mitotic kinase involved in chromosome segregation and cytokinesis. It is overexpressed in many cancers including ATC and represents a potential target for chemotherapy. The effects of AZD1152, a specific Aurora B kinase inhibitor, have been evaluated against ATC, showing G₂/M accumulation, polyploidy and subsequent cell death by mitotic catastrophe upon drug treatment. Only three administrations of AZD1152 significantly reduced the growth of ATC tumour xenografts. Oncolytic viruses in association with other forms of treatment have proven highly promising in preclinical and clinical reports. The oncolytic adenovirus *dl922-947* is active against ATC cells, and we have evaluated the effects of the association between AZD1152 and *dl922-947*. In cells treated with virus and drug, we report additive/synergistic killing effects. Interestingly, the phosphorylation of histone H3 (Ser10), the main Aurora B substrate, is inhibited by *dl922-947* in a dose-dependent manner, and completely abolished in association with AZD1152. The combined treatment significantly inhibited the growth of ATC tumour xenografts with respect to single treatments. Our data demonstrate that the Aurora B inhibitor AZD1152, alone or in combination with oncolytic virus *dl922-947*, could represent a novel therapeutic option for the treatment of ATC.

Endocrine-Related Cancer (2011) 18 129–141

Introduction

Anaplastic thyroid carcinoma (ATC) is one of the most aggressive human malignancies, responsible for up to 40% of mortality from thyroid cancer. Although multimodality treatments are successfully applied for well-differentiated thyroid carcinomas, ATC survival rates have not been improved for decades: after diagnosis, patients have a median survival time of 4–6 months (Smallridge *et al.* 2009). Development and evaluation of novel therapeutic strategies are, therefore, desperately required.

Several approaches of gene therapy have been studied for ATC, such as differentiating therapy to restore radioiodine uptake, suicide therapy and oncolytic viruses. The latter are viral mutants able to replicate selectively in, and destroy tumour cells. The most common approach to achieve selectivity is the deletion of viral genes whose product is necessary for replication in normal cells, but expendable in cancer cells (Mullen & Tanabe 2002).

dl922-947 is an oncolytic adenovirus, which bears a deletion of 24 bp in E1A-conserved region 2 (CR2)

(Heise *et al.* 2000). This region normally binds to, and inactivates, host cell Rb, thus causing the release of E2F, followed by S-phase entry and subsequent viral DNA replication. Lacking a functional E1A-CR2 region, *dl922-947* mutant is unable to trigger S-phase entry of quiescent normal cells, but can actively replicate in cells with an aberrant G₁-S checkpoint. This checkpoint is lost in almost all cancer cells, and several *in vitro* and *in vivo* studies demonstrate the efficacy of *dl922-947* in a range of cancer cell lines (Heise *et al.* 2000). Its killing activity exceeds that of adenovirus 5 wild type (Ad5wt) and of the first generation virus *dl1520* (Heise *et al.* 2000); a phase I trial of *dl922-947* in women with relapsed ovarian cancer is under way (Baird *et al.* 2008).

We have shown that *dl922-947* is active against ATC cell lines and tumour xenografts (Libertini *et al.* 2008). However, data accumulated so far suggest that the oncolytic activity of viruses, although impressive, requires assistance in order to reach full efficacy. Using viruses in association with other forms of treatment has proven highly promising in preclinical and clinical reports. The association of viruses with specific drugs, not only able to directly kill tumour cells but also to increase viral oncolytic activity, would represent a powerful therapeutic tool.

The mitotic serine–threonine kinase Aurora B is a chromosomal passenger protein (Keen & Taylor 2009). Together with INCENP, Borealin and survivin, it exerts essential functions during mitosis, such as modifying histones at the chromatin, correcting misattachments while at the centromere, and regulating cytokinesis at the central spindle and later midbody (Keen & Taylor 2009). Aurora B is over-expressed in several human cancers, and its expression directly correlates with malignancy (Katayama *et al.* 1999, Araki *et al.* 2004, Chieffi *et al.* 2004, 2006, Kurai *et al.* 2005, Smith *et al.* 2005, Sorrentino *et al.* 2005, López-Ríos *et al.* 2006, Vischioni *et al.* 2006, Qi *et al.* 2007, Tanaka *et al.* 2008). Upon Aurora B depletion or inhibition, the cells with intact checkpoint function arrest with 4N DNA content, while those with compromised p53-dependent pathway undergo endoreduplication and apoptosis (Keen & Taylor 2004).

Cells lacking a p53-mediated post-mitotic checkpoint are highly responsive to Aurora B inhibition, thus suggesting a wide therapeutic window between normal and tumour cells (Keen & Taylor 2004). In human ATC, alterations of the p53 tumour suppressor gene are a constant feature (Smallridge *et al.* 2009), and we have previously shown that Aurora B is overexpressed in ATC (Sorrentino *et al.* 2005). All these data indicate

that the treatment of ATC could benefit from the use of an Aurora B inhibitor.

It has been reported that the block in G₂/M phase improves viral entry and replication (Seidman *et al.* 2001); therefore, we have hypothesized that Aurora B inhibition could enhance the oncolytic effects of *dl922-947* adenovirus. We selected AZD1152 as an Aurora B inhibitor due to its high selectivity for Aurora B and its good solubility, which makes it appropriate for clinical use (Wilkinson *et al.* 2007). Recent studies showed that AZD1152 significantly reduces tumour growth in a panel of solid human cancer xenograft models (Wilkinson *et al.* 2007).

In this report, we show that AZD1152 is active against ATC cells, inducing cell death through mitotic catastrophe. We also demonstrate that the drug is able to enhance the anti-neoplastic effects of *dl922-947* oncolytic virus in both *in vitro* and *in vivo* models of ATC. Our data hint towards a mechanism of how AZD1152 and *dl922-947* can synergistically kill ATC cells.

Materials and methods

Cells, adenoviruses and drugs

Human ATC cell lines such as BHT101-5, Cal62, FRO and 8505C have been authenticated as shown previously (Schweppe *et al.* 2008). All ATC cell lines used have a non-functional *p53* gene: in BHT101-5 cells, a 251 Ile→Thr substitution has been reported, 8505C cells present an Arg→Gly in position 248, Cal62 cells are characterized by A161D mutation while FRO cells are p53 null (Schweppe *et al.* 2008).

dl922-947 has a 24-bp deletion in E1A-CR2 (Heise *et al.* 2000). AdGFP is a non-replicating E1-deleted adenovirus encoding green fluorescent protein (GFP; Libertini *et al.* 2007). Viral stocks were expanded, purified, stored and quantified as previously reported (Libertini *et al.* 2007).

AZD1152-HQPA was dissolved in DMSO to a final concentration of 10 mM and stored at –20 °C. AZD1152 was dissolved in 0.3 M Tris–HCl (pH 9) to a final concentration of 10 mg/ml, each mouse received 300 µl of suspension *i.p.*, *i.e.* 3 mg of prodrug, corresponding to 2.5 mg of active drug.

Viability assay

BHT101-5, Cal62, FRO and 8505C cell lines have been treated with a different range of drug concentrations since their sensitivity to AZD1152 treatment varies. Treated cells were fixed with 50% TCA and stained with 0.4% sulforhodamine B in 1% acetic

acid as already described (Libertini *et al.* 2008). The percentages of surviving cells after treatment were calculated by assuming that the number of surviving untreated cells is 100%.

FACS analysis

PH3 and cell cycle

Cells treated with AZD1152, virus or both were harvested by trypsinization, fixed in 70% cold ethanol and prepared as already described (Esposito *et al.* 2009) using antibodies anti-phospho-histone H3 (Ser10) and anti-histone H3 (Upstate, Biotechnology Inc, Waltham, MA, USA).

AdGFP infection

FRO cells were treated for 24 h with AZD1152 25 nM, washed and then infected with AdGFP (0, 25 or 50 pfu/cell). Forty-eight hours post infection, cells were trypsinized, washed, resuspended in 300 µl of PBS and analysed for the emission in FITC channel.

Samples were acquired with a CYAN flow cytometer (DAKO Corporation, San Jose, CA, USA) and analysed using SUMMIT software.

Micronuclei counting

Cells grown on cover slips and treated as described were fixed 15' in 3% paraformaldehyde, permeabilized with 0.2% Triton X-100 10' and then stained 5' with Hoechst 33258 (1 µg/ml, Sigma–Aldrich). The washes were followed by mounting the cover slips onto glass slides with glycerol:PBS 1:1.

Synchronization

Cells were treated for 12 h with thymidine (2 mM), released for 10 h in fresh media and retreated for further 12 h with thymidine. Cells were washed twice in fresh media, then treated and harvested as indicated.

Antibodies for western blot

Procaspase-3 (sc-56053; 1:100, Santa Cruz Biotechnology Inc, Santa Cruz, CA, USA), caspase-3 (ab13585, 1:500, Abcam, Cambridge, MA, USA), phospho-histone H3 (Ser10) (06570, 1:500, Upstate Biotechnology Inc, Waltham, MA, USA), histone H3 rabbit polyclonal IgG (31949; 1:1000, Upstate) and actin (sc-10731, 1:500, Santa Cruz) are the antibodies used for western blot.

Tumourigenicity assay, viral replication and distribution

Experiments were performed in 6-week-old female athymic mice (Charles River Laboratories International Inc, MA, USA). Mice were maintained at the Dipartimento di Biologia e Patologia Animal Facility. Animal experiments were conducted in accordance with accepted standards of animal care and in accordance with the Italian regulations for the welfare of animals used in the studies of experimental neoplasia. The study was approved by our institutional committee on animal care.

To evaluate the effects of *dl922-947* in combination with AZD1152, FRO cells (1×10^7) were injected into the right flank of 80 athymic mice. After 40 days, tumour volume was evaluated, and the animals were divided into four groups (20 animals/group) with similar average tumour size. Tumour diameters were measured with callipers, and tumour volumes (*V*) were calculated by the formula of rotational ellipsoid: $V = A \times B^2 / 2$ (*A* is the axial diameter and *B* is the rotational diameter).

Viral replication and distribution were evaluated as previously described (Libertini *et al.* 2008).

Statistical analysis

The analysis of the cell killing effect *in vitro* was made by isobolograms generated to calculate the concentration of each agent killing 50% of cells (EC_{50}) using untreated cells or cells treated with one agent only as controls, as previously described (Cheong *et al.* 2008).

Comparisons among different treatment groups in the experiments *in vivo* were made by the ANOVA method and the Bonferroni *post hoc* test using commercial software (GraphPad Prism 4, GraphPad Software Inc, La Jolla, CA, USA). Differences in the rate of tumour growth in mice were assessed for each time point of the observation period.

Results

AZD1152 treatment induces cell death in ATC cells

Aurora B kinase is overexpressed in ATC, and blocking its expression or activity reduces ATC cell growth (Sorrentino *et al.* 2005). To confirm Aurora B as a therapeutic target, we have evaluated the effects of Aurora B inhibitor AZD1152 on the survival of human ATC cell lines FRO, BHT101-5, 8505C and Cal62.

All cell lines are highly sensitive to AZD1152, with an IC_{50} ranging from 8 to 50 nM for Cal62 and

FRO cells respectively (Fig. 1A). Aurora B inhibition induces endoreduplication thus increasing cell diameter; this could underestimate drug effects when standard proliferation assays are used. Therefore, the anti-proliferative effect of AZD1152 was also determined by cell counting. As shown in Fig. 1B, the inhibitor significantly reduces cell number after 1 day of treatment, further confirming the high efficacy of the drug.

AZD1152 blocks Ser10 H3 phosphorylation and induces mitotic catastrophe

Aurora B phosphorylates histone H3 on serine 10 during mitosis (Prigent & Dimitrov 2003). To confirm AZD1152 effects on Aurora B activity, we treated FRO and BHT101-5 cells for 24 h and performed a FACS analysis by using a specific anti-phospho-Ser10 histone H3 antibody (Fig. 1C).

To analyse the effects of Aurora B inhibition on cell cycle, cells were stained with propidium iodide. Cell cycle profiles were also analysed after 48 h to monitor the effects of a prolonged exposure.

As shown in Fig. 2A and B, a dose- and time-dependent increase in polyploid cells was observed; this increase was paralleled by the reduction in Ser10 H3 phosphorylation levels (Fig. 1C). After 24 h of treatment, a subG₁ fraction and G₂/M accumulation were observed in both cell lines. Immunofluorescence analysis shows that the inhibition of Ser10 H3 phosphorylation caused by AZD1152 treatment does not affect chromosome condensation (Fig. 1D).

The increase of cells with $\geq 4N$ DNA content and a subsequent subG₁ suggest that AZD1152-treated cells die through mitotic catastrophe, a form of programmed cell death resulting from aberrant mitosis. Such mitosis does not produce proper

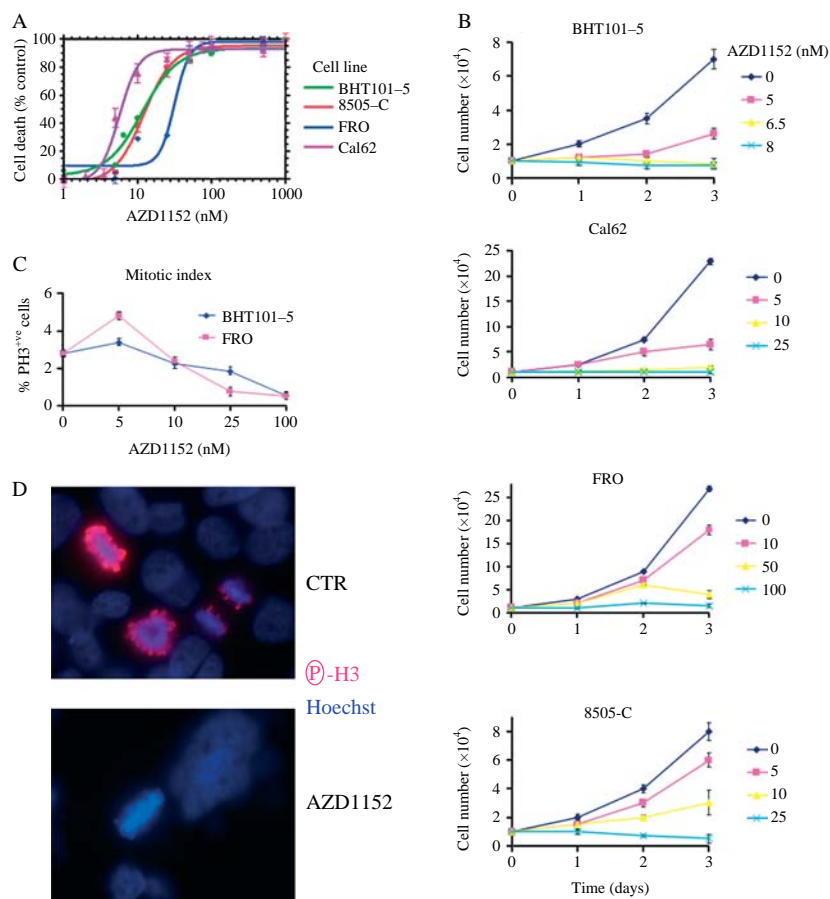


Figure 1 AZD1152 kills ATC cells. (A) ATC cells were treated with AZD1152, and survival was evaluated after 7 days by the sulforhodamine B method. (B) Cells were plated in 12-well plates, treated with different amounts of AZD1152 and counted at the indicated time points. (C) FRO and BHT101-5 cells were treated for 24 h, and phospho-Ser10 H3 levels were evaluated by FACS analysis. The bars in (A), (B) and (C) indicate the s.d. The data are the mean of three different experiments. (D) FRO cells were treated or not for 16 h with 100 nM AZD1152 and phospho-Ser10 H3 visualized by immunofluorescence.

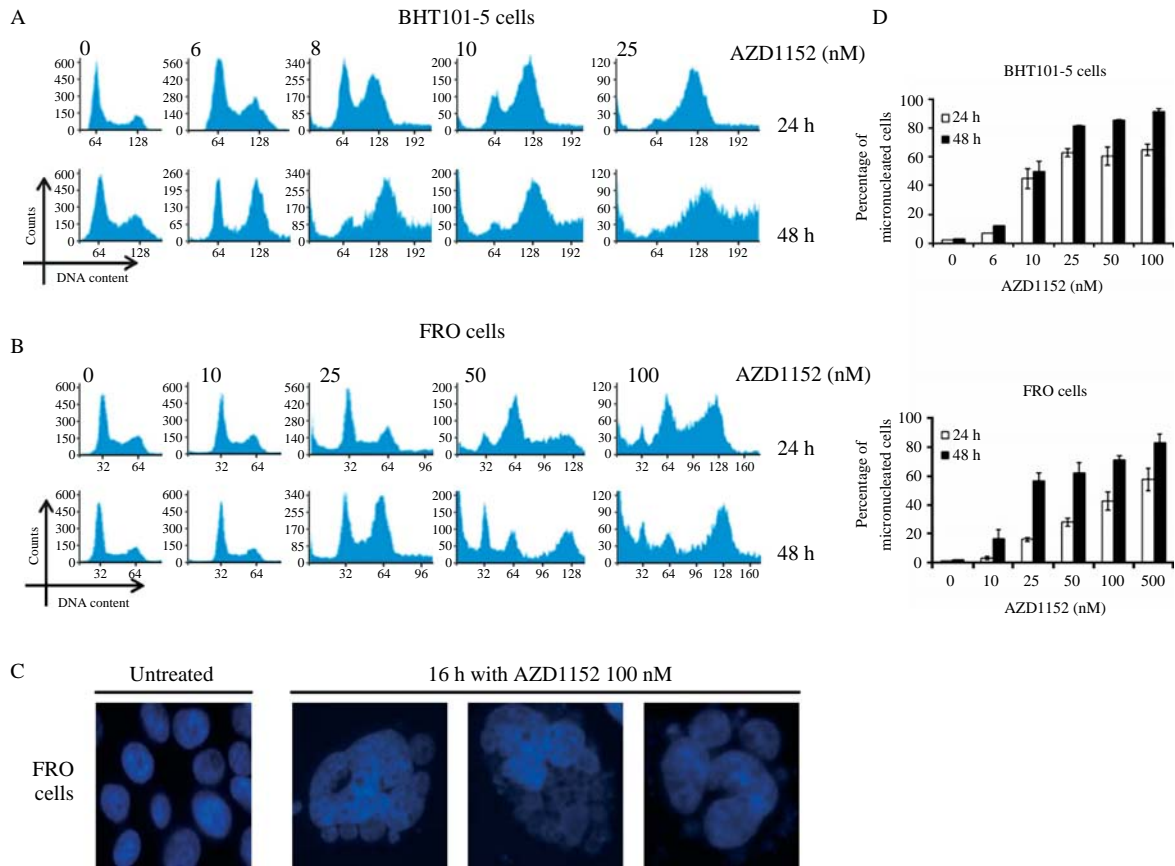


Figure 2 AZD1152 induces mitotic catastrophe. Cell cycle of BHT101-5 (A) and FRO (B) cells was analysed 24 (upper panel) or 48 h (lower panel) after AZD1152 treatment. (C) Hoechst staining of FRO cells treated or not with AZD1152. The same magnification (40×) was used in the images. (D) Quantification of data obtained by Hoechst staining. The cells with ≥3 micronuclei were counted as positive.

chromosome segregation and cell division, and leads to the formation of large non-viable cells characterized by micronuclei (Castedo *et al.* 2004a). Micronuclei are nuclear envelopes around clusters of missegregated chromosomes (examples in Fig. 2C). By immunofluorescence, we have quantified the number of FRO- and BHT101-5-micronucleated cells after AZD1152 treatment (Fig. 2D). A clear dose- and time-dependent increase in the number of micronucleated cells was observed.

AZD1152 and *dl922-947* show synergistic effects on ATC cells

It has been proposed that drugs interfering with mitosis and cytokinesis could potentiate viral oncolysis (Seidman *et al.* 2001). Therefore, we hypothesized that the association with AZD1152 could positively affect the activity of the oncolytic adenovirus *dl922-947*.

FRO and BHT101-5 cells were treated with AZD1152 and simultaneously infected with *dl922-947*; cell survival was evaluated after 7 days, showing additive/synergistic effects (Fig. 3A, Table 1). In order to understand whether AZD1152 sensitizes cells to viral action, we have treated FRO and BHT101-5 cells with AZD1152 for 24 h and then infected with *dl922-947*. The effects were evaluated after 6 days: the data obtained show that 24 h pre-treatment is sufficient to significantly increase the killing activity of *dl922-947* (Fig. 3B, Table 2), confirming that the inhibitor sensitizes cells to viral action. It is also worth noting that 24 h treatment with AZD1152 alone significantly affects cell survival.

AZD1152 does not affect cellular infectivity

It has been proposed that drugs can enhance viral oncolytic activity by increasing viral entry in target cells (Anders *et al.* 2003). To monitor this step, FRO

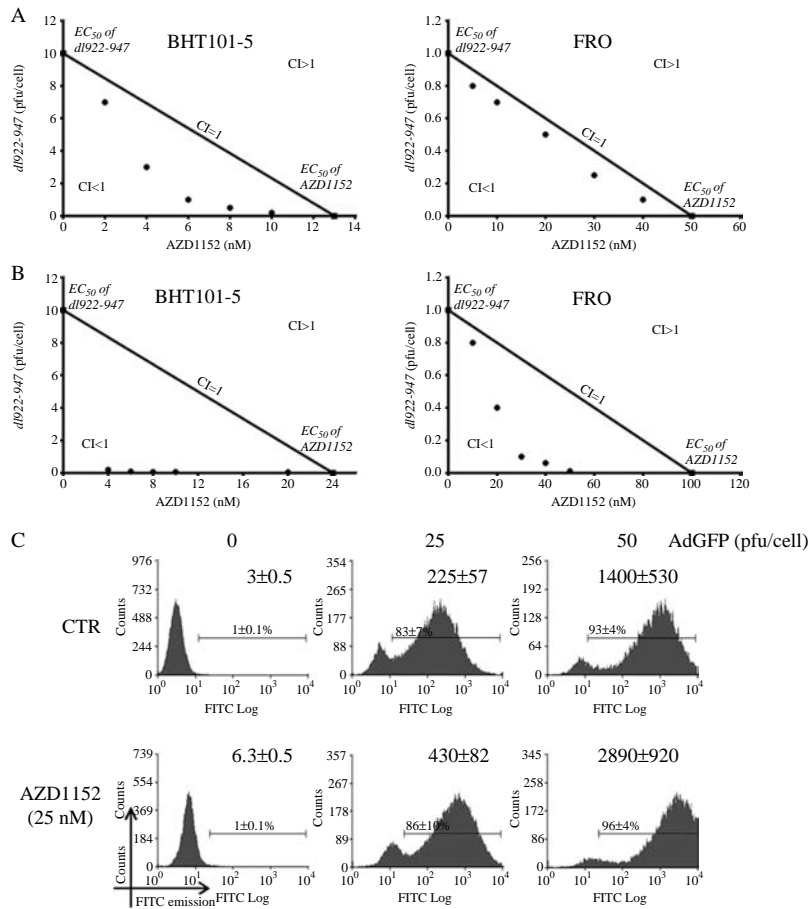


Figure 3 AZD enhances the oncolytic activity of *dI922-947* but does not increase cellular infectivity. (A) FRO and BHT101-5 cells were treated with five fixed combination ratios of *dI922-947* and AZD1152, and cell viability was determined by sulforhodamine B assay 7 days post infection. Dose–response curve and EC₅₀ values were used to construct isobolograms and calculate combination indexes (CI) for each ratio. Ratios are expressed as virus (pfu/cell) to drug (nM). A line is drawn connecting the EC₅₀ values of the virus and drug as a single agent. A ratio producing a CI ≤ 0.8 is considered synergistic, a ratio producing CIs between 0.8 and 1.2 is considered additive and a ratio producing CI ≥ 1.2 is considered antagonistic. (B) Cells were treated for 24 h with the drug; then, the media were replaced with media containing the virus alone. Survival was evaluated after 6 days with isobolograms obtained as above. (C) FRO cells were treated for 24 h with AZD1152, and then infected with AdGFP. Viral entry was quantified by monitoring the percentage of GFP-positive cells (numbers on the bars) and the average expression in FITC channel (numbers on top right) after 24 h. The percentage of GFP-positive cells does not significantly change upon AZD1152 pre-treatment, being ~85% for 25 pfu/cell and ~95% for 50 pfu/cell, regardless of drug pre-treatment. The FITC ratio in infected and uninfected cells upon drug treatment showed no significant change (75 ± 31-fold increase versus 68 ± 19 for 25 pfu/cell and 466 ± 246-fold increase versus 458 ± 182 for 50 pfu/cell).

cells were pre-treated for 24 h with AZD1152 at a low concentration (able to induce G₂/M block but not death after 48 h) and then infected with a non-replicating reporter adenovirus transducing GFP (AdGFP). After additional 24 h, GFP emission was evaluated by cytofluorimetric analysis. The percentage of GFP cells was not modified by AZD1152 pre-treatment, although a positive shift in FITC channel was observed (Fig. 3C). This increase is apparent, since AZD1152 treatment enlarges the cells thus enhancing basal fluorescence. Indeed, analysis of the FITC ratio in infected and uninfected cells treated or not with

AZD1152 showed no significant difference. Similar results were obtained with BHT101-5 cells (data not shown).

***dI922-947* and AZD1152 induce subG₁ phase population in treated cells**

Next, cell cycle profiles in infected cells, treated or not with AZD1152, were evaluated. To better discriminate differences in cell cycle phases, timing and cell death, a double thymidine block was performed to synchronize cells in G₁. As shown in Fig. 4, in untreated cells, 10 h

Table 1 Simultaneous treatment with AZD1152 and *dl922-947*

| Cell line | Ratio ((pfu/cell)/(nM)) | EC ₅₀ | EC ₅₀ | CI |
|-----------|----------------------------|--------------------------------|------------------|------|
| | | <i>dl922-947</i> (pfu/cell) | AZD1152 (nM) | |
| BHT101-5 | AZD1152 alone | 0 | 13 | |
| | <i>dl922-947</i> alone | 10 | 0 | |
| | 1:50 | 0.2 | 10 | 0.79 |
| | 1:16 | 0.5 | 8 | 0.67 |
| | 1:6 | 1 | 6 | 0.56 |
| | 1:1 | 5 | 4 | 0.8 |
| | 4:1 | 8 | 2 | 0.95 |
| FRO | AZD1152 alone | 0 | 50 | |
| | <i>dl922-947</i> alone | 1 | 0 | |
| | 1:400 | 0.1 | 40 | 0.9 |
| | 1:120 | 0.25 | 30 | 0.85 |
| | 1:40 | 0.5 | 20 | 0.9 |
| | 1:14 | 0.7 | 10 | 0.9 |
| | 1:6 | 0.8 | 5 | 0.9 |

after thymidine release, about 30% of the population re-entered G₁ phase; a similar profile was observed in infected cells. Conversely, after 10 h, AZD1152 induced a G₂/M accumulation that was not modified by the association with *dl922-947*. Starting from 20 h, a significant increase in subG₁ phase was observed in both AZD1152- and *dl922-947*-treated cells. Interestingly, the combination between drug and virus increased the percentage of cells in subG₁ fraction compared with single treatments. It is also worth noting that, in the combined treatment, the increase in subG₁ fraction at later time points is associated with a decrease in polyploidy fractions, suggesting that dying cells (subG₁ fraction) are the ones that escaped G₂/M block.

Caspase-3 activation has been observed in some models of mitotic catastrophe (Castedo *et al.* 2004a,b), and *dl922-947* induces subG₁ accumulation and caspase-3 cleavage in ovarian cancer cells (Baird *et al.* 2008). Therefore, we analysed caspase-3 activation in treated ATC cells. As shown in Fig. 5A, while *dl922-947* induces caspase-3 cleavage, AZD1152 does not. Interestingly, in the combined treatment, an earlier decrease of procaspase-3 with respect to virus treatment alone was observed. This observation suggests that the inhibitor could enhance viral-induced cell death by accelerating the activation of caspase-3 pathway.

***dl922-947* reduces H3 phosphorylation**

FRO cells infected with *dl922-947* show G₂/M accumulation and tetraploidy (Fig. 4), suggestive of a mitotic block. During a normal mitosis, histone H3 is phosphorylated on Ser 10 (28–29); the viral effects on

cell cycle prompted us to analyse whether *dl922-947* acted on this substrate.

We treated FRO cells for 24 h with different amounts of virus and drug, alone or in combination. Cells were stained with propidium iodide and with anti-phospho-Ser10 H3 histone antibody to monitor the percentage of PH3-positive cells during the cell cycle (Fig. 5B). *dl922-947* alone is able to decrease the percentage of PH3-positive cells and, together with AZD1152, Ser10 H3 phosphorylation is almost completely abolished: FACS data were confirmed by western blot analysis of PH3 levels (Fig. 5C).

AZD1152 increases *dl922-947* oncolytic activity *in vivo*

To further validate the potential therapeutic use of AZD1152 in association with *dl922-947*, we analysed the effects of the combined treatment on xenograft tumours. To study the effect of the association in the worst possible scenario, FRO cells were chosen, being the least sensitive to AZD1152 effect (Fig. 1) and viral infection (Libertini *et al.* 2008). A low viral dose (1 × 10⁶ pfu) was used to better evaluate the effects of the combined treatment; virus was administered by i.t. injection to avoid first pass effect.

Animals were divided into four groups: untreated, treated with AZD1152, *dl922-947* or both. As shown in Fig. 6A, AZD1152 and *dl922-947* in combination have a stronger anti-tumour activity than when used alone. As already described, no toxicities were observed in virus-treated animals (Libertini *et al.* 2008). Drug-treated animals showed slight weight loss and dehydration on the third day of treatment, but

Table 2 AZD1152 pre-treatment on *dl922-947*-infected cells

| Cell line | Ratio ((pfu/cell)/(nM)) | EC ₅₀ | EC ₅₀ | CI |
|-----------|----------------------------|--------------------------------|------------------|------|
| | | <i>dl922-947</i> (pfu/cell) | AZD1152 (nM) | |
| BHT101-5 | AZD1152 alone | 0 | 24 | |
| | <i>dl922-947</i> alone | 10 | 0 | |
| | 1:500 | 0.04 | 20 | 0.84 |
| | 1:167 | 0.06 | 10 | 0.42 |
| | 1:114 | 0.07 | 8 | 0.34 |
| | 1:62 | 0.08 | 5 | 0.21 |
| | 1:20 | 0.2 | 4 | 0.19 |
| FRO | AZD1152 alone | 0 | 100 | |
| | <i>dl922-947</i> alone | 1 | 0 | |
| | 1:5000 | 0.01 | 50 | 0.51 |
| | 1:667 | 0.06 | 40 | 0.46 |
| | 1:300 | 0.1 | 30 | 0.4 |
| | 1:50 | 0.4 | 20 | 0.6 |
| | 1:12 | 0.8 | 10 | 0.9 |

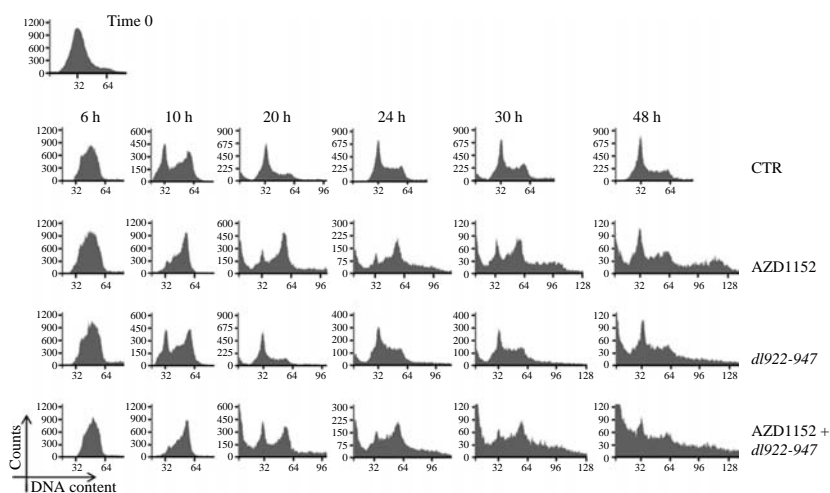


Figure 4 AZD1152 and *dl922-947* induce tetraploidy and cell death. FRO cells were synchronized in G₁ phase and treated with AZD1152 10 nM, *dl922-947* (25 pfu/cell) or both. FACS analysis was performed to analyse the cell cycle.

recovered after 2–3 days. In the combined treatment group, animals took longer to recover (4–5 days), but no other symptoms were observed.

Viral replication analysis in animals pre-treated with AZD1152 showed an increase of genome copies (Fig. 6B). However, this effect was not observed *in vitro* (data not shown). It has been hypothesized that the pre-treatment with anti-neoplastic drugs could improve intratumoural viral diffusion by reducing the number of neoplastic cells (Vähä-Koskela *et al.* 2007). To address this point, FRO xenografts animals, pre-treated or not with AZD1152, were injected intratumourally with AdGFP. GFP expression was evaluated by fluorescence microscopy analysis (Fig. 6C). In control tumours, a faint fluorescence signal was observed, whereas in AZD1152-treated tumours, a more intense fluorescence signal was

detected. It is worth noting that both viral replication and distribution were increased three times upon drug treatment (Fig. 6B and C).

Discussion

ATC is one of the most lethal neoplasia and leads to death in a short time. Active therapies are not available, making the development of novel therapeutic strategies imperative (Smallridge *et al.* 2009).

AZD1152 is a reversible ATP-competitive Aurora inhibitor, which is 1000-fold more selective for Aurora kinase B than for Aurora kinase A (Wilkinson *et al.* 2007). The effects of AZD1152 have been already assessed in *in vivo* models of human leukaemia (Wilkinson *et al.* 2007, Yang *et al.* 2007, Walsby *et al.* 2008, Oke *et al.* 2009), breast cancer (Gully *et al.* 2010),

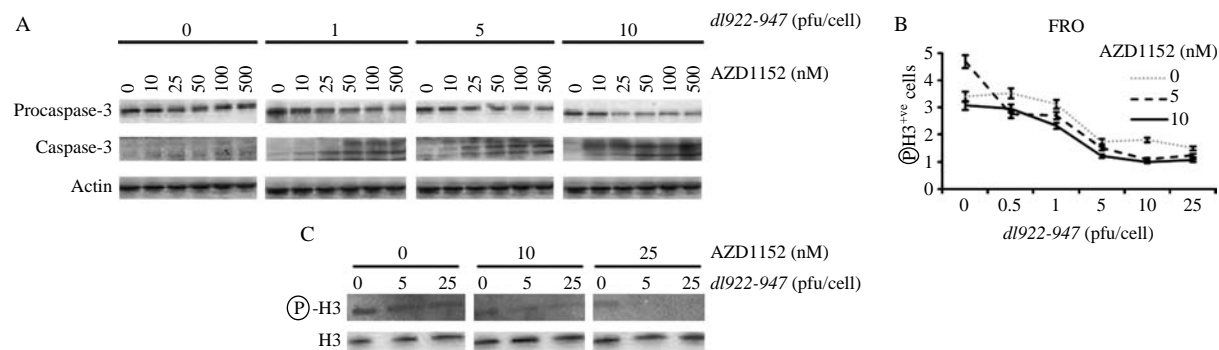


Figure 5 *dl922-947* induces caspase-3 activation and decreases PH3 levels. (A) FRO cells were synchronized in G₁ phase and treated with different combinations of *dl922-947* and AZD1152. Attached and detached cells were harvested, and western blot analysis was performed to quantify procaspase- and activated caspase-3 levels. Fifty micrograms of lysate were loaded in each well. FRO cells were treated for 24 h with different amounts of AZD1152 and *dl922-947*, alone or in combination. Ser10 PH3 levels were evaluated by FACS (B) and western blot analysis (C).

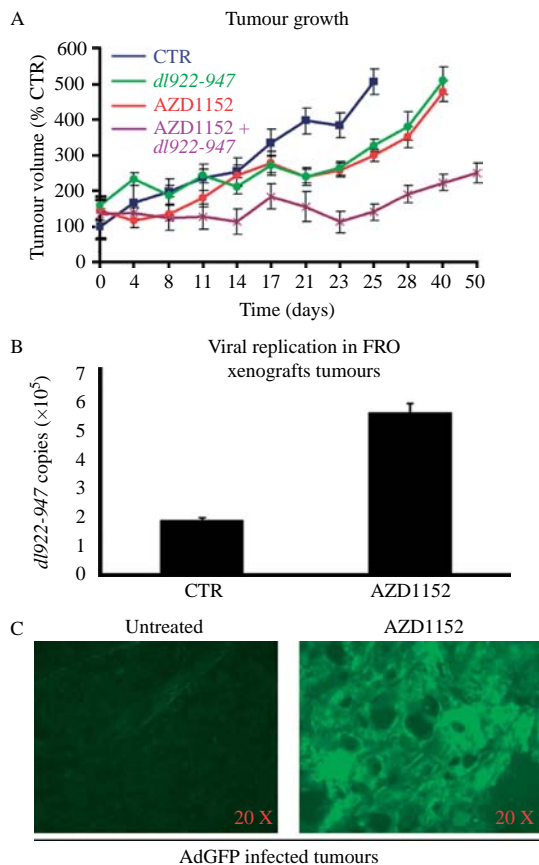


Figure 6 AZD1152 delays tumour growth and facilitates *dl922-947* replication and distribution. (A) Tumour bearing mice were randomized into four groups. Two groups received AZD1152 (100 mg/kg per day) i.p. from T1 to T3 and from T15 to T17. *dl922-947* (1×10^6 pfu, in a volume of 300 μ l) was injected at T4, T8, T11 and T15 into one AZD1152-treated group and one untreated group. The control group was injected with saline solution. Tumour volume is expressed as a percentage of the volume observed at day 0 in the control group. The difference between treated and untreated groups becomes statistically significant ($P < 0.05$) from day 17 for virus versus control and drug versus control, and from day 8 for combined treatment versus control. At day 21, a significant difference ($P < 0.05$) was observed between the combined treatment group and single treatment groups. From day 23 till the end of the treatment, the difference became highly significant ($P < 0.01$). (B) FRO cells (1×10^7 cells) were injected intratumourally within ten athymic mice. Forty days later, when tumours were detectable, animals were divided into two groups, which received respectively AZD1152 (2.5 mg/mouse) or saline solution i.p. After 24 h, *dl922-947* (1×10^6 pfu, in a volume of 300 μ l) was injected intratumourally in both groups. Two days later, animals were killed. DNA was extracted from 100 mg of tumour tissue, and the number of viral copies was evaluated by real-time PCR. The data are the mean of three different experiments. (C) Ten FRO-induced xenograft tumours were injected i.p. with AZD1152 (100 mg/kg per day) or saline solution for 3 consecutive days and, after 2 days, AdGFP (1×10^7 pfu, in a volume of 300 μ l) was injected intratumourally in both groups. Two days later, animals were killed, tumours were excised and GFP distribution was evaluated by confocal microscopy. The quantification of the digitized signal showed a threefold increase upon AZD1152 treatment.

hepatocellular carcinoma (Aihara *et al.* 2010), and colon and lung cancers (Wilkinson *et al.* 2007). AZD1152 and other Aurora inhibitors are currently in early clinical evaluation, showing reversible neutropenia as a major side effect (Keen & Taylor 2009).

In the present study, we have demonstrated that AZD1152 is active against ATC cells and that the effects are observed within 24 h. These data are consistent with the high levels of Aurora B expression (Sorrentino *et al.* 2005), the lack of a functional p53 pathway (Schweppe *et al.* 2008) and the short doubling time (10 h) of ATC cells. In the present study, we have also shown that just three doses of AZD1152 significantly delay the growth of ATC tumour xenografts.

Another Aurora inhibitor, VX-680, has been previously evaluated on ATC cell lines showing inhibition of cell proliferation and cell death; however, the drug was not evaluated *in vivo* (Arlot-Bonnemains *et al.* 2008). Cells treated with VX-680 showed an increase in DNA content ($>4N$), reduction of Ser10 H3 phosphorylation, subG₁ accumulation and activation of caspase-3 (Arlot-Bonnemains *et al.* 2008). The authors concluded that VX-680 activated the apoptotic cascade in ATC cells, and suggested that the effects reported were due to the inhibition of Aurora A rather than Aurora B. VX-680 inhibits Aurora kinases with comparable inhibition constants, ranging from 0.6 nM for Aurora A to 18 nM for Aurora B; hence, it is plausible that the effects exerted by VX-680 on ATC cells are due to the inhibition of both Aurora kinases. In addition, it has been previously reported in other cell models that effects seen with VX-680 closely resemble those described for Aurora B inhibition (Keen & Taylor 2004) and mirror the effects described here with AZD1152 on ATC cells. Moreover, the IC₅₀ of VX-680 on ATC cells ranged from 25 to 150 nM: these concentrations are also sufficient to inhibit the kinase FLT3 (Harrington *et al.* 2004, Arlot-Bonnemains *et al.* 2008). On the other hand, the IC₅₀ of AZD1152 in this study ranges from 5 to 30 nM, indicating that AZD1152 could achieve a therapeutic effect at lower and less toxic concentrations. Therefore, our results clearly indicate using both *in vitro* and *in vivo* models that selective inhibition of Aurora B could represent a therapeutic option for the treatment of ATC.

Oncolytic viruses are emerging as new therapeutic tools for the treatment of cancer, and we previously demonstrated that the mutants *dl1520* and *dl922-947* are active against ATC *in vitro* and *in vivo* (Libertini *et al.* 2007, 2008). It has been reported that drugs able to block cells in G₂/M or inhibit cytokinesis could enhance the effects of oncolytic viruses

(Seidman *et al.* 2001). Since AZD1152 has a clear effect on cell division, we wondered whether it could positively affect *dl922-947* activity. The data presented in this manuscript demonstrate the efficacy of this combination both *in vitro* and *in vivo*.

To understand how AZD1152 enhances oncolytic activity, we first monitored viral entry upon drug treatment. Our data show that AZD1152 does not affect viral entry. The synchronization in G₂/M phase leads to modest, but significant, translocation of CAR receptor to the cell surface of A549 lung carcinoma cells (Seidman *et al.* 2001). Although AZD1152-treated cells accumulate in G₂/M phase, membrane levels of CAR and its co-receptors integrins $\alpha_v\beta_3$, $\alpha_v\beta_5$ and $\alpha_v\beta_1$ do not increase after AZD1152 treatment (data not shown). By using AdGFP, we did not observe any difference in viral entry during each cell cycle phase (data not shown). Our observation is not in agreement with Seidman *et al.* (2001); this discrepancy could be due to the different cellular system used or to a very slight increase in receptor levels hidden by the increase in cellular size.

Secondly, we analysed cell death mechanisms induced by virus and drug, alone or in combination. AZD1152 induces a G₂/M block and tetraploidy in ATC cells. This aberrant mitotic phenotype, the presence of micronuclei and the appearance of subG₁ population demonstrate that AZD1152-treated cells die through mitotic catastrophe. According to the literature, mitotic catastrophe could share biochemical hallmarks with apoptosis, such as mitochondrial membrane permeabilization (MMP) and caspase cleavage (Castedo *et al.* 2004a,b). In our study, despite the clear induction of mitotic catastrophe, AZD1152 did not induce caspase-3 activation (Fig. 5) and MMP (data not shown). Like AZD1152-treated cells, ATC-infected cells show enlargement and polyploidy. However, it is possible to exclude death by mitotic catastrophe since, upon infection, cells detach, a feature not observed in mitotic catastrophe. Moreover, in the few adhering cells, we have not observed the presence of micronuclei (data not shown). We have also excluded autophagic cell death, since neither beclin 1 activation nor LC3I-II conversion were induced, and accumulation of autophagic vesicular organelles was not observed by FACS analysis in acridine orange-stained cells (data not shown). Our data extend to ATC cells the observation of Baird *et al.* (2008) that infection with mutant oncolytic adenovirus leads to programmed cell death lacking the features of classical apoptosis, but showing some apoptotic markers, such as subG₁ accumulation and caspase-3 activation. Interestingly, the association with

AZD1152 accelerates the appearance of cleaved caspase-3 and increases the percentage of cells in subG₁ phase. Our results indicate that AZD1152 enhances the cytotoxic effects of oncolytic viruses, although the cell death mechanisms are not yet defined.

During mitosis, Aurora B is involved in phosphorylation of histone H3 on Ser10 (Ditchfield *et al.* 2003, Hauf *et al.* 2003). Accordingly, AZD1152 strongly reduces H3 phosphorylation. It has been reported that the oncolytic herpes virus G47D decreases phospho-Ser10 H3 levels (Passer *et al.* 2009), and we observed that the oncolytic adenovirus *dl922-947* (Fig. 5B) and Ad5wt (personal observation) have a similar effect. These data suggest that modulation of PH3 levels is a common feature of viral infections; it is conceivable that viruses prematurely end mitosis in order to switch cell machinery to viral replication.

The first oncolytic adenovirus described, *dl1520* (Heise *et al.* 1997), has shown improved effects in clinical trials in combinations with chemotherapy (Kumar *et al.* 2008). In 2005, China approved the world's first oncolytic virus therapy for cancer treatment, with modified adenovirus H101, similar to *dl1520* (Yu & Fang 2007). In a phase III trial, a 79% response rate for H101 plus chemotherapy, compared with 40% for chemotherapy alone, was observed (Yu & Fang 2007). Other oncolytic viruses have entered into clinical trials: their efficacy and safety, and synergistic effects in association with other drugs have been demonstrated, confirming virotherapy as a promising direction for the treatment of cancer (Liu *et al.* 2007). Oncolytic viruses target neoplastic cells using a mechanism different from that of anti-neoplastic drug; therefore, the combination treatment could contribute to avoid the development of resistant cancer cells, thus increasing the cure rate.

Data presented here demonstrate that the selective inhibitor of Aurora B kinase AZD1152 is highly effective against ATC cell lines and tumour xenografts, and could represent a novel therapeutic option for the treatment of this dismal disease. We have also shown that AZD1152 enhances the effects of *dl922-947* against ATC; similar combined approaches could be used for the treatment of ATC and other aggressive and incurable human cancers.

Declaration of interest

The authors declare that there is no conflict of interest that could be perceived as prejudicing the impartiality of the research reported.

Funding

This study was supported by the Associazione Italiana per la Ricerca sul Cancro (AIRC). S Libertini was recipient of FIRC fellowship.

Acknowledgements

We thank Dr Elizabeth Anderson and Odedra Rajesh, AstraZeneca UK, for their help in the preparation of this article. We also thank AstraZeneca for kindly providing us with AZD1152 and AZD1152-HQPA. We thank Salvatore Sequino for his excellent technical assistance and Joanne Smith for proofreading this manuscript.

References

- Aihara A, Tanaka S, Yasen M, Matsumura S, Mitsunori Y, Murakata A, Noguchi N, Kudo A, Nakamura N, Ito K *et al.* 2010 The selective Aurora B kinase inhibitor AZD1152 as a novel treatment for hepatocellular carcinoma. *Journal of Hepatology* **52** 63–71. (doi:10.1016/j.jhep.2009.10.013)
- Anders M, Christian C, McMahon M, McCormick F & Korn WM 2003 Inhibition of the Raf/MEK/ERK pathway up-regulates expression of the coxsackievirus and adenovirus receptor in cancer cells. *Cancer Research* **63** 2088–2095.
- Araki K, Nozaki K, Ueba T, Tatsuka M & Hashimoto N 2004 High expression of Aurora-B/Aurora and Ip11-like midbody-associated protein (AIM-1) in astrocytomas. *Journal of Neuro-Oncology* **67** 53–64. (doi:10.1023/B:NEON.0000021784.33421.05)
- Arlot-Bonnemains Y, Baldini E, Martin B, Delcros JG, Toller M, Curcio F, Ambesi-Impiombato FS, D'Armiento M & Ulisse S 2008 Effects of the Aurora kinase inhibitor VX-680 on anaplastic thyroid cancer-derived cell lines. *Endocrine-Related Cancer* **15** 559–568. (doi:10.1677/ERC-08-0021)
- Baird SK, Aerts JL, Eddaoudi A, Lockley M, Lemoine NR & McNeish IA 2008 Oncolytic adenoviral mutants induce a novel mode of programmed cell death in ovarian cancer. *Oncogene* **27** 3081–3090. (doi:10.1038/sj.onc.1210977)
- Castedo M, Perfettini JL, Roumier T, Valent A, Raslova H, Yakushijin K, Horne D, Feunteun J, Lenoir G, Medema R *et al.* 2004a Mitotic catastrophe constitutes a special case of apoptosis whose suppression entails aneuploidy. *Oncogene* **23** 4362–4370. (doi:10.1038/sj.onc.1207572)
- Castedo M, Perfettini JL, Roumier T, Andreau K, Medema R & Kroemer G 2004b Cell death by mitotic catastrophe: a molecular definition. *Oncogene* **23** 2825–2837. (doi:10.1038/sj.onc.1207528)
- Cheong SC, Wang Y, Meng JH, Hill R, Sweeney K, Kim D, Lemoine NR & Halldén G 2008 E1A-expressing adenoviral E3B mutants act synergistically with chemotherapeutics in immunocompetent tumor models. *Cancer Gene Therapy* **15** 40–50. (doi:10.1038/sj.cgt.7701099)
- Chieffi P, Troncone G, Caleo A, Libertini S, Linardopoulos S, Tramontano D & Portella G 2004 Aurora B expression in normal testis and seminomas. *Journal of Endocrinology* **181** 263–270. (doi:10.1677/joe.0.1810263)
- Chieffi P, Cozzolino L, Kisslinger A, Libertini S, Staibano S, Mansueto G, De Rosa G, Villacci A, Vitale M, Linardopoulos S *et al.* 2006 Aurora B expression directly correlates with prostate cancer malignancy and influence prostate cell proliferation. *Prostate* **66** 326–333. (doi:10.1002/pros.20345)
- Ditchfield C, Johnson VL, Tighe A, Ellston R, Haworth C, Johnson T, Mortlock A, Keen N & Taylor SS 2003 Aurora B couples chromosome alignment with anaphase by targeting BubR1, Mad2, and Cenp-E to kinetochores. *Journal of Cell Biology* **161** 267–280. (doi:10.1083/jcb.200208091)
- Espósito F, Libertini S, Franco R, Abagnale A, Marra L, Portella G & Chieffi P 2009 Aurora B expression in post-puberal testicular germ cell tumours. *Journal of Cellular Physiology* **221** 435–439. (doi:10.1002/jcp.21875)
- Gully CP, Zhang F, Chen J, Yeung JA, Velazquez-Torres G, Wang E, Yeung SC & Lee MH 2010 Antineoplastic effects of an Aurora B kinase inhibitor in breast cancer. *Molecular Cancer* **9** 42. (doi:10.1186/1476-4598-9-42)
- Harrington EA, Bebbington D, Moore J, Rasmussen RK, Ajose-Adeogun AO, Nakayama T, Graham JA, Demur C, Hercend T, Diu-Hercend A *et al.* 2004 VX-680, a potent and selective small-molecule inhibitor of the Aurora kinases, suppresses tumor growth *in vivo*. *Nature Medicine* **10** 262–267. (doi:10.1038/nm1003)
- Hauf S, Cole RW, LaTerra S, Zimmer C, Schnapp G, Walter R, Heckel A, van Meel J, Rieder CL & Peters JM 2003 The small molecule Hesperadin reveals a role for Aurora B in correcting kinetochore-microtubule attachment and in maintaining the spindle assembly checkpoint. *Journal of Cell Biology* **161** 281–294. (doi:10.1083/jcb.200208092)
- Heise C, Sampson-Johannes A, Williams A, McCormick F, Von Hoff DD & Kirn DH 1997 ONYX-015, an E1B gene-attenuated adenovirus, causes tumor-specific cytolysis and antitumoral efficacy that can be augmented by standard chemotherapeutic agents. *Nature Medicine* **3** 639–645. (doi:10.1038/nm0697-639)
- Heise C, Hermiston T, Johnson L, Brooks G, Sampson-Johannes A, Williams A, Hawkins L & Kirn D 2000 An adenovirus E1A mutant that demonstrates potent and selective systemic anti-tumoral efficacy. *Nature Medicine* **6** 1134–1139. (doi:10.1038/80474)
- Katayama H, Ota T, Jisaki F, Ueda Y, Tanaka T, Odashima S, Suzuki F, Terada Y & Tatsuka M 1999 Mitotic kinase expression and colorectal cancer progression. *Journal of the National Cancer Institute* **91** 1160–1162. (doi:10.1093/jnci/91.13.1160)
- Keen N & Taylor S 2004 Aurora-kinase inhibitors as anticancer agents. *Nature Reviews. Cancer* **4** 927–936. (doi:10.1038/nrc1502)

- Keen N & Taylor S 2009 Mitotic drivers – inhibitors of the Aurora B kinase. *Cancer Metastasis Reviews* **28** 185–195. (doi:10.1007/s10555-009-9184-9)
- Kumar S, Gao L, Yeagy B & Reid T 2008 Virus combinations and chemotherapy for the treatment of human cancers. *Current Opinion in Molecular Therapeutics* **10** 371–379.
- Kurai M, Shiozawa T, Shih HC, Miyamoto T, Feng YZ, Kashima H, Suzuki A & Konishi I 2005 Expression of Aurora kinases A and B in normal, hyperplastic, and malignant human endometrium: Aurora B as a predictor for poor prognosis in endometrial carcinoma. *Human Pathology* **36** 1281–1288. (doi:10.1016/j.humpath.2005.09.014)
- Libertini S, Iacuzzo I, Ferraro A, Vitale M, Bifulco M, Fusco A & Portella G 2007 Lovastatin enhances the replication of the oncolytic adenovirus dl1520 and its antineoplastic activity against anaplastic thyroid carcinoma cells. *Endocrinology* **148** 5186–5194. (doi:10.1210/en.2007-0752)
- Libertini S, Iacuzzo I, Perruolo G, Scala S, Ieranò C, Franco R, Hallden G & Portella G 2008 Bevacizumab increases viral distribution in human anaplastic thyroid carcinoma xenografts and enhances the effects of E1A-defective adenovirus dl922-947. *Clinical Cancer Research* **14** 6505–6514. (doi:10.1158/1078-0432.CCR-08-0200)
- Liu TC, Galanis E & Kim D 2007 Clinical trial results with oncolytic virotherapy: a century of promise, a decade of progress. *Nature Clinical Practice. Oncology* **4** 101–117. (doi:10.1038/npcnc0736)
- López-Ríos F, Chuai S, Flores R, Shimizu S, Ohno T, Wakahara K, Illei PB, Hussain S, Krug L, Zakowski MF et al. 2006 Global gene expression profiling of pleural mesotheliomas: overexpression of aurora kinases and P16/CDKN2A deletion as prognostic factors and critical evaluation of microarray-based prognostic prediction. *Cancer Research* **66** 2970–2979. (doi:10.1158/0008-5472.CAN-05-3907)
- Mullen JT & Tanabe KK 2002 Viral oncolysis. *Oncologist* **7** 106–119. (doi:10.1634/theoncologist.7-2-106)
- Oke A, Pearce D, Wilkinson RW, Crafter C, Odedra R, Cavenagh J, Fitzgibbon J, Lister AT, Joel S & Bonnet D 2009 AZD1152 rapidly and negatively affects the growth and survival of human acute myeloid leukemia cells *in vitro* and *in vivo*. *Cancer Research* **69** 4150–4158. (doi:10.1158/0008-5472.CAN-08-3203)
- Passer BJ, Castelo-Branco P, Buhman JS, Varghese S, Rabkin SD & Martuza RL 2009 Oncolytic herpes simplex virus vectors and taxanes synergize to promote killing of prostate cancer cells. *Cancer Gene Therapy* **16** 551–560. (doi:10.1038/cgt.2009.10)
- Prigent C & Dimitrov S 2003 Phosphorylation of serine 10 in histone H3, what for? *Journal of Cell Science* **116** 3677–3685. (doi:10.1242/jcs.00735)
- Qi G, Ogawa I, Kudo Y, Miyauchi M, Siriwardena BS, Shimamoto F, Tatsuka M & Takata T 2007 Aurora-B expression and its correlation with cell proliferation and metastasis in oral cancer. *Virchows Archiv* **450** 297–302. (doi:10.1007/s00428-006-0360-9)
- Schweppe RE, Klopper JP, Korch C, Pugazhenth U, Benezra M, Knauf JA, Fagin JA, Marlow LA, Copland JA, Smallridge RC et al. 2008 Deoxyribonucleic acid profiling analysis of 40 human thyroid cancer cell lines reveals cross-contamination resulting in cell line redundancy and misidentification. *Journal of Clinical Endocrinology and Metabolism* **93** 4331–4341. (doi:10.1210/jc.2008-1102)
- Seidman MA, Hogan SM, Wendland RL, Worgall S, Crystal RG & Leopold PL 2001 Variation in adenovirus receptor expression and adenovirus vector-mediated transgene expression at defined stages of the cell cycle. *Molecular Therapy* **4** 13–21. (doi:10.1006/mthe.2001.0414)
- Smallridge RC, Marlow LA & Copland JA 2009 Anaplastic thyroid cancer: molecular pathogenesis and emerging therapies. *Endocrine-Related Cancer* **16** 17–44. (doi:10.1677/ERC-08-0154)
- Smith SL, Bowers NL, Betticher DC, Gautschi O, Ratschiller D, Hoban PR, Booton R, Santibáñez-Koref MF & Heighway J 2005 Overexpression of aurora B kinase (AURKB) in primary non-small cell lung carcinoma is frequent, generally driven from one allele, and correlates with the level of genetic instability. *British Journal of Cancer* **93** 719–729. (doi:10.1038/sj.bjc.6602779)
- Sorrentino R, Libertini S, Pallante PL, Troncone G, Palombini L, Bavetsias V, Spalletti-Cernia D, Laccetti P, Linardopoulos S, Chieffi P et al. 2005 Aurora B overexpression associates with the thyroid carcinoma undifferentiated phenotype and is required for thyroid carcinoma cell proliferation. *Journal of Clinical Endocrinology and Metabolism* **90** 928–935. (doi:10.1210/jc.2004-1518)
- Tanaka S, Aarii S, Yasen M, Mogushi K, Su NT, Zhao C, Imoto I, Eishi Y, Inazawa J, Miki Y et al. 2008 Aurora kinase B is a predictive factor for the aggressive recurrence of hepatocellular carcinoma after curative hepatectomy. *British Journal of Surgery* **95** 611–619. (doi:10.1002/bjs.6011)
- Vähä-Koskela MJ, Heikkilä JE & Hinkkanen AE 2007 Oncolytic viruses in cancer therapy. *Cancer Letters* **254** 178–216. (doi:10.1016/j.canlet.2007.02.002)
- Vischioni B, Oudejans JJ, Vos W, Rodriguez JA & Giaccone G 2006 Frequent overexpression of aurora B kinase, a novel drug target, in non-small cell lung carcinoma patients. *Molecular Cancer Therapeutics* **5** 2905–2913. (doi:10.1158/1535-7163.MCT-06-0301)
- Walsby E, Walsh V, Pepper C, Burnett A & Mills K 2008 Effects of the aurora kinase inhibitors AZD1152-HQPA and ZM447439 on growth arrest and polyploidy in acute myeloid leukemia cell lines and primary blasts. *Haematologica* **93** 662–669. (doi:10.3324/haematol.12148)

- Wilkinson RW, Odedra R, Heaton SP, Wedge SR, Keen NJ, Crafter C, Foster JR, Brady MC, Bigley A, Brown E *et al.* 2007 AZD1152, a selective inhibitor of Aurora B kinase, inhibits human tumor xenograft growth by inducing apoptosis. *Clinical Cancer Research* **13** 3682–3688. (doi:10.1158/1078-0432.CCR-06-2979)
- Yang J, Ikezoe T, Nishioka C, Tasaka T, Taniguchi A, Kuwayama Y, Komatsu N, Bandobashi K, Togitani K, Koeffler HP *et al.* 2007 AZD1152, a novel and selective aurora B kinase inhibitor, induces growth arrest, apoptosis, and sensitization for tubulin depolymerizing agent or topoisomerase II inhibitor in human acute leukemia cells *in vitro* and *in vivo*. *Blood* **110** 2034–2040. (doi:10.1182/blood-2007-02-073700)
- Yu W & Fang H 2007 Clinical trials with oncolytic adenovirus in China. *Current Cancer Drug Targets* **7** 141–148. (doi:10.2174/156800907780058817)

Inhibition of autophagy enhances the effects of E1A defective oncolytic adenovirus dl922-947 against glioma cells in vitro and in vivo

| | |
|-------------------------------|--|
| Journal: | <i>Human Gene Therapy</i> |
| Manuscript ID: | HUM-2011-120 |
| Manuscript Type: | Research Article |
| Date Submitted by the Author: | 06-Jul-2011 |
| Complete List of Authors: | <p>Botta, Ginevra; Università degli Studi di Napoli "Federico II", Dipartimento di Biologia e Patologia Cellulare e Molecolare "L.Califano"</p> <p>Passaro, Carmela; Università degli Studi di Napoli "Federico II", Dipartimento di Biologia e Patologia Cellulare e Molecolare "L.Califano"</p> <p>Libertini, Silvana; Beatson Institute for Cancer Research; Università degli Studi di Napoli "Federico II", Dipartimento di Biologia e Patologia Cellulare e Molecolare "L.Califano"</p> <p>Abagnale, Antonella; Università degli Studi di Napoli "Federico II", Dipartimento di Biologia e Patologia Cellulare e Molecolare "L.Califano"</p> <p>Barbato, Sara; Università degli Studi di Napoli "Federico II", Dipartimento di Biologia e Patologia Cellulare e Molecolare "L.Califano"</p> <p>Hallden, Gunnel; School of Medicine and Dentistry Queen Mary University of London, Centre for Molecular Oncology and Imaging Institute of Cancer Barts and the London</p> <p>Beguinet, Francesco; Università degli Studi di Napoli "Federico II", Dipartimento di Biologia e Patologia Cellulare e Molecolare "L.Califano"</p> <p>Formisano, Pietro; Università degli Studi di Napoli "Federico II", Dipartimento di Biologia e Patologia Cellulare e Molecolare "L.Califano"</p> <p>Portella, Giuseppe; Università di Napoli Federico II, Biologia e Patologia Cellulare e Molecolare</p> |
| Keyword: | Cancer - Apoptosis < C. Disease Models and Clinical Applications |
| | |

1
2
3
4
5
6
7
8
9
10
11
12
13
14
15
16
17
18
19
20
21
22
23
24
25
26
27
28
29
30
31
32
33
34
35
36
37
38
39
40
41
42
43
44
45
46
47
48
49
50
51
52
53
54
55
56
57
58
59
60



1
2
3 **Inhibition of autophagy enhances the effects of E1A defective oncolytic adenovirus *dl922-947***
4 **against glioma cells *in vitro* and *in vivo***
5
6
7
8
9

10 Ginevra Botta¹, Carmela Passaro¹, Silvana Libertini^{1,2}, Antonella Abagnale¹, Sara Barbato¹, Gunnel
11 Hallden³, Francesco Beguinot¹, Pietro Formisano¹ and Giuseppe Portella^{1,§}.
12
13
14
15
16

17 ¹Dipartimento di Biologia e Patologia Cellulare e Molecolare Università Federico II, Naples-Italy.

18 ²Beatson Institute for Cancer Research, Garscube Estate, Switchback Road, Glasgow, UK.

19 ³Centre for Molecular Oncology and Imaging, Institute of Cancer, Barts and the London School of
20
21
22
23
24
25
26
27
28
29
30
31
32
33
34
35
36
37
38
39
40
41
42
43
44
45
46
47
48
49
50
51
52
53
54
55
56
57
58
59
60

Medicine, Queen Mary University of London, London, UK.

Running Title: chloroquine and *dl922-947* for glioma treatment

Key words: glioma, oncolytic virus, autophagy, Chloroquine

§ Correspondence should be addressed to: Giuseppe Portella,

Dipartimento di Biologia e Patologia Cellulare e Molecolare, Facoltà di Medicina e

Chirurgia, Università di Napoli Federico II,

via S. Pansini 5, 80131 Napoli, Italy.

Tel: ++39 081 7463056; Fax: 39 081 7463037; e-mail: portella@unina.it

Abstract

1
2
3
4
5
6 Oncolytic viruses represent a novel therapeutic approach for aggressive tumours, such as
7
8 glioblastoma multiforme, which are resistant to available treatments. Autophagy has been observed
9
10 in cells infected with oncolytic viruses, however its role on cell death/survival is unclear. To
11
12 elucidate the potential therapeutic use autophagy modulators in association with viral therapy, we
13
14 analyzed autophagy induction in human glioma cell lines U373MG and U87MG infected with the
15
16 oncolytic adenovirus *dl922-947*. *dl922-947* infection triggered autophagy, as shown by
17
18 development of acidic vesicular organelles, LC3-I→LC3-II conversion, reduction of p62 levels.
19
20 Upon infection, Akt/mTOR/p70s6k pathway, a negative regulator of autophagy, was activated,
21
22 while ERK1/2 pathway, which positively regulates autophagy, was inhibited. Accordingly, MEK
23
24 inhibition by PD98059 sensitized glioma cells to *dl922-947* effects, whereas autophagy induction
25
26 by rapamycin protected cells from *dl922-947*-induced death. Treatment with two inhibitors of
27
28 autophagy, chloroquine and 3-methyladenine, increased the cytotoxic effects of *dl922-947 in vitro*.
29
30 *In vivo*, the growth of U87MG induced xenografts was further reduced by adding chloroquine to
31
32 *dl922-947* treatment. In conclusion, autophagy acts as survival response in glioma cells infected
33
34 with *dl922-947*, thus suggesting autophagy inhibitors as adjuvant/neoadjuvant drugs in oncolytic
35
36 viruses based treatments.
37
38
39
40
41
42
43
44
45
46
47
48
49
50
51
52
53
54
55
56
57
58
59
60

Introduction

Malignant glioma of astrocytic origin or glioblastoma multiforme (GBM) is one of the most aggressive human tumours (Furnari *et al.*, 2007; Brandes *et al.*, 2008) with a median survival time of about 12-15 months. The standard treatment protocol for newly diagnosed GBM includes surgical resection, radiotherapy and chemotherapy (Furnari *et al.*, 2007; Brandes *et al.*, 2008). However, this therapeutic approach has achieved only a moderate increase in survival (Ahmadi *et al.*, 2009), highlighting the need for the development of novel and more effective treatments.

Conditionally replicating oncolytic viruses (OVs) are a novel promising platform for the treatment of cancer. Several studies have demonstrated the feasibility and safety of this therapeutic strategy in glioblastoma patients (Haseley *et al.*, 2009). *dl922-947* is a replication-selective oncolytic adenoviral mutant harbouring a 24-bp deletion in the E1A-Conserved Region 2 (CR2), that is necessary for binding and inactivation of pRb (Heise *et al.*, 2000), which regulates the G1 to S phase transition. Thus, *dl922-947* virus is unable to induce G1 to S phase transition in normal cells, but can replicate with high efficiency in cells with an abnormal G1-S checkpoint. Previous studies have confirmed the efficacy of E1A CR2-deleted adenoviruses for glioma cells such as Delta24 (Fueyo *et al.*, 2000; Jiang *et al.*, 2007) and we have demonstrated that *dl922-947* exerts antineoplastic activity against the glioma cell lines U373MG and U343MG (Botta *et al.*, 2010). Recently, a phase I clinical trial for the use of an E1ACR2-deleted mutant (Ad5- Δ 24RGD) in recurrent malignant gliomas has been completed (<http://clinicaltrialsfeeds.org/clinical-trials/show/NCT00805376>).

Although efficacy and safety of OVs have been clearly demonstrated in preclinical and clinical studies, most of the molecular and/or biochemical pathways activated in cancer cells, including the cell death mechanisms, are not fully understood. A better understanding of such mechanisms would be advantageous for future selection of novel drugs or treatments to further enhance the efficacy of oncolytic viruses. In different studies, it has been shown that OVs activate the autophagic machinery in some cancer cells (Ito *et al.*, 2006; Jiang *et al.*, 2007; Baird *et al.*, 2008; Tyler *et al.*,

1
2
3 2009). Autophagy is an evolutionarily conserved process whereby cytoplasm and cellular organelles
4 are degraded in lysosomes for amino acid and energy recycling (Mizushima, 2007). The role of
5 autophagy as an alternate energy source, and thus as a temporary survival mechanism under
6 stressful conditions, is well recognized. However, it has also been reported that autophagy plays an
7 active role in cell death (Baehrecke, 2005; Loos and Engelbrecht, 2009).

8
9 Here, we showed that infection with the oncolytic virus *dl922-947* induces formation of acidic
10 vesicular organelles and LC3I-II conversion, indicative of an autophagic response.

11 Regulation of autophagy requires multiple signaling pathways (Meijer and Codogno, 2004),
12 therefore we decided to further study this process. Akt/mTOR/p70s6k is the main pathway involved
13 in the negative regulation of autophagy (Blommaart *et al.*, 1995; Yang *et al.*, 2005). Class I
14 phosphatidylinositol 3-phosphate kinase (PI3K) is activated by ligand binding to growth factor
15 receptors. PI3K activates the downstream target AKT, leading to activation of mammalian target of
16 rapamycin (mTOR) (Diaz-Troya *et al.*, 2008). TOR is a serine/threonine kinase that exerts an
17 inhibitory effect on autophagy, which is achieved by either controlling translation and transcription
18 or either directly or indirectly affecting the Atg (autophagy related genes) proteins (Diaz-Troya *et*
19 *al.*, 2008). p70S6k is considered a candidate of the substrates of mTOR and of the control of
20 autophagy downstream of mTOR (Blommaart *et al.*, 1995). In the presence of amino acids, mTOR
21 promotes phosphorylation of S6 through activation of p70S6K, thus facilitating the translation
22 initiation of mRNAs (Diaz-Troya *et al.*, 2008). On the other side, the ERK1/2 pathway has been
23 described as a positive regulator pathway of autophagy (Pattingre *et al.*, 2003).

24 Surprisingly, we found that, even though *dl922-947* infection induces autophagy, it also activates
25 the main negative regulator of autophagy—the Akt/mTOR/p70S6K pathway— and inhibits the
26 positive regulator—the ERK1/2 pathway. In line with this, viral cytotoxicity is decreased by
27 rapamycin (an mTOR inhibitor) and increased by ERK1/2 inhibitor PD98059, as well as by specific
28 inhibitors of autophagy (3-Methyladenine and Chloroquine) or genetic tools such as Atg5 shRNA.
29 Although these data seem to contrast with previous results suggesting autophagy as a cell death

1
2
3 mechanism induced by oncolytic viruses in glioma cells (Ito *et al.*, 2006), our results led us to
4
5 speculate that autophagy might play a survival/defensive role in glioma cells infected with *dl922-*
6
7 947. Consistently, we demonstrated that chloroquine treatment of athymic mice bearing glioma
8
9 tumour xenografts enhances the effects of *dl922-947* in reducing tumor growth.
10
11

12 13 14 15 **Material and methods**

16 17 *Cell lines and reagents*

18
19 Human glioma cell lines U373MG and U87MG were purchased from American Type Culture
20
21 Collection and grown as described (Botta *et al.*, 2010).
22
23

24
25 Acridine orange and 3-Methyladenine (3-MA), an inhibitor of class-III-phosphatidylinositol-3
26
27 kinase (PI3KIII), which is known to inhibit autophagic sequestration (Kondo *et al.*, 2005), were
28
29 purchased from Sigma-Aldrich (St. Louis, Missouri).
30

31
32 Chloroquine (CQ), which prevents the fusion of autophagosomes and lysosomes (Kondo *et al.*,
33
34 2005), was purchased from Fluka, Biochemika (Buchs, Switzerland). PD98059, a mitogen-activated
35
36 protein kinase/extracellular signal-regulated kinase kinase 1 (MEK 1) inhibitor, and rapamycin, a
37
38 natural product which binds directly to mTOR and suppresses mTOR-mediated phosphorylation of
39
40 its downstream target p70S6K, were purchased from Sigma-Aldrich (St. Louis, Missouri).
41
42
43
44

45 46 *Preparation of adenoviruses, infection and viability assay*

47
48 *dl922-947* is a second generation adenoviral mutant that has a 24-bp deletion in E1A Conserved
49
50 Region 2 (CR2). AdGFP is a non replicating E1A-deleted adenovirus encoding green fluorescent
51
52 protein. *dl312* is a non replicating adenovirus (Δ E1A, Δ E3B) (Cheong *et al.*, 2008). Viral stocks
53
54 were expanded, purified and stored as previously reported (Botta *et al.*, 2010). Virus titre was
55
56 determined by plaque-forming units (pfu) on the HEK-293 cells.
57
58

59
60 For the evaluation of the cytotoxic effects of the *dl922-947* virus, 1×10^3 cells were seeded in 96-well
plates, and 24 hours later cells infected with at different Multiplicity Of Infection (MOIs), in

1
2
3 presence or not of 1.0 mM 3-MA or 10 μ M CQ. After seven days, cells were fixed with 10% TCA
4
5 and stained with 0.4 % sulforhodamine B in 1% acetic acid (Libertini *et al.*, 2010). The bound dye
6
7 was solubilised in 200 μ l of 10 mM unbuffered Tris solution and the optical density was determined
8
9 at 490 nm in a microplate reader (Biorad; Hercules, California). The percent of cell death rates of
10
11 treated cells were calculated. Dose response curves were generated to calculate the concentration at
12
13 which each agent killed 50% of cells (LD₅₀), using untreated cells or cells treated with single agents
14
15 as a control.
16
17
18
19
20
21

22 *Quantification of Acidic Vesicular Organelles With Acridine Orange*

23
24 Autophagy is characterized by the development of acidic vesicular organelles. The cytoplasm and
25
26 nucleoli of acridine orange–stained cells fluoresce bright green and dim red, respectively, whereas
27
28 acidic compartments fluoresce bright red (Paglin *et al.*, 2001). Therefore, autophagy was assessed
29
30 in U373MG and U87MG cells by the quantification of acidic vesicular organelles with supravital
31
32 cell staining using acridine orange. Treated cells were detached with 0.05% trypsin–EDTA and
33
34 stained with 1.0 μ g/mL acridine orange for 15 minutes at 37°C. Stained cells were then analyzed
35
36 on a FACS cytometer (Dako Cytomation, Carpinteria, California) and Summit V4.3 software
37
38 (Dako).
39
40
41
42
43
44

45 *Generation of stable clones*

46
47 The green fluorescent protein (GFP)-tagged LC3 expressing cells were used to demonstrate
48
49 induction of autophagy (Kabeya *et al.*, 2000). The LC3 expression vector (pCAG-LC3) was kindly
50
51 provided by Drs. N. Mizushima and T.Yoshimori (Osaka University, Suita, Japan). To obtain
52
53 pGFP-LC3, LC3 cDNA was inserted into the *Bgl*III and *Eco*RI sites of pEGFP-C1, a GFP fusion
54
55 protein expression vector (Clontech laboratories; Mountain View, California) (Kabeya *et al.*, 2000).
56
57 Stable expression of GFP-LC3 cDNA in U373MG cells (U373GFP-LC3) was accomplished by
58
59 using the Lipofectamine (Invitrogen; Carlsbad, California) method according to the manufacturer's
60

1
2
3 instructions. Briefly, cells were cultured in 60 mm dishes (Corning Incorporated, Corning, NY) and
4
5 incubated for 24 h in serum-free DMEM supplemented with 5 μ g of cDNA and 15 μ l of
6
7 Lipofectamine reagent. An equal volume of DMEM supplemented with 20% fetal calf serum was
8
9 then added for 5 h followed by replacement with DMEM supplemented with 10% serum for 24 h
10
11 before the assays. At 48 h after the medium change, cells were selected in medium containing 400
12
13 mg/ml of G418 (GIBCO; Carlsbad, California) and G-418 resistant clones were established.
14
15 Expression of GFP-LC3 in the selected clones was evaluated by western blot analysis using anti
16
17 GFP antibody.
18
19
20
21

22 To stably inhibit the expression of ATG5 gene, APG5 shRNA (sc-41445-sh) and control shRNA
23
24 (sc-108060) plasmids were purchased from Santa Cruz biotech (Santa Cruz, California) and
25
26 transfected/selected in U373MG and U87MG cell lines as described above.
27
28
29
30

31 *Analysis of LC3 localization by immunofluorescence staining*

32
33 U373MG cells stably expressing GFP-LC3 plasmid were seeded in 12-wells dishes. After
34
35 treatment, cells were fixed with 3% paraformaldehyde and then examined. Images were acquired
36
37 with a LSM510 inverted confocal microscope (Zeiss, Oberkochen, Germany) using a x40 oil
38
39 objective and processed using LSM software (Zeiss, Oberkochen, Germany).
40
41
42
43
44

45 *Western blot analysis*

46
47 For protein extraction, cells were homogenised into lysis buffer (50 mM HEPES, 150 mM NaCl, 1
48
49 mM EDTA, 1 mM EGTA, 10% glycerol, 1% Triton-X-100, 1 mM phenylmethylsulfonyl fluoride, 1
50
51 μ g/ml aprotinin, 0.5 mM sodium orthovanadate, 20 mM sodium pyrophosphate).
52
53
54

55 Tumour tissue samples were homogenised in a Polytron (Brinkman Instruments, Westbury, New
56
57 York) in 20 ml T-PER reagent (Pierce, Rockford, Illinois) per gram of tissue according to
58
59 manufacturer's instructions. After centrifugation at 5000 \times g for 5 min, supernatant fraction was
60
collected.

1
2
3 Total homogenates were separated by SDS-PAGE under reducing conditions. Membranes were
4
5 incubated overnight with the following primary antibodies: LC3-I/II (ab51520, 1:3000) and
6
7 caspase-3 (ab13585, 1:500) from Abcam (Cambridge, United Kingdom); p62 (#5114, 1:1000) , p-
8
9 ERK1/2 (#9101S, 1:1000), p-Akt (#9271, 1:1000) and p-p70s6k (#9205S, 1:500), from Cell
10
11 Signalling (Danvers, Massachusetts), ATG5 (sc-8666, 1:500), ERK1/2 (sc-93-G, 1:1000) and β -
12
13 actin (sc-10731, 1:2000) from Santa Cruz biotech (Santa Cruz, California); AKT (#28745, 1:1000)
14
15 from Upstate Biotechnology (Billerica, Massachusetts).
16
17
18
19
20
21

22 *In vivo antitumor activity*

23
24 Experiments were performed in six-week-old female CD-1 athymic mice (Charles-River,
25
26 Wilmington, Massachusetts). U87MG cells (5×10^6) were injected into the right flank of 80 athymic
27
28 mice. After 20 days, when tumours were clearly detectable, tumours volumes were evaluated and
29
30 the animals were randomised into four groups (T=0) with similar average tumour size: untreated,
31
32 treated with CQ, *dl922-947*, or both. CQ (45 mg/Kg) was administered *i.p.* every third day, virus
33
34 was administered three times per week by intratumoural injection to avoid first pass effect. A low
35
36 viral dose (1×10^7 pfu) was used to better evaluate the effects of the combined treatment. The control
37
38 group was injected with saline solution. Tumours diameters were measured with calipers and
39
40 tumours volumes (V) were calculated by the formula of rotational ellipsoid: $V = A \times B^2 / 2$ (A=axial
41
42 diameter, B=rotational diameter).
43
44
45
46
47

48 Experiment was stopped when tumors reached 1 cm^3 in volume and/or symptomatic tumor
49
50 ulceration occurred.
51

52
53 Mice were maintained at the Dipartimento di Biologia e Patologia Animal Facility. Animal
54
55 experiments were conducted in accordance with accepted standards of animal care and in
56
57 accordance with the Italian regulations for the welfare of animals used in studies of experimental
58
59 neoplasia. The study was approved by our institutional committee on animal care.
60

Statistical analysis

The analysis of the cell killing effect *in vitro* was made by calculating the concentration at which each agent killed 50% of cells (LD₅₀), using untreated cells or cells treated with one agent only as controls. Comparisons among different treatment groups in the experiments *in vivo* were made by the ANOVA method and the Bonferroni post hoc test using commercial software (GraphPad Prism 4). Differences in the rate of tumour growth in mice were assessed for each time point of the observation period.

Results

Induction of autophagy in malignant glioma cells by dl922-947

First, we evaluated the cytotoxic effects of *dl922-947* in U87MG and U373MG glioma cells, confirming its efficacy. U373MG cell line displayed higher sensitivity to *dl922/947* with an EC₅₀ of 0.003 pfu/cell, compared to U87MG EC₅₀ at 0.019 pfu/cell (Fig. 1A).

Next, we evaluated the activation of autophagy in glioma cells infected with *dl922-947*. To this end, we analysed the formation of acidic vesicular organelles (AVOs), a peculiar feature of autophagy, after infection with *dl922-947*. Quantification of AVOs in U373MG and U87MG cells was performed with acridine orange supravital cell staining. U373MG and U87MG cells were infected at increasing MOIs of *dl922-947* and acridine orange vital staining performed 72 hpi (hours post infection). FACS analysis showed an increase in bright red fluorescence in infected cells, in a MOI-dependent manner, up to 18% (U373MG) or up to 14% (U87MG). Untreated cells exhibited mainly green fluorescence (Fig. 1B). Cells infected with a non replicating control adenovirus, *dl312* exhibited a similar pattern (not shown). This indicates an accumulation of AVOs in glioma cells infected with *dl922-947*.

In amino acid starvation-induced autophagy, the microtubule-associated protein 1 light chain 3, LC3-I, undergoes a series of ubiquitination-like reactions, and is modified to LC3-II. LC3-I is located in the cytoplasm, conversely LC3-II is a tightly membrane bound protein and is attached to

1
2
3 pre-autophagosomal (PAS) and autophagosomal structures. LC3-II amount reflects the abundance
4 of autophagosomes and variations in the ratio of LC3-II to LC3-I are indicative of autophagy
5 induction (Kabeya *et al.*, 2000). LC3-I to LC3-II conversion was analyzed in U373MG and U87MG
6 cells infected with *dl922-947* at 72 hpi by western blotting. An increase of LC3-II levels, paralleled
7 by a strong reduction of LC3-I levels, was observed in U373MG and U87MG infected cells, in a
8 MOI-dependent manner (Fig. 1C).

9
10 During the autophagic process, LC3-II is recruited to autophagosome membranes, therefore we
11 decided to monitor LC3 localization during *dl922-947* infection. U373MG clones expressing LC3
12 fused to green fluorescent protein were generated (U373 GFP-LC3) by stable transfection and GFP-
13 LC3 tracked by immunofluorescence.

14
15 In untreated U373 GFP-LC3 cells or in cells infected with the non replicating adenoviral mutant
16 *dl312*, a diffuse and mostly cytosolic distribution of fluorescence was observed (Fig. 1E). A less
17 diffuse and more punctate pattern was observed after infection with 0.1 pfu of *dl922-947* 72 hpi,
18 indicating that LC3-II is recruited to the autophagosomal membranes. As a positive control, U373
19 GFP-LC3 cells were treated with the autophagy inducer rapamycin, showing the typical LC3-II
20 localization pattern.

21
22 The accumulation of LC3-II could be due to the autophagy flux or to an interference with
23 autophagosomal/lysosomal function. To discriminate between the two options, we have evaluated
24 the levels of the specific autophagy substrate p62/SQSTM1. During autophagy, p62 levels are
25 reduced whereas, in the absence of autophagy, p62 levels are unmodified (Komatsu and Ichimura,
26 2010). As shown in Fig 1C, a clear decrease of p62 levels was observed, demonstrating that *dl922-*
27 *947* enhances the autophagic flux.

28
29 To confirm that autophagy is due to the infection with a replicating virus, glioma cells were also
30 infected with a non replicating adenovirus expressing green fluorescence protein (AdGFP). AdGFP
31 infection did not induce changes in LC3-II/LC3-I ratio nor in p62 levels (Fig. 1D).

1
2
3 Taken together, these data demonstrate that glioma cells infected with the *dl922-947* virus activate
4
5 autophagic processes.
6
7

8
9
10 *dl922-947* infection modulates autophagic signalling pathways and its effects are modified by
11
12 *specific pharmacological inhibitors*
13
14

15 We evaluated the effects of *dl922-947* infection on Akt/mTOR/p70s6k and ERK1/2 pathways,
16
17 respectively negative and positive regulatory pathways of autophagy.
18

19 U373MG and U87MG cells were infected with *dl922-947* in a dose-response experiment.
20
21 Phosphorylation of p70s6k and AKT increased in a dose-dependent manner (Fig. 2A) in both cell
22
23 lines, indicating activation of the negative regulatory pathway. Conversely, ERK1/2
24
25 phosphorylation was reduced upon infection with *dl922-947* in a dose-dependent manner (Fig. 2A),
26
27 indicating an inhibition of the positive regulatory pathway. AdGFP infection did not induce any of
28
29 these effects (Fig. 2B). These data suggest that, along with autophagy activation occurring in
30
31 infected cells, *dl922-947* also induces compensatory mechanisms.
32
33
34

35 To clarify the effects of ERK1/2 pathway on autophagy upon infection, glioma cells were infected
36
37 with *dl922-947* in the presence of MEK 1 inhibitor PD98059. An inhibitory dose of 25 μ M was
38
39 used for all the experiments. The combined treatment led to further reduction of ERK 1/2
40
41 phosphorylation (Fig. 3A) along with a reduction on LC3 conversion; conversely, in uninfected
42
43 cells, the drug did not modify LC3I/LC3II ratio (Fig. 3A). Accordingly, PD98059 enhanced *dl922-*
44
45 *947* induced cytotoxicity. A significant reduction of LD₅₀ values was obtained in both cell lines:
46
47 from 0.14 to 0.02 in U373MG cells, and from 0.33 to 0.1 in U87MG cells (Fig. 3B).
48
49
50

51 To investigate the role of Akt/mTOR/p70s6k pathway in *dl922-947* infection, glioma cells were
52
53 treated with the mTOR inhibitor rapamycin, a well known autophagy inducer (Meijer and Codogno,
54
55 2004), and then infected with *dl922-947*. Treatment with rapamycin led to a reversion of p70S6K
56
57 phosphorylation induced by the virus, paralleled by an increase of LC3-II/LC3 I ratio (Fig. 4A). In
58
59
60

1
2
3 both cell lines, rapamycin treatment led to a significant reduction of viral cytotoxicity, with more
4
5 than hundred fold increase in LD₅₀ (Fig. 4B).
6

7
8 These data strongly indicate that autophagy plays a survival role in glioma cells infected with
9
10 *dl922-947* and that the attenuation of autophagic response could increase viral cytotoxicity.
11
12

13 14 15 *Inhibition of autophagy increases dl922-947 cytotoxicity in glioma cells*

16
17 Next, we evaluated the effect of pharmacological inhibition of autophagy on *dl922-947* infection.
18
19 To this aim, we used two well known inhibitors of autophagy: 3-methyladenine (3-MA) and
20
21 hydroxychloroquine (CQ), acting at early and late stages of autophagy, respectively. CQ blocks the
22
23 formation of autolysosomes where LC3-II degradation occurs, thus inducing LC3II accumulation
24
25 (Amaravadi *et al.*, 2007), whereas 3-MA, an inhibitor of class-III-phosphatidylinositol-3 kinase
26
27 (PI3KIII), blocks early autophagocytic signaling, preventing LC3I-LCII conversion (Kondo *et al.*,
28
29 2005).
30
31

32
33 Accordingly, *dl922-947*-mediated LC3-II induction and AVOs formation were further increased by
34
35 CQ, while treatment with 3-MA partially reverted the LC3-II increase and AVOs formation (Fig.
36
37 5A).
38
39

40
41 The treatment with a single dose of CQ (10 μ M) or 3-MA (1 mM) increased *dl922-947* induced
42
43 cytotoxicity, with a reduction of LD₅₀ values ranging from two to thirty fold (Fig. 5B). At the
44
45 concentrations used, CQ or 3-MA treatment alone did not induce any toxic effect (not shown).
46
47

48
49 Since CQ and 3-MA have a wide range of effects, not only specifically linked to autophagy, we
50
51 have evaluated the effects of autophagy inhibition by generating stable glioma cells clones
52
53 expressing Atg5 shRNA. We have chosen Atg5 being this gene involved in both canonical and not
54
55 canonical autophagy (Scarlati *et al.*, 2008). Although we did not obtain a complete gene silencing,
56
57 in all transfected clones a strong increase of viral induced cell death was observed (Fig. 5C).
58
59

60
Our data confirm that inhibition of autophagy sensitises glioma cells to the oncolytic effect of
dl922-947.

Chloroquine increases dl922-947 oncolytic activity in vivo

To validate the potential therapeutic use of anti-autophagic drugs in association with *dl922-947*, we analyzed the effects of the virus combined with CQ in U87MG xenograft tumours. Athymic mice were injected with U87MG cells and after 20 days animals were randomised in four groups (T=0).

In mice receiving the single treatments (*dl922-947* or CQ), a non significant reduction of tumor growth was observed, whereas CQ and *dl922-947* combination treatment resulted in a highly significant tumor growth inhibition (Fig. 6A). Starting from T=11, a significant difference ($*p<0.05$) was observed between the group receiving the combined treatment, the untreated and the groups receiving single treatments. At T=23, the difference became highly significant ($**p<0.01$).

No toxicities were observed in virus-treated animals, or in CQ-treated animals.

As shown in Fig. 6B, CQ and *dl922-947* were both able to increase LC3-II/LC3 I ratio, this effect was further increased in the combined treatment.

The existence of a double switch between apoptosis and autophagy has been suggested (Platini *et al.*, 2010), and recent studies have demonstrated that the inhibition of autophagy increased apoptotic cell death in cancer cells (Kanzawa *et al.*, 2004; Boya *et al.*, 2005; Dalby *et al.*, 2010). Therefore, we analysed caspase-3 activation in treated tumours.

Cleaved caspase 3 levels were undetectable in control tumours and barely detectable in *dl922-947* infected tumours. At variance, in CQ-treated tumours, *dl922-947* led to more intense caspase 3 activation, compared to the tumours undergoing the CQ single treatment (Fig. 6B), thus indicating that chloroquine is effective in increasing the antitumour activity of *dl922-947* and in inducing apoptosis in experimental glioma *in vivo*.

Discussion

Glioblastoma multiforme (GBM) is one of the deadliest human cancer (Furnari *et al.*, 2007). The therapy for GBM, which includes surgical resection, radiotherapy, and chemotherapy, has shown a

1
2
3 limited success. Consequently, there is an urgent need for the development of novel therapeutic
4 approaches to improve patient survival. A number of promising oncolytic viruses have
5 demonstrated anti-glioma activity in both preclinical and clinical settings (Brandes *et al.*, 2008).
6
7

8
9
10 In the present study, we have analysed the effects of E1A mutated adenovirus *dl922-947* against
11 glioma cells, confirming its efficacy and showing that glioma cells undergo autophagy in response
12 to *dl922-947* infection, as confirmed by the dose-dependent development of acidic vesicular
13 organelles, the increase of LC3-II levels and the reduction of p62 levels. These effects were not
14 observed upon infection with control non replicating adenoviruses (AdGFP or *dl312*), indicating
15 that the activation of autophagy is dependent on viral replication.
16
17
18
19
20
21
22
23

24 In contrast with the induction of autophagy observed in infected cells, we show that *dl922-947*
25 infection activates the Akt/mTOR/p70s6k pathway, which is considered the main negative
26 regulatory mechanism for autophagy (Blommaert *et al.*, 1995; Yang *et al.*, 2005), and
27 simultaneously inhibits ERK1/2 pathway, which is known to promote it (Pattingre *et al.*, 2003).
28
29
30
31
32
33
34 Non replicating control adenovirus AdGFP did not induce these effects. This apparent discrepancy
35 could be possible due to compensatory mechanisms selectively operated by glioma cells to escape
36 *dl922-947* killing.
37
38
39

40
41 To address the role of these modulatory pathways in *dl922-947*-infected cells, we have used
42 pharmacological inhibitors. The MEK1 inhibitor PD98059 induced a block of autophagy, as shown
43 by a reduction of LC3 conversion. Interestingly, this block was paralleled by an increase of *dl922-*
44 *947* cytotoxicity. Conversely, the induction of autophagy by rapamycin in infected cells sharply
45 increased cell survival. All together, our data suggest that autophagy plays a defensive/survival role
46 during the infection with *dl922-947*, the autophagic machinery probably being involved in the
47 destruction of viral structures. On the other hand, the effects exerted by *dl922-947* infection on
48 intracellular signal could likely represent an attempt of the virus to overcome the cellular
49 autophagic response by modulating important autophagic signalling pathways.
50
51
52
53
54
55
56
57
58
59
60

1
2
3 It is known that viral infections have complex interconnections with the autophagic process. It has
4
5 been suggested that autophagosomes could serve as sites of viral replication during some viral
6
7 infections and therefore autophagy can support viral replication and assembly (Lin *et al.*, 2010).
8
9 Moreover, it has been observed that Hepatitis C virus (Dreux *et al.*, 2009; Tanida *et al.*, 2009), polio
10
11 virus (Suhy *et al.*, 2000) and Dengue Virus serotypes 2 and 3 (Panyasrivanit *et al.*, 2009) subvert or
12
13 induce autophagy to create membrane alterations advantageous for their replication. On the other
14
15 hand, it has been suggested that autophagy may confine viral replication within vesicles as a
16
17 defense mechanism, since it is well documented that autophagy acts as a host defense against
18
19 intracellular pathogens (xenophagy) (Lin *et al.*, 2010). An antiviral effect of autophagy has been
20
21 confirmed during neurotropic Sindibis virus infection and in HSV 1 encephalitis (Lin *et al.*, 2010).
22
23 Oncolytic viruses can modulate autophagy in target cells, including glioma cells. Delta-24-RGD
24
25 oncolytic adenovirus has been shown to induce autophagic cell death in brain tumour stem cells
26
27 (Jiang *et al.*, 2007; Jiang *et al.*, 2011). Auto-phagosomal-mediated cell death was also observed in
28
29 glioma cells infected with an oncolytic adenovirus driven by the survivin promoter (Ulasov *et al.*,
30
31 2009). Furthermore, hTERT-Ad, an oncolytic adenovirus regulated by the human telomerase
32
33 reverse transcriptase promoter, induced autophagic cell death in human malignant glioma through
34
35 inactivation of the AKT/TOR pathway (Ito *et al.*, 2006) and the inhibition of autophagy reduced
36
37 viral cytotoxicity (Yokoyama *et al.*, 2008). These results have led to the speculation that autophagy
38
39 is the main pathway of cell death in cells infected with replicating adenoviral vectors (Ito *et al.*,
40
41 2006). In line with this hypothesis, recent *in vitro* studies showed that autophagy inhibition can
42
43 decrease the oncolytic activity of Delta-24-RGD on glioma cell lines (Jiang *et al.*, 2011) and of the
44
45 E1B deleted adenovirus Adhz60 on lung carcinoma cell lines (Rodriguez-Rocha *et al.*, 2011).
46
47 Here, we show *in vitro* and *in vivo* that inhibition of autophagic pathways increases the activity of
48
49 the E1A deleted oncolytic virus of *dl922-947*, indicating that autophagy acts as cell survival
50
51 response. Our observation is consistent with Baird and colleagues (Baird *et al.*, 2008), that have
52
53 already shown that 3MA and chloroquine enhanced the effects of *dl922-947* in ovarian carcinoma
54
55
56
57
58
59
60

1
2
3 cells, but in contrast with the above mentioned studies from Jiang et al (Jiang *et al.*, 2011) and
4
5 Rodriguez-Rocha et al (Rodriguez-Rocha *et al.*, 2011). The discrepancies could be due to the
6
7 different oncolytic adenoviruses analysed. It is also conceivable that different viruses elicit different
8
9 cellular responses depending on cancer cell type. In this regard, in anaplastic thyroid carcinoma
10
11 cells, we did not observe autophagy following *dl922-947* infection (Libertini *et al.*, 2010),
12
13 suggesting that the activation of the autophagic process and the subsequent cellular fate are most
14
15 likely virus-and cell type-dependent. Further studies are required to better understand how
16
17 adenoviruses interact with host cells.
18
19
20

21
22 Autophagy inhibition is receiving attention as a novel strategy for cancer treatment. New autophagy
23
24 inhibitors have been reported as potent anticancer drugs and/or to sensitize cancer cells to the
25
26 activity of anticancer agents (Amaravadi *et al.*, 2007; Carew *et al.*, 2007; Rubinsztein *et al.*, 2007;
27
28 Shingu *et al.*, 2009). Chloroquine itself is emerging as a potential anticancer agent against various
29
30 cancers, including gliomas (Degtyarev et al., 2008; Solomon and Lee, 2009). Here, we show that
31
32 chloroquine strongly enhances the oncolytic effects of *dl922-947* both *in vitro* and *in vivo*,
33
34 encouraging the use of anti-autophagic drugs for the development of therapies based on the use of
35
36 *dl922-947* virus for the treatment of gliomas.
37
38
39
40
41
42

43 **Acknowledgments**

44
45 We thank Dr Tamotsu Yoshimori (Osaka University) and Prof Noboru Mizushima (Tokyo Medical
46
47 and Dental University) for kindly providing the plasmid containing LC3 cDNA. We thank Salvatore
48
49 Sequino for his excellent technical assistance and Joanne Smith for proofreading this manuscript.
50
51

52
53 We thank Angela Serena Maione for help with the confocal microscope.

54
55 Silvana Libertini was the recipient of a FIRC fellowship and is now recipient of a Marie Curie
56
57 fellowship. This study was supported by the Associazione Italiana per la Ricerca sul Cancro
58
59 (AIRC).
60

1
2
3
4
5
6
7
8
9
10
11
12
13
14
15
16
17
18
19
20
21
22
23
24
25
26
27
28
29
30
31
32
33
34
35
36
37
38
39
40
41
42
43
44
45
46
47
48
49
50
51
52
53
54
55
56
57
58
59
60

Author Disclosure Statement

No competing financial interests exist

1
2
3
4
5
6
7
8
9
10
11
12
13
14
15
16
17
18
19
20
21
22
23
24
25
26
27
28
29
30
31
32
33
34
35
36
37
38
39
40
41
42
43
44
45
46
47
48
49
50
51
52
53
54
55
56
57
58
59
60**References**

Ahmadi R, Dictus C, Hartmann C, Zürn O, Edler L, Hartmann M. Long-term outcome and survival of surgically treated supratentorial low-grade glioma in adult patients. *Acta Neurochir (Wien)*. 2009;151:1359-65.

Amaravadi RK, Yu D, Lum JJ, Bui T, Christophorou MA, Evan GI, Thomas-Tikhonenko A, Thompson CB. Autophagy inhibition enhances therapy-induced apoptosis in a Myc-induced model of lymphoma. *J Clin Invest*. 2007;117:326-36.

Baehrecke EH. Autophagy: dual roles in life and death? *Nat Rev Mol Cell Biol*. 2005 Jun;6:505-10.

Baird SK, Aerts JL, Eddaoudi A, Lockley M, Lemoine NR, McNeish IA. Oncolytic adenoviral mutants induce a novel mode of programmed cell death in ovarian cancer. *Oncogene*. 2008;27:3081-90.

Blommaart EF, Luiken JJ, Blommaart PJ, van Woerkom GM, Meijer AJ. Phosphorylation of ribosomal protein S6 is inhibitory for autophagy in isolated rat hepatocytes. *J Biol Chem*. 1995;270:2320-6.

1
2
3 Botta G, Perruolo G, Libertini S, Cassese A, Abagnale A, Beguinot F, Formisano P, Portella G.
4
5 PED/PEA-15 Modulates Coxsackievirus-Adenovirus Receptor Expression and Adenoviral
6
7 Infectivity via ERK-Mediated Signals in Glioma Cells. *Hum Gene Ther.* 2010;21:1067-76.
8
9

10
11
12
13
14
15 Boya P, González-Polo RA, Casares N, Perfettini JL, Dessen P, Larochette N, Métivier D, Meley
16
17 D, Souquere S, Yoshimori T, Pierron G, Codogno P, Kroemer G. Inhibition of macroautophagy
18
19 triggers apoptosis. *Mol Cell Biol.* 2005;25:1025-40.
20
21

22
23
24
25
26
27 Brandes AA, Tosoni A, Franceschi E, Reni M, Gatta G, Vecht C. Glioblastoma in adults. *Crit Rev*
28
29 *Oncol Hematol.* 2008;67:139-52. Epub 2008 Apr 3. Review
30
31

32
33
34
35 Carew JS, Nawrocki ST, Kahue CN, Zhang H, Yang C, Chung L, Houghton JA, Huang P, Giles FJ,
36
37 Cleveland JL. Targeting autophagy augments the anticancer activity of the histone deacetylase
38
39 inhibitor SAHA to overcome Bcr-Abl-mediated drug resistance. *Blood.* 2007;110:313-22.
40
41

42
43
44
45 Cheong SC, Wang Y, Meng JH, Hill R, Sweeney K, Kirn D, Lemoine NR, Halldén G. E1A-
46
47 expressing adenoviral E3B mutants act synergistically with chemotherapeutics in
48
49 immunocompetent tumor models. *Cancer Gene Ther.* 2008; 15: 40–50.
50
51

52
53
54
55
56
57 Dalby KN, Tekedereli I, Lopez-Berestein G, Ozpolat B. Targeting the prodeath and prosurvival
58
59 functions of autophagy as novel therapeutic strategies in cancer. *Autophagy.* 2010;6:322-9.
60

1
2
3 Degtyarev M, De Mazière A, Orr C, Lin J, Lee BB, Tien JY, Prior WW, van Dijk S, Wu H, Gray
4
5 DC, Davis DP, Stern HM, Murray LJ, Hoeflich KP, Klumperman J, Friedman LS, Lin K. Akt
6
7 inhibition promotes autophagy and sensitizes PTEN-null tumors to lysosomotropic agents. *J Cell*
8
9 *Biol.* 2008;183:101-16.

10
11
12
13
14
15
16
17 Díaz-Troya S, Pérez-Pérez ME, Florencio FJ, Crespo JL. The role of TOR in autophagy regulation
18
19 from yeast to plants and mammals. *Autophagy.* 2008;4:851-65.

20
21
22
23
24
25
26 Dreux M, Gastaminza P, Wieland SF, Chisari FV. The autophagy machinery is required to initiate
27
28 hepatitis C virus replication. *Proc Natl Acad Sci U S A.* 2009;106:14046-51

29
30
31
32
33
34
35 Fueyo J, Gomez-Manzano C, Alemany R, Lee PS, McDonnell TJ, Mitlianga P, Shi YX, Levin VA,
36
37 Yung WK, Kyritsis AP. A mutant oncolytic adenovirus targeting the Rb pathway produces anti-
38
39 glioma effect in vivo. *Oncogene.* 2000;19:2-12.

40
41
42
43
44
45
46
47 Furnari FB, Fenton T, Bachoo RM, Mukasa A, Stommel JM, Stegh A, Hahn WC, Ligon KL, Louis
48
49 DN, Brennan C, Chin L, DePinho RA, Cavenee WK. Malignant astrocytic glioma: genetics,
50
51 biology, and paths to treatment. *Genes Dev.* 2007;21:2683-710. Review.

52
53
54
55
56
57
58
59 Haseley A, Alvarez-Breckenridge C, Chaudhury AR, Kaur B. Advances in oncolytic virus therapy
60
for glioma. *Recent Pat CNS Drug Discov.* 2009;4:1-13

1
2
3 Heise C, Hermiston T, Johnson L, Brooks G, Sampson-Johannes A, Williams A, Hawkins L, Kirn
4
5 D. An adenovirus E1A mutant that demonstrates potent and selective systemic anti-tumoral
6
7 efficacy. *Nat Med.* 2000;6:1134-9.
8
9

10
11
12
13
14
15 Ito H, Aoki H, Kühnel F, Kondo Y, Kubicka S, Wirth T, Iwado E, Iwamaru A, Fujiwara K, Hess
16
17 KR, Lang FF, Sawaya R, Kondo S. Autophagic cell death of malignant glioma cells induced by a
18
19 conditionally replicating adenovirus. *J Natl Cancer Inst.* 2006; 98:625-36.
20
21

22
23
24
25
26
27 Jiang H, Gomez-Manzano C, Aoki H, Alonso MM, Kondo S, McCormick F, Xu J, Kondo Y,
28
29 Bekele BN, Colman H, Lang FF, Fueyo J. Examination of the therapeutic potential of Delta-24-
30
31 RGD in brain tumor stem cells: role of autophagic cell death. *J Natl Cancer Inst.* 2007;99:1410-4.
32
33

34
35
36
37
38
39 Jiang H, White EJ, Ríos-Vicil CI, Xu J, Gomez-Manzano C, Fueyo J. Human adenovirus type 5
40
41 induces cell lysis through autophagy and autophagy-triggered caspase activity. *J Virol.* 2011
42
43 May;85(10):4720-9.
44
45

46
47
48
49
50
51 Kabeya Y, Mizushima N, Ueno T, Yamamoto A, Kirisako T, Noda T, Kominami E, Ohsumi Y,
52
53 Yoshimori T. LC3, a mammalian homologue of yeast Apg8p, is localized in autophagosome
54
55 membranes after processing. *EMBO J.* 2000;19:5720-8.
56
57
58
59
60

1
2
3
4
5
6
7
8
9
10
11
12
13
14
15
16
17
18
19
20
21
22
23
24
25
26
27
28
29
30
31
32
33
34
35
36
37
38
39
40
41
42
43
44
45
46
47
48
49
50
51
52
53
54
55
56
57
58
59
60

Kanzawa T, Germano IM, Komata T, Ito H, Kondo Y, Kondo S. Role of autophagy in temozolomide-induced cytotoxicity for malignant glioma cells. *Cell Death Differ.* 2004;11:448-57.

Komatsu M, Ichimura Y. Physiological significance of selective degradation of p62 by autophagy. *FEBS Lett.* 2010 Apr 2;584(7):1374-8. Epub 2010 Feb 12. Review.

Kondo Y, Kanzawa T, Sawaya R, Kondo S. The role of autophagy in cancer development and response to therapy. *Nat Rev Cancer.* 2005;5:726-34.

Libertini S, Abagnale A, Passaro C, Botta G, Barbato S, Chieffi P, Portella G. AZD1152 negatively affects the growth of anaplastic thyroid carcinoma cells and enhances the effects of oncolytic virus *dl922-947*. *Endocr Relat Cancer.* 2011;18:129-41.

Lin LT, Dawson PW, Richardson CD. Viral interactions with macroautophagy: a double-edged sword. *Virology.* 2010;402:1-10.

Loos B, Engelbrecht AM. Cell death: a dynamic response concept. *Autophagy.* 2009;5:590-603.

Meijer AJ, Codogno P. Regulation and role of autophagy in mammalian cells. *Int J Biochem Cell Biol.* 2004;36:2445-62.

1
2
3 Mizushima N. Autophagy: process and function. *Genes Dev.* 2007;21:2861-73.
4
5
6
7

8
9 Paglin S, Hollister T, Delohery T, Hackett N, McMahon M, Sphicas E, Domingo D, Yahalom J. A
10 novel response of cancer cells to radiation involves autophagy and formation of acidic vesicles.
11
12 *Cancer Res.* 2001;61:439-44.
13
14
15
16
17

18
19
20
21 Panyasrivanit M, Khakpoor A, Wikan N, Smith DR. Linking dengue virus entry and
22 translation/replication through amphisomes. *Autophagy.* 2009;5:434-5.
23
24
25
26
27

28
29
30 Pattingre S, Bauvy C, Codogno P. Amino acids interfere with the ERK1/2-dependent control of
31 macroautophagy by controlling the activation of Raf-1 in human colon cancer HT-29 cells. *J Biol*
32 *Chem.* 2003;278:16667-74.
33
34
35
36
37
38
39
40
41

42 Platini F, Pérez-Tomás R, Ambrosio S, Tessitore L. Understanding autophagy in cell death control.
43
44 *Curr Pharm Des.* 2010;16:101-13.
45
46
47
48
49
50

51
52 Rodriguez-Rocha H, Gomez-Gutierrez JG, Garcia-Garcia A, Rao XM, Chen L, McMasters KM,
53
54 Zhou HS. Adenoviruses induce autophagy to promote virus replication and oncolysis. *Virology.*
55
56 2011 Jul 20;416(1-2):9-15.
57
58
59
60

1
2
3
4
5
6
7
8
9
10
11
12
13
14
15
16
17
18
19
20
21
22
23
24
25
26
27
28
29
30
31
32
33
34
35
36
37
38
39
40
41
42
43
44
45
46
47
48
49
50
51
52
53
54
55
56
57
58
59
60

Rubinsztein DC, Gestwicki JE, Murphy LO, Klionsky DJ. Potential therapeutic applications of autophagy. *Nat Rev Drug Discov.* 2007;6:304-12.

Scarlatti F, Maffei R, Beau I, Ghidoni R, Codogno P. Non-canonical autophagy: an exception or an underestimated form of autophagy? *Autophagy.* 2008 Nov 16;4(8):1083-5.

Shingu T, Fujiwara K, Bögl O, Akiyama Y, Moritake K, Shinojima N, Tamada Y, Yokoyama T, Kondo S. Inhibition of autophagy at a late stage enhances imatinib-induced cytotoxicity in human malignant glioma cells. *Int J Cancer.* 2009;124:1060-71.

Solomon VR, Lee H. Chloroquine and its analogs: a new promise of an old drug for effective and safe cancer therapies. *Eur J Pharmacol.* 2009;625:220-33. Review.

Suhy DA, Giddings TH Jr, Kirkegaard K.J *Virology.* Remodeling the endoplasmic reticulum by poliovirus infection and by individual viral proteins: an autophagy-like origin for virus-induced vesicles. 2000;74:8953-65.

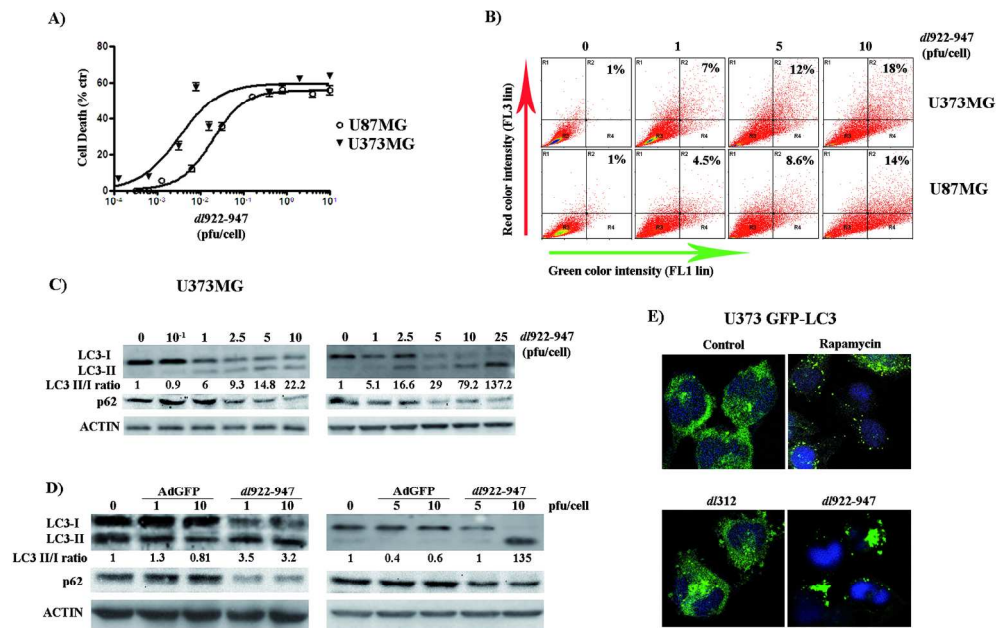
Tanida I, Fukasawa M, Ueno T, Kominami E, Wakita T, Hanada K. Knockdown of autophagy-related gene decreases the production of infectious hepatitis C virus particles. *Autophagy.* 2009;5:937-45.

1
2
3 Tyler MA, Ulasov IV, Lesniak MS. Cancer cell death by design: apoptosis, autophagy and glioma
4 virotherapy. *Autophagy*. 2009;5:856-7.
5
6
7
8
9

10
11
12 Ulasov IV, Tyler MA, Zhu ZB, Han Y, He TC, Lesniak MS. Oncolytic adenoviral vectors which
13 employ the survivin promoter induce glioma oncolysis via a process of beclin-dependent
14 autophagy. *Int J Oncol*. 2009;34:729-42.
15
16
17
18
19

20
21
22
23
24 Yang YP, Liang ZQ, Gu ZL, Qin ZH. Molecular mechanism and regulation of autophagy. *Acta*
25 *Pharmacol Sin*. 2005;26:1421-34.
26
27
28
29
30

31
32
33
34 Yokoyama T, Iwado E, Kondo Y, Aoki H, Hayashi Y, Georgescu MM, Sawaya R, Hess KR, Mills
35 GB, Kawamura H, Hashimoto Y, Urata Y, Fujiwara T, Kondo S. Autophagy-inducing agents
36 augment the antitumor effect of telerase-selve oncolytic adenovirus OBP-405 on glioblastoma cells.
37
38
39
40
41
42
43
44
45
46
47
48
49
50
51
52
53
54
55
56
57
58
59
60
Gene Ther. 2008;15:1233-9.

Fig. 1, Botta *et al.*

- Fig. 1 *di922-947* induces cell death and autophagy in malignant glioma cells
- (A) U373MG and U87MG cells were infected at the indicated MOIs and cell survival was analyzed seven days post-infection. The percent survival rates of cells exposed to the virus were calculated by assuming the survival rate of untreated cells to be 100%.
- (B) U373MG and U87MG cells were infected with *di922-947* for 72 h, stained with acridine orange for 15 min and then subjected to flow cytometric analysis.
- Red-positive cells in upper quadrants were considered as AVOs and calculated percentages shown.
- (C-D) Cells were infected with *di922-947* (C, D) or with AdGFP (D) and LC3I-II expression analysed after 72 hours. β -actin was used as a loading control.
- (E) Stable clones of U373MG cells expressing a fusion protein GFP-LC3 (U373 LC3-GFP) were infected with *di922-947* or *di312* (0.1 pfu/cell), or treated with rapamycin (500 nM) for 72 h and analysed by confocal microscope.

Experiments shown are representative of three independent experiments.

180x121mm (300 x 300 DPI)

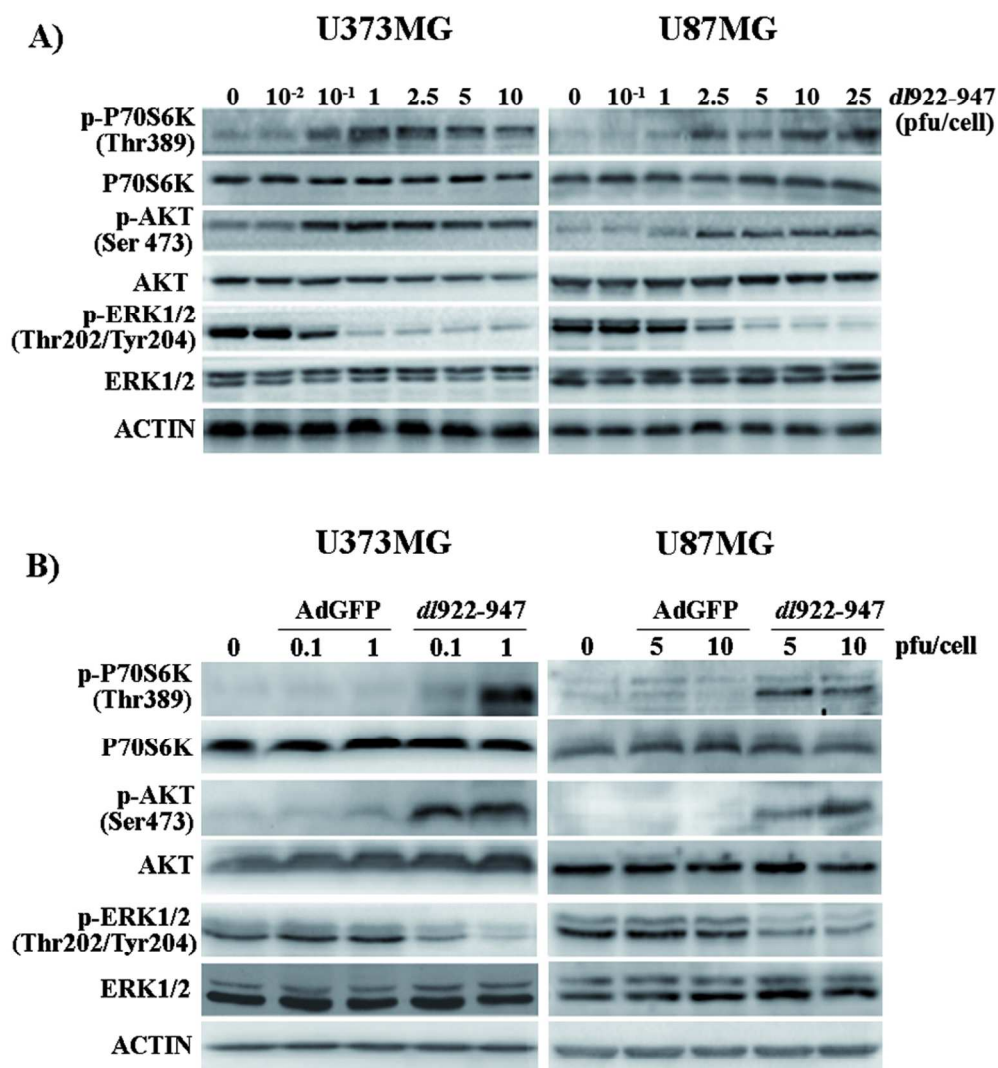
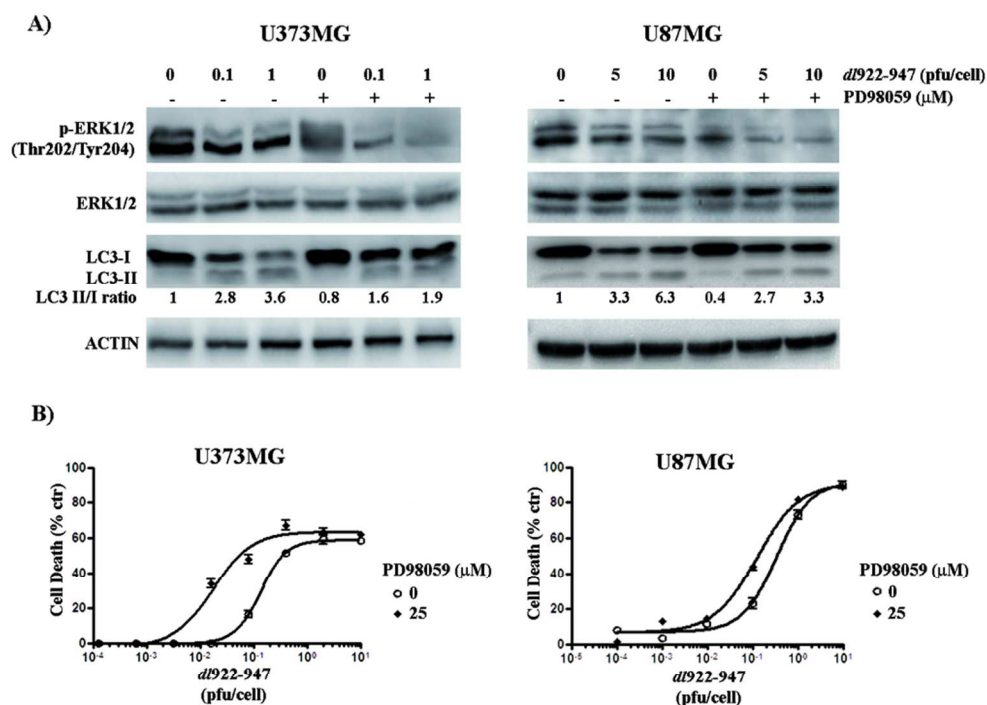


Fig. 2, Botta *et al.*

Fig. 2 Autophagy signalling pathways are modulated in response to *dl922-947* infection in glioma cells
 (A) U373MG and U87MG cells were infected with *dl922-947* at indicated MOIs for 72 h.
 (B) Cells were infected with *dl922-947* or AdGFP at indicated MOIs for 72 h. Expression of total and phosphorylated (p-) P70S6K, AKT and ERK1/2 were analysed by western blot.
 Results shown are representative of three independent experiments.

87x102mm (300 x 300 DPI)



33
34
35
36
37
38
39
40
41
42
43
44
45
46
47
48
49
50
51
52
53
54
55
56
57
58
59
60

Fig. 3, Botta *et al.*

Fig. 3 Inhibition of ERK1/2 pathway inhibits autophagy and enhances dI922-947-induced cytotoxicity (A) U373MG and U87MG cells were treated with PD98059 (25 μ M) for 2 h and then infected with dI922-947 at indicated MOIs. Expression of total and phosphorylated (p)-ERK1/2, and LC3I-II were analysed by western blot after 72 hours.

(B) Cells were treated with PD98059 (25 μ M) and after 2 hours infected with dI922-947 at indicated MOIs. Cell survival was evaluated after 7 days. PD98059 treatment alone induced 15% and 20% of cytotoxicity in U373MG cells in U87MG cells, respectively.

Results shown are representative of three independent experiments.

87x68mm (300 x 300 DPI)

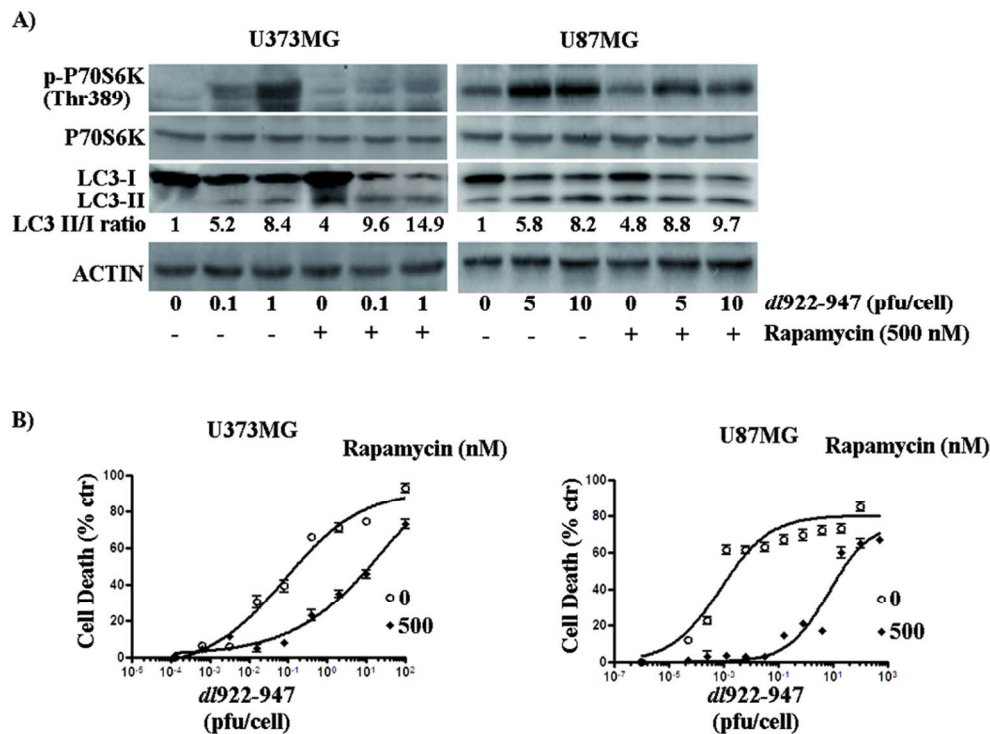


Fig. 4, Botta *et al.*

Fig. 4 Inhibition of mammalian target of rapamycin (mTOR) pathway induces autophagy and decreases dl922-947-induced cytotoxicity

(A) U373MG and U87MG cells were treated with rapamycin (500 nM) for 2 h and infected with dl922-947 at indicated MOIs. Expression of total and phosphorylated (p-) P70S6k, and LC3I-II were analysed by western blot after 72 hours.

(B) Cells were treated with rapamycin (500 nM) and infected with dl922-947 after 2 hours at indicated MOIs. Cell survival was evaluated after 7 days. A significant increase of LD50 values was obtained in both cell lines in the presence of rapamycin: from 0.09 to 9.18 in U373MG cells, and from 0.01 to 31.9 in U87MG cells.

Results shown are representative of three independent experiments.

87x70mm (300 x 300 DPI)

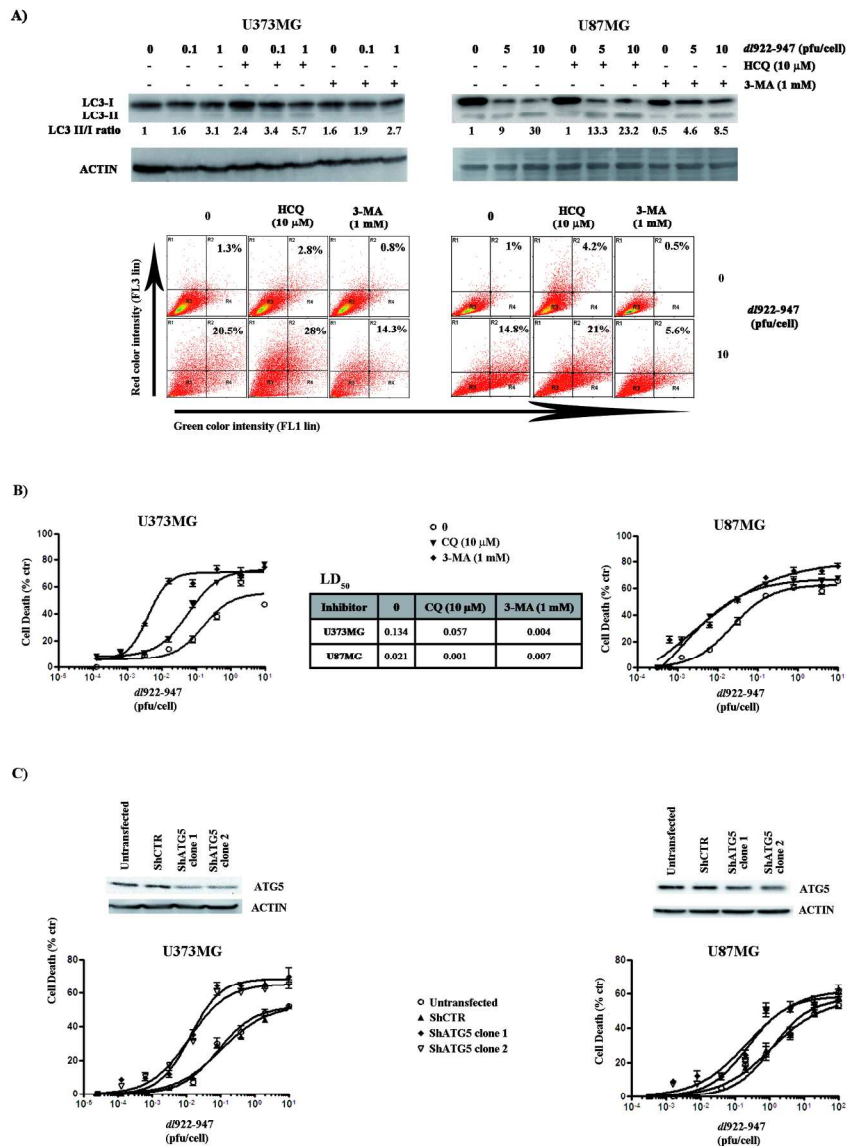
Fig. 5, Botta *et al.*

Fig. 5 Pharmacological autophagy inhibitors enhance dI922-947-induced cytotoxicity
 (A) U373MG (left) and U87MG cells (right) were treated with CQ (10 μ M) or 3-MA (1mM) for 2 hours, infected with different MOIs of dI922-947 for 72 hours and LC3I-II levels or AVOs formation analysed after 72 hours respectively by western blot (upper panel) and FACS analysis (lower).
 (B) Cells were treated with CQ or 3-MA for 2 hours and then infected at different MOIs of dI922-947. Cell survival was evaluated after 7 days.
 (C) U373MG and U87MG clones stably expressing a scrambled (ShCTR) or a specific shRNA for ATG5 (shATG5) were infected with different MOI of dI922-947 and cell survival evaluated 7 days.
 Results shown are representative of three independent experiments.

180x240mm (300 x 300 DPI)

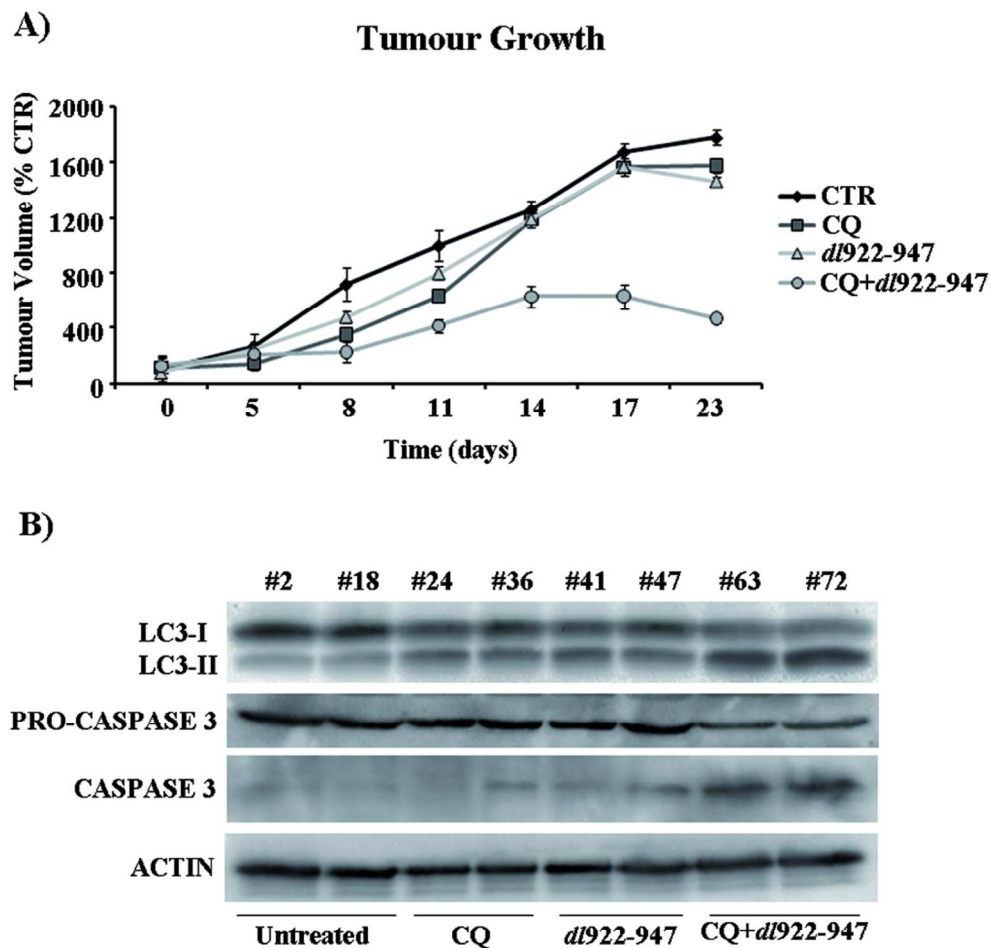


Fig. 6, Botta *et al.*

Fig. 6 Chloroquine enhances the activity of dl922-947 and delays the growth of glioma tumour xenografts (A) Animals bearing U87MG tumour xenografts were randomised into four groups. Two groups received CQ (45mg/kg/die) i.p. every third day. dl922-947 ($1 \times 10^6 \times 10^6$ pfu, in a volume of 200 μ l) was injected three times per week into one CQ-treated group and one untreated group. Tumour volume is expressed as a percentage of the volume observed at day 0 in the control group. The difference between the untreated group or the group receiving the combined treatment become statistically significant ($*p < 0.05$) from day 11. From day 17, until the end of the treatment, the difference became highly significant ($**p < 0.01$).

A statistically significant difference was also observed between the group receiving the combined treatment and single treatment groups ($*p < 0.05$) from day 11 and from day 17 ($**p < 0.01$).

No statistically significant difference was observed between the groups receiving the single treatments and the untreated control group.

(B) Animals bearing U87MG xenograft were treated or not with CQ (45mg/Kg) and intratumourally injected with dl922-947 (1×10^7 pfu) after 24 hours. Tumour tissue samples were homogenized after 48 hours and LC3I-II or caspase-3 levels analysed by western blot. β -actin was used as loading control.

87x90mm (300 x 300 DPI)

1
2
3 **Figure legends**
4
5
6
7

8 **Fig. 1** *dl922-947 induces cell death and autophagy in malignant glioma cells*
9

10 (A) U373MG and U87MG cells were infected at the indicated MOIs and cell survival was analyzed
11 seven days post-infection. The percent survival rates of cells exposed to the virus were calculated
12 by assuming the survival rate of untreated cells to be 100%.
13
14

15
16
17 (B) U373MG and U87MG cells were infected with *dl922-947* for 72 h, stained with acridine orange
18 for 15 min and then subjected to flow cytometric analysis.
19

20 Red-positive cells in upper quadrants were considered as AVOs and calculated percentages shown.
21

22 (C-D) Cells were infected with *dl922-947* (C, D) or with AdGFP (D) and LC3I-II expression
23 analysed after 72 hours. β -actin was used as a loading control.
24

25
26
27 (E) Stable clones of U373MG cells expressing a fusion protein GFP-LC3 (U373 LC3-GFP) were
28 infected with *dl922-947* or *dl312* (0.1 pfu/cell), or treated with rapamycin (500 nM) for 72 h and
29 analysed by confocal microscope.
30
31

32 Experiments shown are representative of three independent experiments.
33
34
35
36
37
38
39
40

41 **Fig. 2** *Autophagy signalling pathways are modulated in response to dl922-947 infection in glioma*
42 *cells*
43
44

45 (A) U373MG and U87MG cells were infected with *dl922-947* at indicated MOIs for 72 h.
46
47

48 (B) Cells were infected with *dl922-947* or AdGFP at indicated MOIs for 72 h. Expression of total
49 and phosphorylated (p-) P70S6K, AKT and ERK1/2 were analysed by western blot.
50
51

52 Results shown are representative of three independent experiments.
53
54
55
56
57

58 **Fig. 3** *Inhibition of ERK1/2 pathway inhibits autophagy and enhances dl922-947-induced*
59 *citotoxicity*
60

1
2
3 (A) U373MG and U87MG cells were treated with PD98059 (25 μ M) for 2 h and then infected with
4 *dl922-947* at indicated MOIs. Expression of total and phosphorylated (p)-ERK1/2, and LC3I-II
5
6 were analysed by western blot after 72 hours.
7
8

9
10 (B) Cells were treated with PD98059 (25 μ M) and after 2 hours infected with *dl922-947* at
11
12 indicated MOIs. Cell survival was evaluated after 7 days. PD98059 treatment alone induced 15%
13
14 and 20% of cytotoxicity in U373MG cells in U87MG cells, respectively.
15
16

17 Results shown are representative of three independent experiments.
18
19
20
21

22 **Fig. 4** *Inhibition of mammalian target of rapamycin (mTOR) pathway induces autophagy and*
23
24 *decreases dl922-947-induced cytotoxicity*
25
26

27 (A) U373MG and U87MG cells were treated with rapamycin (500 nM) for 2 h and infected with
28
29 *dl922-947* at indicated MOIs. Expression of total and phosphorylated (p-) P70S6k, and LC3I-II
30
31 were analysed by western blot after 72 hours.
32
33

34 (B) Cells were treated with rapamycin (500 nM) and infected with *dl922-947* after 2 hours at
35
36 indicated MOIs. Cell survival was evaluated after 7 days. A significant increase of LD₅₀ values was
37
38 obtained in both cell lines in the presence of rapamycin: from 0.09 to 9.18 in U373MG cells, and
39
40 from 0.01 to 31.9 in U87MG cells.
41
42

43 Results shown are representative of three independent experiments.
44
45
46
47

48 **Fig. 5** *Pharmacological autophagy inhibitors enhance dl922-947-induced cytotoxicity*
49
50

51 (A) U373MG (left) and U87MG cells (right) were treated with CQ (10 μ M) or 3-MA (1mM) for 2
52
53 hours, infected with different MOIs of *dl922-947* for 72 hours and LC3I-II levels or AVOs
54
55 formation analysed after 72 hours respectively by western blot (upper panel) and FACS analysis
56
57 (lower).
58
59

60 (B) Cells were treated with CQ or 3-MA for 2 hours and then infected at different MOIs of *dl922-947*. Cell survival was evaluated after 7 days.

1
2
3
4
5
6
7
8
9
10
11
12
13
14
15
16
17
18
19
20
21
22
23
24
25
26
27
28
29
30
31
32
33
34
35
36
37
38
39
40
41
42
43
44
45
46
47
48
49
50
51
52
53
54
55
56
57
58
59
60

(C) U373MG and U87MG clones stably expressing a scrambled (ShCTR) or a specific shRNA for ATG5 (shATG5) were infected with different MOI of *dl922-947* and cell survival evaluated 7 days. Results shown are representative of three independent experiments.

Fig. 6 *Chloroquine enhances the activity of dl922-947 and delays the growth of glioma tumour xenografts*

(A) Animals bearing U87MG tumour xenografts were randomised into four groups. Two groups received CQ (45mg/kg/die) *i.p.* every third day. *dl922-947* ($1 \times 10^6 \times 10^6$ pfu, in a volume of 200 μ l) was injected three times per week into one CQ-treated group and one untreated group. Tumour volume is expressed as a percentage of the volume observed at day 0 in the control group. The difference between the untreated group or the group receiving the combined treatment become statistically significant ($*p < 0.05$) from day 11. From day 17, until the end of the treatment, the difference became highly significant ($**p < 0.01$).

A statistically significant difference was also observed between the group receiving the combined treatment and single treatment groups ($*p < 0.05$) from day 11 and from day 17 ($**p < 0.01$).

No statistically significant difference was observed between the groups receiving the single treatments and the untreated control group.

(B) Animals bearing U87MG xenograft were treated or not with CQ (45mg/Kg) and intratumourally injected with *dl922-947* (1×10^7 pfu) after 24 hours. Tumour tissue samples were homogenized after 48 hours and LC3I-II or caspase-3 levels analysed by western blot. β -actin was used as loading control.